HDL-CR-76-090-1

EMP RESPONSE AND DAMAGE MODELING OF DIODES, JUNCTION FIELD EFFECT TRANSISTOR DAMAGE TESTING AND SEMICONDUCTOR DEVICE FAILURE ANALYSIS--FINAL TECHNICAL REPORT

APRIL 1976

Prepared By

General Electric Company
Space Division
Philadelphia, PA 19101

Under Contract

DAAG39-74-C-0090

This work was sponsored by the Defense Nuclear Agency under Subtask R99QAXEB099/42, Work Unit 42

U.S. Army Materiel Command
HARRY DIAMOND LABORATORIES
Adelphi, Maryland 20783

The findings in this report are not to be construed as an official Department of the Army position unless so designated by other authorized documents.

Citation of manufacturers' or trade names does not constitute an official indorsement or approval of the use thereof.

Destroy this report when it is no longer needed. Do not return it to the originator.

(14) 75SDS-4226

UNCLASSIFIED

SECURITY CLASSIFICATION OF THIS PAGE (When Data Entered)

REPORT DOCUMENTATION PAGE	READ INSTRUCTIONS BEFORE COMPLETING FORM
1. REPORT NUMBER (19) HDL-CR-76-090-1	2. GOVT ACCESSION NO. 3. RECIPIENT'S CATALOG NUMBER
4. TITLE (and Subtitle) (6) EMP RESPONSE AND DAMAGE MODELING OF DIODES, JUNCTION FIELD EFFECT TRANSISTOR DAMAGE TESTING & SEMICONDUCTOR DEVICE FAILURE ANALYSIS	5. TYPE OF REPORT & PERIOD COVERED (1) FINAL TECHNICAL REPORT, 6/75 TO 12/75 Aug 74 - Dec 75 (3) 6. PERFORMING ORG. REPORT NUMBER 75SDS4279
7. AUTHOR(s) (10) DANTE M. TASCA AND SAMUEL J. STOKES, III	8. CONTRACT OR GRANT NUMBER(s) HDL PROJECT NO. E143E1 DRCMS CODE: 691000.22. 10560
9. PERFORMING ORGANIZATION NAME AND ADDRESS (1) GENERAL ELECTRIC COMPANY (5) SPACE DIVISION (2) PHILADELPHIA, PENNA 19101	10. PROGRAM ELEMENT, PROJECT, TASK AREA & WORK UNIT NUMBERS MIPR: 3-626 PROG.ELEMENT:6.11.02.H
11. CONTROLLING OFFICE NAME AND ADDRESS DEFENSE NUCLEAR AGENCY	12. REPORT DATE (11) APRIL 1976 13. NUMBER OF PAGES 204 (12) 211
14. MONITORING AGENCY NAME & ADDRESS(if different from Controlling Office) U.S. ARMY MATERIEL DEVELOPMENT AND READINESS COMMAND HARRY DIAMOND LABORATORIES	15. SECURITY CLASS. (of this report) UNCLASSIFIED 15a. DECLASSIFICATION/DOWNGRADING SCHEDULE
16. DISTRIBUTION STATEMENT (of this Report) (15) DAAG39-74-C-0094 APPROVED FOR PUBLIC RELEASE; DISTRIBUTION UNLIMITED.	
17. DISTRIBUTION STATEMENT (of the abstract entered in Block 20, if different from Report)	
18. SUPPLEMENTARY NOTES THIS WORK WAS SPONSORED BY THE DEFENSE NUCLEAR AGENCY UNDER SUBTASK R99QAXEB097, WORK UNIT #41.	
19. KEY WORDS (Continue on reverse side if necessary and identify by block number) EMP (ELECTROMAGNETIC PULSE) SEMICONDUCTOR DEVICE DAMAGE DIODE DAMAGE MODELS JFET PULSE DAMAGE SEMICONDUCTOR FAILURE ANALYSIS	
20. ABSTRACT (Continue on reverse side if necessary and identify by block number) Engineering type damage models to predict both surge impedance and failure levels of silicon semiconductor diodes when exposed to EMP type environments were developed from multiple regression analyses of a large experimental data base which was supplied by the U.S. Army/HDL and the U.S. Air Force/AFWL. The models were developed for both forward and reverse polarities of junction current conduction. The models are expressed in terms	

DD FORM 1 JAN 73 1473 EDITION OF 1 NOV 65 IS OBSOLETE UNCLASSIFIED

1 SECURITY CLASSIFICATION OF THIS PAGE (When Data Entered)

405 025

of published device parameters and, as such, do not require a "hands on" device evaluation. The models were developed both for conditions where the device construction was unknown and for conditions where specific device construction is known. Separate models were develcped for devices functionally classified as "rectifiers, diodes and switches" and for devices functionally classified as "non-temperature compensated Zener diodes". This study was undertaken to provide a supplement to the damage mode ing techniques presently contained in the DNA EMP Handbook, Report No. DNA 2114H.

Extensive pulse damage testing was performed on the Motorola 2N4392 N-Channel silicon JFET. The 2N4392 is a depletion mode device designed for chopper and high speed switching applications. A total of 215 units were evaluated for various combinations of terminal pairs in biased and unbiased configurations. The experiments were performed in order to provide sufficient information to determine the basic pulse response and damage characteristics of JFET structures.

Failure analyses were performed on a variety of semiconductor device types which were subjected to EMP pulse damage in order to determine the nature of the failure mechanisms in the respective device types. The device types examined were the 1N4148 diode, 2N918 transistor, RD211 gate expander, MEM806A MOSFET and SN5404 microcircuit which were previously subjected to pulse damage testing under Contract DAAG 39-72-C-0066, together with the 2N4392 JFET which was subjected to pulse damage testing under the present program. The failure analyses consisted of a surface examination, microprobing, surface etching, device cross-sectioning and electron microscopy.

FOREWORD

This Final Technical Report was prepared by the General Electric Company, Space Division, Philadelphia, Pennsylvania, under U. S. Army Contract DAAG 39-74-C-0090, DNA NWED Subtask R99QAXEB097, Work Unit 41, "EMP Induced Damage in Semiconductor Circuits". The work was administered under the direction of the U.S. Army, Harry Diamond Laboratories, Electromagnetic Effects Laboratory, 2800 Powder Mill Road, Adelphi, Maryland 20783. Technical monitoring of the contract at USA/HDL was under the direction of J. Miletta, A. Renner and J. Kreck. The program manager at General Electric Company was J. C. Peden and the principle investigators, D. M. Tasca and S. J. Stokes III.

The authors express their sincere appreciation to J. Miletta of U. S. Army, Harry Diamond Laboratories and R. A. Hays of U. S. Air Force, Air Force Weapons Laboratory for providing detailed experimental damage data on semiconductor devices. The authors also wish to acknowledge J. R. Greenwald, B. A. Pokol, R. R. Boileau and F. C. Frey of the General Electric Company, Space Division, for their contributions to the work reported here.

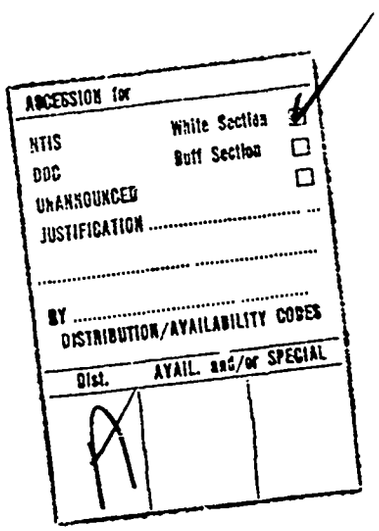

SUMMARY

The objective of the experimental and analytical work performed on this program was threefold. The first was to develop an engineering model to predict the EMP response and damage levels of semiconductor diodes. This study was undertaken to provide a supplement to the damage modeling techniques presently contained in the DNA EMP Handbook, Report No. DNA 2114H, and was the area in which the primary emphasis of the program was placed. The second and third objectives were to perform pulse damage testing on a junction field effect transistor type and to perform failure analyses on various semiconductor device types which were subjected to pulse damage.

Engineering type damage models to predict both surge impedance and failure levels of silicon semiconductor diodes were developed from multiple regression analyses of a large experimental data base which was supplied by the U. S. Army/HDL and the U. S. Air Force/AFWL. The models were developed for both forward and reverse polarities of junction current conduction. The models are expressed in terms of published device parameters, and, as such, do not require a "hands on" device evaluation. The models were developed both for conditions where the device construction was unknown and for conditions where specific device construction is known. Separate models were developed for devices functionally classified as "rectifiers, diodes and switches" and for devices functionally classified as "non-temperature compensated Zener diodes"

The analysis showed that, under high pulse current injection levels, the forward polarity surge impedance of both diode classes exhibited conductivity modulation effects whereby the impedance was inversely proportional to I^N where N was between 0.3 and 0.4. The forward polarity pulse damage in both classes of diodes was found to be due to I^2R bulk heating under non-adiabatic conditions for the pulse widths and device junction areas evaluated. The conductivity modulation effects caused the exponents of the time dependence for damage to lie in the range of 0.3 as would be expected for these effects.

Under reverse pulse polarity conditions, the low and medium voltage Zener diodes also exhibited a surge impedance associated with the bulk material and also partially dependent on conductivity modulation effects. The reverse polarity surge impedance of the "rectifiers, diodes and switches" was found to be strongly dependent on both device breakdown voltage level and pulse current level. The reverse polarity pulse damage in the Zener diodes was found to be due also to I^2R bulk heating under non-adiabatic conditions. The rectifiers, diodes and switches, however, exhibited junction heating effects which were also characteristic of non-adiabatic conditions.

Extensive pulse damage testing was performed on the Motorola 2N4392 N-Channel silicon JFET. The 2N4392 is a depletion mode device designed for chopper and high speed switching applications. A total of 215 units were evaluated for various combinations of terminal pairs in biased and unbiased configurations. In the forward polarity the gate-source junction behaves like a normal forward biased diode. Because of the relatively large junction to metallization area ratio in the device, metallization burnout occurred before junction damage. The damage characteristics of the drain and source terminal pair and the reverse bias gate-source junction were somewhat similar. Here, the devices exhibited a second breakdown response which was initiated at a relatively constant pulse current injection level from 30 nanoseconds to 100 microseconds. The pulse current required for damage increased sharply below 30 nanoseconds and in this region the damage levels are significantly higher than the second breakdown initiation levels.

Failure analyses were performed on a variety of semiconductor device types which were subjected to EMP pulse damage. The device types examined were the 1N4148 diode, 2N918 transistor, RD211 gate expander, MEM806A MOSFET and SN5404 microcircuit which were previously subjected to pulse damage testing under Contract DAAG 39-72-C-0066, together with the 2N4392 JFET which was subjected to pulse damage testing under the present program. The failure analyses consisted of a surface examination, microprobing, surface etching, device cross-sectioning and electron microscopy. Junction and metallization damage in bipolar devices was observed. Gate oxide damage in the MOSFET device was observed while the JFET device exhibited failures which were observable on the device surface. Metallization damage was also observed in the unipolar devices.

TABLE OF CONTENTS

LIST OF FIGURES

LIST OF FIGURES
(CONTINUED)

LIST OF FIGURES
(CONTINUED)

LIST OF FIGURES
(CONTINUED)

LIST OF FIGURES
(CONTINUED)

LIST OF FIGURES
(CONTINUED)

LIST OF FIGURES
(CONTINUED)

LIST OF TABLES

1. Introduction

This document is the Final Technical Report for U. S. Army, Harry Diamond Laboratories Contract DAAG 39-74-C-0090, "EMP Response and Damage Modeling of Diodes, Junction Field Effect Transistor Damage Testing and Semiconductor Device Failure Analysis". The program consisted of three tasks. The first task was to develop an engineering model to predict the EMP response and damage levels of semiconductor diodes. This task was the one in which the primary emphasis of the program was placed. The second and third tasks were to perform pulse damage testing on a junction field effect transistor type and to perform failure analyses on various semiconductor device types which were subjected to pulse damage.

The objective of the Diode Damage Model Task was to develop engineering type damage models to predict both surge impedances and failure levels of silicon semiconductor diodes when exposed to EMP type environments. The models were to be developed for both the forward and reverse polarities of junction current conduction. A further requirement was that the models should not require a "hands on" device evaluation but should relate the surge impedance and failure levels to some associated device parameter which could easily be obtained from a manufacturer's data sheet or other published information. This study was undertaken to provide a supplement to the damage modeling techniques presently contained in the DNA EMP Handbook, Report No. DNA 2114H. The experimental data base used to develop the desired models consisted of the pulse damage data supplied by the U. S. Army, Harry Diamond Laboratories on the Pershing and Lance Programs, the pulse damage data supplied by the U. S. Air Force, Air Force Weapons Laboratory on the EMP Assessment and Hardening of Aeronautical Systems Program, together with the pulse damage data generated by the General Electric Company, Re-Entry and Space Divisions on various missile and technology programs.

The objective of the second task was to perform a detailed experimental pulse damage characterization of a typical JFET device in order to provide sufficient information to determine the basic pulse response and damage characteristics of JFET structures. Bipolar semiconductor devices have been studied in detail in the past and their associated pulse response and damage characteristics are well known. Junction field effect transistors, in contrast, have not received anywhere near the attention that bipolar devices have. As a result, comparitively little is known about their pulse response and damage characteristics.

The objective of the Semiconductor Device Failure Analysis Task was to physically examine a variety of semiconductor device types which were subjected to EMP pulse damage in order to determine the nature of the failure mechanisms in the respective device types. The device types examined were the 1N4148 diode, 2N918 transistor, RD211 gate expander, MEM806A MOSFET and SN5404 microcircuit which

were previously subjected to pulse damage testing under Contract DAAG 39-72-C-0066, together with the 2N4392 JFET which was subjected to pulse damage testing under the present program. The failure analyses consisted of a surface examination, microprobing, surface etching, device cross-sectioning and electron microscopy.

2. Diode Damage Model Development

The objective of the Diode Damage Model Task was to develop engineering type damage models to predict both surge impedances and failure levels of silicon semiconductor diodes when exposed to EMP type environments. The models were to be developed for both the forward and reverse polarities of junction current conduction. A further requirements was that the models should not require a "hands on" device evaluation but should relate the surge impedance and failure levels to some associated device parameter which could easily be obtained from a manufacturer's data sheet or other published information.

This study was undertaken to provide a supplement to the damage modeling techniques presently contained in the DNA EMP Handbook, Report No. DNA 2114H. The present handbook model does not provide any quantitative methods for evaluating device surge impedance (either forward or reverse polarity) nor does it provide any quantitative methods for evaluating forward polarity vulnerability level. The diode models presented in the handbook are primarily based on one dimensional heat flow conditions in a reverse biased junction with bulk heating effects neglected. The resulting model is expressed in terms of a simplified single termed, time dependent expression of the form "$K\sqrt{t}$". Although "K" is evaluated empirically, a quantitative measure of the statistical errors associated with the empirical evaluation is not provided. Thus, the results of this study are intended to provide the supplemental information required to expand upon the damage model definition in these particular areas. In view of the large data base that was made available, the damage modeling was restricted to purely analytical efforts with no new test data being generated in order to maximize the output of the program. A considerable effort was devoted to obtaining the data base in the configuration required together with obtaining device rating and construction information.

The approach taken in the present model development program was: (1) obtain existing pulse damage data on semiconductor diodes; (2) define the various published device specifications and construction type for each unique device identification number/manufacturer combination in the data base; (3) identify the published specification parameters which were common to all device types within certain functional classifications; (4) perform multiple regression analyses of the pulse damage data versus the common specification parameters within each functional classification; and, (5) identify the relevant device parameters which correlated best to the experimental surge impedance and failure level values together with the prediction errors associated with each empirical model. The data base used consisted of the pulse damage data supplied by the U. S. Army, Harry Diamond Laboratories on the Pershing and Lance Programs, the pulse damage data supplied by the U. S. Air Force, Air Force Weapons Laboratory on the EMP

Assessment and Hardening of Aeronautical Systems Program, together with the pulse damage data generated by the General Electric Company, Re-Entry and Space Divisions on various missile and technology programs. Since diode surge impedance was one of the device characteristics to be modeled, the data base was required to be defined down to the level of the peak voltages and current associated with each device experiment rather than down to just a power-time definition.

Table 1 shows a summary of the number of different device types (i.e., unique identification number/manufacturer/data source) in the present data base with respect to functional classification and construction type. The functional classifications shown are those defined in the 34th Edition of the "Semiconductor Diode D.A.T.A. Book". The device construction information shown was obtained from each manufacturer whose device was listed in the data base. Each manufacturer was contacted twice (once in the beginning of the program and once toward the end of the program) in an effort to complete the construction characterization of the data base. Device construction information, though, is generally, difficult to obtain being considered either proprietary or too troublesome for manufacturer's representatives to ferret out. Evidence of this can be seen from the number of devices listed as diffused (which in reality are generally either mesa or planar) and unknown.

Figures 1 and 2 show the range of variation in device ratings for the diode data base considered in the present study. Figure 1 shows the range of peak inverse voltage and maximum average rectified current ratings for diodes functionally classified as rectifiers, diodes and switches. Figure 2 is a similar display for a zener diode functional classification with respect to zener voltage and power ratings. Tables 2, 3, and 4 give a parametric description of each device type within the data base. Shown here are the data file number (F #) which contains the detailed pulse damage data for each device type, the data source, the device functional classification, the device type (i.e., identification alpha-numeric code), the device manufacturer (MFG) per the D.A.T.A. Book code, the device ratings and the construction type (CONST.). The "PIV" and "IO" ratings given in Tables 2 and 4 refer to the diode peak inverse voltage in volts and maximum average rectified current in amperes rating, respectively. The "VZ" and "PWR" ratings given in Tables 3 and 4 refer to the diode zener voltage in volts and power in watts rating, respectively. The detailed pulse damage data for each device type shown in Tables 2, 3 and 4 is given in Appendix A and is listed there in numerical sequence with respect to the appropriate data file number (F #).

The results of the diode damage model development are described in detail below. Surge impedance and failure level models are presented for both the forward and reverse polarities of junction current conduction. The results are given in graphical form show-

Table 1. Functional Classifications and Construction Types for the Silicon Semiconductor Diodes in the Present Data Base.

DIODE FUNCTIONAL CLASSIFICATION	NUMBER OF TYPES FOR EACH CONSTRUCTION					
	ALLOY	MESA	PLANAR	DIFFUSED	UNKNOWN	TOTAL
RECTIFIER	9	17	5	4	7	42
DIODE	1	3	2	1	0	7
SWITCH	2	2	10	0	1	15
ZENER	15	18	15	1	13	62
T.C. ZENER	1	1	0	1	6	9
STABISTOR	0	0	1	0	1	2
TUNNEL DIODE	0	0	0	0	1	1
POINT CONTACT	0	0	0	0	1	1

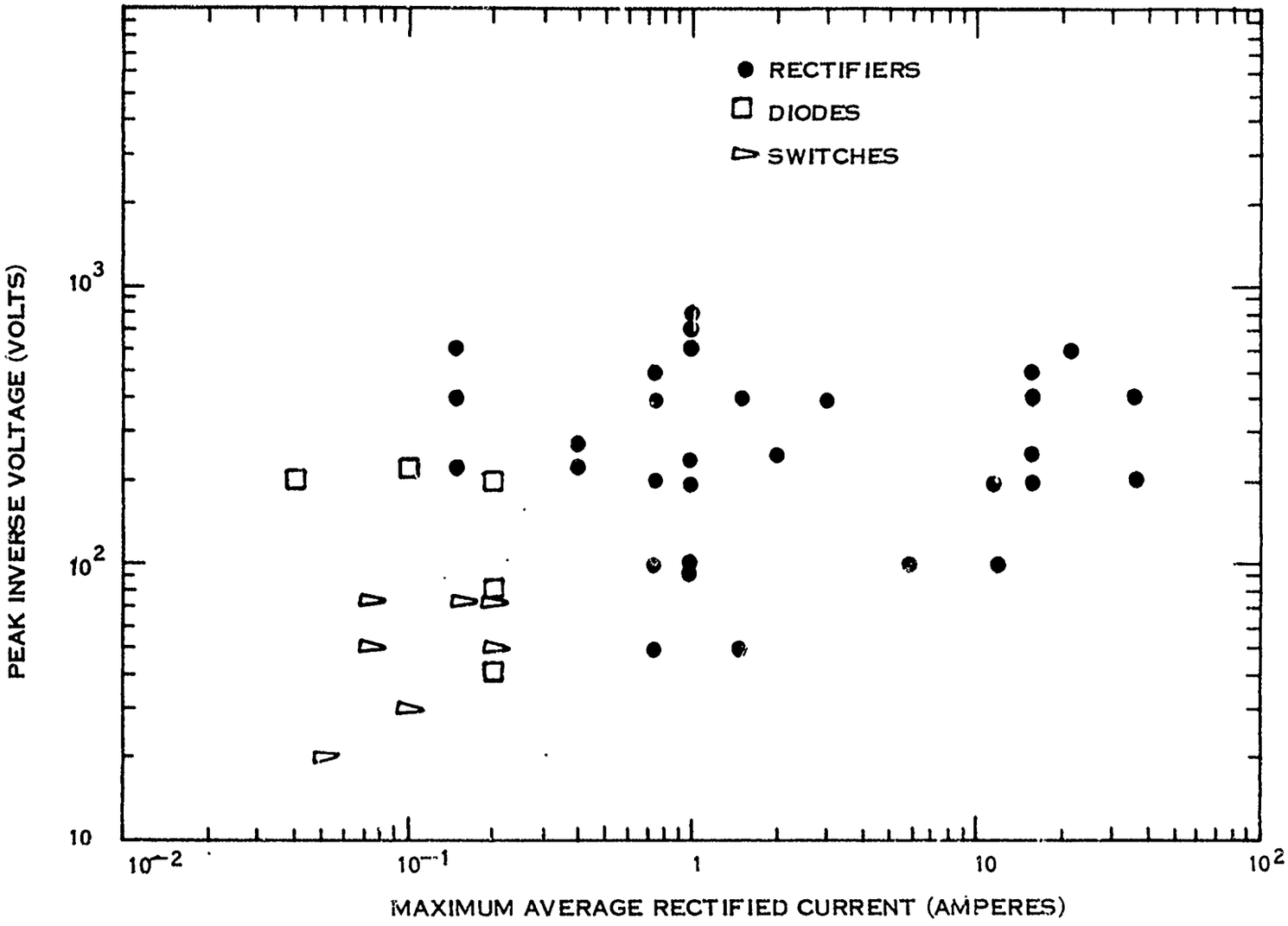

Figure 1. Range of Peak Inverse Voltage & Maximum Average Rectified Current Ratings for Diodes in the Present Data Base Functionally Classified as Rectifiers, Diodes and Switches.

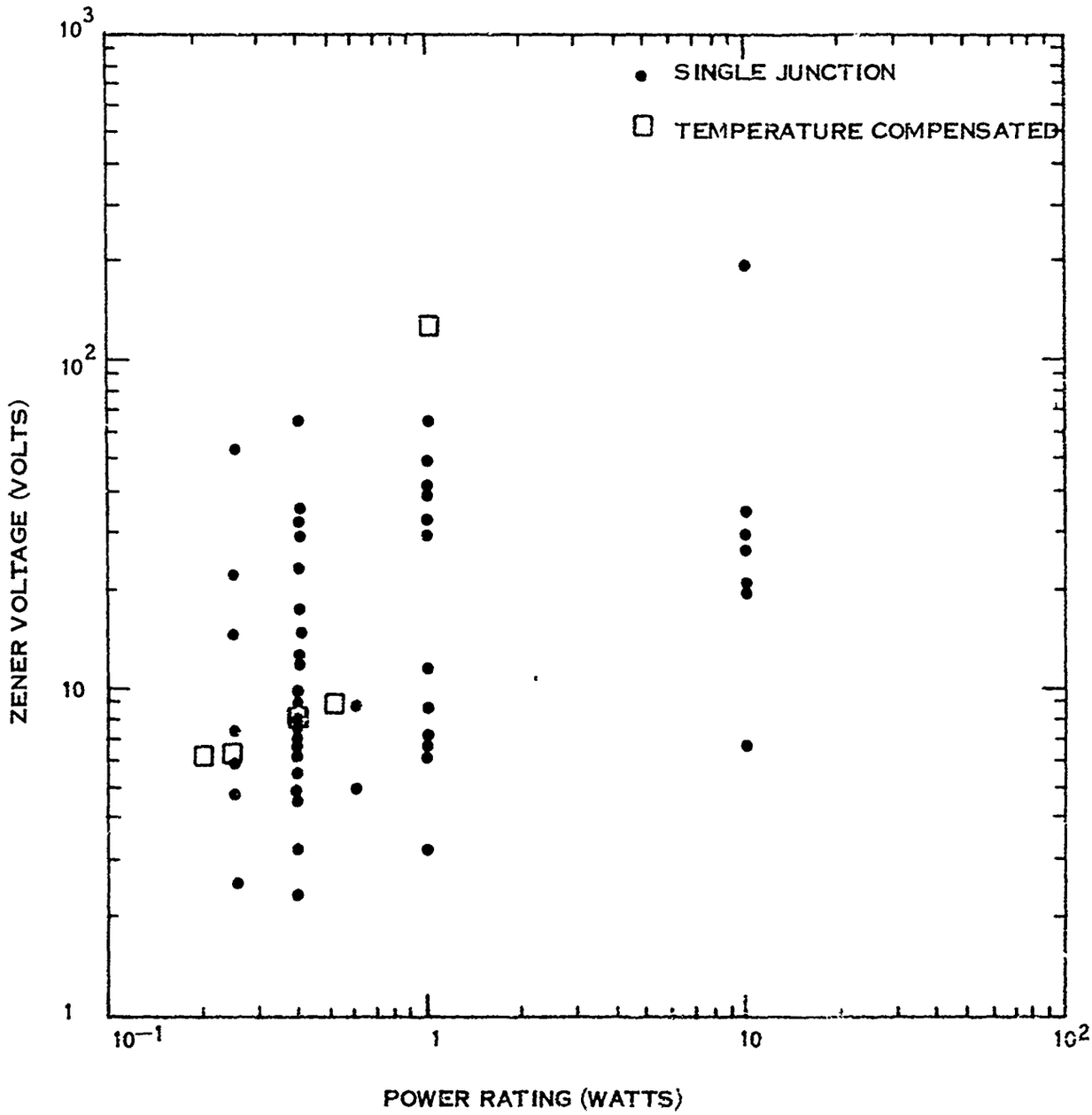

Figure 2. Range of Zener Voltage & Power Ratings for Diodes in the Present Data Base Functionally Classified as Zener Diodes.

Table 2. Device Ratings and Construction Types for Diodes Functionally Classified as Rectifiers, Diodes and Switches

F#	SOURCE	FUNCTION	TYPE	MFG	PIV	IØ	CONST
65	HDL	RECTIFIER	1N1202A	BEN	200	12.00	MESA
28	HDL	RECTIFIER	1N1095	GESY	500	.75	ALLØY
61	HDL	RECTIFIER	1N1200G	GESY	100	12.00	MESA
63	HDL	RECTIFIER	1N1202	GESY	200	12.00	MESA
2	HDL	RECTIFIER	1N250A	GESY	200	37.00	MESA
3	HDL	RECTIFIER	1N253	GESY	95	1.00	MESA
9	HDL	RECTIFIER	1N536	GESY	50	.75	ALLØY
10	HDL	RECTIFIER	1N537	GESY	100	.75	ALLØY
11	HDL	RECTIFIER	1N540	GESY	400	.75	ALLØY
55	HDL	RECTIFIER	983B6152	GESY	---	---	MLTSUB
12	HDL	RECTIFIER	1N645	GIC	225	.15	MESA
13	HDL	RECTIFIER	1N647	GIC	400	.15	MESA
14	HDL	RECTIFIER	1N649	GIC	600	.15	MESA
62	HDL	RECTIFIER	1N1200M	MØTA	100	12.00	MESA
64	HDL	RECTIFIER	1N1202M	MØTA	200	12.00	MESA
67	HDL	RECTIFIER	1N4003M	MØTA	240	1.00	MESA
69	HDL	RECTIFIER	1N4005	MØTA	720	1.00	MESA
58	HDL	RECTIFIER	1N645	TII	275	.40	MESA
30	HDL	RECTIFIER	1N1585	TEC	400	3.00	MESA
4	HDL	RECTIFIER	1N338	TEC	100	1.00	MESA
68	HDL	RECTIFIER	1N4003T	TRW	240	1.00	---
29	HDL	RECTIFIER	1N1342A	WESY	100	6.00	PLANAR
35	HDL	RECTIFIER	1N4816	WESY	50	1.50	PLANAR
36	HDL	RECTIFIER	1N4820	WESY	400	1.50	PLANAR
47	HDL	RECTIFIER	W6807WS	WESY	---	---	PLANAR
48	HDL	RECTIFIER	W6807ZU	WESY	---	---	PLANAR
56	HDL	RECTIFIER	MIS17007	GIC	---	---	---
117	AFWL	RECTIFIER	1N3189	GESY	200	1.00	MESA
73	AFWL	RECTIFIER	1N538B	GIC	200	.75	DIFF
124	AFWL	RECTIFIER	1N4385J	ITT	600	1.00	---
74	AFWL	RECTIFIER	1N645	ITT	225	.40	DIFF
121	AFWL	RECTIFIER	1N4006	MØTA	800	1.00	---
93	AFWL	RECTIFIER	1N1124A	SYN	250	16.00	ALLØY
96	AFWL	RECTIFIER	1N1206	SYN	600	22.00	ALLØY
98	AFWL	RECTIFIER	1N1615	SYN	400	16.00	ALLØY
99	AFWL	RECTIFIER	1N2158	SYN	400	37.00	ALLØY
94	AFWL	RECTIFIER	IN1126A	SYN	500	16.00	ALLØY
95	AFWL	RECTIFIER	1N1202A	---	200	12.00	DIFF
97	AFWL	RECTIFIER	1N1614	---	200	16.00	---
132	AFWL	RECTIFIER	1N3191	---	600	1.00	---
75	AFWL	RECTIFIER	1N645	---	225	.40	DIFF
149	GE	RECTIFIER	UR225	UNI	250	2.00	MESA

Table 2. Continued

F#	SOURCE	FUNCTION	TYPE	MFG	PIV	IO	CONST
7	HDL	DIODE	1N459A	CRL	200	.20	MESA
8	HDL	DIODE	1N482A	SYL	40	.20	ALLOY
6	HDL	DIODE	1N459	TEC	200	.04	PLANAR
37	HDL	DIODE	DHD936	GESY	---	.20	PLANAR
54	HDL	DIODE	998A562-6/2	GESY	---	6.00	MESA
70	AFWL	DIODE	1N483B	---	80	.20	MESA
71	AFWL	DIODE	1N486	---	225	.10	DIFF
59	HDL	SWITCH	1N914	TII	75	.08	MESA
131	AFWL	SWITCH	1N914	---	75	.08	---
122	AFWL	SWITCH	1N4148	FSC	75	.20	PLANAR
115	AFWL	SWITCH	1N3064	---	50	.08	PLANAR
118	AFWL	SWITCH	1N3600	---	50	.20	PLANAR
133	AFWL	SWITCH	1N4610	---	50	.20	PLANAR
144	GE	SWITCH	1N914J	CDC	75	.08	ALLOY
146	GE	SWITCH	1N914JT	CDC	75	.08	ALLOY
141	GE	SWITCH	1N914	CDC	75	.08	PLANAR
143	GE	SWITCH	1N914J	FSC	75	.08	PLANAR
145	GE	SWITCH	1N914JT	TII	75	.08	MESA
142	GE	SWITCH	1N914	GESY	75	.15	PLANAR
147	GE	SWITCH	FD700	FSC	20	.05	PLANAR
148	GE	SWITCH	HPA1001	HPA	30	.10	PLANAR
150	GE	SWITCH	1N4148	GESY	75	.15	PLANAR

Table 3. Device Ratings and Construction Types for Diodes Functionally Classified as Zener Diodes

F#	SOURCE	FUNCTION	TYPE	MFG	VZ	PWR	CONST
26	HDL	ZENER	1N967B	CDC	18.0	.40	---
31	HDL	ZENER	1N1770A	CRL	9.1	1.00	MESA
17	HDL	ZENER	1N711A	CRL	7.5	.25	MESA
34	HDL	ZENER	1N3016B	DIC	6.8	1.00	PLANAR
27	HDL	ZENER	1N981B	DIC	68.0	.40	PLANAR
32	HDL	ZENER	1N1783	HOFF	33.0	1.00	---
60	HDL	ZENER	1N965B	MOTA	15.0	.40	PLANAR
52	HDL	ZENER	R0510746	MOTA	11.0	---	---
18	HDL	ZENER	1N751A	TII	5.1	.40	PLANAR
19	HDL	ZENER	1N752A	TII	5.6	.40	PLANAR
20	HDL	ZENER	1N753A	TII	6.2	.40	PLANAR
40	HDL	ZENER	MC357	TII	120.0	---	---
15	HDL	ZENER	1N702A	TEC	2.6	.25	ALLOY
16	HDL	ZENER	1N705A	TEC	4.9	.25	ALLOY
21	HDL	ZENER	1N763	TEC	7.0	.40	MESA
53	HDL	ZENER	9838649	TEC	33.0	---	---
50	HDL	ZENER	MIS17149	TEC	170.0	---	PLANAR
43	HDL	ZENER	SV138	TEC	15.0	.25	MESA
44	HDL	ZENER	SV589	TEC	22.8	.25	MESA
46	HDL	ZENER	SV9847	TEC	7.0	.40	MESA
41	HDL	ZENER	PS10245	TRW	14.5	---	---
49	HDL	ZENER	MIS17027	TRW	6.5	---	---
100	AFWL	ZENER	1N2970B	CRL	6.8	10.00	MESA
101	AFWL	ZENER	1N2984B	CRL	20.0	10.00	MESA
102	AFWL	ZENER	1N2985B	CRL	22.0	10.00	MESA
104	AFWL	ZENER	1N2988B	CRL	27.0	10.00	MESA
105	AFWL	ZENER	1N2989B	CRL	30.0	10.00	MESA
106	AFWL	ZENER	1N2991B	CRL	36.0	10.00	MESA
107	AFWL	ZENER	1N3015B	CRL	200.0	10.00	MESA
108	AFWL	ZENER	1N3017B	CRL	7.5	1.00	MESA
109	AFWL	ZENER	1N3019	CRL	9.1	1.00	MESA
112	AFWL	ZENER	1N3035B	CRL	43.0	1.00	MESA
113	AFWL	ZENER	1N3037B	CRL	51.0	1.00	MESA
114	AFWL	ZENER	1N3040B	CRL	68.0	1.00	MESA
128	AFWL	ZENER	LNA351	CODI	5.1	.60	ALLOY
129	AFWL	ZENER	LNA391	CODI	9.1	.60	ALLOY
110	AFWL	ZENER	1N3022B	DIC	12.0	1.00	D-A
119	AFWL	ZENER	1N3821A	DIC	3.3	1.00	ALLOY
120	AFWL	ZENER	1N3828A	DIC	6.2	1.00	ALLOY
86	AFWL	ZENER	1N963B	DIC	12.0	.40	PLANAR
88	AFWL	ZENER	1N965B	DIC	15.0	.40	PLANAR
89	AFWL	ZENER	1N970B	DIC	24.0	.40	PLANAR
90	AFWL	ZENER	1N972B	DIC	30.0	.40	PLANAR

Table 3. Continued

F#	SOURCE	FUNCTION	TYPE	MFG	VZ	PWR	CONST
87	AFWL	ZENER	1N964B	FSC	13.0	.40	PLANAR
125	AFWL	ZENER	1N5556	GSI	40.3	1.00	---
111	AFWL	ZENER	1N3031B	HOFF	30.0	1.00	---
91	AFWL	ZENER	1N973B	HOFF	33.0	.40	ALLOY
92	AFWL	ZENER	1N974B	HOFF	36.0	.40	DIFF
103	AFWL	ZENER	1N2985RB	MOTA	22.0	10.00	PLANAR
76	AFWL	ZENER	1N746A	NPC	3.3	.40	PLANAR
80	AFWL	ZENER	1N754A	NPC	6.8	.40	PLANAR
123	AFWL	ZENER	1N4370	TEC	2.4	.40	---
78	AFWL	ZENER	1N752A	TEC	5.6	.40	ALLOY
79	AFWL	ZENER	1N753A	TEC	6.2	.40	ALLOY
81	AFWL	ZENER	1N755A	TEC	7.5	.40	ALLOY
83	AFWL	ZENER	1N757A	TEC	9.1	.40	ALLOY
84	AFWL	ZENER	1N758A	TEC	10.0	.40	ALLOY
82	AFWL	ZENER	1N756	TRW	8.2	.40	ALLOY
126	AFWL	ZENER	LVA51A	TRW	5.1	.40	ALLOY
127	AFWL	ZENER	LVA91A	TRW	9.1	.40	ALLOY
130	AFWL	ZENER	1N4127	---	56.0	.25	---
77	AFWL	ZENER	1N750A	---	4.7	.40	---

Table 4. Device Ratings and Construction Types for Diodes Functionally Classified as Temperature Compensated Zener Diodes, Stabistors, Tunnel Diodes and Point Contact Diodes

F#	SØURCE	FUNCTIØN	TYPE	MFG	VZ	PWR	CØNST
5	HDL	TC ZENER	1N429	IRC	6.2	.20	A+1D
23	HDL	TC ZENER	1N823	TEC	6.2	.25	MESA
25	HDL	TC ZENER	1N939A	DIC	9.0	.50	D+2D
38	HDL	TC ZENER	1N429	DIC	6.2	.20	---
42	HDL	TC ZENER	S1655	SCE	140.0	---	---
57	HDL	TC ZENER	1N429	HØFF	6.2	.20	---
66	HDL	TC ZENER	1N3047B	IRC	130.0	1.00	---
116	AFWL	TC ZENER	1N3157	DIC	8.4	.40	DIFF
85	AFWL	TC ZENER	1N821	TEC	6.2	.25	ALLØY

F#	SØURCE	FUNCTIØN	TYPE	MFG	PIV	IØ	CØNST
39	HDL	STABISTER	G129	TII	10	1.5	PLANAR
45	HDL	STABISTER	SV3145	DELTA	3	0.4	---
33	AFWL	TUNNEL	1N2929A	HØFF	---	---	--
1	GE	PT CØNT	1N82A	SYL	---	---	---

ing the correlation of the actual data points to the predicted values for each diode model developed. The range of device variables and prediction error associated with each analysis are identified on each graph. The graphs are the analytical results and associated data plots of multiple regression analyses performed on the General Electric Mark III computer system. The format for the data points shown in the graphs is as follows:

(a) the symbol "*" corresponds to 1 data point;
(b) the numbers "2" through "9" correspond to 2 through 9 data points, respectively;
(c) the number "0" corresponds to 10 data points;
(d) the letters "A" through "Z" correspond to 11 through 36 data points, respectively;
(e) the symbol "$" corresponds to greater than 36 data points.

A glossary of symbols used in the various model presentations is shown in Table 5.

The data analyses revealed that the rectifier, diode and switch functional classifications were essentially similar in their correlation to specific device parameters and are considered below in terms of one functional classification. Non-temperature compensated zener diodes form the other functional classification considered. Damage modeling was not performed for temperature compensated zener diodes, stabistors, point contact and tunnel diodes. The amount of pulse test data and device rating variations in the present data base was not considered to be sufficient to yield statistically significant results.

The damage models for each diode functional classification are presented for both the conditions when all construction types are taken together as well as for each individual construction type when sufficient data exists to warrant such an analysis. The first condition shows the prediction accuracy that can be achieved when construction information is unavailable or difficult to obtain. The latter condition shows the prediction accuracy obtainable when such information is available. In all cases, the results for the surge impedance and failure level models for both the forward and reverse polarities are preceded by a discussion of the results obtained with the General Electric 1N4148 diode. This device was tested on a prior U.S. Army, Harry Diamond Laboratory Contract.[1] This device, which is shown in detail in Figure 3, was obtained from the General Electric Company, Semiconductor Products Department under closely controlled diffusion profiles. The pulse testing on the device was well defined and carefully instrumented to eliminate the inductive response of

---

1 Tasca, D. M., Peden, J. C. and Andrews, J. L., "Theoretical & Experimental Studies of Semiconductor Device Degradation Due to High Power Electrical Transients", Final Technical Report, Contract DAAG 39-72-C-0066, U.S. Army, HDL, General Electric Company, Space Division, Document #73SD3289, December 1973.

Table 5. Glossary of Symbols Used in the Diode Pulse Damage Model Development

I_o	MAXIMUM AVERAGE RECTIFIED CURRENT RATING (AMPERES) FOR RECTIFIERS, DIODES AND SWITCHES
I_{PF}	FORWARD POLARITY PULSE CURRENT (AMPERES)
I_{PR}	REVERSE POLARITY PULSE CURRENT (AMPERES)
P_R	POWER RATING FOR ZENER DIODES (WATTS)
t	PULSE WIDTH (MICROSECONDS)
V_{JF}	FORWARD POLARITY JUNCTION VOLTAGE (VOLTS)
V_{JR}	REVERSE POLARITY JUNCTION VOLTAGE (VOLTS) $V_{JR} = V_Z$
V_{PF}	DIODE FORWARD POLARITY PULSE VOLTAGE (VOLTS)
V_{PR}	DIODE REVERSE POLARITY PULSE VOLTAGE (VOLTS)
V_Z	LOW CURRENT LEVEL JUNCTION BREAKDOWN VOLTAGE VOLTS
Z_{DF}	FORWARD POLARITY TOTAL DEVICE IMPEDANCE (OHMS) $Z_{DF} = \frac{V_{PF}}{I_{PF}}$
Z_{DR}	REVERSE POLARITY TOTAL DEVICE IMPEDANCE (OHMS) $Z_{DR} = \frac{V_{PR}}{I_{PR}}$
Z_{SF}	FORWARD POLARITY SURGE IMPEDANCE (OHMS) $Z_{SF} = \frac{V_{PF}-V_{JF}}{I_{PF}} \sim \frac{V_{PF}}{I_{PF}}$
Z_{SR}	REVERSE POLARITY SURGE IMPEDANCE (OHMS) $Z_{SR} = \frac{V_{PR}- V_Z}{I_{PR}}$

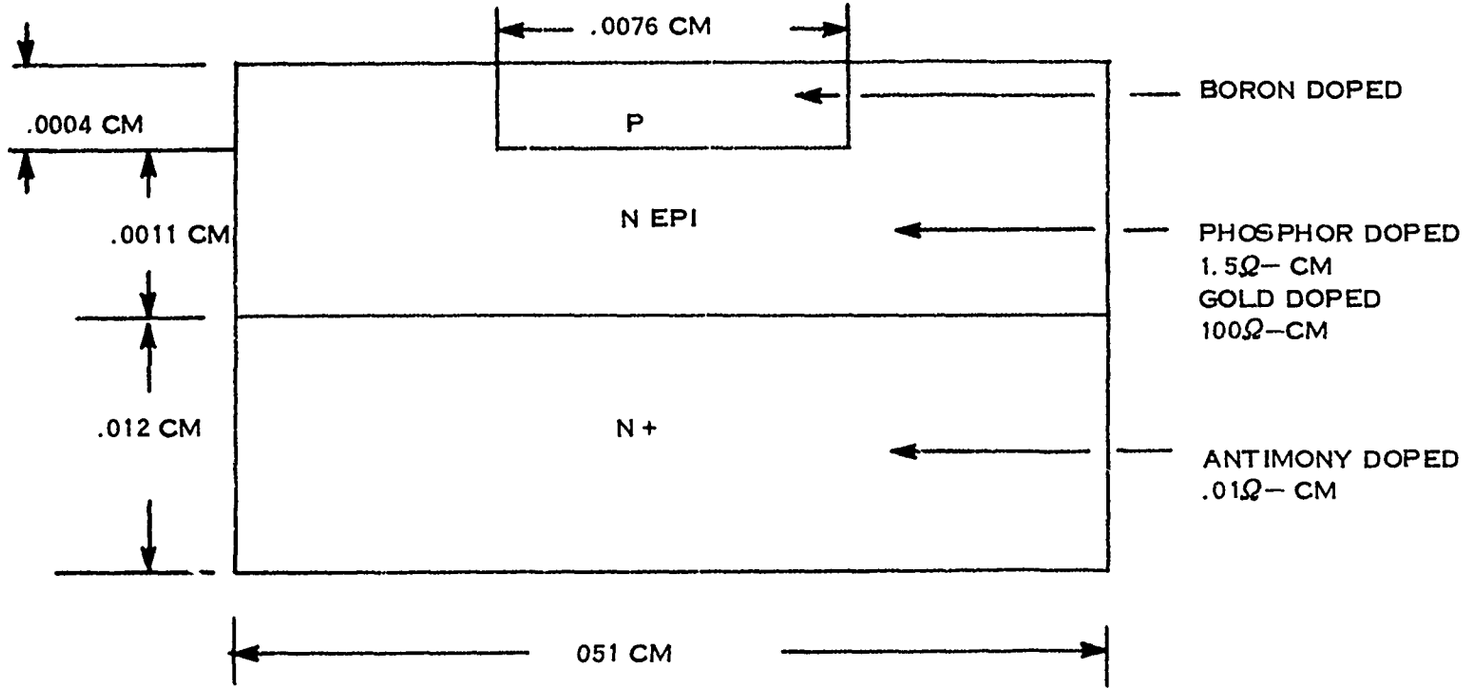

Figure 3. Construction & Diffusion Details of the General Electric 1N4148 Diode.

device leads and instrumentation noise. Furthermore, the increments in pulse stress level were controlled to eliminate large separations in the "no-fail" and "fail" levels applied to the device. As such, the data base for this device, which is given in File # 150, is considered to represent an excellent example of thermal damage mechanisms and responses in semiconductor diodes.

The pulse impedance models for the diodes were developed for both the total device impedance as well as for the diode surge impedance whereby the junction voltage is subtracted from the total device response. The failure levels are given in terms of the failure current rather than the failure power. The failure current representation was chosen for a number of reasons. First, the damage current representation provides a direct insight into the predominant damage model exhibited by a particular class of devices. Here, by examining the time dependence of the diode damage current, one can ascertain whether, for instance, bulk (I^2R) type heating or direct junction (VI) type heating is the prevalent failure mode. Furthermore, when diodes are pulsed at very high current levels, the device power one measures is a combination of junction and bulk power. As such, a total power representation of a device could lead to some erroneous conclusions if one attributes all the measured device power to directly producing device damage. A second reason for choosing the current representation is associated with the relative pulse impedance levels of the diodes and EMP disturbance source. When pulsed in the forward direction, the diodes exhibit a small impedance (generally less than 1 ohm) and when pulsed in the reverse direction, they exhibit a moderately small impedance (generally in the range of 1 to 100 ohms). In many cases, the EMP disturbance source would have a comparable or greater source impedance. As such, the EMP disturbance would approximate a constant current source, where the pulse current is primarily determined by the EMP source impedance. Hence, the current representation is a directly relatable quantity. Once the diode impedance is defined, it is a relatively simple task to determine the pulse current in the diode from a knowledge of the EMP source voltage and source impedance. Similarly, the damage power can be obtained, if so desired, from the device impedance and damage current.

2.1 Foward Polarity Models

The diode models developed for the forward polarity of junction current conduction are presented in this subsection. In general, the forward polarity represents a well-behaved junction condition in comparison to the reverse polarity condition. In performing forward polarity pulse testing on diodes, other than temperature compensated devices, the pulse response that one measures is generally that associated with the bulk semiconductor material in the diode rather than that of the junction. In fact, previous testing[1] has indicated that the failure mode is probably associated with bulk heating and

subsequent heat transfer to the junction, rather than due to direct junction heating.

2.1.1 Forward Polarity Surge Impedance

The forward polarity surge impedance, Z_{SF}, is defined by

$$Z_{SF} = \frac{V_{PF} - V_{JF}}{I_{PF}} \tag{1}$$

where

V_{PF} = Forward polarity pulse voltage
V_{JF} = Forward polarity junction voltage
I_{PF} = Forward polarity pulse current

In general, under forward polarity pulsing

$$V_{JF} << V_{PF} \tag{2}$$

and

$$Z_{SF} \sim \frac{V_{PF}}{I_{PF}} = Z_{DF} \tag{3}$$

where

Z_{DF} = Total device pulse impedance

If, for the moment, the increase in junction potential with current level increase is neglected, then one can consider the surge impedance to be associated with the bulk material (under high injection level conditions it is). Under low injection level conditions the surge impedance for a uniform cylindrical bulk piece of silicon can then be approximated as

$$Z_{SF} \sim \frac{\rho \ell}{A} \tag{4}$$

where

ρ = Resistivity of the bulk material
ℓ = Length of the bulk silicon
A = Cross sectional area of the uniform cylindrical bulk silicon

Similarly, if one considers the diode current to spread out from the junction through the bulk silicon in the form of a conic frustum from a diameter, d_1, to a diameter, d_2, then

$$Z_{SF} \sim \frac{4 \rho \ell}{\pi d_1 d_2} \tag{5}$$

In any event, this can be generalized to

$$Z_{SF} \sim K_1 \tag{6}$$

where

K_1 = Constant dependent on device doping and geometry

Under high injection level conditions one can anticipate significant conductivity modulation to occur. If the current path geometry through the device does not change significantly from that existing under low injection level conditions, then the effects on device surge impedance due to high injection level conductivity modulation are a function of current density and can be approximated to the first degree as

$$Z_{SF} \sim \frac{K_1}{1 + K_2 \left(\frac{I_{PF}}{A}\right)^N} \tag{7}$$

where

K_2 = constant

A = average cross sectional area for the current path

which can be generalized as

$$Z_{SF} \sim \frac{K_1}{1 + K_3 (I_{PF})^N} \tag{8}$$

under high injection levels, we would expect

$$K_3 (I_{PF})^N >> 1 \tag{9}$$

which yields

$$Z_{SF} \sim \frac{K}{(I_{PF})^N} \tag{10}$$

where

K = constant dependent on device construction

Hence, if one were to perform a pulse voltage-pulse current characterization for a particular device type, then the expected results would be of the form

$$V_{PF} = I_{PF} \quad Z_{SF} = K(I_{PF})^{1-N} \tag{11}$$

Figure 4 shows that such a relationship is indeed exhibited by the experimental data for the G.E. 1N4148 diode. Here, the 1N4148 diode exhibits a surge impedance which is of the form

$$Z_{SF} = \frac{3.4}{(I_{PF})^{0.31}} \tag{12}$$

where

Z_{SF} = Ohms
I_{PF} = Amperes

This relationship is exhibited over a wide range of pulse current to within 3 σ limits of $\pm$ a factor of 1.45.

Figure 5 shows a similar relationship which was developed for diodes functionally classified as "rectifiers, diodes, and switches" when one considers all construction types together. Here, the forward surge impedance was found to be related to the maximum average rectified current rating, I_O, of the diodes. It is interesting to note the similarity of exponents for the conductivity modulation between Figures 4 and 5. Almost all data points lie within $\pm$ a factor of 3.16. The statistical 3 σ limits are $\pm$ a factor of $\sqrt{6}$. Figures 6, 7 and 8 show the surge impedance results for rectifiers, diodes and switches of alloy, mesa and

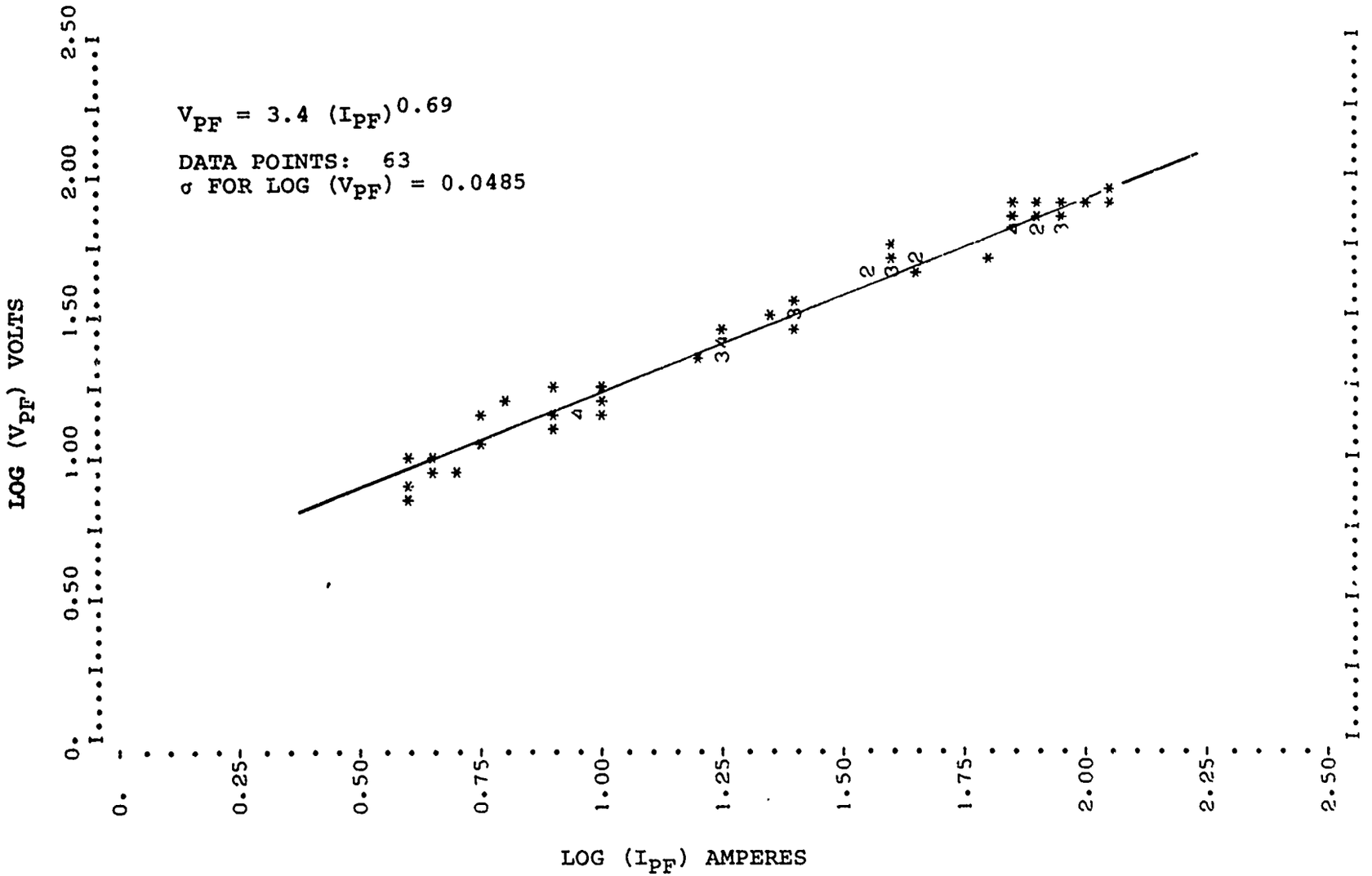

Figure 4. Forward Polarity, Pulse Voltage-Current Characteristics of the GE 1N4148 Diode Illustrating Conductivity Modulation at High Injection Levels.

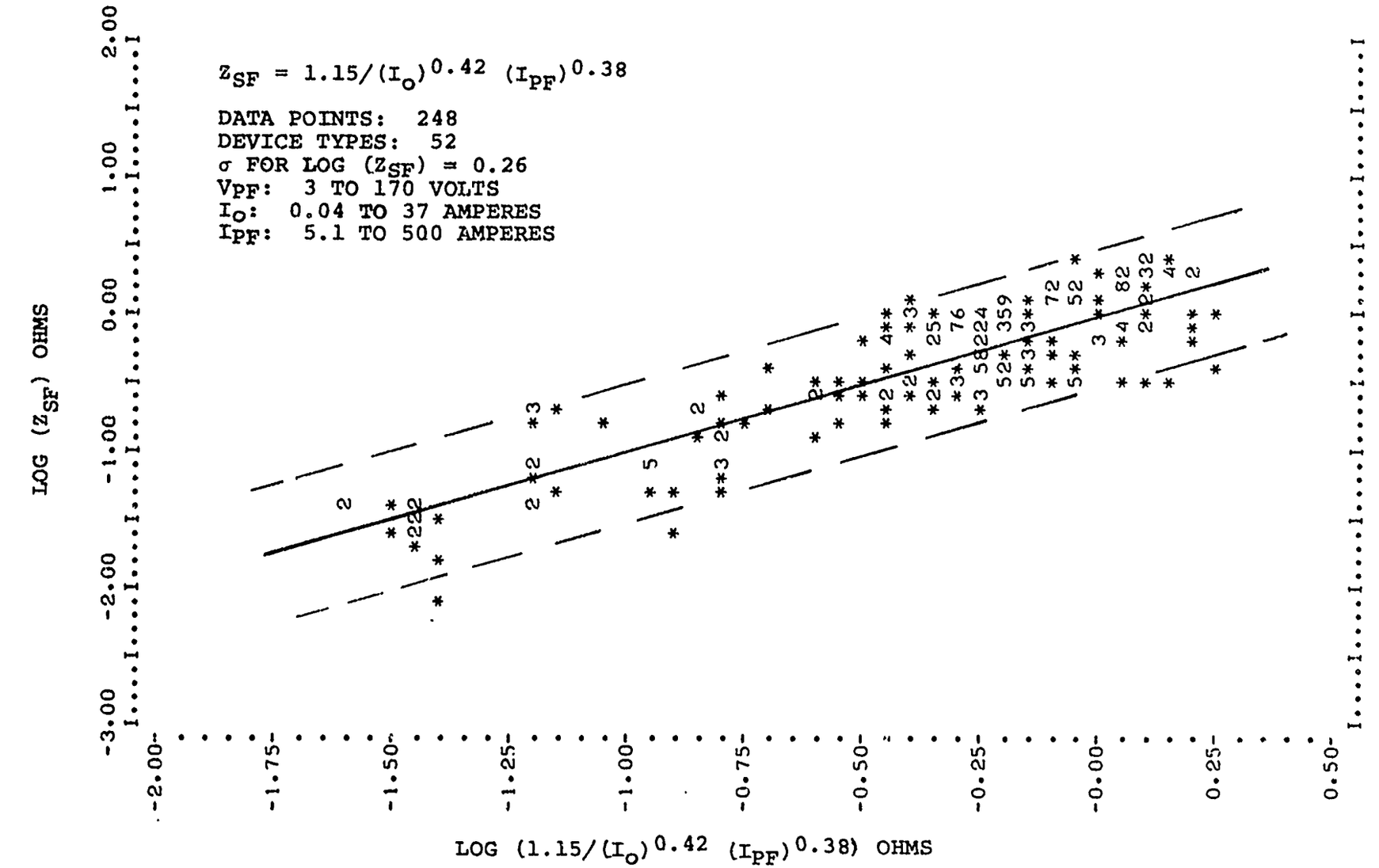

Figure 5. Forward Surge Impedance Characteristics for all Construction Type Diodes Functionally Classified as Rectifiers, Diodes and Switches.

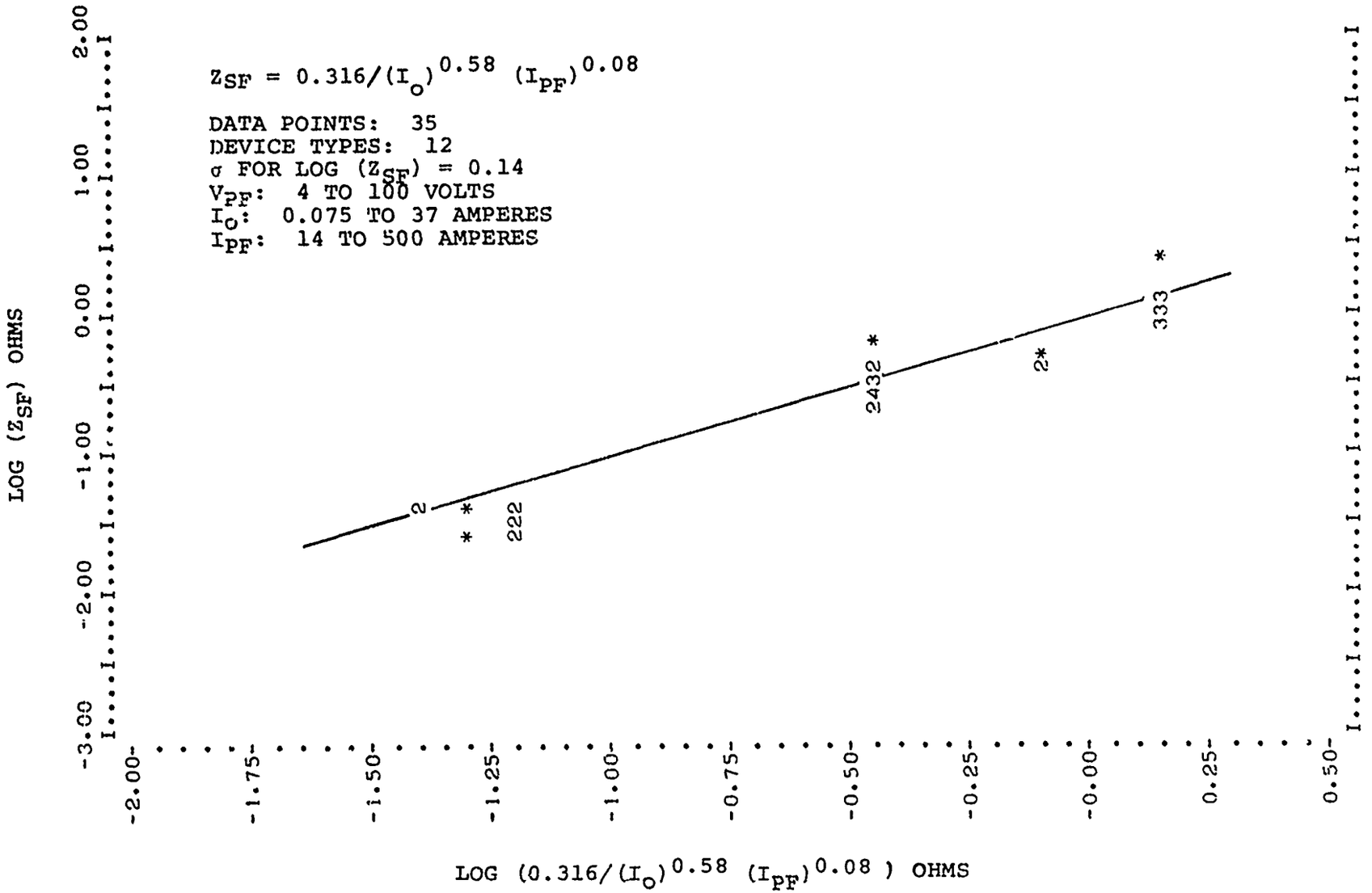

Figure 6. Forward Surge Impedance Characteristics of Alloy Diodes Functionally Classified as Rectifiers, Diodes & Switches.

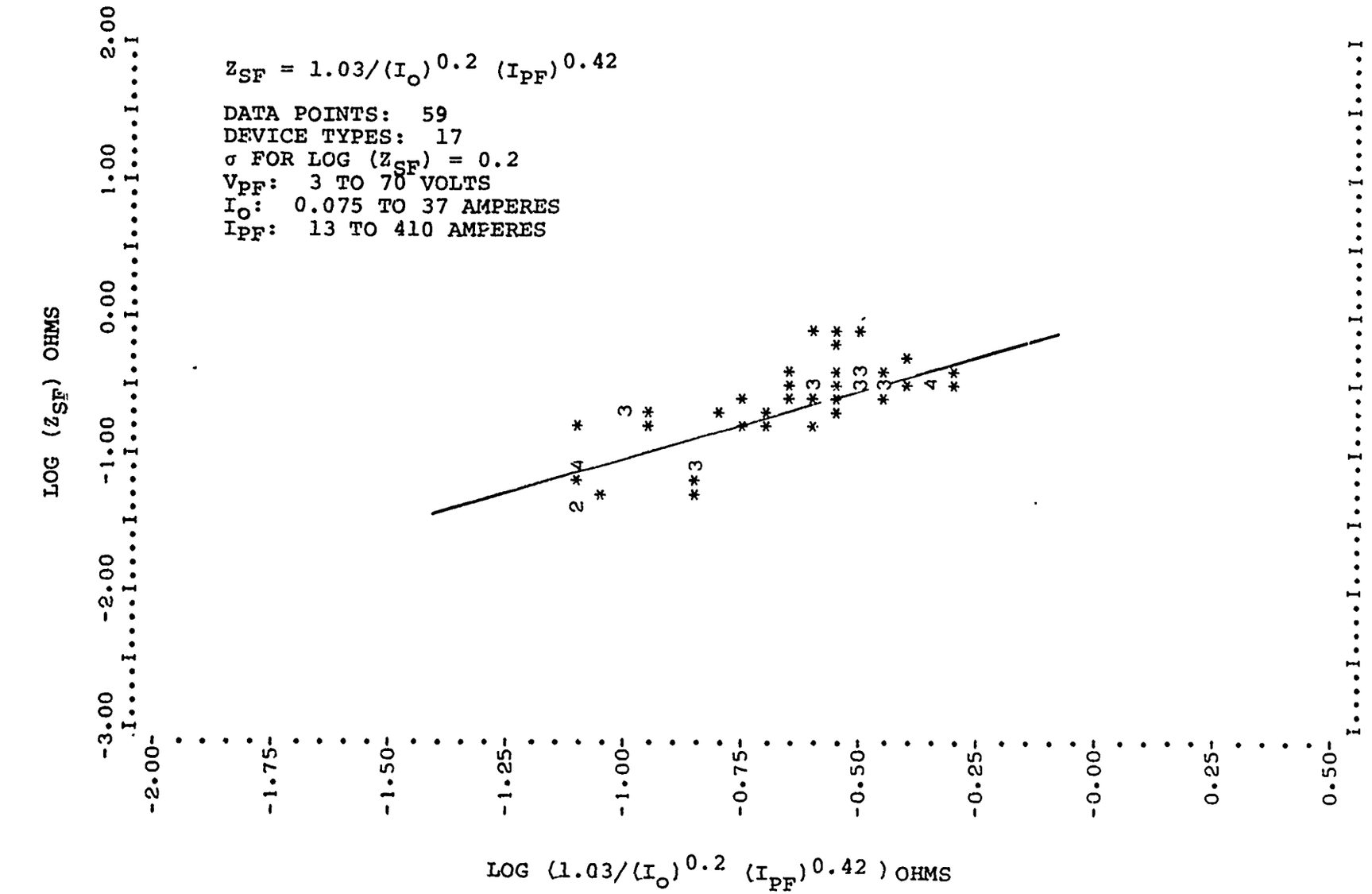

Figure 7. Forward Surge Impedance Characteristics of Mesa Diodes Functionally Classified as Rectifiers, Diodes & Switches.

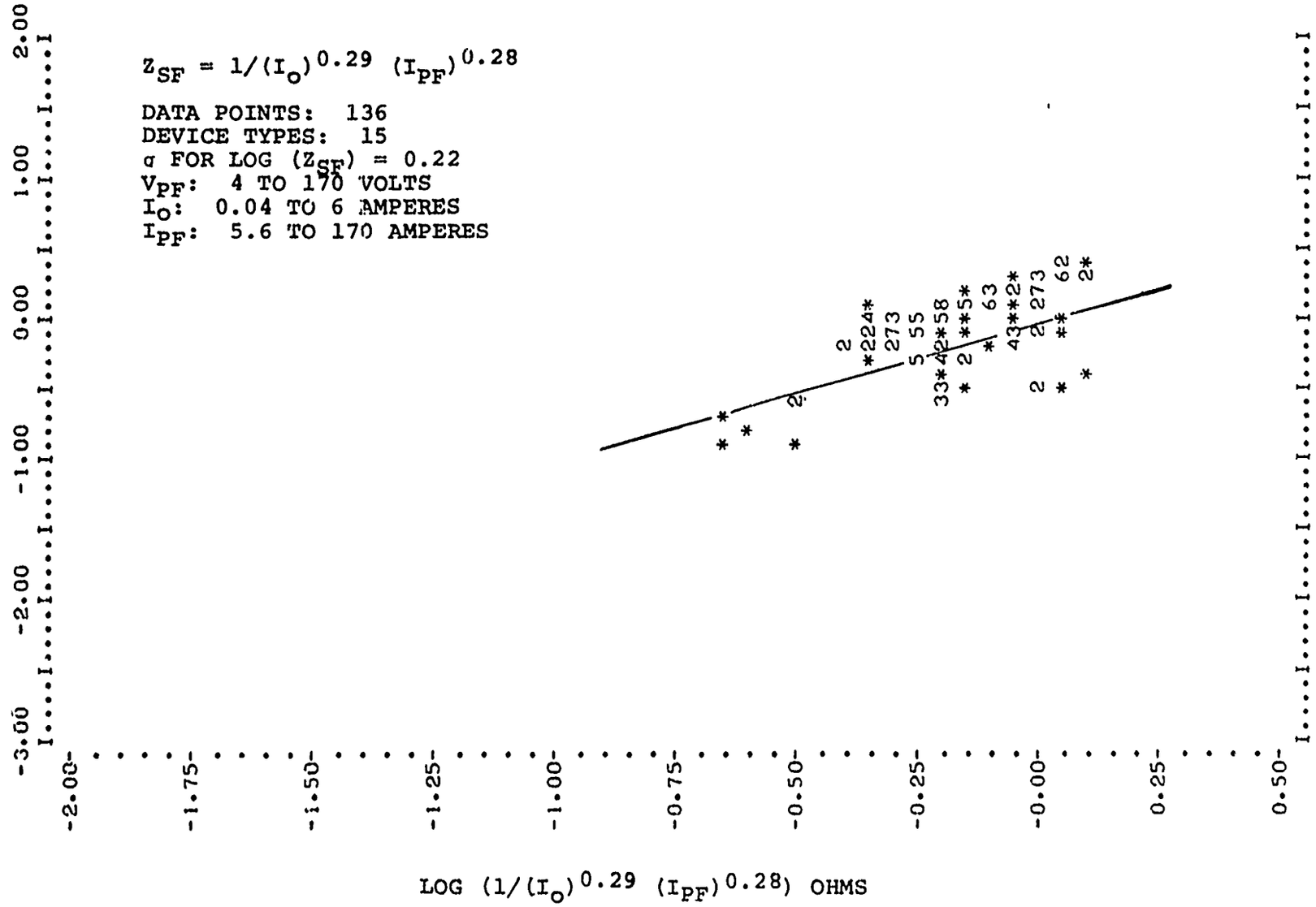

Figure 8. Forward Surge Impedance Characteristics of Planar Diodes Functionally Classified as Rectifiers, Diodes and Switches.

planar constructions, respectively. Note that the alloy devices do not exhibit a strong dependence on pulse current level as do the mesa and planar devices.

Figure 9 shows the correlation results developed for the forward surge impedance of diodes functionally classified as "Zener" diodes when one considers all construction types together. Here, the forward surge impedance was found to be related to both the Zener power rating, P_R, as well as the pulse current level, I_{PF}. The similarity between the conductivity modulation exponent in Figures 4 and 9 can again be seen. Almost all data points lie within $\pm$ a factor of 3.16. The statistical 3 σ limits are $\pm$ a factor of 5.4. The correlation results obtained for alloy, mesa and planar constructions are shown in Figures 10, 11 and 12. The low exponent of dependence on pulse current level exhibited by alloy devices can again be seen.

2.1.2 Forward Polarity Damage Current

Semiconductor devices which exhibit thermal damage mechanisms fail under pulse power stressing when the temperature of the junction reaches a certain critical value. If heat is produced at a constant rate per unit time (square wave power pulsing) per unit volume, then the time dependent temperature rise of any heat producing general volumetric geometry which is immersed in an infinite medium of the same material can be approximated as[2]

$$\Delta T = \frac{E}{\rho C v + \sqrt{\rho C k t}\, s + \frac{8}{3}\pi k t r} \qquad (13)$$

where

ΔT = Temperature rise above ambient

E = Energy dissipated in the volume

ρ = Material density

C = Material specific heat (temperature dependent)

k = Material thermal conductivity (temperature dependent)

v = Volume of the heat producing region

s = Total surface area of the heat producing region

---

[2] Tasca, D.M., "Pulse Power Failure Modes in Semiconductors", in IEEE Transactions on Nuclear Science, Volume NS-17, No. 6, pp. 364-372, December 1970.

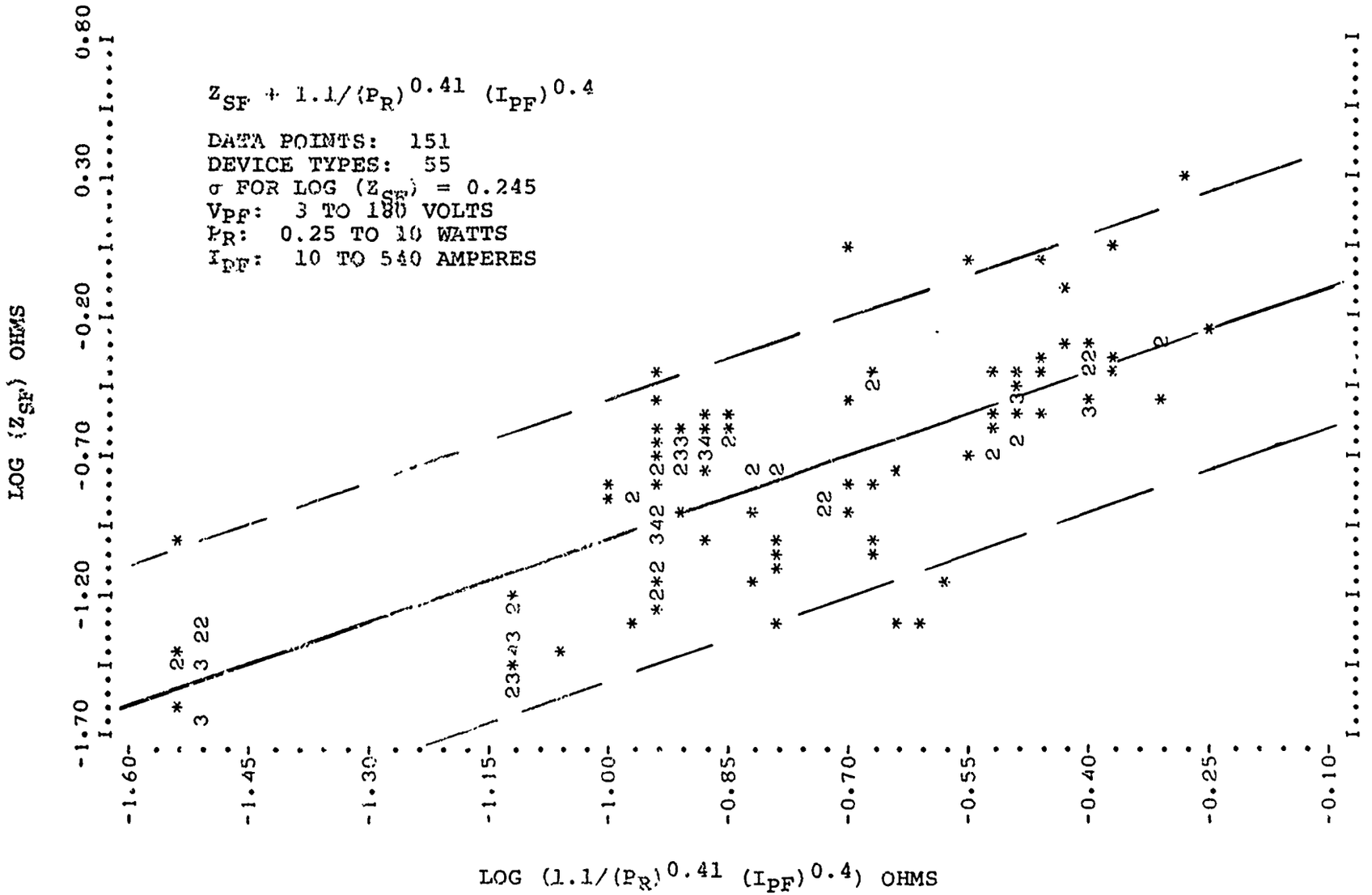

Figure 9. Forward Surge Impedance Characteristics for all Construction Type Diodes Functionally Classified as Zener Diodes.

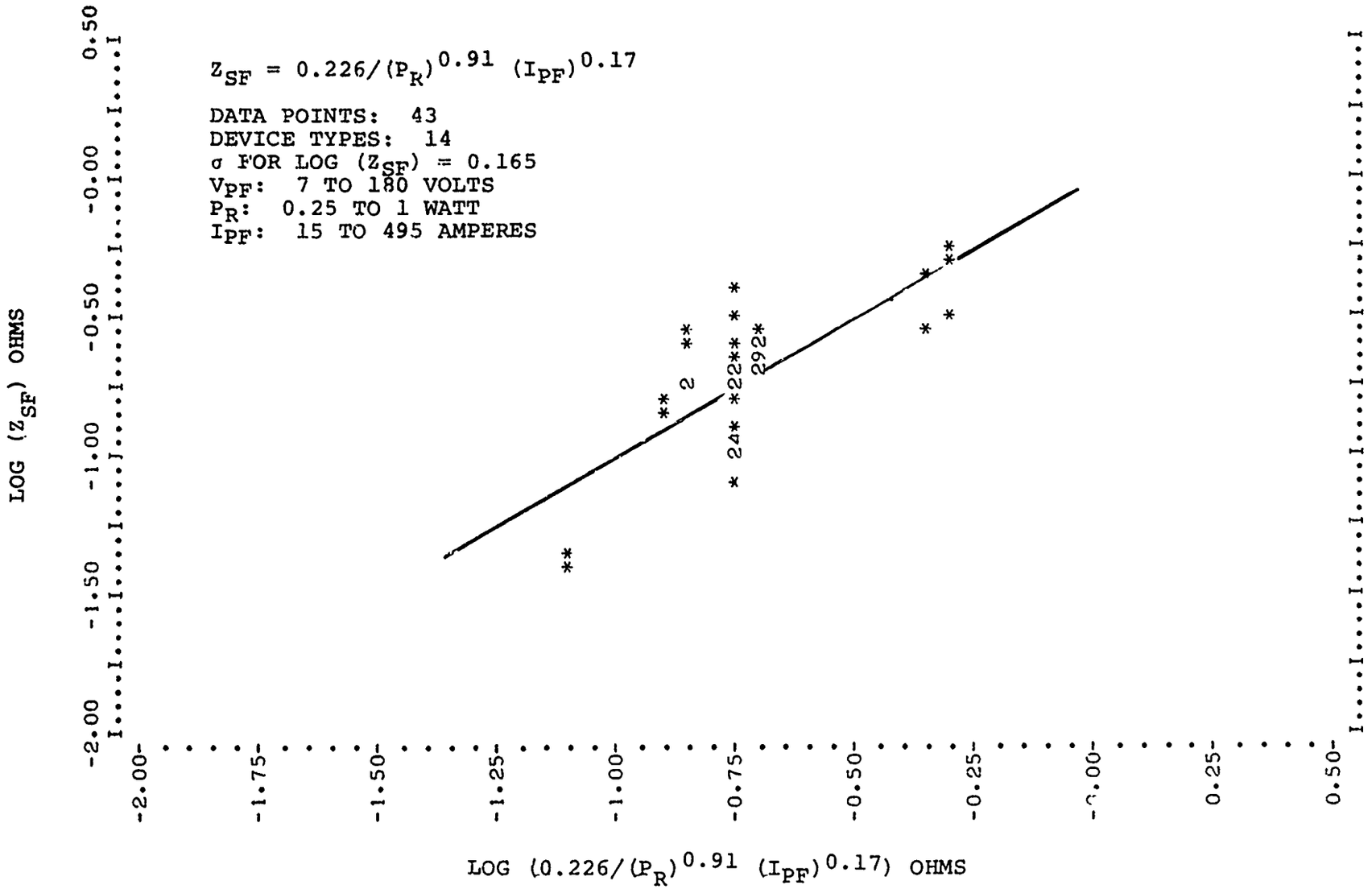

Figure 10. Forward Surge Impedance Characteristics of Alloy Diodes Functionally Classified as Zener Diodes.

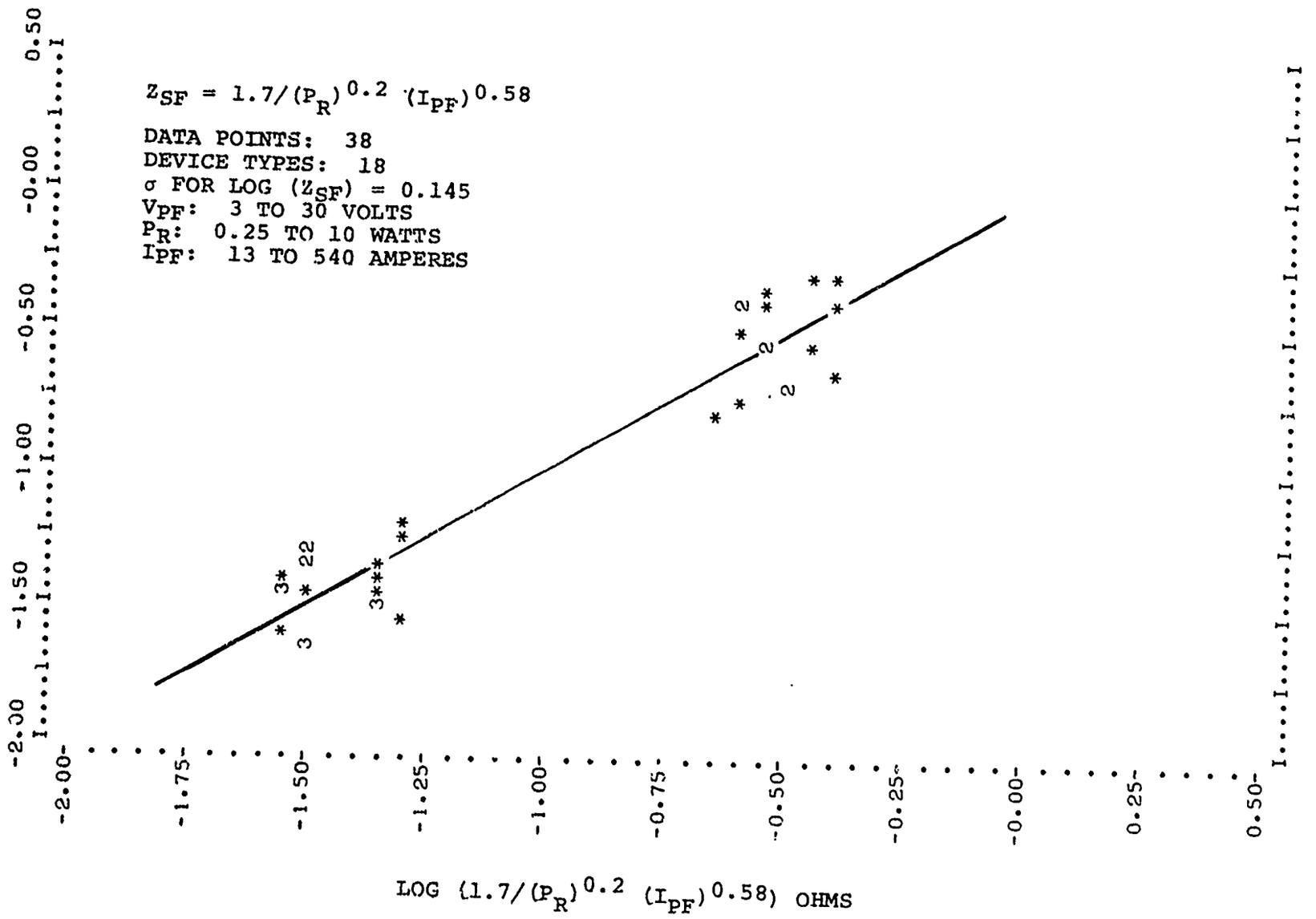

Figure 11. Forward Surge Impedance Characteristics of Mesa Diodes Functionally Classified as Zener Diodes.

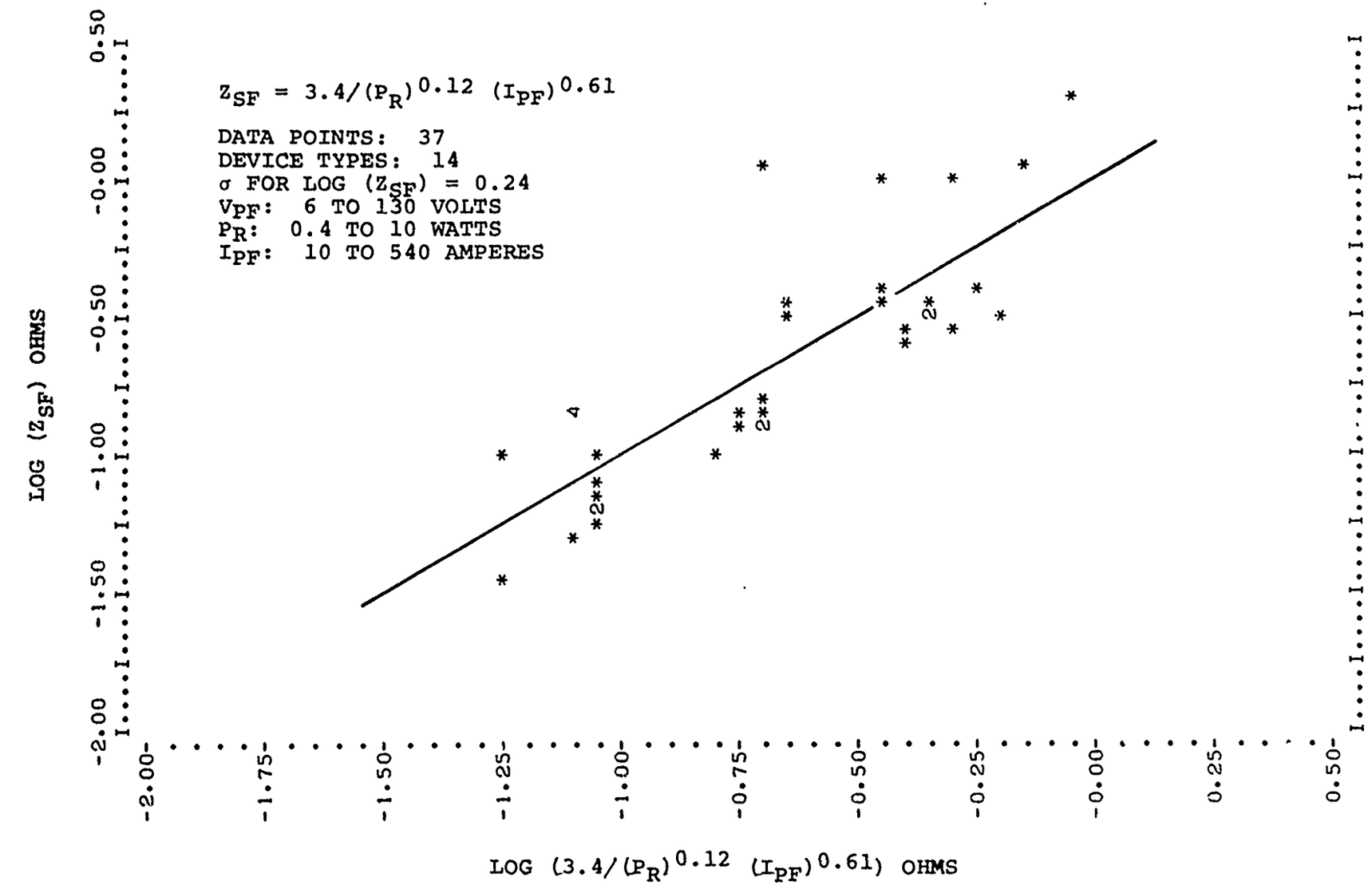

Figure 12. Forward Surge Impedance Characteristics of Planar Diodes Functionally Classified as Zener Diodes.

r = Average radius of the heat producing region

t = Time

The corresponding expression for non-square wave power pulsing conditions has been previously developed[1] and will not be repeated here. Due to the relatively short time duration of EMP type environments, the third term in (13) can generally be neglected. If the critical temperature rise for junction failure is defined as a value, T, then the required energy to produce device damage can be approximated from (13) as

$$E = (\rho Cv + \sqrt{\rho Ckt}\, s\ )\ T \tag{14}$$

As previously noted, the existing experimental data indicates that diode failure under forward polarity pulsing is due to bulk material heating and subsequent heat transfer to the junction. Since the junction surface is in intimate contact with the bulk surface, and if one neglects direct junction heating, then (14) can be considered to approximate the temperature conditions of the junction-bulk material interface. Here, the energy term relates to the energy dissipated in the bulk material, while the volume and surface area are those of the bulk region. Since the bulk material is a conductivity modulated resistance, the heat production in the bulk material is due to I^2R heating and (14) can be written as

$$E = (I_{PF})^2\ Rt = (\rho Cv + \sqrt{\rho Ckt}\, s)\ T \tag{15}$$

which can be generalized to

$$(I_{PF})^2\ R\ t = K_1 + K_2\sqrt{t} \tag{16}$$

From (10) the bulk resistance is of the form

$$R = Z_{SF} = \frac{K}{(I_{PF})^N} \tag{17}$$

Hence, (16) is of the form

$$\frac{(I_{PF})^2 \, K \, t}{(I_{PF})^N} = K_1 + K_2\sqrt{t} \tag{18}$$

which can be further generalized to

$$(I_{PF})^2 = K_1 \, (I_{PF})^N \left(\frac{1}{t} + \frac{K_2}{\sqrt{t}}\right) \tag{19}$$

Recalling the expression given in (12) for surge impedance, the corresponding expression for the GE 1N4148 diode would be

$$(I_{PF})^2 \text{ for GE 1N4148} = K_1 \, (I_{PF})^{0.31} \left(\frac{1}{t} + \frac{K_2}{\sqrt{t}}\right) \tag{20}$$

Figure 13 shows that such a relationship is indeed exhibited by the GE 1N4141 diode. Furthermore, this relationship is exhibited over a wide range of pulse width (0.01 to 300 microseconds) and pulse current (3.9 to 180 amperes) to within 3 σ limits of $\pm$ a factor of 1.47. The break point between adiabatic and heat diffusion is about 28 nanoseconds, which indicates a relatively large surface area to volume region in the bulk material.

It should be noted that when diodes (other than temperature compensated Zener diodes) are pulsed in the forward direction, they do not generally exhibit a distinct failure point as does reverse polarity pulsing, where second breakdown is exhibited. Hence, when analyzing forward polarity pulse data, one is forced to examine the highest "no-fail" pulse stress level and the lowest "fail" stress level and conclude that the actual failure level lies somewhere in between. The corresponding uncertainty is associated with the relative spread between "no-fail" and "fail" levels. As such, one should endeavor to minimize the spread between these two levels and, if possible, limit the data to be analyzed to only those devices which have sets of "no-fail" - "fail" data pairs. The experimental data shown in Figure 13 has been restricted to such data pair sets. Furthermore, the allowable data spread here, and in subsequent analyses, has been restricted to those pairs which are separated by no more than a factor of three between "no fail" and "fail" levels within each respective data pair. In actuality, the data points shown in Figure 13 are

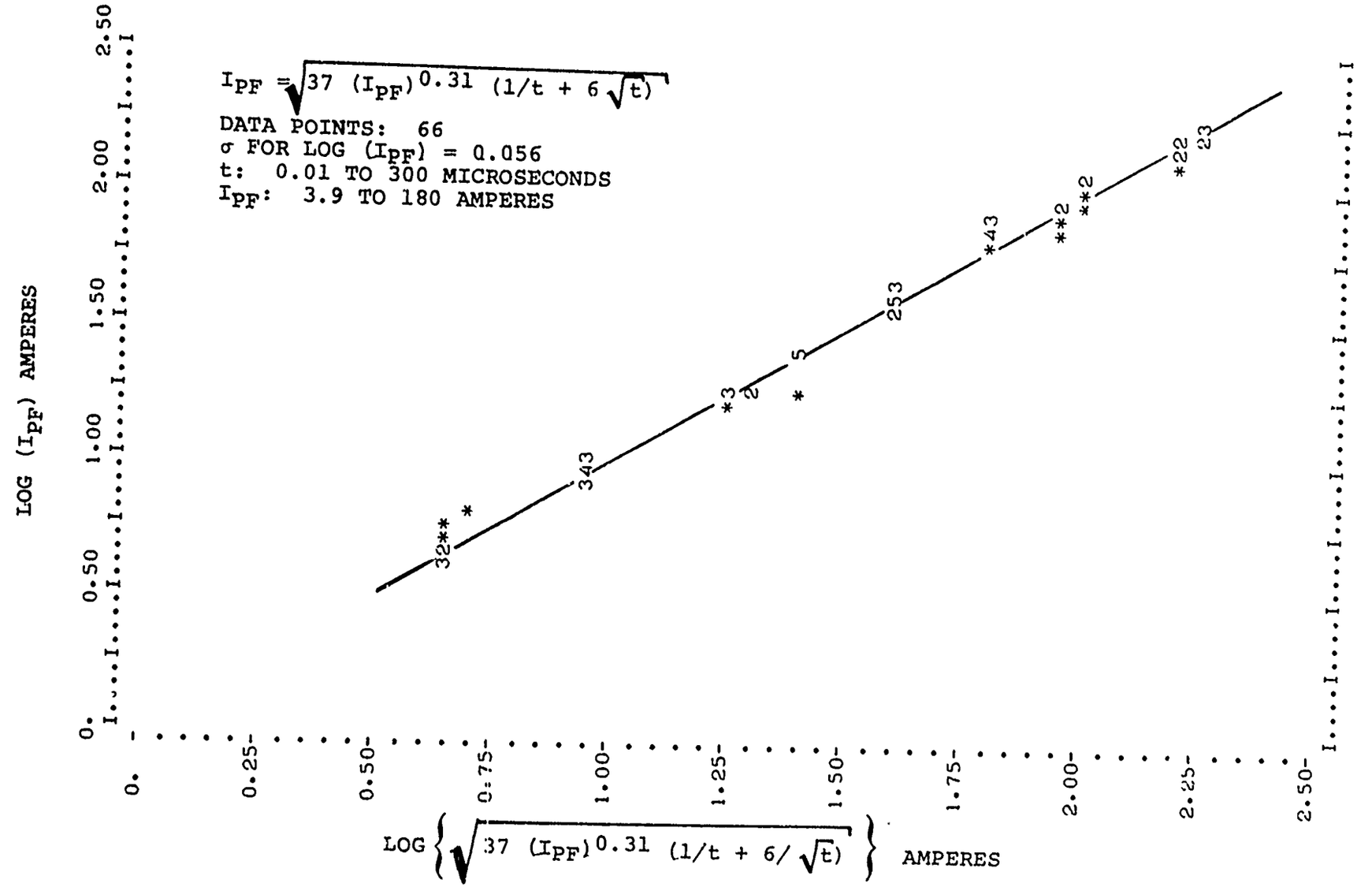

Figure 13. Forward Polarity, Pulse Damage Current Characteristics of the GE 1N4148 Diode Illustrating Bulk I^2R Heating and Conductivity Modulation Effects (Paired No-Fail and Fail Data Point Within a Factor of Three).

all within less than a factor of two spread as a result of the close experimental controls exercised during the pulse testing of this particular diode type. One final note is that the units of time are in microseconds for the data shown here and in all subsequent data graphs which contain a time dependent term.

A relationship similar to (20) was developed for diodes functionally classified as "rectifiers, diodes and switches". Here, the analysis showed that the break point between adiabatic and heat diffusion conditions was less than 10 nanoseconds. Due to the overall sparsity of data in this region, it was felt that the general two termed time expression in (19) could not be accurately evaluated. As such, the regression analysis was restricted to a general single time term for more accuracy. As partial compensation, the conductivity modulated surge impedance was not restricted to a predefined form (such as that developed in Figures 5, 6, 7 and 8) but was also represented by a general expression. Hence, the regression analysis took the form

$$I_{PF} = \frac{K}{(t)^m} \tag{21}$$

where

K = Constant dependent on device parameters

Figure 14 shows the damage model developed from (21) for rectifiers, diodes and switches of all construction types. Here, the damage current was found to be dependent on the maximum average rectified current, I_O. Almost all data point lie within $\pm$ a factor of 3.16 with statistical 3 σ limits of $\pm$ a factor of $\overline{4}.5$. It is interesting to note that by approximating (19) by the single term $\sqrt{t}$ expression, yields

$$(I_{PF})^2 \sim \frac{K_1 (I_{PF})^N}{\sqrt{t}} \tag{22}$$

Recalling that the exponent, N, as defined in Figure 5 is 0.38 yields

$$(I_{PF})^{1.62} \sim \frac{K_1}{\sqrt{t}} \tag{23}$$

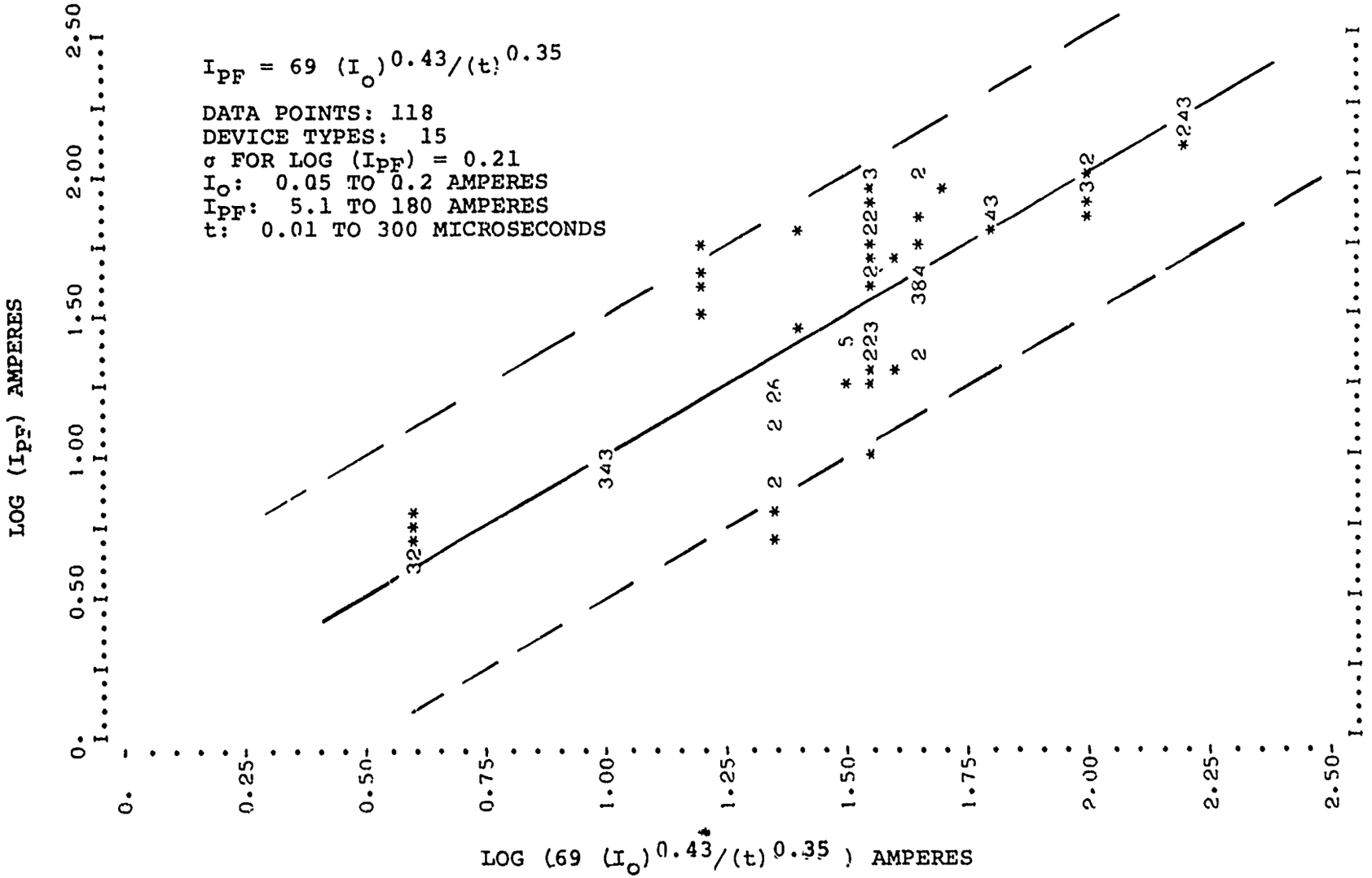

Figure 14. Forward Pulse Damage Current Characteristics for all Construction Type Diodes Functionally Classified as Rectifiers, Diodes and Switches(Paired No Fail and Fail Data Points Within a Factor of Three).

or

$$I_{PF} \sim \frac{K_2}{(t)^{0.308}} \tag{24}$$

Note the close agreement between the time exponents in (24) and Figure 14. Figures 15 and 16 show the comparison of the regression line developed in Figure 14 with all the "fail" data and "no fail" data in the present data base.

Similar relationships for the forward polarity damage current of individual construction types was not performed due to the small amount of data available on an individual construction type level.

A similar situation was encountered when attempting to model the forward damage current of Zener diodes. This was further compounded by the fact that the data base for all construction types consisted of only 25 pairs of "no-fail"-"fail" data, 20 of which were for a 1 microsecond pulse width and a 0.4 watt power rating. In an attempt to define at least a preliminary damage model the following procedure was resorted to. By considering only a $\sqrt{t}$ time dependency, (16) can be generalized as

$$(I_{PF})^2 \sim \frac{K_2}{Z_{SF}\sqrt{t}} \tag{25}$$

From Figure 9

$$Z_{SF} = \frac{1.1}{(P_R)^{0.41}\ (I_{PF})^{0.4}} \tag{26}$$

Thus

$$(I_{PF})^2 \sim \frac{K_2\ (P_R)^{0.41}\ (I_{PF})^{0.4}}{1.1\ \sqrt{t}} \tag{27}$$

Recalling that

$$K_2 = \sqrt{\rho C k}\ \Delta T\ s \tag{28}$$

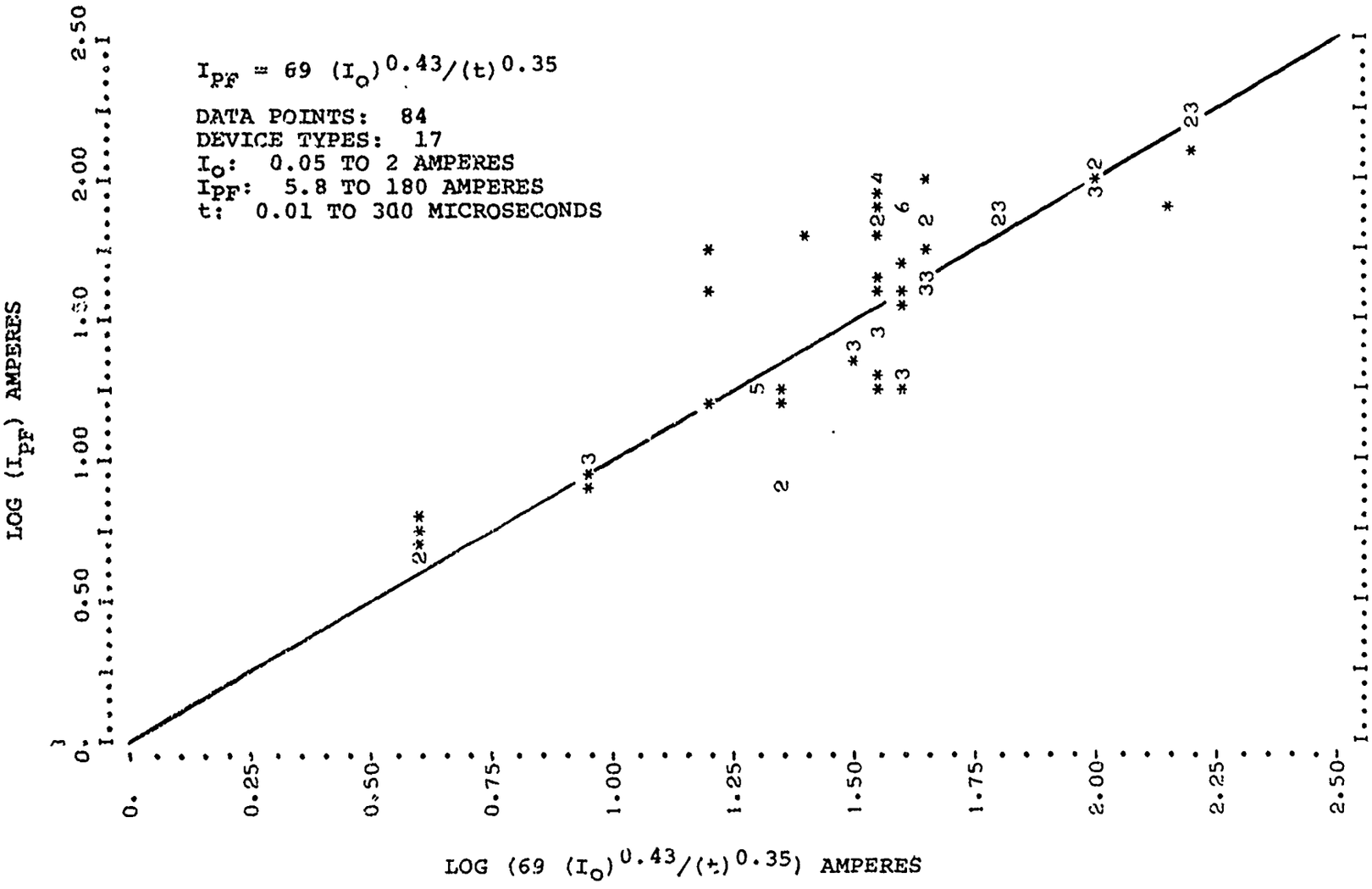

Figure 15. Comparison of the Forward Pulse Damage Current Model of all Construction Type Rectifiers, Diodes & Switches with all Fail Points in Data Base.

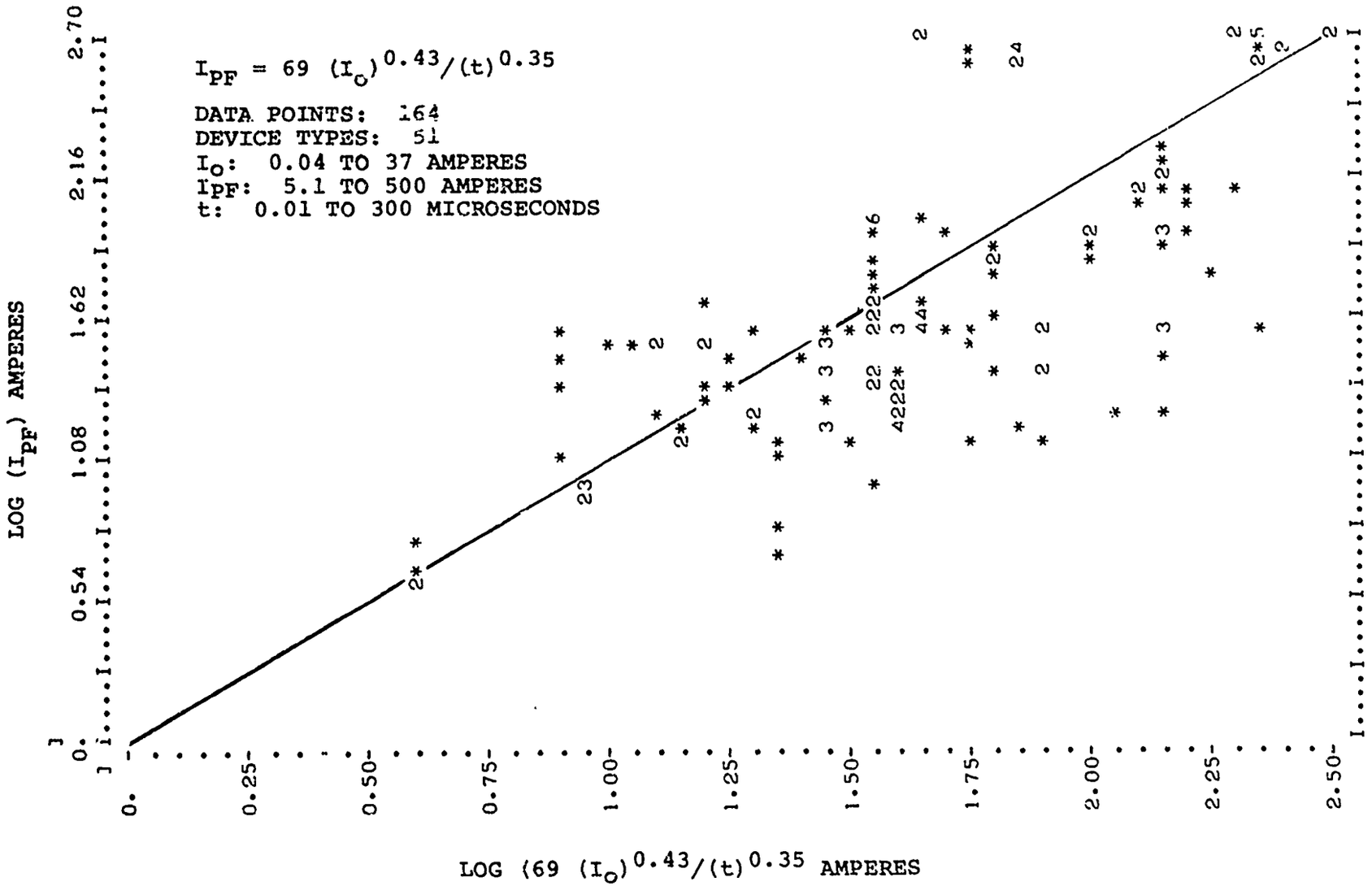

Figure 16. Comparison of the Forward Pulse Damage Current Model of all Construction Type Rectifiers, Diodes and Switches with all No-Fail Points in Data Base.

and making the tacit assumption that

$$s \propto P_R \tag{29}$$

and letting

$$\sqrt{\rho C k}\ \Delta T/1.1 = \text{constant} \tag{30}$$

then

$$(I_{PF})^2 = \frac{K\ (P_R)^{1.41}\ (I_{PF})^{0.4}}{\sqrt{t}} \tag{31}$$

and

$$I_{PF} = \frac{K\ (P_R)^{0.88}}{(t)^{0.312}} \tag{32}$$

Figure 17 shows the results of the regression analysis using the predefined form given in (32) and the paired "no-fail"-"fail" data points in the present data base. The overall 3 σ limits associated with this model are $\pm$ a factor of 11.2 and is a direct result of the rather limited range of device variables in the data base. Figure 18 shows the comparison of the model with all "fail" points in the data base, while Figure 19 is a similar comparison for all "no-fail" points.

2.2 Reverse Polarity Models

The diode models developed for the reverse polarity of junction current conduction are presented in this subsection. Junction conditions in the reverse direction are not nearly as well behaved as that in forward conduction. Rectifiers, diodes and switches exhibit a high variability in reverse conduction characteristics. The reverse conduction process in ideal diodes is controlled by a reverse voltage avalanche breakdown in the depletion region. Real devices, however, are prone to surface breakdown over surface geometries which vary from device to device. This is also dependent on device construction type, surface conditions, and, to a large extent, breakdown voltage level. Higher breakdown voltage devices are generally more susceptible to this than lower voltage devices. Zener diodes, on the other hand, are designed to avalanche breakdown

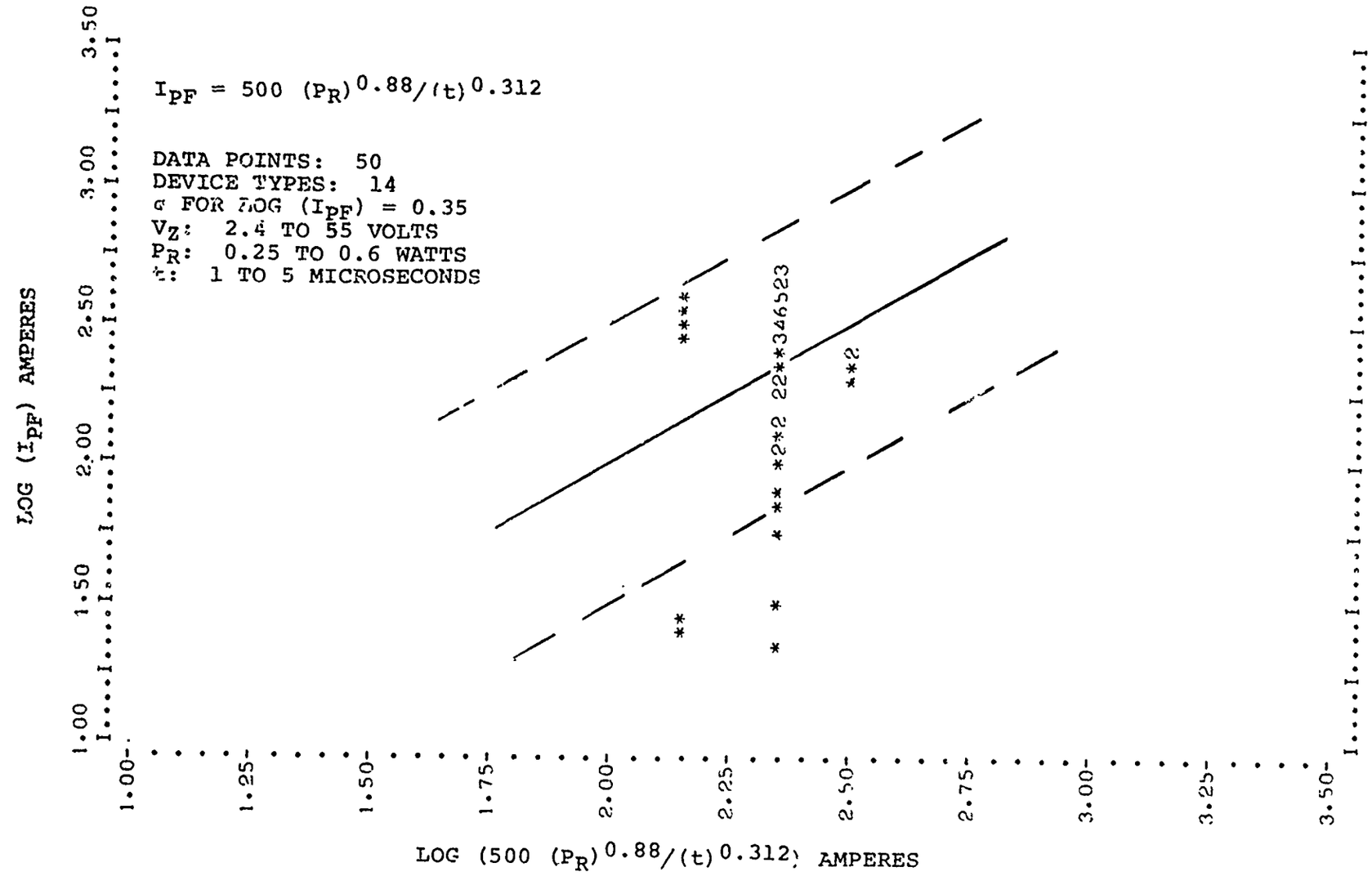

Figure 17. Forward Pulse Damage Current Characteristics for all Construction Type Diodes Functionally Classified as Zener Diodes (Paired No Fail and Fail Data Points Within a Factor of Three).

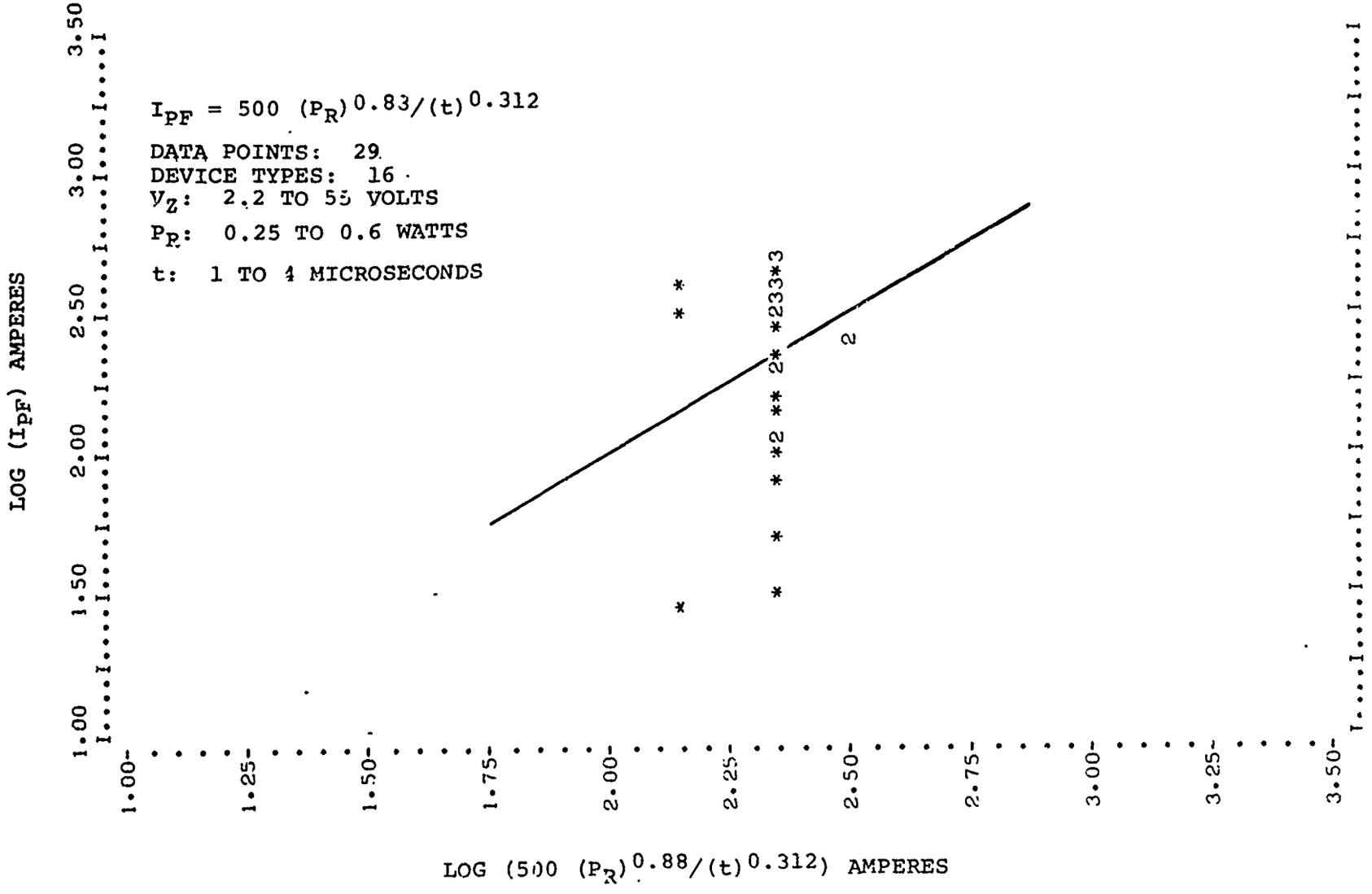

Figure 18. Comparison of the Preliminary Forward Pulse Damage Current Model of all Construction Type Zener Diodes with All Fail Points in the Data Base.

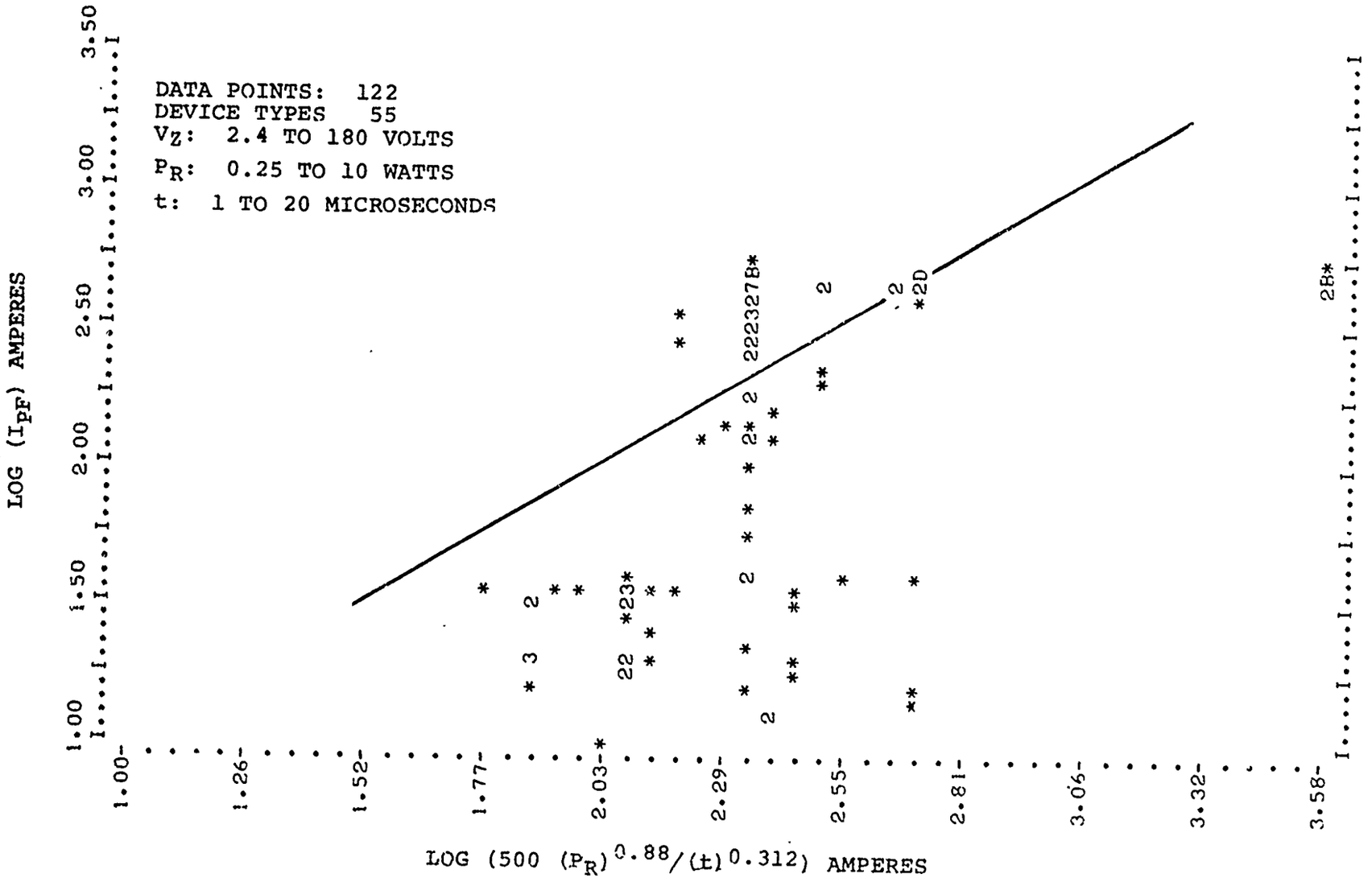

Figure 19. Comparison of the Preliminary Forward Pulse Damage Current Model of all Construction Type Zener Diodes with all No Fail Points in the Data Base.

in the depletion region. The majority of Zener diodes, though, are relatively low voltage units being generally less than 100 volts. Higher voltage units could exhibit surface breakdown depending on the particular junction construction used.

2.2.1 Reverse Polarity Surge Impedance

The reverse polarity surge impedance is defined by

$$Z_{SR} = \frac{V_{PR}-V_{JR}}{I_{PR}} \tag{33}$$

where

V_{PR} = Reverse polarity pulse voltage
V_{JR} = Reverse polarity junction voltage
I_{PR} = Reverse polarity pulse current

V_{JR} is generally taken as the low level junction breakdown voltage, V_Z, that one normally measures on a curve tracer. Hence

$$Z_{SR} = \frac{V_{PR}-V_Z}{I_{PR}} \tag{34}$$

Z_{SR} is attributable to either an increase in the low injection level junction voltage due to high injection level effects or to an IR type voltage drop in the bulk semiconductor region. In many practical cases, if

$$V_{PR} - V_Z < V_Z \tag{35}$$

then the surge impedance can be neglected. One can also treat the diode from a total device standpoint and define a total device impedance, Z_{DR}, by

$$Z_{DR} = \frac{V_{PR}}{I_{PR}} \tag{36}$$

The General Electric 1N4148 diode described in Figure 3 is an excellent example of a diode which exhibits ideal avalanche breakdown in the depletion region. The device is a relatively low voltage diode ($V_Z \sim 100$ Volts) with a well-controlled and

passivated surface and is designed for avalanche breakdown in the depletion region before punchthrough in the epitaxial region occurs. As such, the device is a good choice for use as a baseline configuration in order to evaluate what should be expected from a well-controlled device. From this, one can then expect the situation to get progressively worse as more and more device variables are considered.

Figure 20 shows the total device impedance, Z_{DR}, characteristics exhibited by the GE 1N4148 diode. The statistical 3 σ limits for the impedance relationship shown are $\pm$ a factor of 1.2 over a very large current range. The relationship shown is what one would nearly expect from an ideal diode with no bulk impedance. Here, Z_{DR} would be of the form

$$Z_{DR} = \frac{V_Z}{I_{PR}} \tag{37}$$

and the device voltage would not increase significantly above the low current breakdown voltage level. Figure 21, however, shows that the increase in total device voltage becomes comparable at high current levels to the low current breakdown voltage level and, as such, the device has a surge impedance associated with it. Furthermore, a closer examination of the surge impedance characteristics reveals some very interesting observations. Figure 22, for example, shows the reverse surge impedance characteristics associated with the GE 1N4148 diode. Here, all but one of the data points lie within a factor of $\pm$ 3.16 and the statistical 3 σ limits are $\pm$ a factor of 3.97. One could still consider the device to be of an ideal diode nature with respect to the junction but to consist of a simple bulk resistance, R, in series with the ideal junction. However, the characteristics show that the reverse polarity surge impedance is far from being just a simple fixed resistance, R, in series with an ideal junction of breakdown voltage, V_Z. If this were the case, then Z_{SR} would be of the form

$$Z_{SR} = \frac{V_{PR}-V_Z}{I_{PR}} = R \tag{38}$$

However, Figure 22 shows Z_{SR} to be of the form

$$Z_{SR} = \frac{25.6}{(I_{PR})^{0.85}} \tag{39}$$

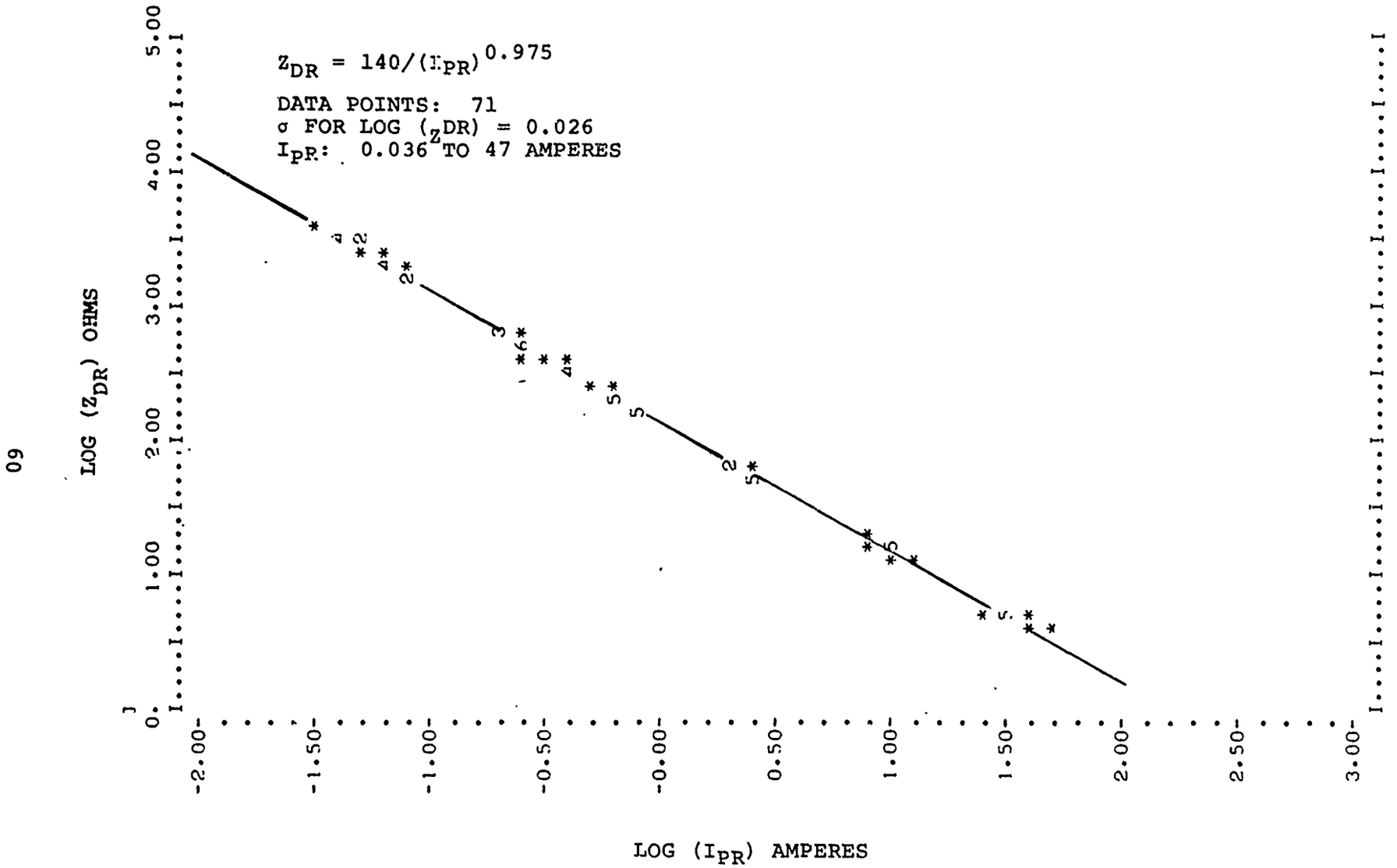

Figure 20. Reverse Total Device Impedance Characteristics of the GE 1N4148 Diode.

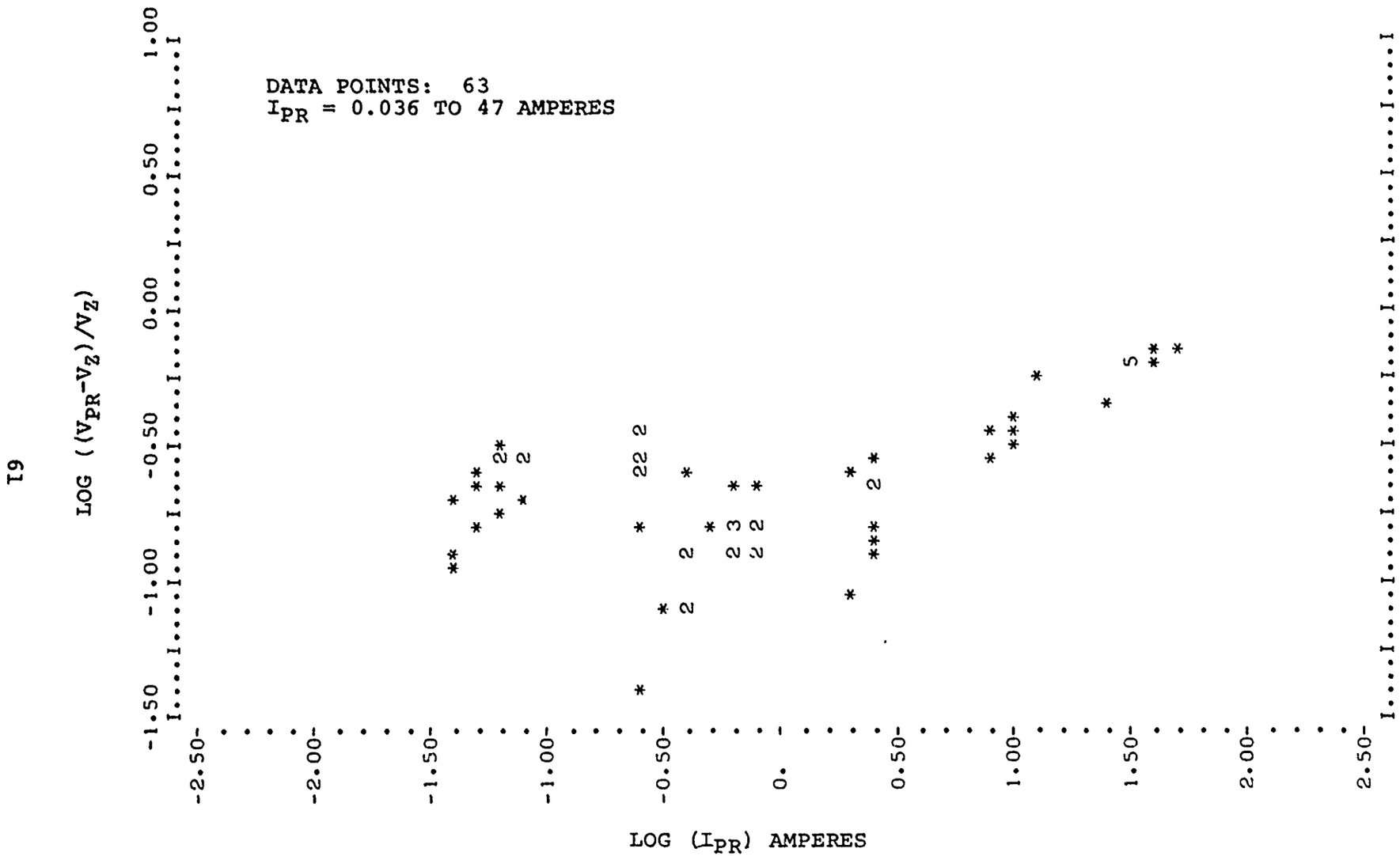

Figure 21. Voltage Increase Above Breakdown for the GE 1N4148 Diode Pulsed in the Reverse Direction.

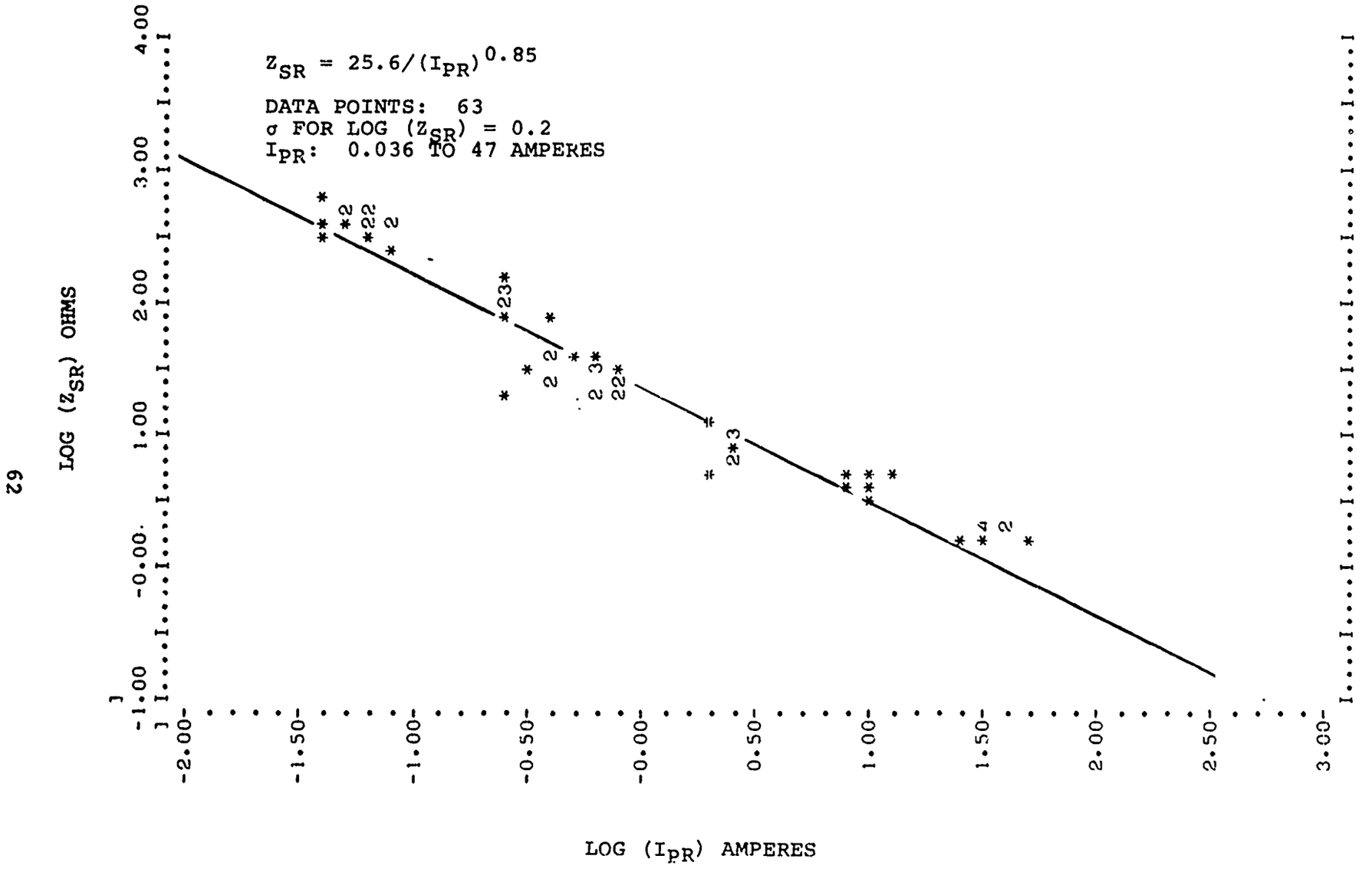

Figure 22. Reverse Surge Impedance Characteristics of the GE 1N4148 Diode.

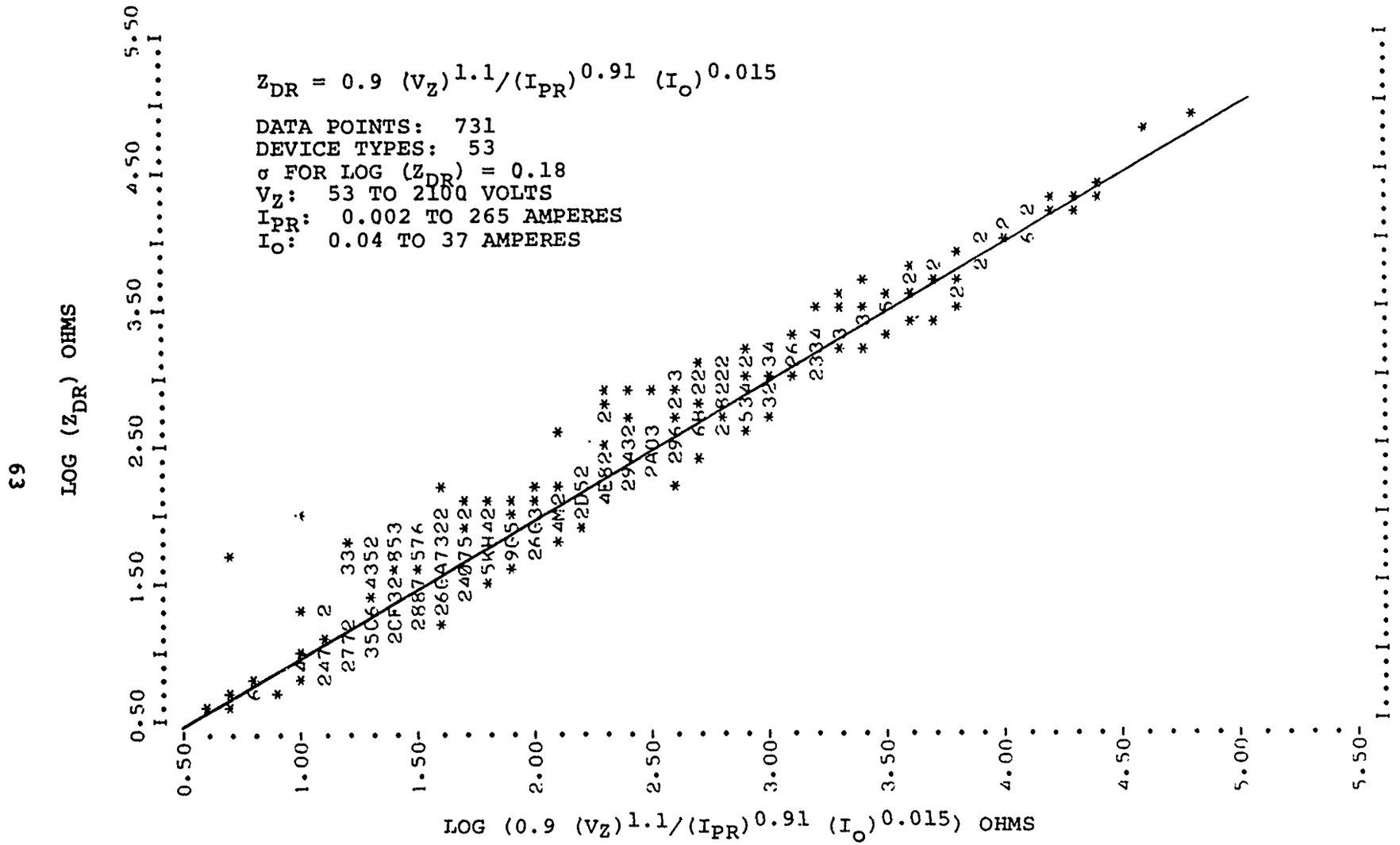

Figure 23. Reverse Total Device Impedance Characteristics for all Construction Type Diodes Functionally Classified as Rectifiers, Diodes and Switches.

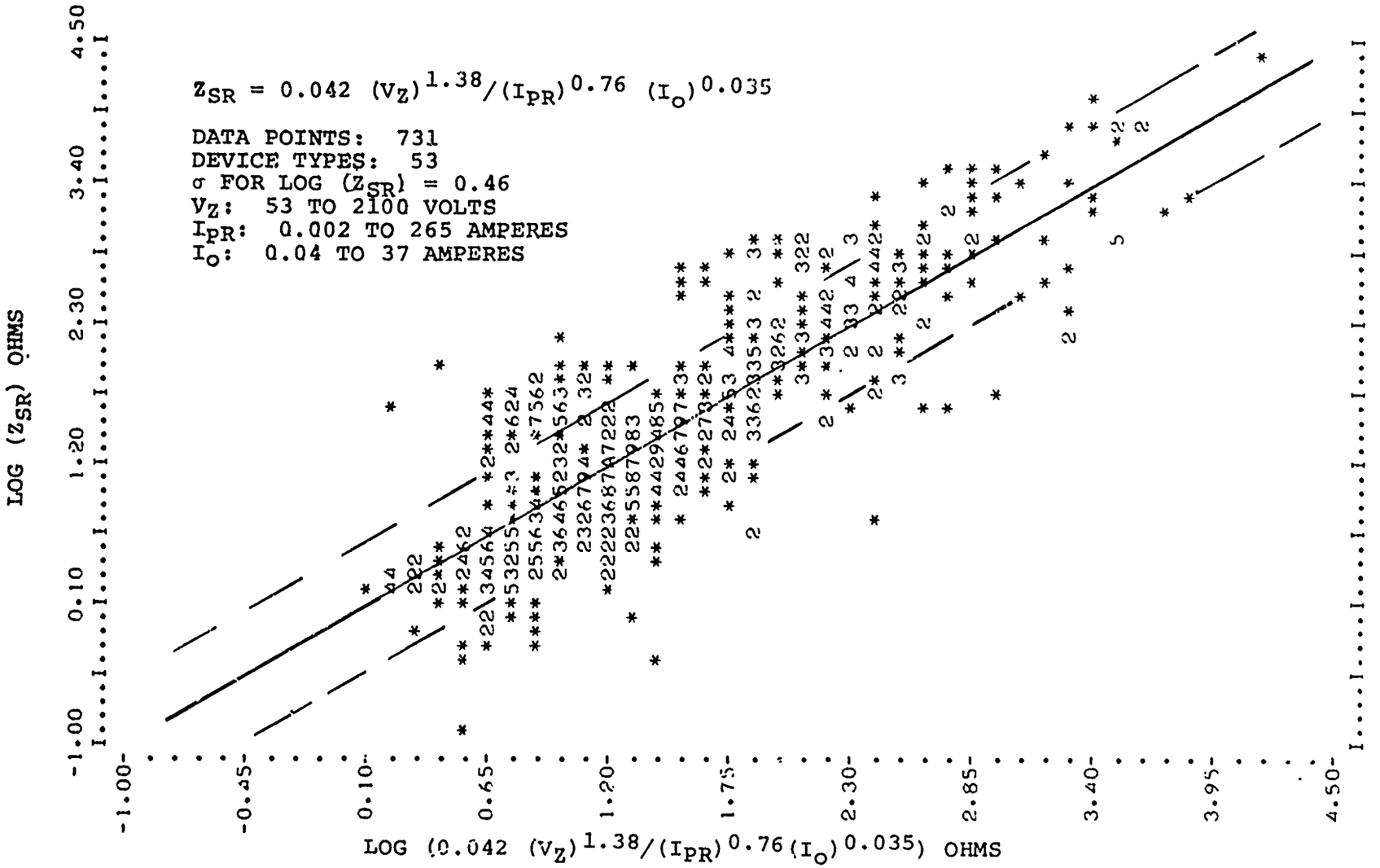

Figure 24. Reverse Surge Impedance Characteristics for all Construction Type Diodes Functionally Classified as Rectifiers, Diodes & Switches.

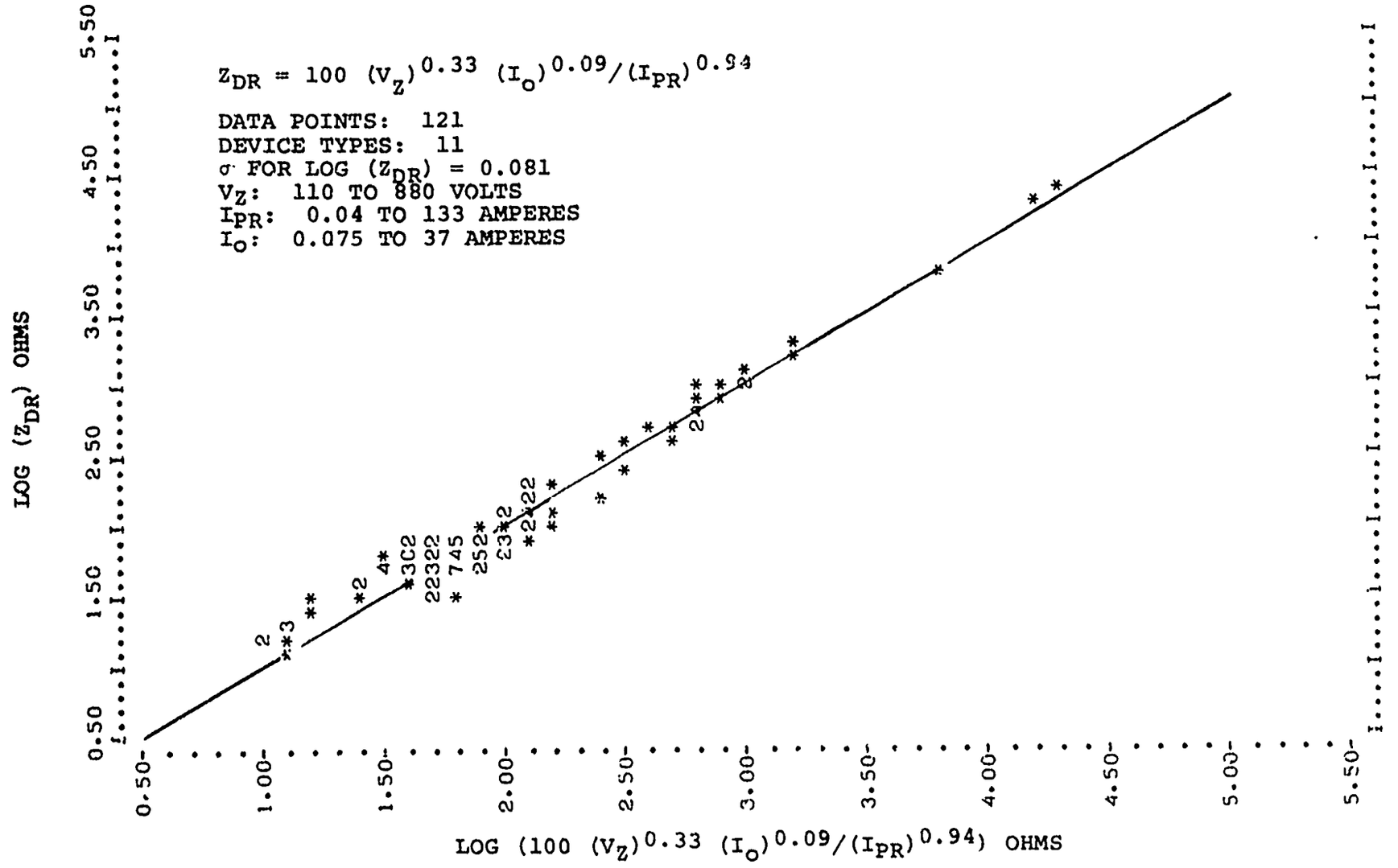

Figure 25. Reverse Total Device Impedance Characteristics of Alloy Diodes Functionally Classified as Rectifiers, Diodes & Switches.

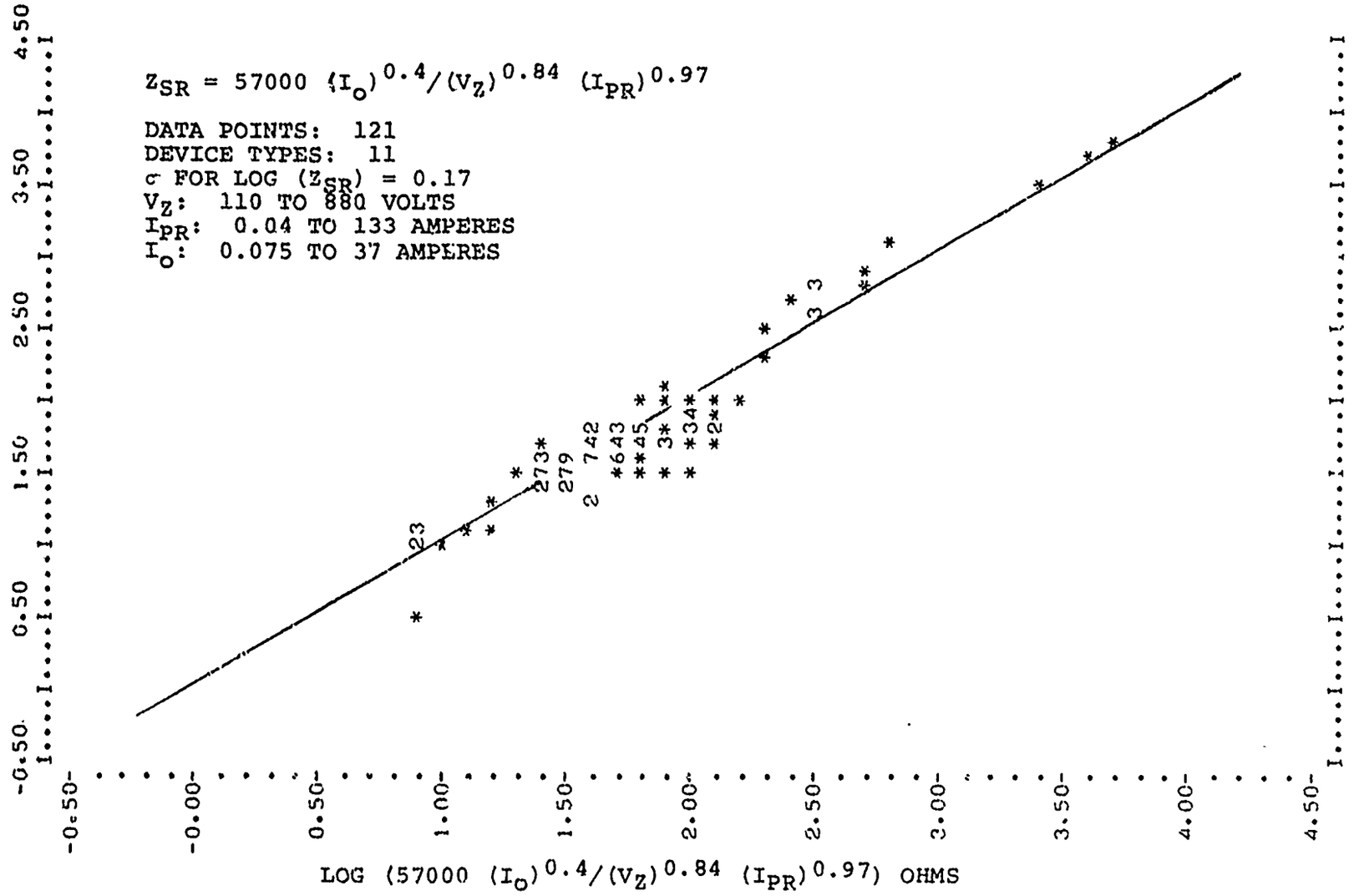

Figure 26. Reverse Surge Impedance Characteristics of Alloy Diodes Functionally Classified as Rectifiers, Diodes & Switches.

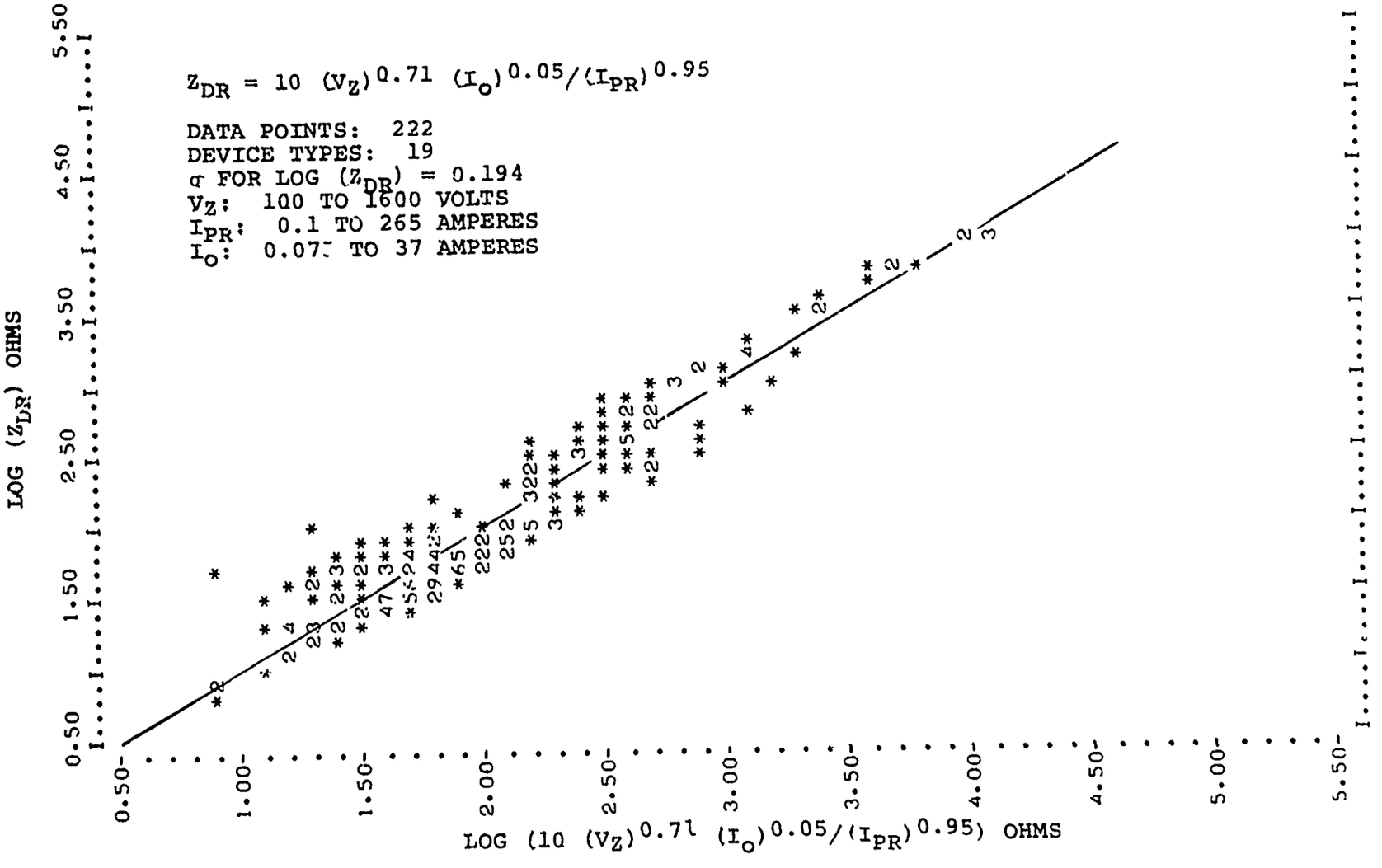

Figure 27. Reverse Total Device Impedance Characteristics of Mesa Diodes Functionally Classified as Rectifiers Diodes & Switches.

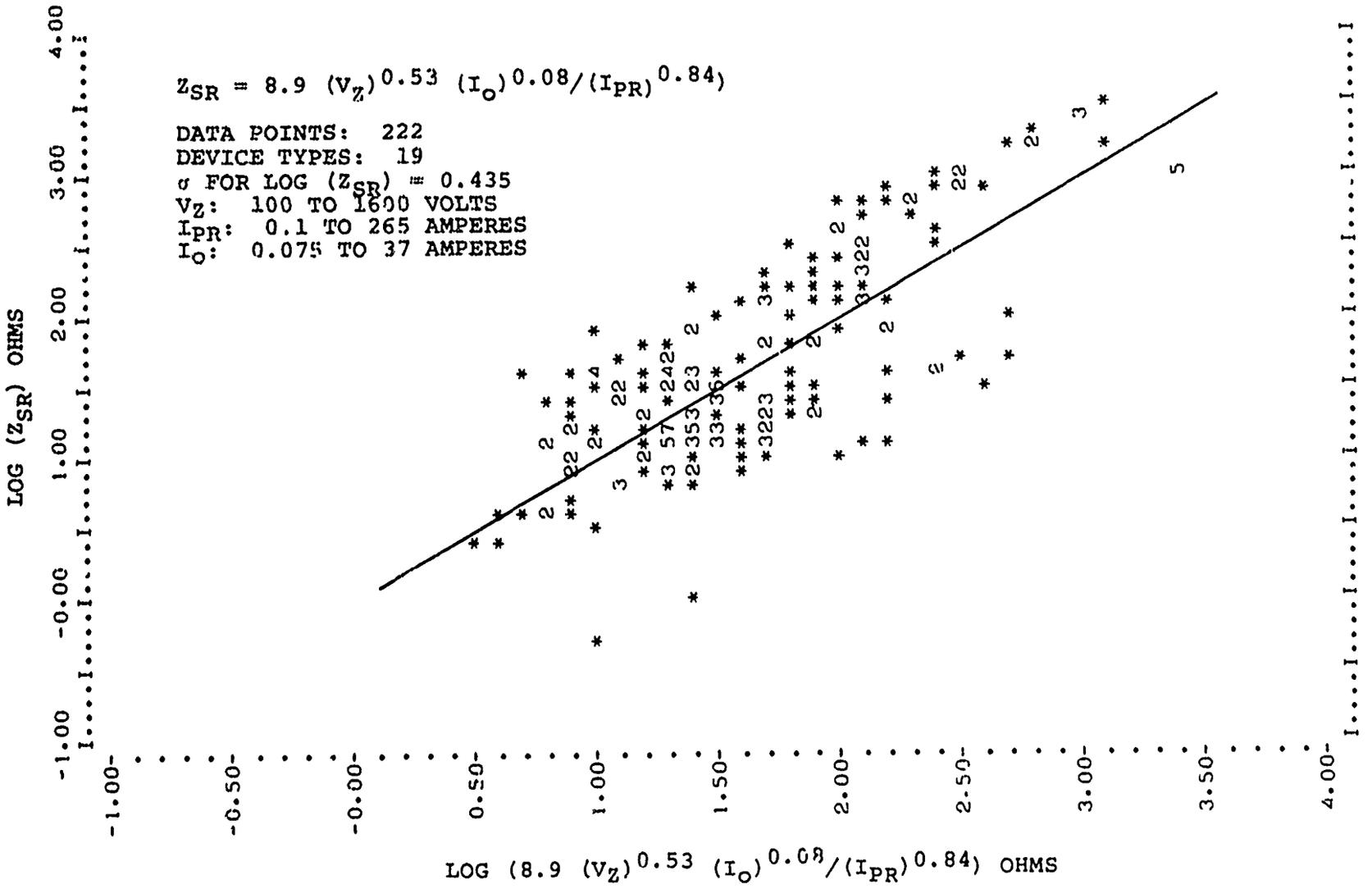

Figure 28. Reverse Surge Impedance Characteristics of Mesa Diodes Functionally Classified as Rectifiers, Diodes & Switches.

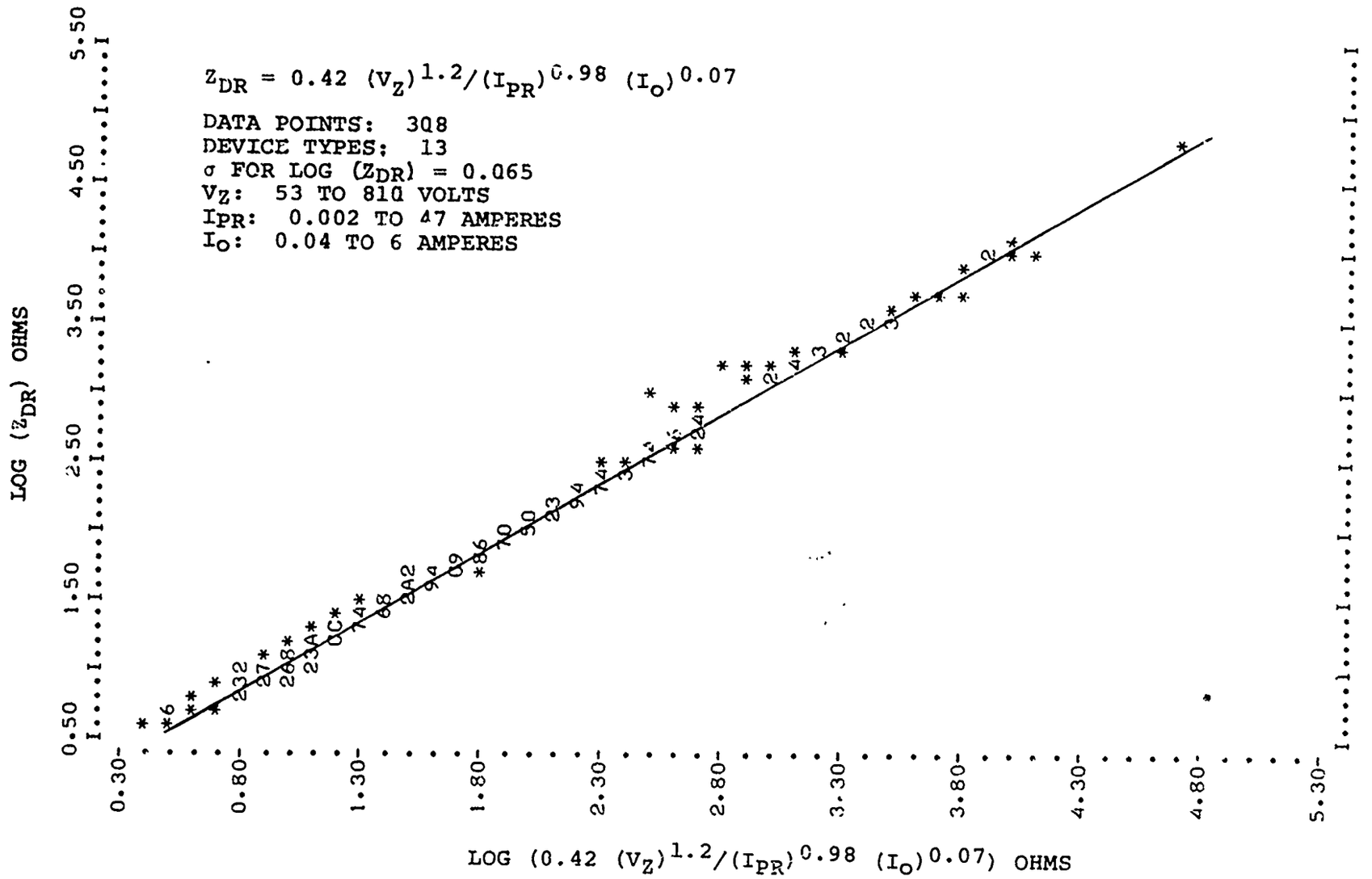

Figure 29. Reverse Total Device Impedance Characteristics of Planar Diodes Functionally Classified as Rectifiers, Diodes & S itches.

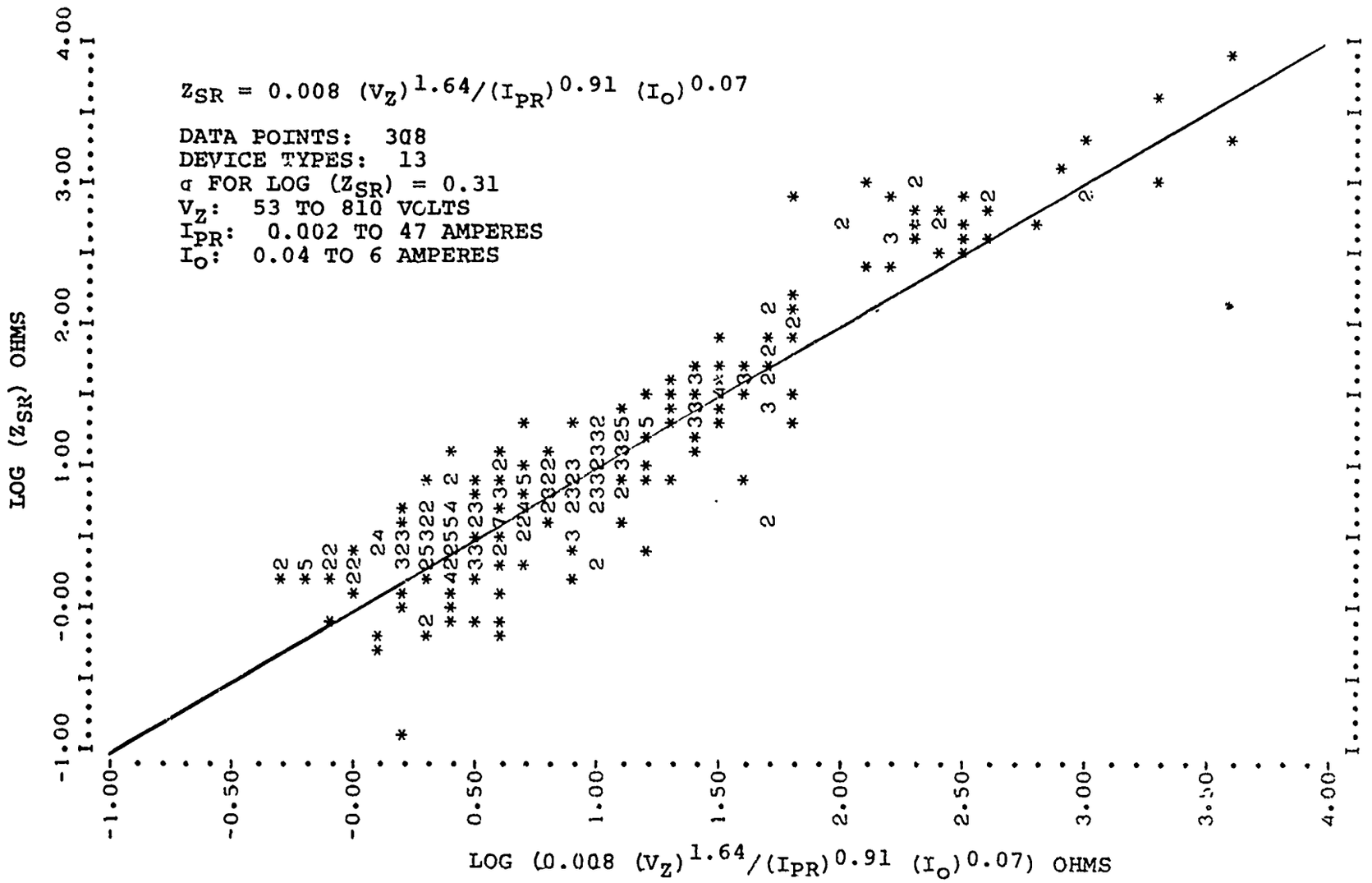

Figure 30. Reverse Surge Impedance Characteristics of Planar Diodes Functionally Classified as Rectifiers, Diodes & Switches.

Since the exponent for conductivity modulation in the forward polarity was found to be 0.31 over a wide range of current, the characteristics shown in (39) could indicate a combination of conductivity modulation in the bulk material and junction voltage increase under high injection levels. This, however, is only speculative at this time and is mentioned only as an interesting point for future discussion.

Figures 23 and 24 show the total device impedance, Z_{DR}, and surge impedance, Z_{SR}, characteristics developed for diodes functionally classified as "rectifiers, diodes and switches" when one considers all construction types together. Figure 23 shows that when one considers the diodes on a total device basis, the characteristics are again indicative of a near ideal diode as evidenced by the near unity values for the exponents of V_Z and I_{PR}, the near unity value of the constant multiplier and the small dependence on the device current rating, I_O. Here the 3 σ statistical limits are within $\pm$ a factor of 3.47 over five oders of magnitude in current. Figure 24, however, shows that the devices do exhibit a surge impedance characteristic which is current level dependent and quite variable as evidenced by the data point scatter. Here the statistical 3 σ limits are $\pm$ a factor of 24. It is interesting to note that the surge impedance is relatively independent of the device current rating, I_O. The corresponding device impedance and surge impedance characteristics of the individual device construction types are shown in Figures 25 through 30. The statistical 3 σ limits are somewhat smaller when the devices are considered on an individual construction type basis. In general, though, the impedance characteristics still follow the trends shown in Figures 23 and 24. Interestingly enough, the alloy devices were the only construction type to exhibit a moderate dependence on the I_O current rating parameter.

The total device impedance, Z_{DR}, and surge impedance, Z_{SR}, characteristics developed for diodes functionally classified as "Zener diodes" when one considers all construction types together is shown in Figures 31 and 32. Both impedance characteristics exhibit a dependence on device parameters other than junction breakdown voltage, V_Z. In fact, if one considers that the device power rating, P_R, is related to the junction area, then one could conclude that the characteristics are indicative of depletion region avalanche over a sizeable portion of the junction area. This should not be too suprising, however, since the data base is proliferated with a wealth of low voltage (i.e., < 100 volts) Zener diode types which should not be as susceptible to surface breakdown. Furthermore, if one compares the surge impedance characteristics shown in Figure 32 with those shown in Figure 9 then one would be tempted to write

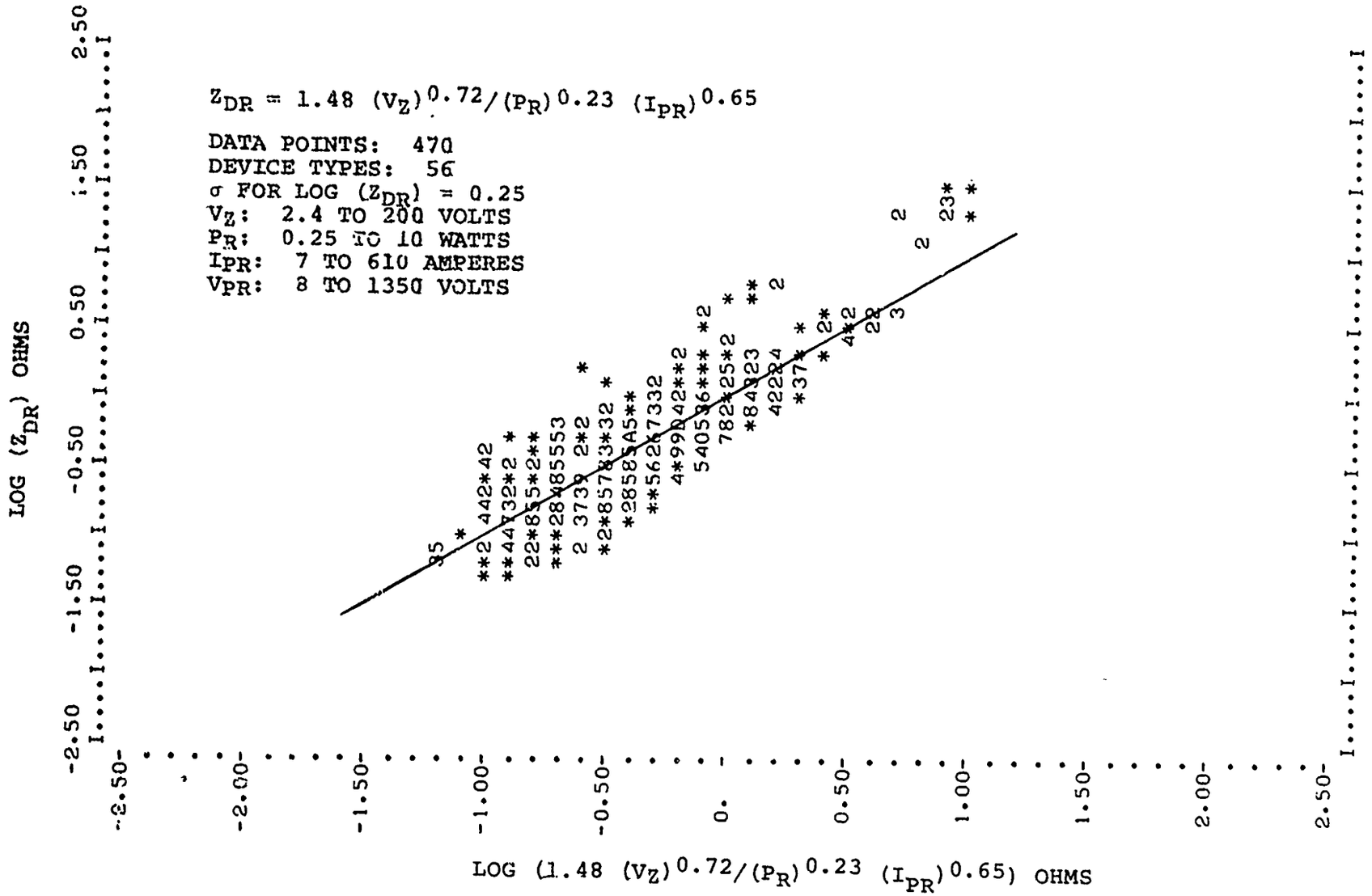

Figure 31. Reverse Total Device Impedance Characteristics for all Construction Type Diodes Functionally Classified as Zener Diodes.

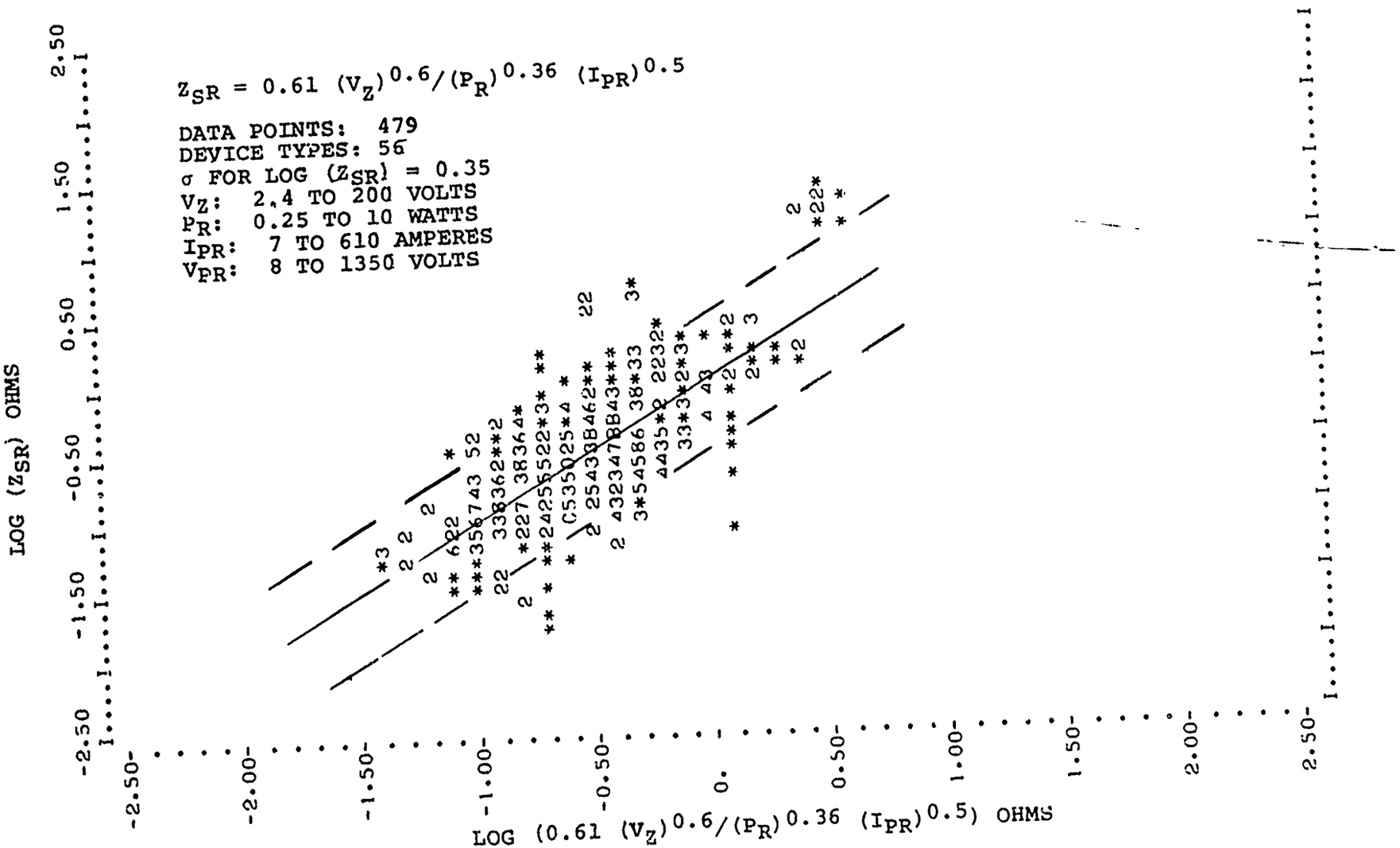

Figure 32. Reverse Surge Impedance Characteristics for all Construction Type Diodes Functionally Classified as Zener Diodes.

$$Z_{SR} = \frac{0.61(V_Z)^{0.6}}{(I_{PR})^{0.5}\ (P_R)^{0.36}} \qquad (40$$

$$Z_{SF} = \frac{1.1}{(I_{PR})^{0.4}\ (P_R)^{0.41}} \qquad (41)$$

therefore

$$Z_{SR} = \frac{0.55\ (V_Z)^{0.6}\ (P_R)^{0.05}}{(I_{PR})^{0.1}}\ Z_{SF} \qquad (42)$$

and

$$Z_{SR} \sim 0.55\ (V_Z)^{0.6}\ Z_{SF} \qquad (43)$$

As such, one would then conclude that a significant part of the device surge impedance is due to a bulk IR type voltage drop in the device. The damage current model developed in Section 2.2.2 for Zener diodes also tends to indicate that the failure mechanism for the lower voltage units is indicative of I^2R heating in the bulk material.

The corresponding models for total device impedance, Z_{DR}, and surge impedance, Z_{SR}, when considering individual construction types is shown in Figures 33 through 38. Again, the devices are observed to follow trends similar to those for all construction types together. The statistical 3 σ limits, though, are somewhat smaller when one considers the devices on an individual construction basis, with the higher 3 σ limits being associated with the higher voltage devices and, in particular, the high voltage mesa units. The statistical 3 σ limits for all device constructions together are $\pm$ a factor of 5.6 and $\pm$ a factor of 11.2 for Z_{DR} and Z_{SR}, respectively, with the majority of data points being within $\pm$ a factor of 3.16.

2.2.2 Reverse Polarity Damage Current

The reverse surge impedance characteristics developed for "rectifiers, diodes and switches" was found to be relatively independent of the device current rating, I_O. The I_O rating of a diode is a qualitative measure of the junction area, and hence the area of the bulk conducting region. Thus, one would conclude that a significant amount of the reverse pulse power applied to

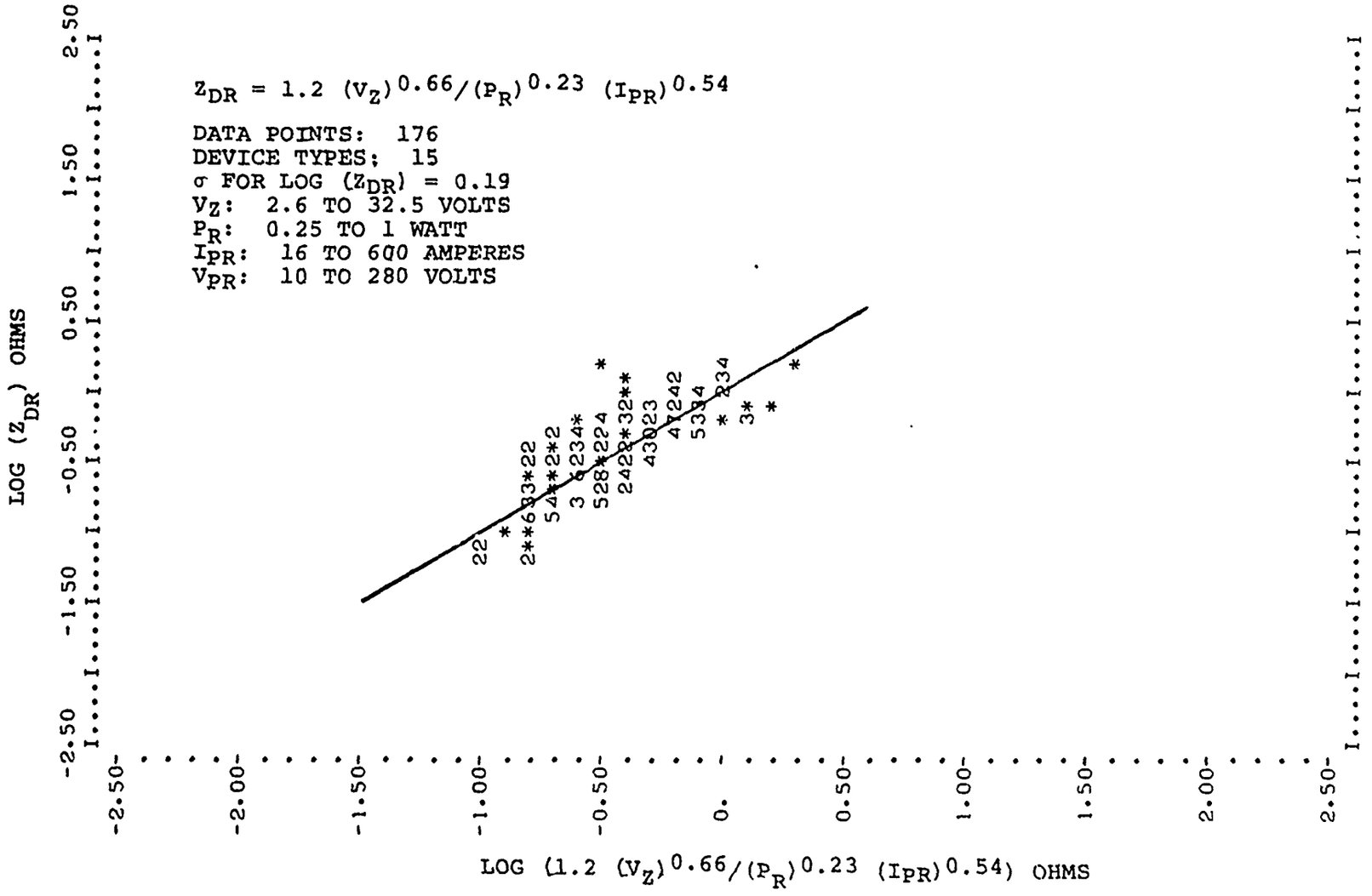

Figure 33. Reverse Total Device Impedance Characteristics of Alloy Diodes Functionally Classified as Zener Diodes.

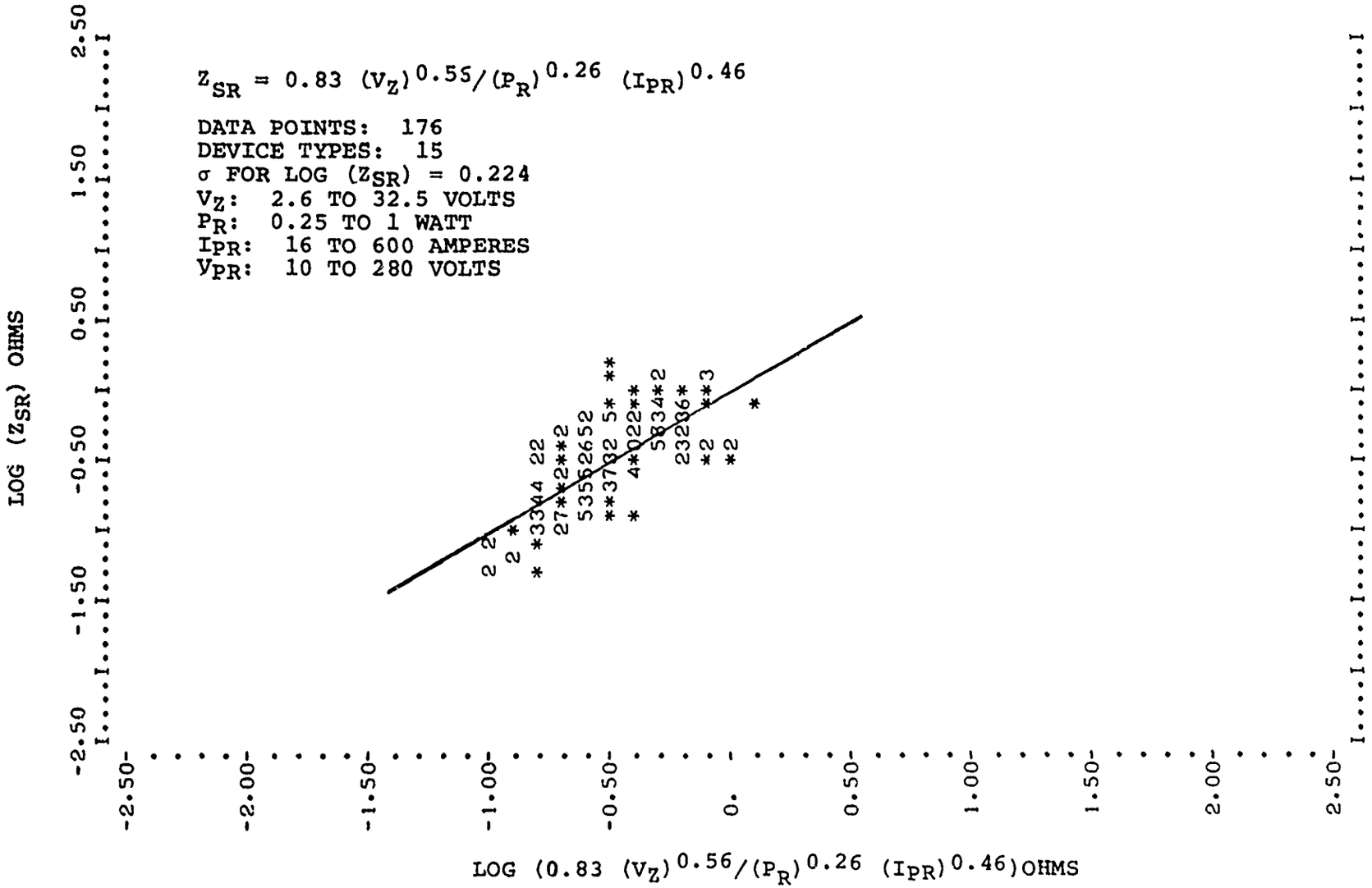

Figure 34. Reverse Surge Impedance Characteristics of Alloy Diodes Functionally Classified as Zener Diodes.

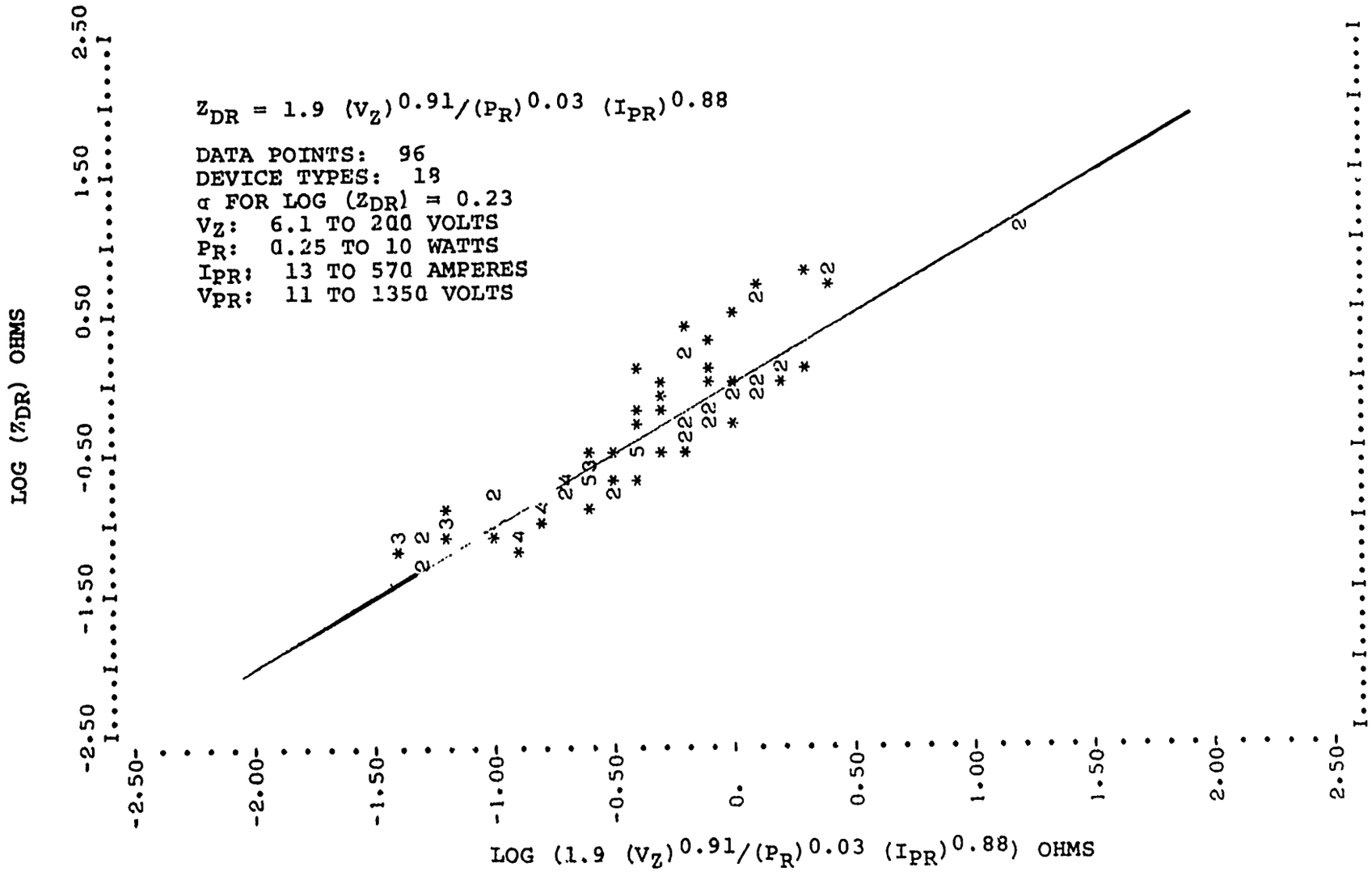

Figure 35. Reverse Total Device Impedance Characteristics of Mesa Diodes Functionally Classified as Zener Diodes.

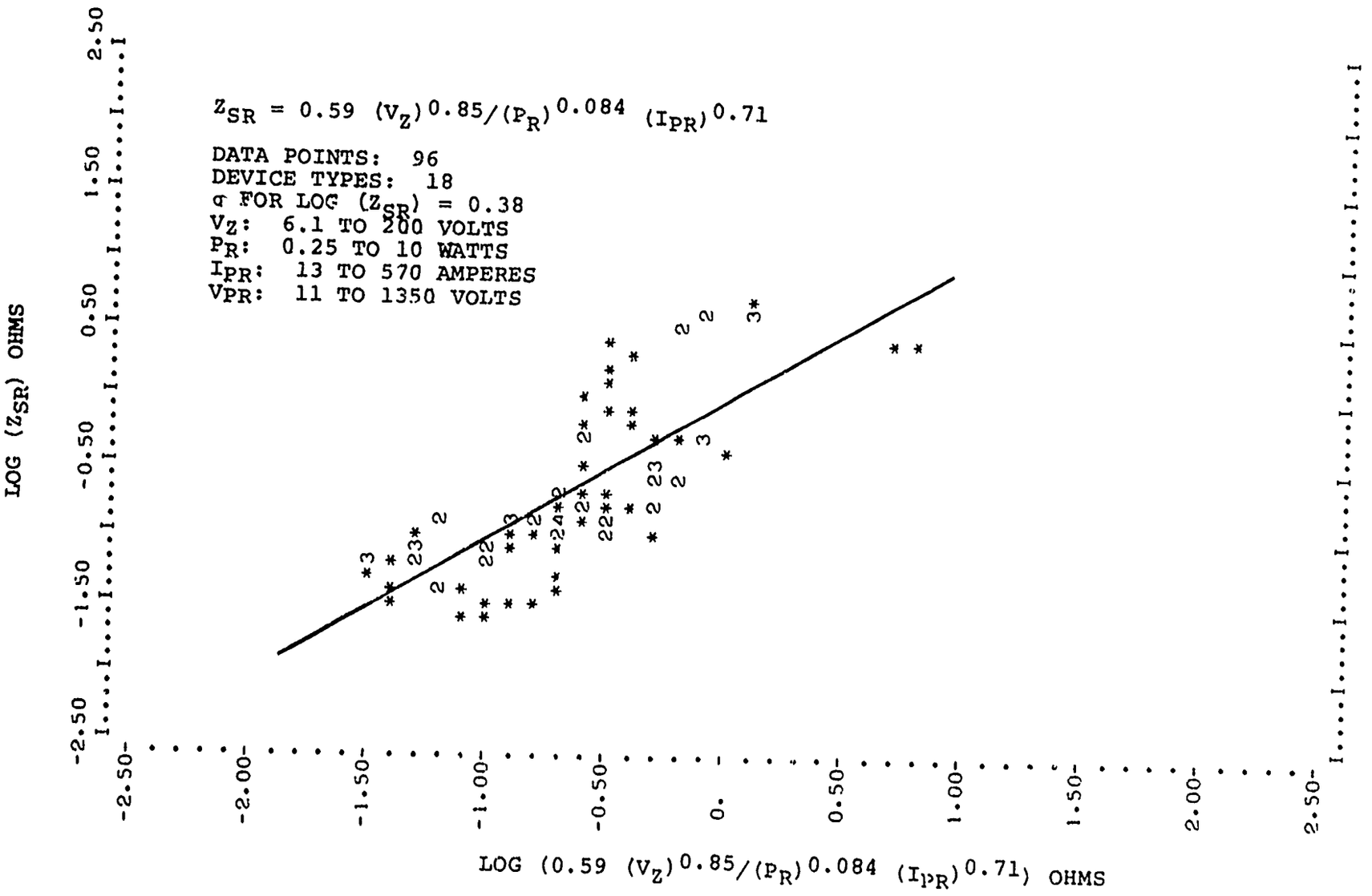

Figure 36. Reverse Surge Impedance Characteristics of Mesa Diodes Functionally Classified as Zener Diodes.

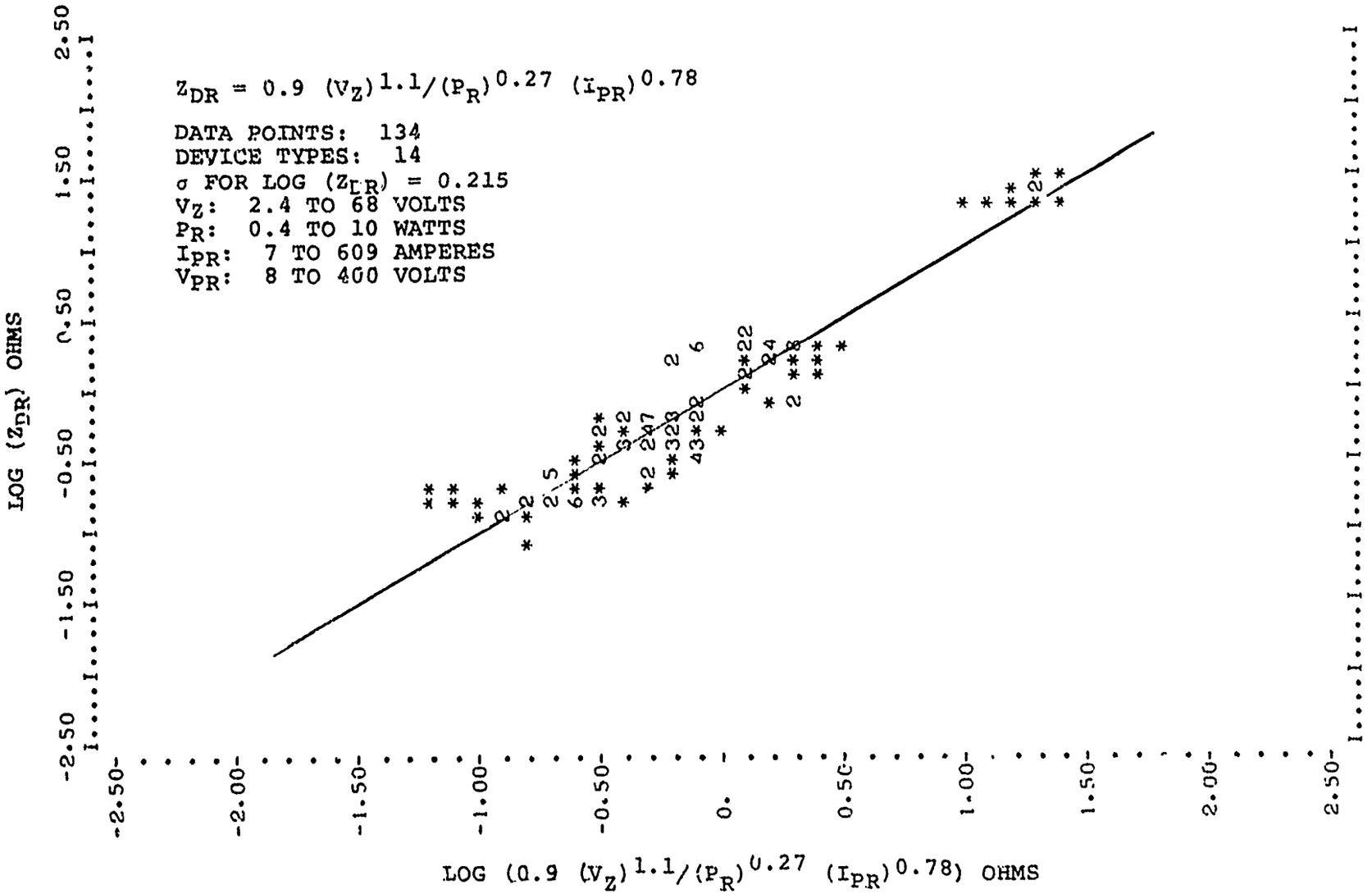

Figure 37. Reverse Total Device Impedance Characteristics Planar Diodes Functionally Classified as Zener Diodes.

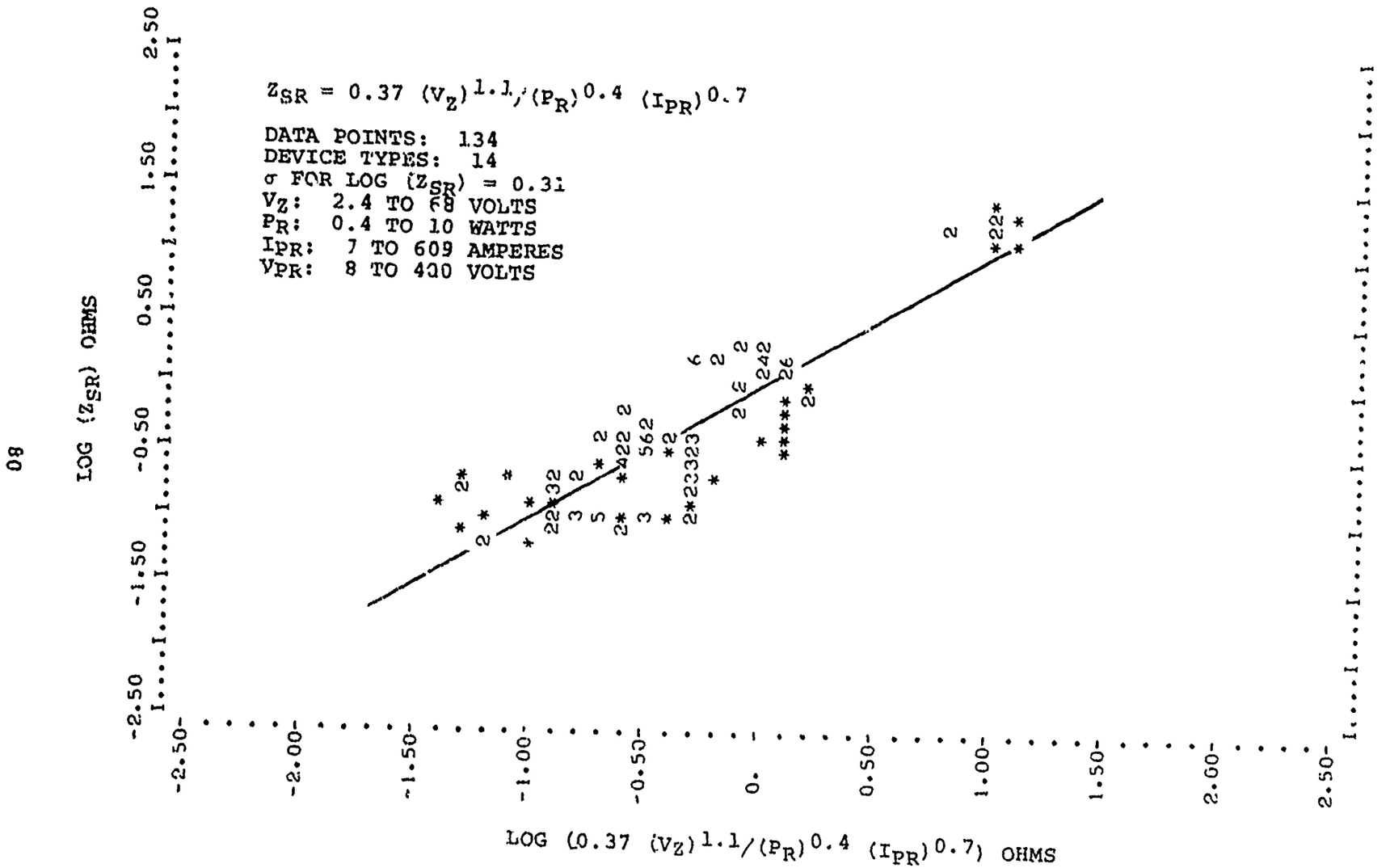

Figure 38. Reverse Surge Impedance Characteristics of Planar Diodes Functionally Classified as Zener Diodes.

the device is being dissipated at the junction rather than in I^2R bulk heating. As such, the energy transfer relationship defined in (14) would be associated with the diode junction where "v" and "s" refer to the junction volume and surface area, respectively.

From Figure 23, it is observed that total device impedance characteristics of the "rectifiers, diodes and switches" is given by

$$\frac{V_{PR}}{I_{PR}} = \frac{0.9\ (V_Z)^{1.1}}{(I_{PR})^{0.91}\ (I_o)^{0.0148}} \tag{44}$$

Since the exponent on the I_o term is so small, one can write

$$\frac{V_{PR}}{V_Z} \sim 0.9\ (V_Z)^{0.1}\ (I_{PR})^{0.09} \tag{45}$$

For a 10 ampere pulse current level in a 100 volt device the increase in device voltage beyond the low current level breakdown voltage, V_Z, is then

$$\frac{V_{PR}}{V_Z} \sim 1.75 \tag{46}$$

Hence to within a factor of two the diodes can be considered to act as ideal diodes with no heat production in the bulk material. As such, the energy, E, in (14) would be defined by

$$E \sim V_Z\ I_{PR}\ t \tag{47}$$

and (14) can be generalized as

$$I_{PR} = K_1 \left(\frac{1}{t} + \frac{K_2}{\sqrt{t}} \right) \tag{48}$$

Figure 39 shows that the experimental data for the reverse damage current of the GE 1N4148 diode does, indeed, follow such a form. This relationship is exhibited over a wide range of pulse width (0.004 to 300 microseconds) and pulse current (0.04 to

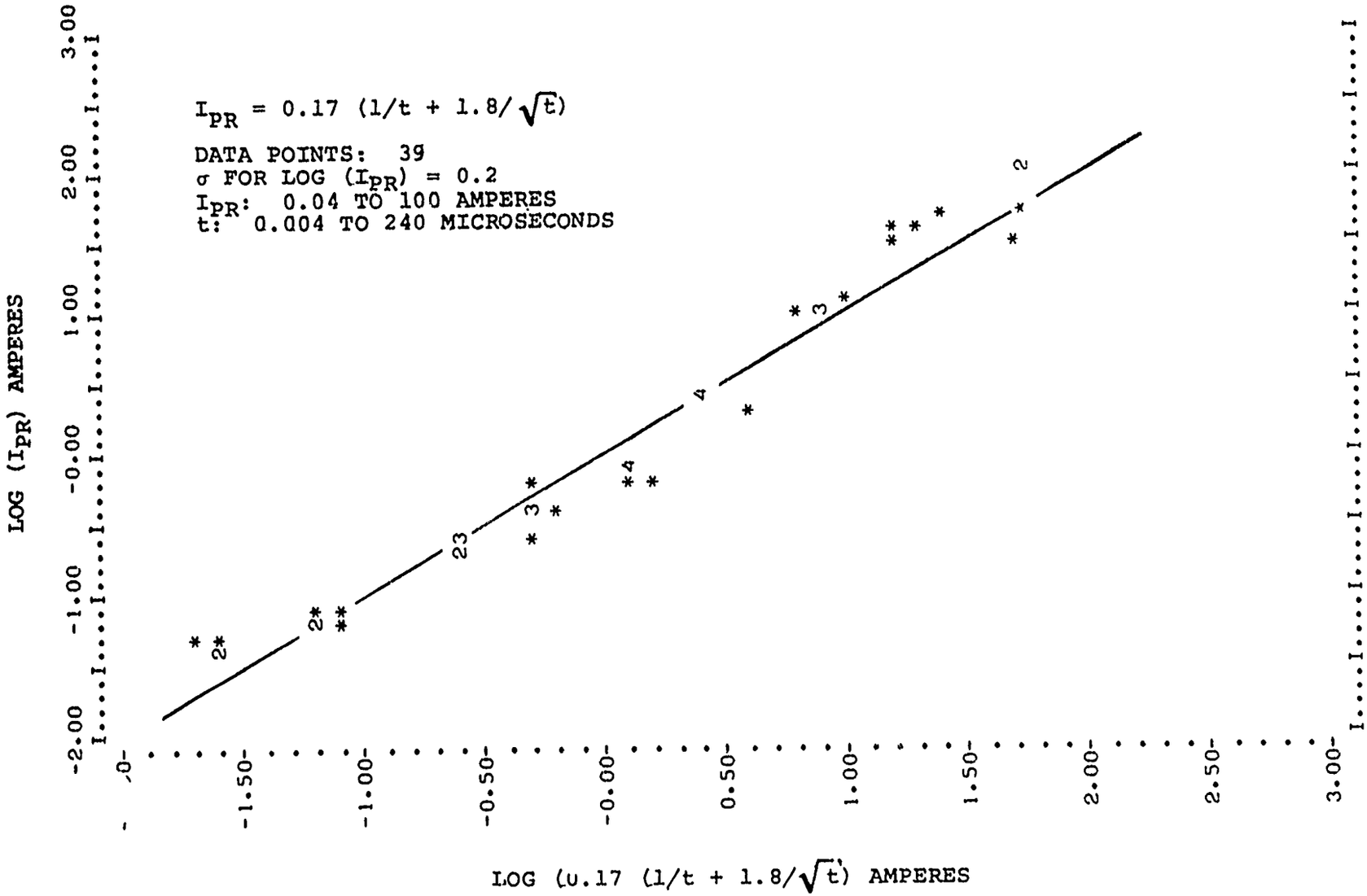

Figure 39. Reverse Polarity Pulse Damage Current Characteristics of the GE 1N4148 Diode.

100 amperes) to within 3 σ limits of ± a factor of 3.97. The break point between adiabatic and heat diffusion is about 310 nanoseconds.

A relationship similar to (48) was developed for diodes functionally classified as "rectifiers, diodes and switches". The analysis indicated that the break point between adiabatic and heat diffusion conditions was less than 30 nanoseconds. Due to the overall sparsity of data in this region, it was felt that the general two termed time expression given in (48) could not be accurately evaluated. As such, the regression analysis was restricted to a general single time term for more accuracy, and took the form

$$I_{PR} = \frac{K}{(t)^m} \qquad (49)$$

where

K = Constant dependent on device parameters

The damage model developed from (49) is shown in Figure 40 for all construction types taken together. Here, the damage current was found to be dependent on the current rating, I_O, and relatively independent of low current avalanche voltage, V_Z. This is not too suprising since relatively large junction area devices are included in the model given in Figure 40 and the analysis indicated that heat diffusion term, $\sqrt{t}$, was significant. As such, a parameter indicative of diode surface area, such as I_O, should be expected. The close agreement of the time exponent, 0.64, with the theoretical 0.5 should also be noted. The 3 σ statistical limits for the model are ± a factor of 16.

Figures 41, 42 and 43 show the damage models developed for individual construction type "rectifiers, diodes and switches". As would be expected, the 3 σ limits are smaller when construction types are considered individually. The smaller time exponents (0.41 and 0.46) for the alloy and mesa devices which have larger area devices is contrasted with the larger exponent (0.77) of the quasi-adiabatic planar devices which have much smaller junction area devices in the data base.

For the Zener diode model, recourse is once again made to an examination of the total device impedance characteristics. From Figure 31, it is observed that Z_{SR} is given by

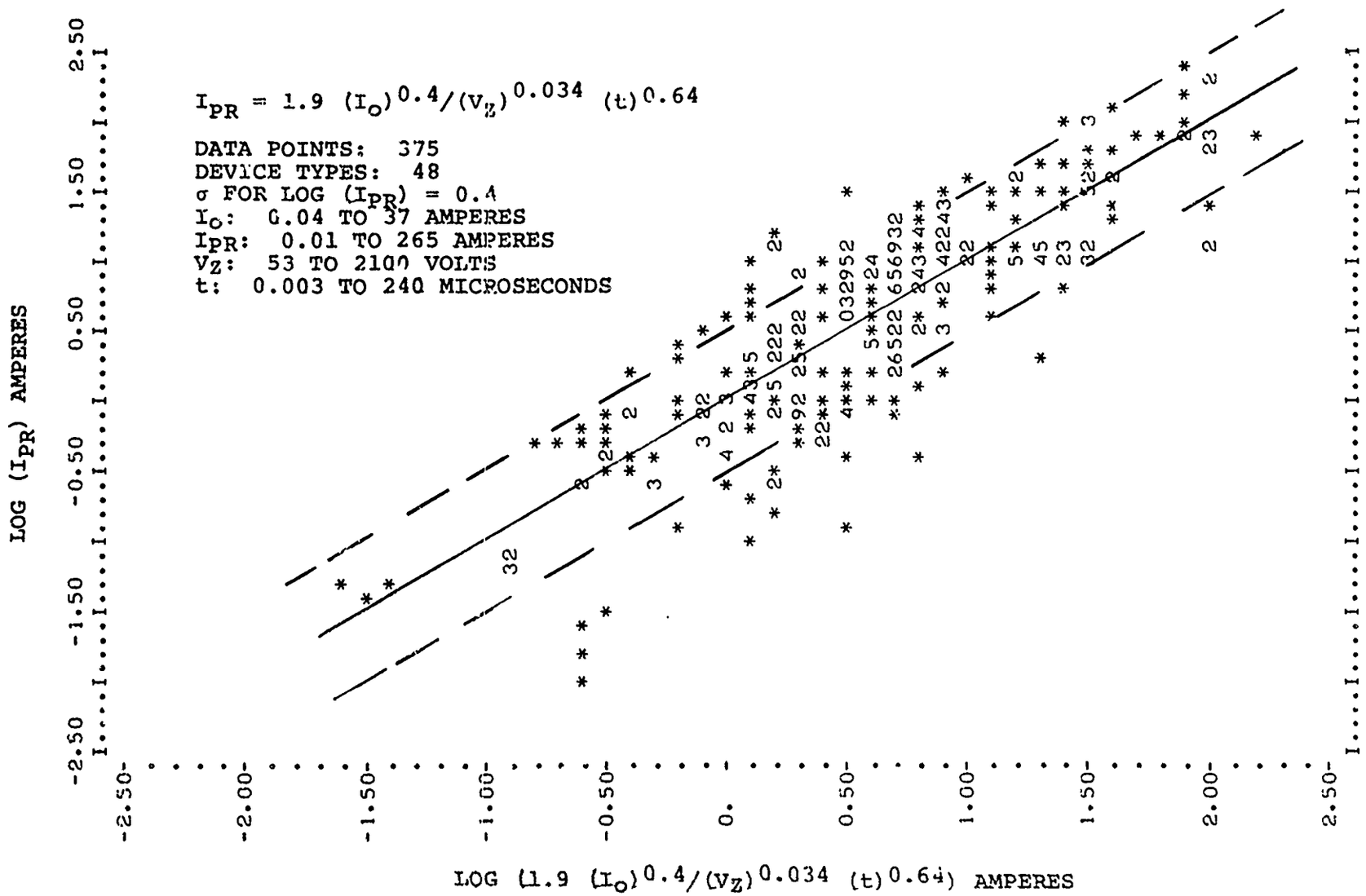

Figure 40. Reverse Pulse Damage Current Characteristics for all Construction Type Diodes Functionally Classified as Rectifiers, Diodes & Switches.

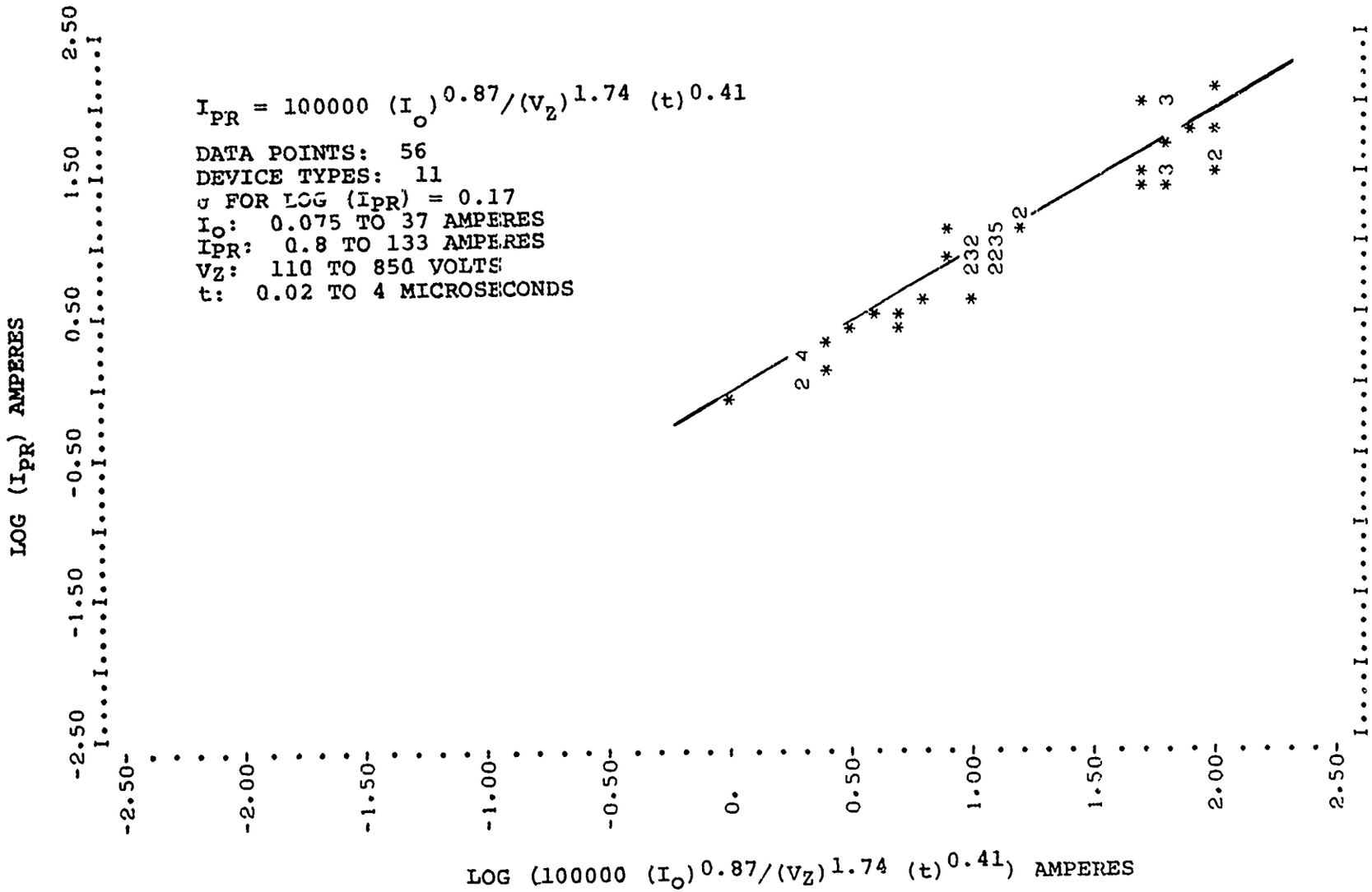

Figure 41. Reverse Pulse Damage Current Characteristics of Alloy Diodes Functionally Classified as Rectifiers, Diodes & Switches.

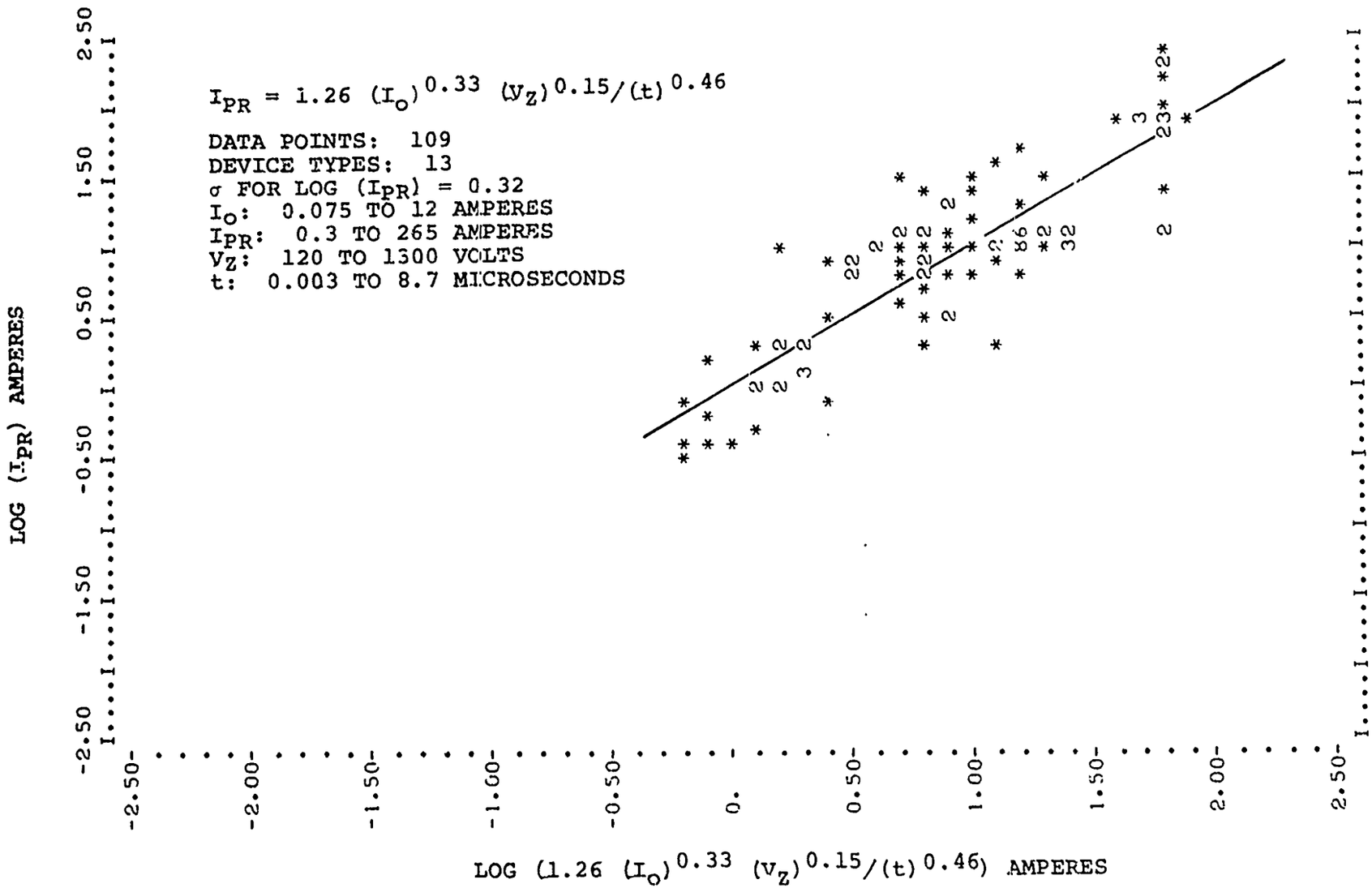

Figure 42. Reverse Pulse Damage Current Characteristics of Mesa Diodes Functionally Classified as Rectifiers, Diodes & Switches.

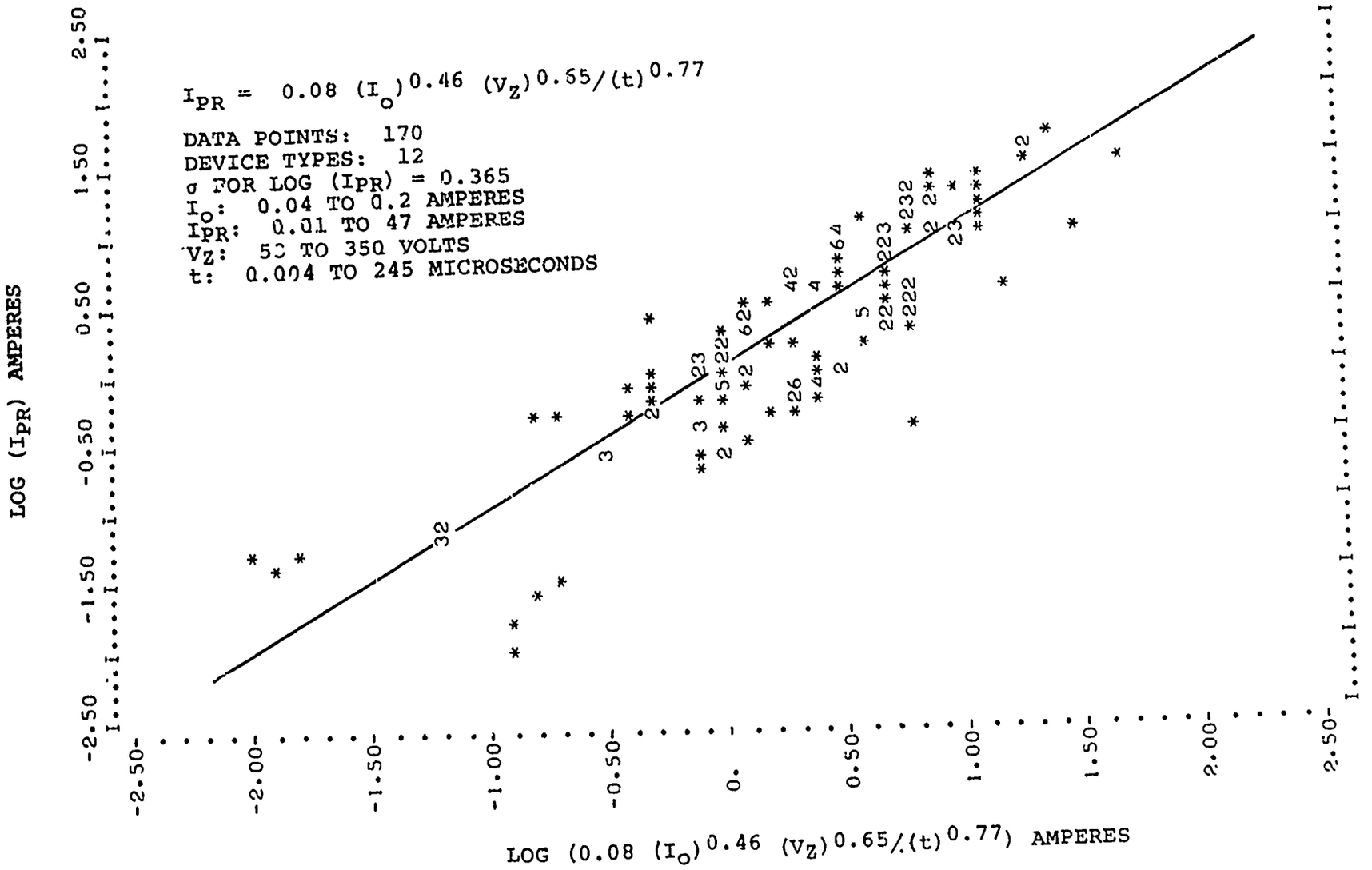

Figure 43. Reverse Pulse Damage Current Characteristics of Planar Diodes Functionally Classified as Rectifiers, Diodes & Switches.

$$\frac{V_{PR}}{I_{PR}} = \frac{1.48\ (V_Z)^{0.72}}{(P_R)^{0.23}\ (I_{PR})^{0.65}} \tag{50}$$

and

$$\frac{V_{PR}}{V_Z} = \frac{1.48\ (I_{PR})^{0.35}}{(P_R)^{0.23}\ (V_Z)^{0.28}} \tag{51}$$

For a 6 volt, 1 watt Zener diode pulsed at 30 amperes, this becomes

$$\frac{V_{PR}}{V_Z} = 2.96 \tag{52}$$

While for a 100 volt, 1 watt device pulsed at 30 amperes

$$\frac{V_{PR}}{V_Z} = 1.34 \tag{53}$$

For the low voltage Zener diodes, the increase in device voltage above the Zener level is significant and is primarily a result of an IR drop in bulk material. The higher voltage Zener diodes, on the other hand, approximate ideal diodes whereby the pulse power is dissipated primarily in the junction region. Hence, the low voltage devices would be susceptible to I^2R heating and the higher voltage units to direct junction heating. Medium voltage diodes, though, would be susceptible to a combination of these effects, whereby the heat transfer from the bulk material to the junction would be comparable to the heat generated in the junction.

Thus, in general, the temperature rise in the junction, ΔT, would be expressed as

$$\Delta T_J \propto Q_J + \alpha Q_B \tag{54}$$

where

Q_J = Heat directly generated in the junction

Q_B = Heat generated in the bulk material

α = Time and diode geometry dependent heat coupling factor

or, in terms of the time truncated expression given in (13)

$$\Delta T_J = \frac{E_{JR}}{\rho C v_J + \sqrt{\rho C k t}\, s_J} + \frac{\alpha\, E_{BR}}{\rho C v_B + \sqrt{\rho C k t}\, s_B} \tag{55}$$

where the subscripts "J" and "B" refer to the junction and bulk, respectively.

If the junction is an ideal junction, then

$$E_{JR} = V_Z\, I_{PR}\, t \tag{56}$$

and the energy dissipated in the bulk is

$$E_{BR} = (I_{PR})^2\, Z_{SR}\, t \tag{57}$$

$$E_{BR} = I_{PR}\, (V_{PR} - V_Z)\, t \tag{58}$$

In the low voltage diodes, the heating effect will be similar to that in the forward direction where non-adiabatic conditions predominated. One would expect the larger power rated, higher voltage diodes to exhibit a somewhat similar response due to their relatively larger surface area to volume ratios. Hence, if one neglects adiabatic heating for simplification, then

$$\Delta T_J = \frac{V_Z\, I_{PR} \sqrt{t}}{K_2\, s_J} + \frac{\alpha I_{PR}\, (V_{PR} - V_Z) \sqrt{t}}{K_2\, s_B} \tag{59}$$

where $K_2 = \sqrt{\rho C k}$

If uniform heating and temperature rise of the bulk is assumed, then "α" can be considered to be related to the time that it takes heat to diffuse from the surface of the bulk through the entire junction width. This time is related to the heat diffusion length, L_H, by

$$L_H = \sqrt{\frac{kt}{C\rho}} \tag{60}$$

and "α" is also related to the junction width "X_J". As a first approximation, "α" can be considered to be of the form

$$\alpha = \frac{1}{1 + \left(\frac{X_J}{L_H}\right)} \tag{61}$$

such that at very short times (i.e., $L_H \sim 0$) "α" is very small and no coupling occurs and at very large times (i.e., $L_H \sim \infty$) "α" is unity and complete coupling occurs. The junction width, X_J, can be considered to be of the form

$$X_J = K\ (V_Z)^P \tag{62}$$

Phillips[3] gives relationships which enable one to evaluate "K" and "P" in (62) for both abrupt and graded base junctions. For abrupt junctions, this is

$$K = 1.97 \times (10)^{-6} \tag{63}$$

$$P = 1.215 \tag{64}$$

and for graded junctions

$$K = 1.35 \times 10^{-6} \tag{65}$$

$$P = 1.25 \tag{66}$$

which yields average values of

$$K = 1.66 \times 10^{-6} \tag{67}$$

$$P = 1.23 \tag{68}$$

The diffusion length, L_H, can be evaluated from the following

$$k = 0.714 \text{ average from } 25°C \text{ to } 600°C \tag{69}$$

---

[3]Phillips, A.B., "Transistor Engineering", McGraw-Hill Book Company, Inc., 1962.

$$C = 0.935 \text{ @ } 725°C \tag{70}$$

$$\rho = 2.42 \tag{71}$$

Thus,

$$L_H = \sqrt{0.316\ t} \text{ cm} \tag{72}$$

and

$$\alpha = \frac{1}{1 + \frac{1.66 \times 10^{-6} (V_Z)^{1.23}}{\sqrt{0.316\ t}}} \tag{73}$$

Finally, if we make the admittedly questionable oversimplification that

$$S_J \sim S_B \sim P_R \ \& \ V_Z \tag{74}$$

then, from (59) we obtain

$$I_{PR} = \frac{K\ (V_Z)^A\ (P_R)^B}{\left[V_Z + \alpha\ (V_{PR}-V_Z)\right] \sqrt{t}} \tag{75}$$

where "α" is given by (73).

A regression analysis of the Zener diode damage data was performed using the relationship defined in (75). Since the data base consisted of numerous low voltage devices where a distinct time point of damage could not be observed, the data was analyzed only for pairs of "no-fail"-"fail" points which were separated by no more than a factor of three. Also, the time term was not constrained to a 0.5 exponent, but for additional accuracy, was expressed in general form to be solved by the regression analysis. The results of this are shown in Figure 44. The relationship shown provides a reasonable, although not very accurate, representation of the Zener diode damage data. The statistical 3 σ error is $\pm$ a factor of 25. Note that the regression analysis defined the exponent of time to be 0.56 which is in close agreement to the non-adiabatic assumption of 0.5.

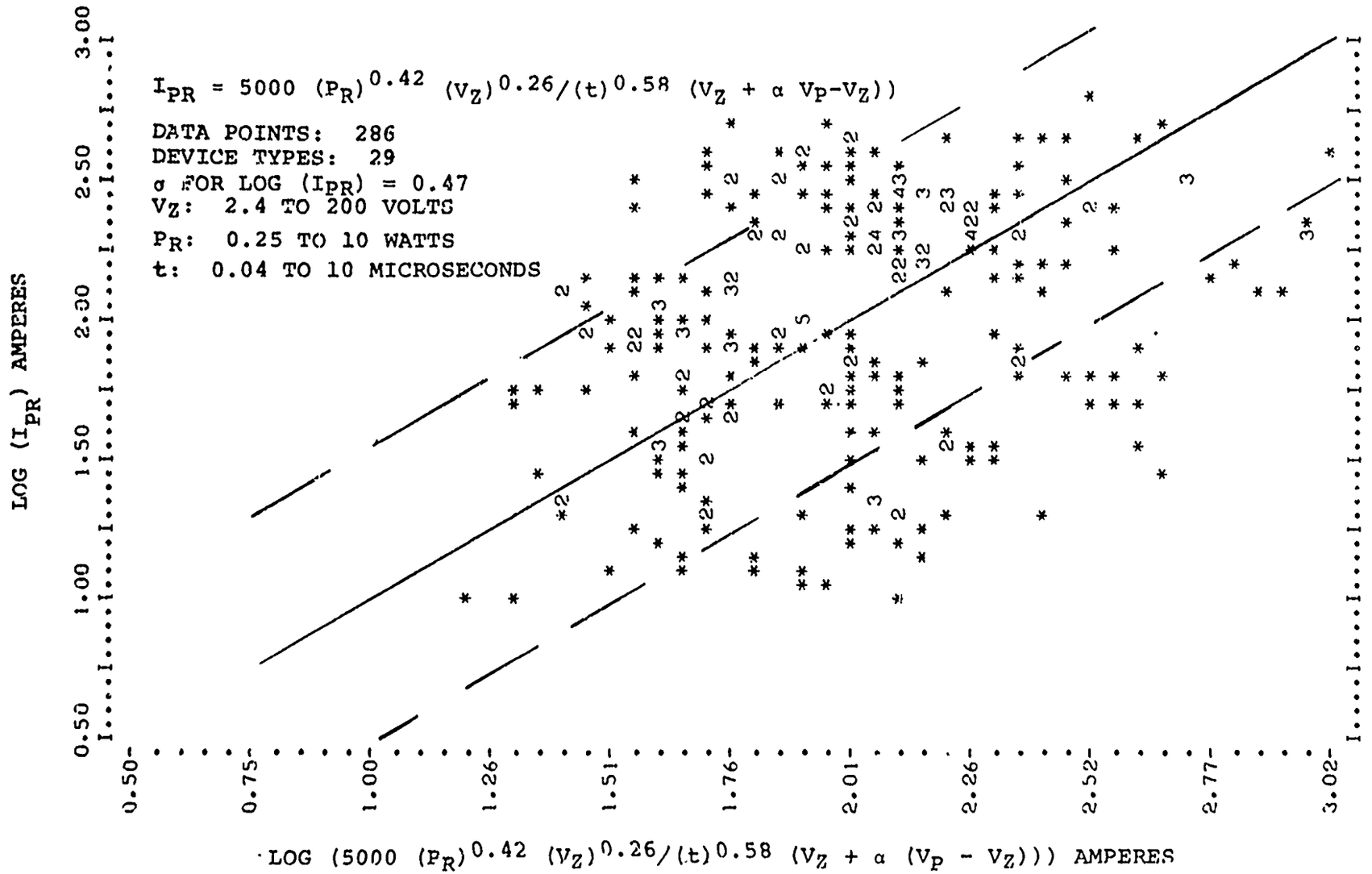

Figure 44. Preliminary Model Describing the Coupling of Bulk Generated Heat to the Diode Junction.

The majority of the data points in the present data base are associated with low and medium voltage Zener diodes (i.e., 40 volts or less) in which direct junction heating should not be as significant as bulk heating. In view of this, and in light of the difficulty associated with obtaining an accurate representation for (55) recourse was made to assuming that the entire damage energy was dissipated only in bulk heating. For this condition, (55) can be expressed as

$$(I_{PR})^2 \, Z_{SR} \, t = \rho C v_B + \sqrt{\rho C k t} \; s_B \tag{76}$$

Since the previous regression analysis indicated that non-adiabatic heating was predominant and recalling from Figure 32 that

$$Z_{SR} = \frac{0.61 \; (V_Z)^{0.6}}{(P_R)^{0.36} \; (I_{PR})^{0.5}} \tag{77}$$

yields, in general terms

$$(I_{PR})^{1.5} = \frac{K}{\sqrt{t}} \tag{78}$$

where

K = Device geometry and material thermal property dependent

which in terms of I_{PR} yields

$$I_{PR} = \frac{K}{(t)^{0.333}} \tag{79}$$

A regression analysis was again performed using the form defined in (79). Again time was expressed in general terms rather than in a predefined value. Figure 45 shows the damage model which was developed. Here, almost all data points lie within $\pm$ a factor of 3.16 and the statistical 3 σ limits are $\pm$ a factor of 9.8. Note the similarity in the exponent as shown in Figure 45 (0.38) with that derived above (0.333). Figures 46 and 47 show a comparison of the damage model with all the "fail" and "no fail" points respectively which are in the data base.

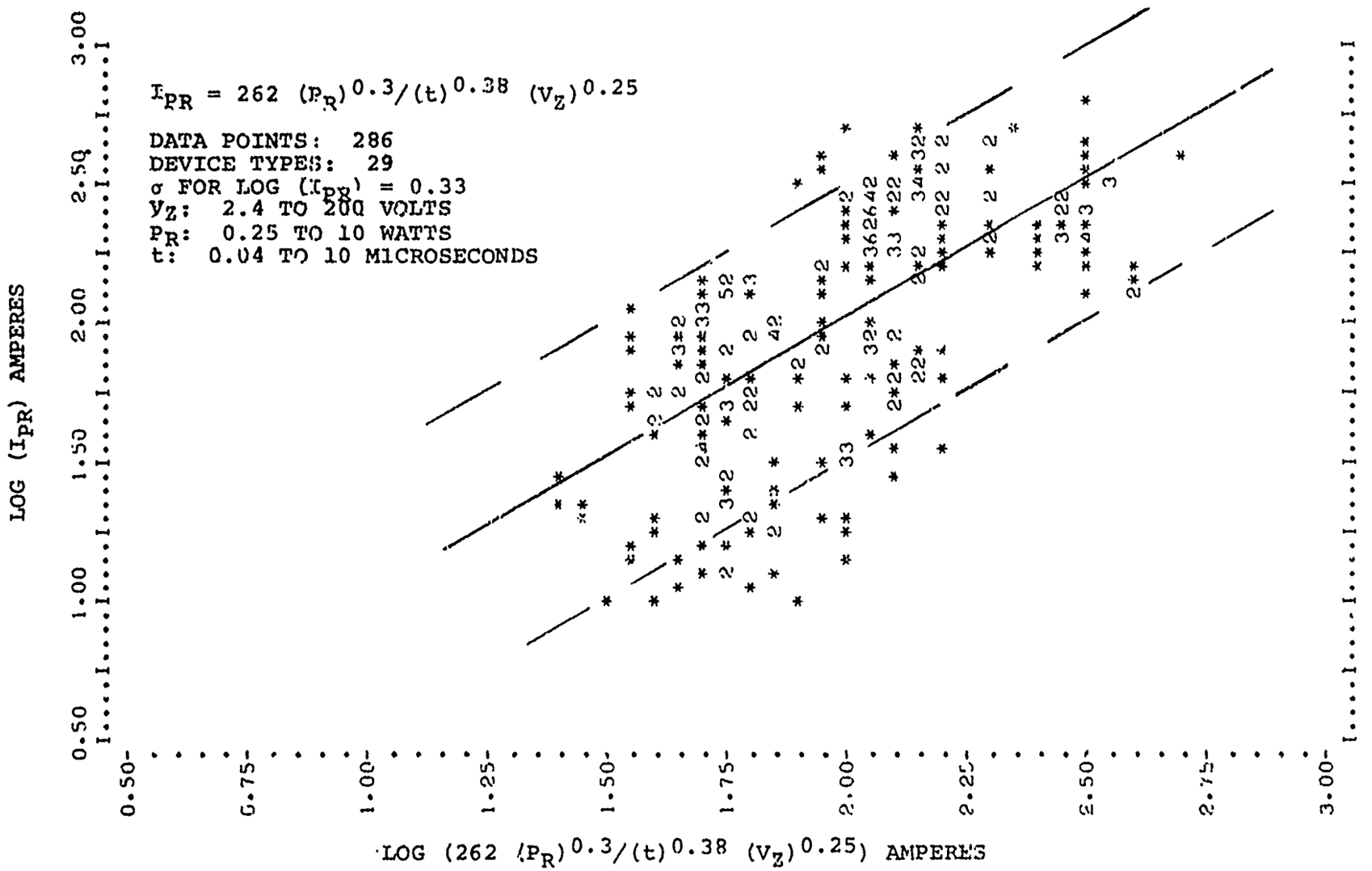

Figure 45. Reverse Pulse Damage Current Characteristics for all Constructi . Type Diodes Functionally Classified as Zener Diodes (Paired No Fail & Fail Data Points Within a Factor of Three).

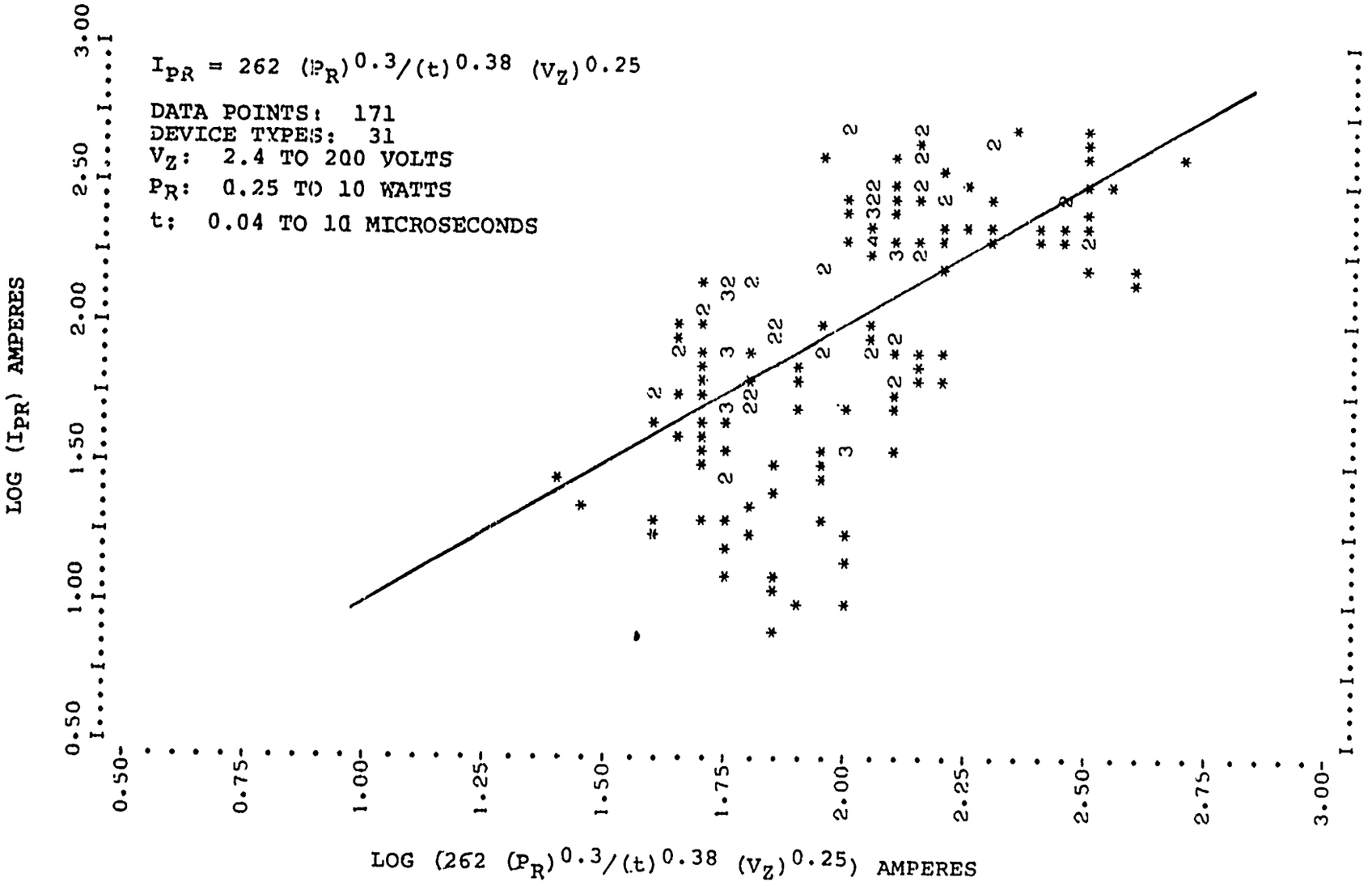

Figure 46. Comparison of the Reverse Pulse Damage Current Model for All Construction Type Zener Diodes with all Fail Points in the Data Base.

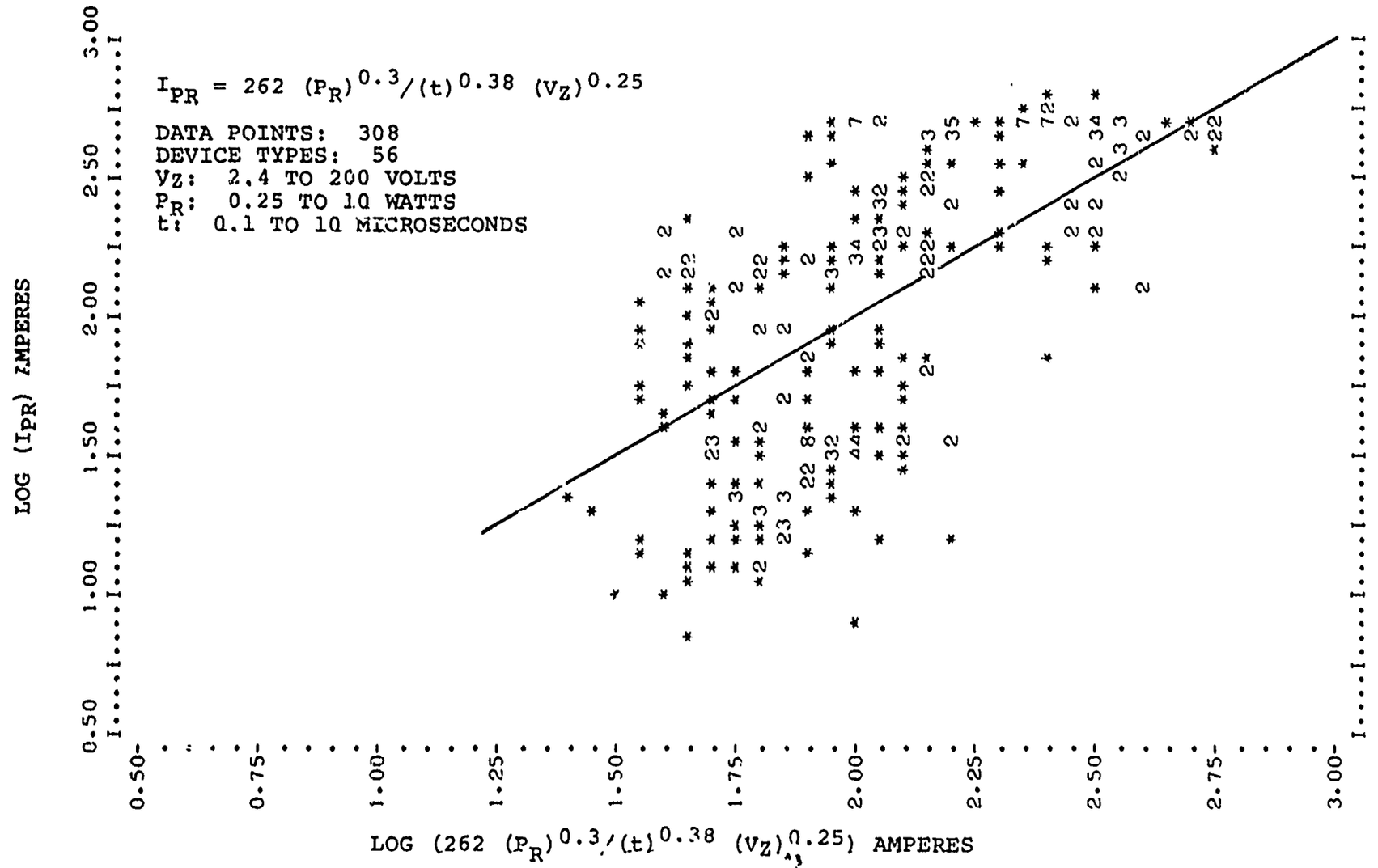

Figure 47. Comparison of the Reverse Pulse Damage Current Model for all Construction Type Zener Diodes with all No Fail Points in the Data Base.

A similar regression analysis was also performed on the individual construction types in the data base. Again, just the paired data points within a factor of three were used. Although the statistical 3 σ error limits are lower in this case, it should be observed that the total range of all variables is much less than that for the entire data base. (Figures 48, 49 and 50)

2.3 Model Development Summary

Engineering type damage models to predict both surge impedance and failure levels of silicon semiconductor diodes when exposed to EMP type environments were developed from multiple regression analyses of a large experimental data base which was supplied by the U. S. Army/HDL and the U. S. Air Force/AFWL. The models were developed for both forward and reverse polarities of junction current conduction. The models are expressed in terms of published device parameters and, as such, do not require a "hands on" device evaluation. The models were developed both for conditions where the device construction was unknown and for conditions where specific device construction is known. Separate models were developed for devices functionally classified as "rectifiers, diodes and switches" and for devices functionally classified as "non-temperature compensated Zener diodes".

The analysis showed that, under high pulse current injection levels, the forward polarity surge impedance of both diode classes exhibited conductivity modulation effects whereby the impedance was inversely proportional to I^N where N was between 0.3 and 0.4. The forward polarity pulse damage in both classes of diodes was found to be due to I^2R bulk heating under non-adiabatic conditions for the pulse widths and device junction areas evaluated. The conductivity modulation effects caused the exponent of the time dependence for damage to lie in the range of 0.3 as would be expected from these effects.

Under reverse pulse polarity conditions the low and medium voltage Zener diodes also exhibited a surge impedance associated with the bulk material and also partially dependent on conductivity modulation effects. The reverse polarity surge impedance of the "rectifiers, diodes and switches" was found to be strongly dependent on both device breakdown voltage level and pulse current level. The reverse polarity pulse damage in the Zener diodes was found to be due also to I^2R bulk heating under non-adiabatic conditions. The rectifiers, diodes and switches, however, exhibited junction heating effects which were also characteristic of non-adiabatic conditions.

A summary of the various models developed, together with the associated 1 σ statistical error limits, is given in Table 6. The models are shown only for the conditions where diode construction information is unknown. For practicality, all parameters which exhibited an exponent of dependency less than 0.035 have been omitted.

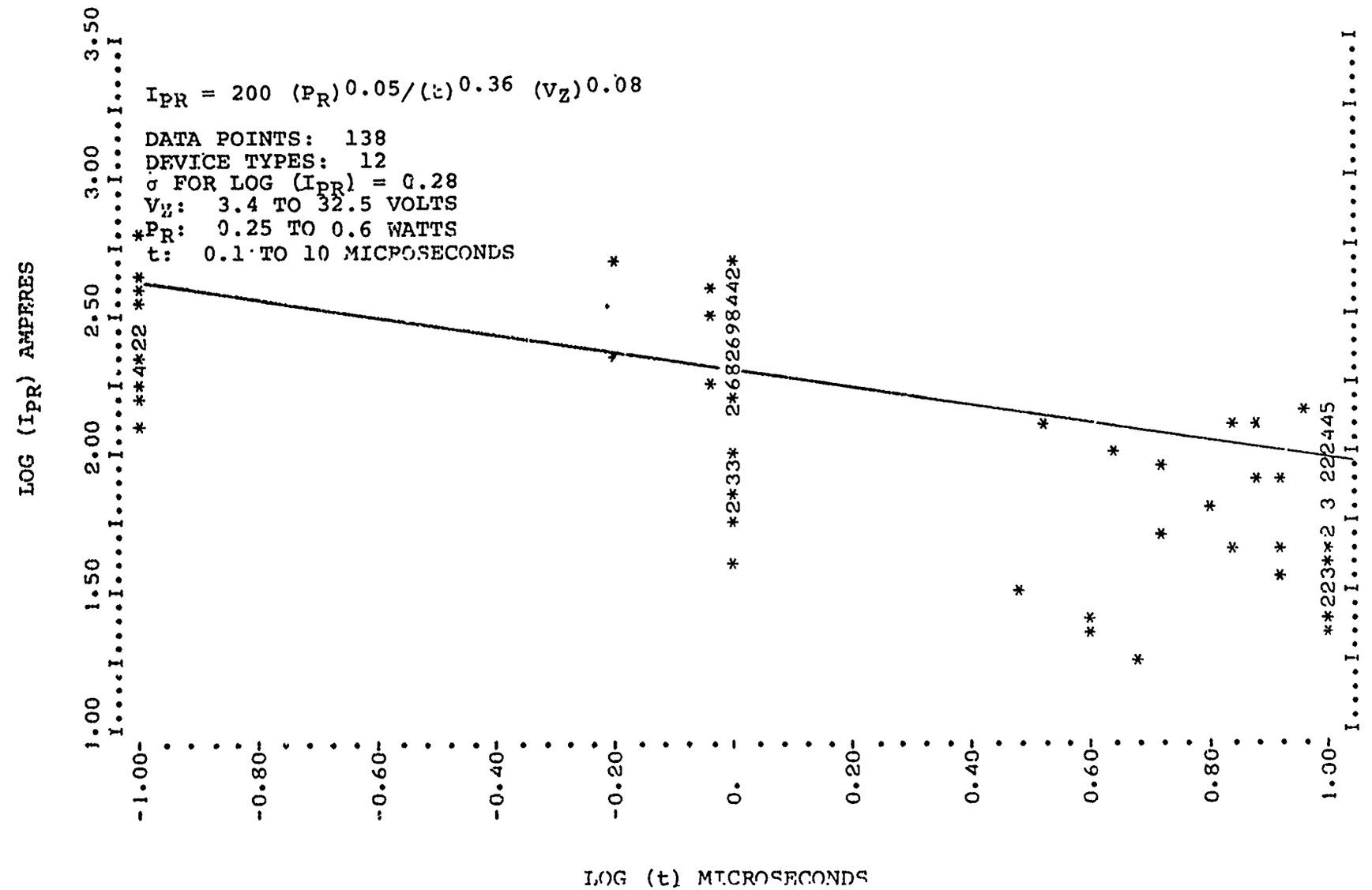

Figure 48. Reverse Pulse Damage Current Characteristics of Alloy Diodes Functionally Classified as Zener Diodes (Paired No Fail & Fail Points Within a Factor of Three).

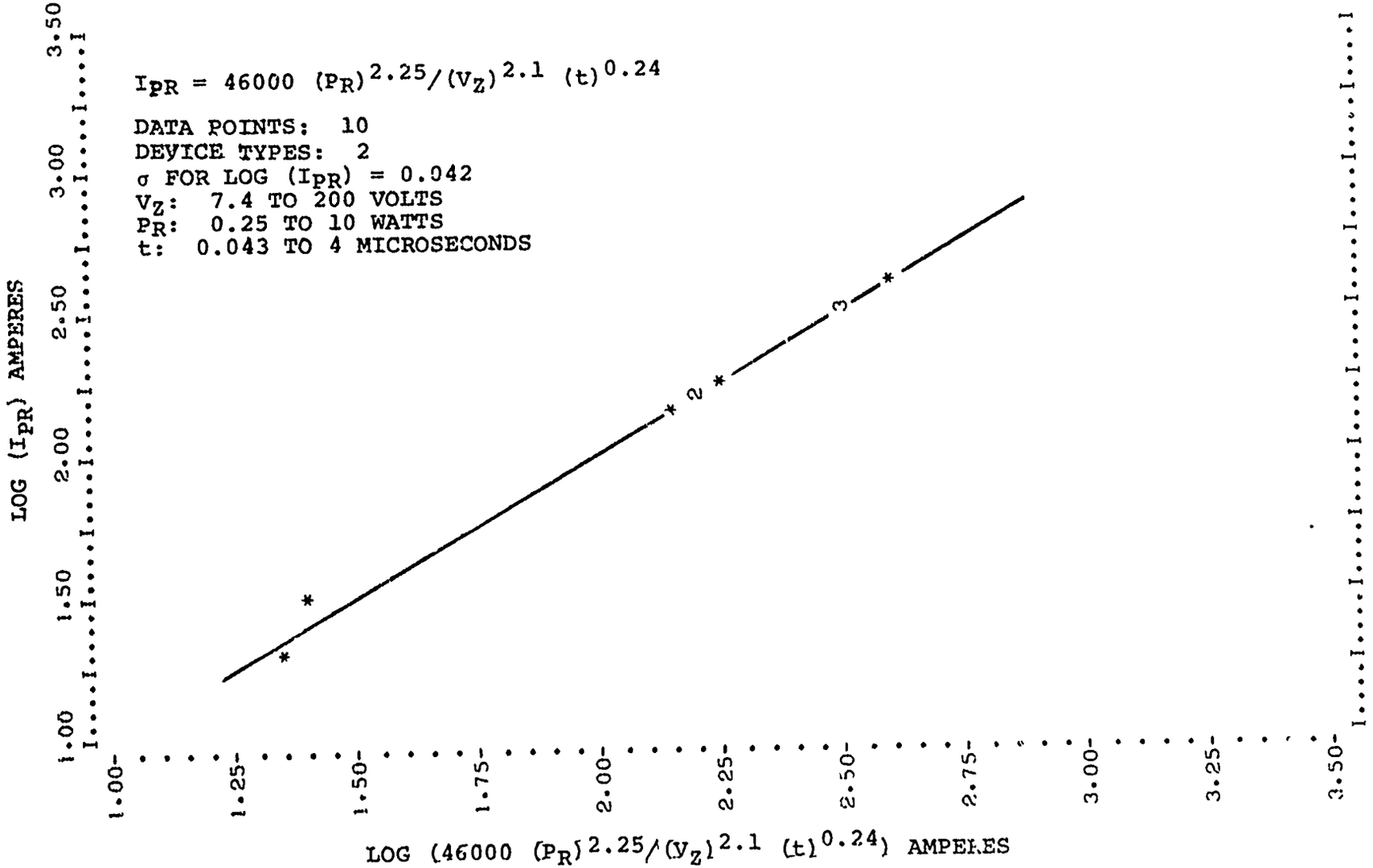

Figure 49. Reverse Pulse Damage Current Characteristics of Mesa Diodes Functionally Classified as Zener Diodes (Paired No Fail & Fail Points Within a Factor of Three).

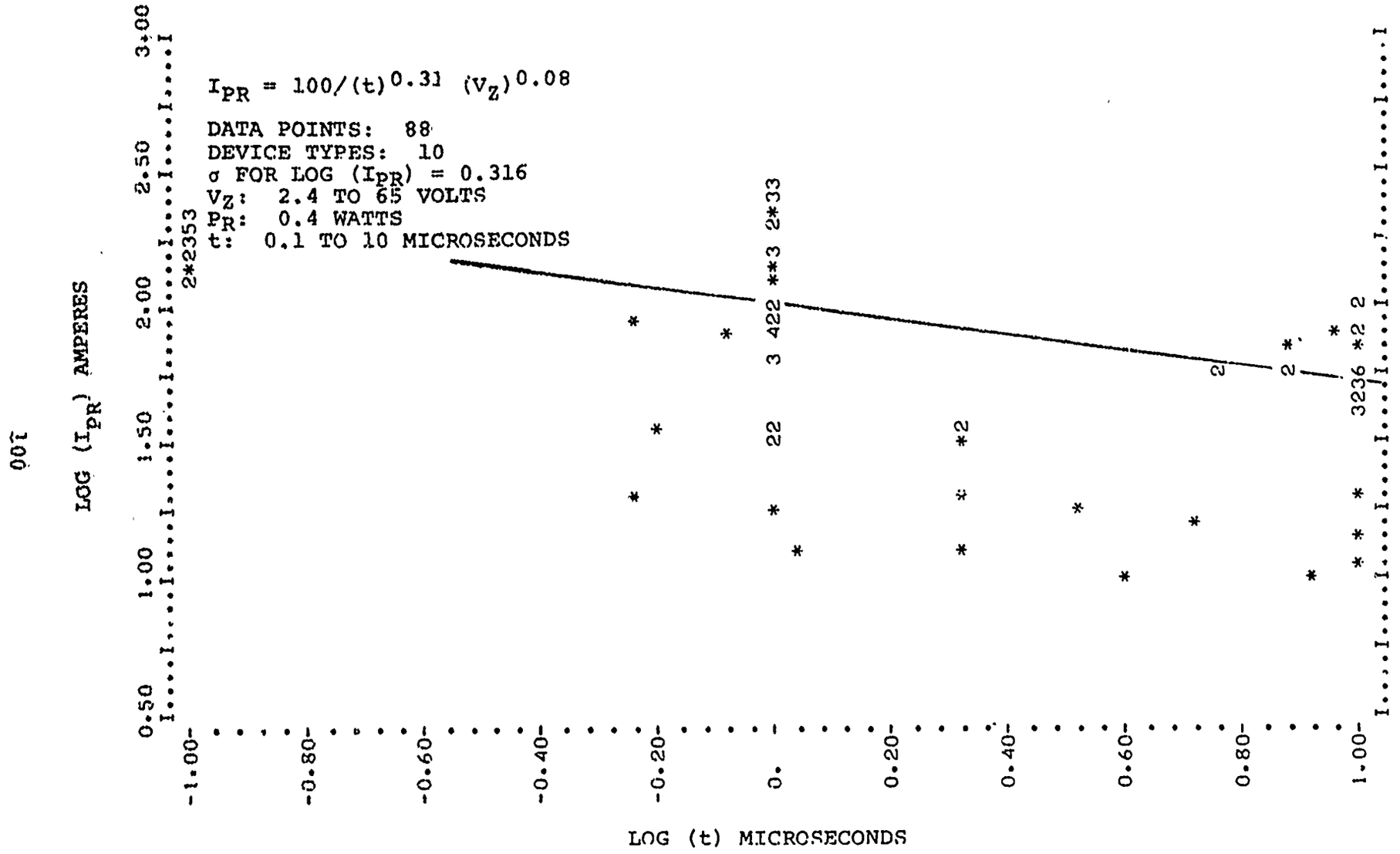

Figure 50. Reverse Pulse Damage Current Characteristics of Planar Diodes Functionally Classified as Zener Diodes (Paired No Fail and Fail Points Within a Factor of Three).

Table 6. Summary of Pulse Damage Models Developed for Diodes Independent of Construction Type

DIODE TYPE	Z_{SF}	I_{PF}	Z_{DR}	Z_{SR}	I_{PR}
G.E. IN4148	$\frac{3.4}{(I_{PF})^{0.31}}$ σ = 1.12 X	$\left(\frac{37}{t} + \frac{220}{\sqrt{t}}\right)^{0.59}$ σ = 1.16 X	$\frac{140}{(I_{PR})^{0.975}}$ σ = 1.06 X	$\frac{25.6}{(I_{PR})^{0.85}}$ σ = 1.59 X	$\frac{0.17}{t} + \frac{0.306}{\sqrt{t}}$ σ = 1.58 X
RECTIFIERS, DIODES AND SWITCHES	$\frac{1.15}{(I_O)^{0.42}(I_{PF})^{0.38}}$ σ = 1.82X	$\frac{69\,(I_O)^{0.43}}{(t)^{0.35}}$ σ = 1.62X	$\frac{0.9\,(V_Z)^{1.1}}{(I_{PR})^{0.91}}$ σ = 1.51 X	$\frac{0.042\,(V_Z)^{1.38}}{(I_{PR})^{0.76}}$ σ = 2.88 X	$\frac{1.9\,(I_O)^{0.4}}{(t)^{0.64}}$ σ = 2.51 X
ZENER DIODES (NON TEMPERATURE) COMPENSATED)	$\frac{1.1}{(P_R)^{0.41}(I_{PF})^{0.4}}$ σ = 1.76X	$\frac{500\,(P_R)^{0.88}}{(t)^{0.312}}$ σ = 2.24X	$\frac{1.48\,(V_Z)^{0.72}}{(P_R)^{0.23}(I_{PR})^{0.65}}$ σ = 1.78X	$\frac{0.61\,(V_Z)^{0.6}}{(P_R)^{0.36}(I_{PR})^{0.5}}$ σ= 2.24X	$\frac{262\,(P_R)^{0.3}}{(V_Z)^{0.25}(t)^{0.38}}$ σ = 2.14X

3. Junction Field Effect Transistor Damage Testing

Bipolar semiconductor devices have been studied in detail in the past and their associated pulse response and damage characteristics are well known. Junction field effect transistors (JFET's), in contrast, have not received anywhere near the attention that bipolar devices have. As a result, comparitively little is known about their pulse response and damage characteristics. As such, the objective of this task was to perform a detailed experimental pulse damage characterization of a typical JFET device in order to provide sufficient information to determine the basic pulse response and damage characteristics of JFET structures.

To meet this objective extensive pulse damage testing was performed on the Motorola 2N4392 N-Channel silicon JFET. The 2N4392 is a depletion mode device designed for chopper and high speed switching applications. A total of 215 units were evaluated in the test program for various combinations of terminal pairs in biased and unbiased configurations. The pulse damage testing consisted of the following pulse conditions: square wave testing without bias (3 nanosecond to 100 microsecond pulse widths) ; square wave testing with bias (10 nanoseconds to 1 microsecond pulse widths); multiple square wave testing; bipolarity square wave testing and 5 MHz damped sinusoid testing. The gate-source and source-drain terminal pairs were evaluated under both positive and negative pulse polarities.

The permanent damage experiments were of a step-stress nature. That is, single pulses of increasing energy level and fixed time duration were consecutively applied to a selected device terminal pair until permanent damage occurred. The occurrence of damage was determined by examing the device characteristic curves which were obtained prior to the initial pulse and following each subsequent pulse of energy. Device damage was taken as the point where the first minimum discernable change in device characteristics was observed. After examing the safe-fail energy levels of this device, the energy increments were then changed and the procedure repeated for a number of similar devices using the same bias conditions and terminal pair input.

The high injection level pulse V-I characteristics of the gate-source and source-drain terminal pairs for each pulse polarity are shown in Figures 51 to 54. Figure 51 shows that when the gate-source junction is pulsed in the forward direction, a normal forward bias junction characteristic is observed. Similarly, Figure 52 shows that under reverse bias conditions the gate-source junction exhibits a second breakdown response together with a moderate reverse surge impedance characteristic. The corresponding V-I characteristics for the source-drain terminal pair with the gate open is shown in Figures 53 and 54. Both terminal pairs exhibit normal depletion and pinch-off characteristics as well as avalanche characteristics. At high avalanche injection levels, a

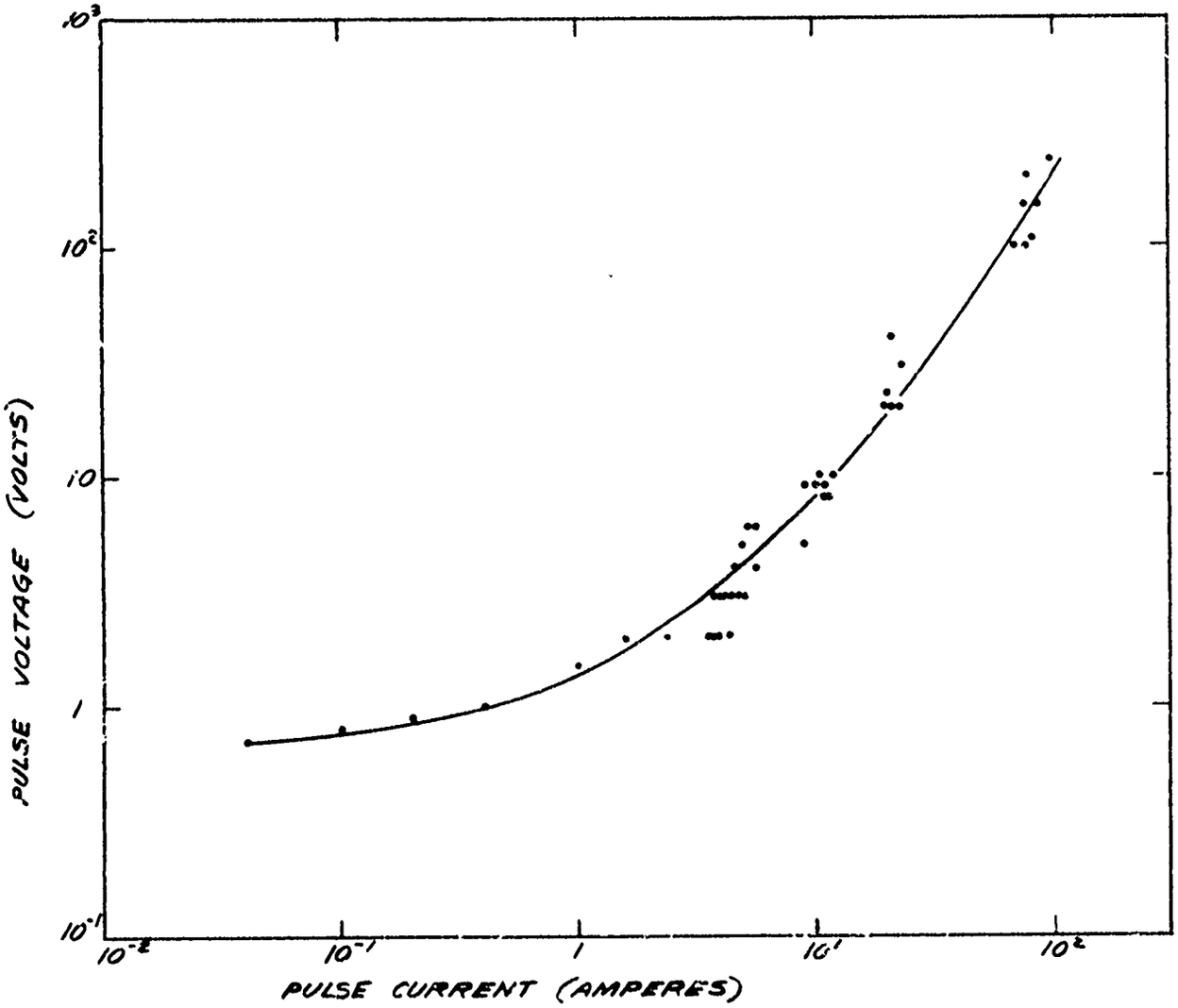

Figure 51. Voltage-Current Characteristics of the Motorola 2N4392 JFET Pulsed in the Gate-to-Source Polarity with the Drain Open.

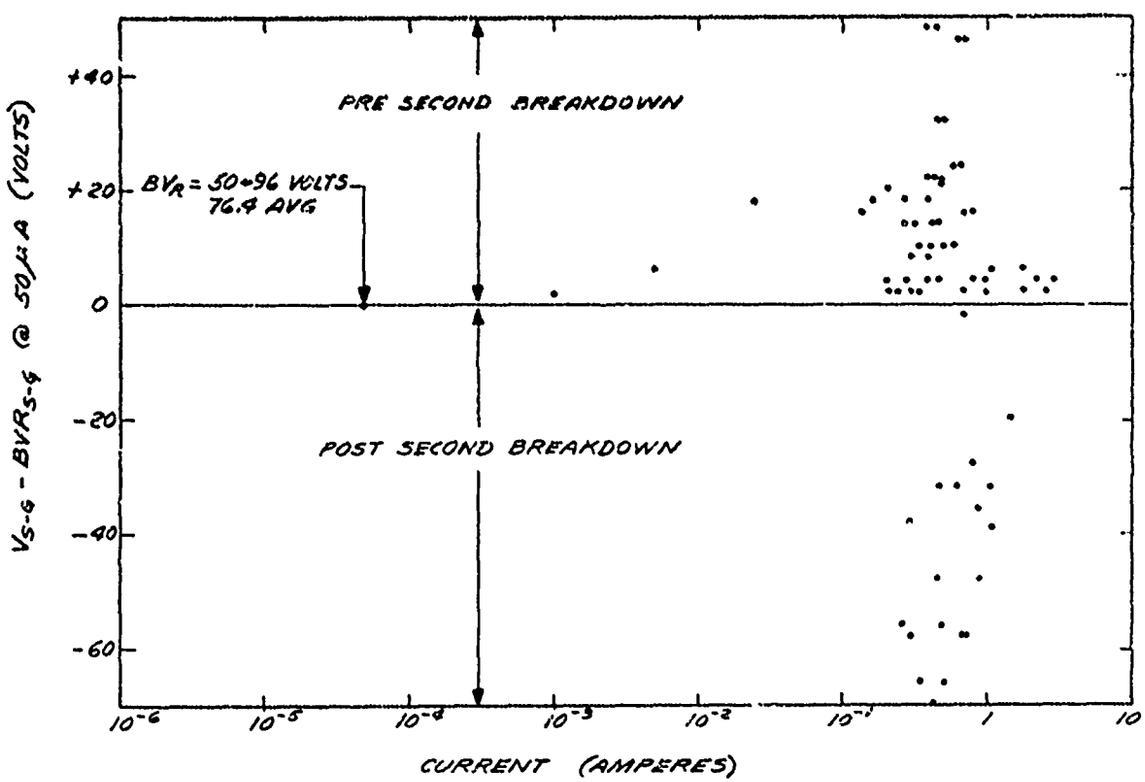

Figure 52. Voltage-Current Characteristics of the Motorola 2N4392 JFET Pulsed in the Source-to-Gate Polarity with the Drain Open.

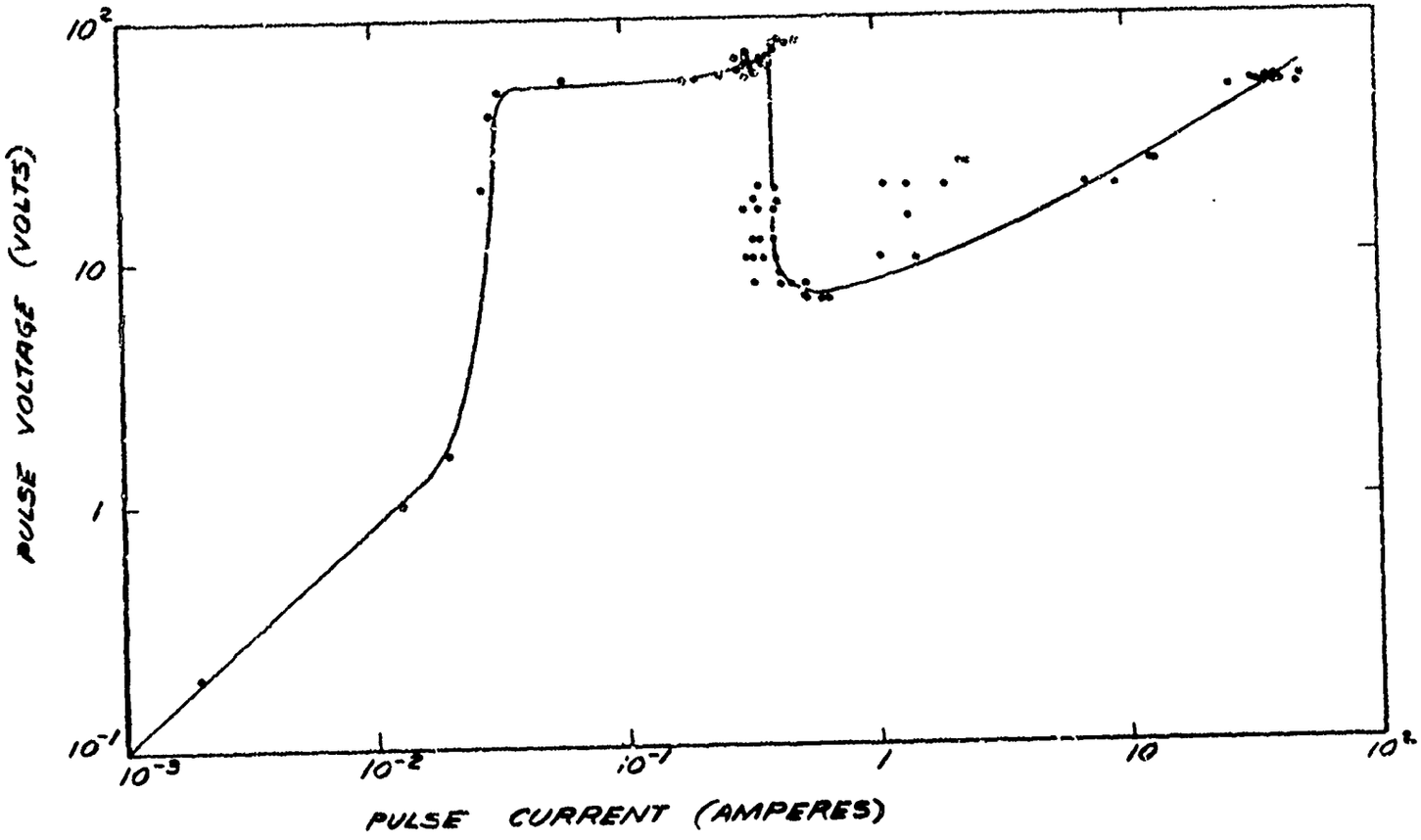

Figure 53. Voltage-Current Characteristics of the Motorola 2N4392 JFET Pulsed in the Source-to-Drain Polarity with the Gate Open.

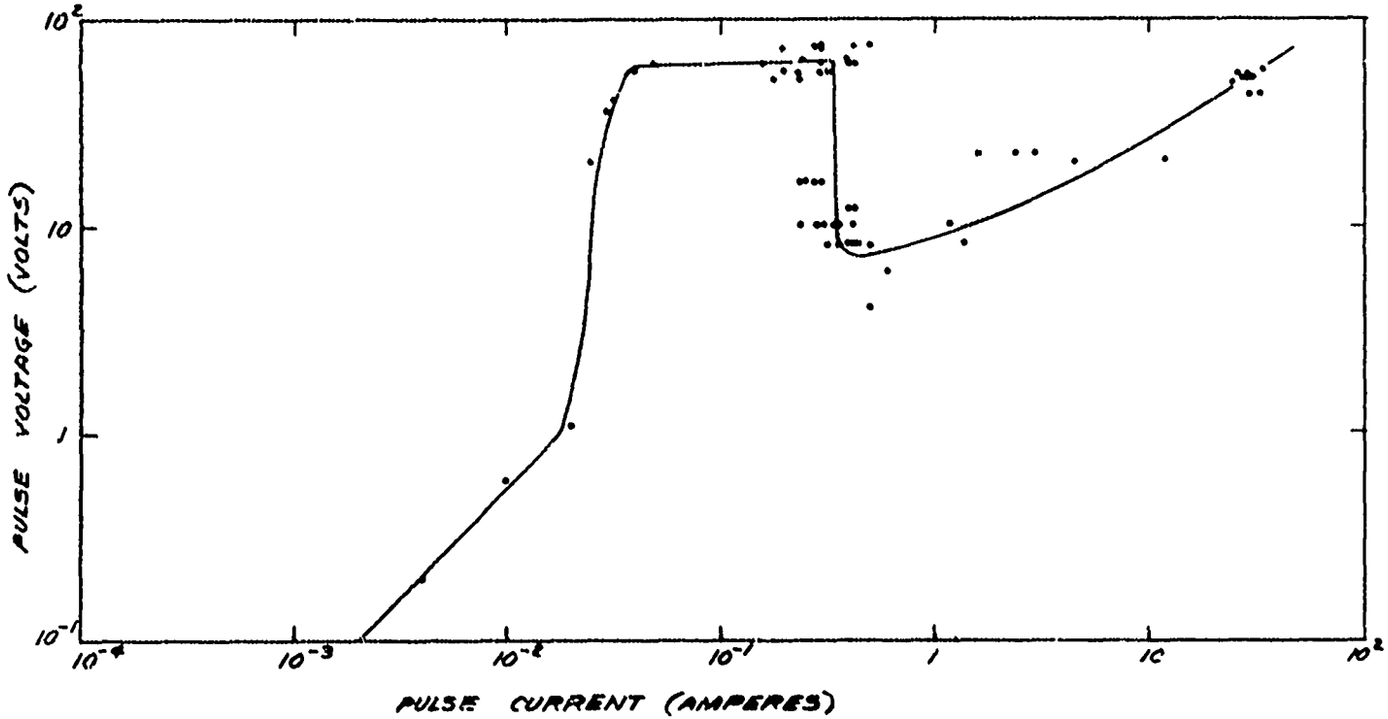

Figure 54. Voltage-Current Characteristics of the Motorola 2N4392 JFET Pulsed in the Drain-to-Source Polarity with the Gate Open.

second breakdown occurs at a relatively fixed injection level (i.e., pulse current levels in the range of 0.1 to 1 ampere) in spite of the wide range of pulse testing performed (i.e., 3 nanoseconds to 100 microseconds). As such, one would expect the device behaviour to be significantly different from the traditional, well-defined energy-time characteristics of bipolar devices which exhibit avalanche breakdown in the depletion region. This is, indeed, the case as is evidenced from a close examination of the device damage characteristics.

In the forward polarity the gate-source junction behaves like a normal forward biased diode. Because of the relatively large junction to metallization area ratio in the device, metallization burnout occurred before junction damage. Figure 55 shows the square wave damage current characteristics of the device in the forward direction. The current versus time profile follows exactly what one would expect[1] for metallization burnout and comparisons with theoretical models[2] show a predicted value of 12 to 19 amperes (based on minimum and maximum metallization controls) at a 1 microsecond pulse width which agrees with the 9 to 13 ampere experimentally observed levels.

The reverse polarity gate-source junction, however, exhibited some very interesting characteristics, as shown in Figure 56. Here, the device was observed to exhibit a second breakdown response which was initiated at a relatively constant pulse current injection level from 30 nanoseconds to 100 microseconds. Whenever second breakdown occurred, device damage resulted even though the post second breakdown currents were within a factor of 1.5 of the pre-second breakdown levels. At the 10 nanosecond and 3 nanosecond pulse levels, a second breakdown response was not clearly discernible for either the "no-fail" or "fail" conditions. Hence, it is unclear whether these levels shown represent pre- or post-second breakdown conditions. Nonetheless, the pulse current levels required for device damage increased sharply below 30 nanoseconds.

The pulse response and damage characteristics of the source-drain terminal are similar to the reverse bias gate-source junction and are somewhat more interesting. The device was again observed to exhibit a second breakdown response which as initiated at a relatively constant pulse current injection level as shown in Figures 57 and 58. The response was similar for either direction of pulse polarity. Note, however, that in this case second breakdown could be initiated without producing device damage. Also, the pulse current required for damage is seen to again increase sharply below 30 nanoseconds and in this region the damage levels are significantly higher than the second breakdown initiation levels.

Figures 59, 60 and 61 show a summary of the pulse damage levels associated with the reverse bias gate-source junction and the drain-source terminal pair. These characteristics are shown in terms of the range of "safe" and "fail" currents which were experi-

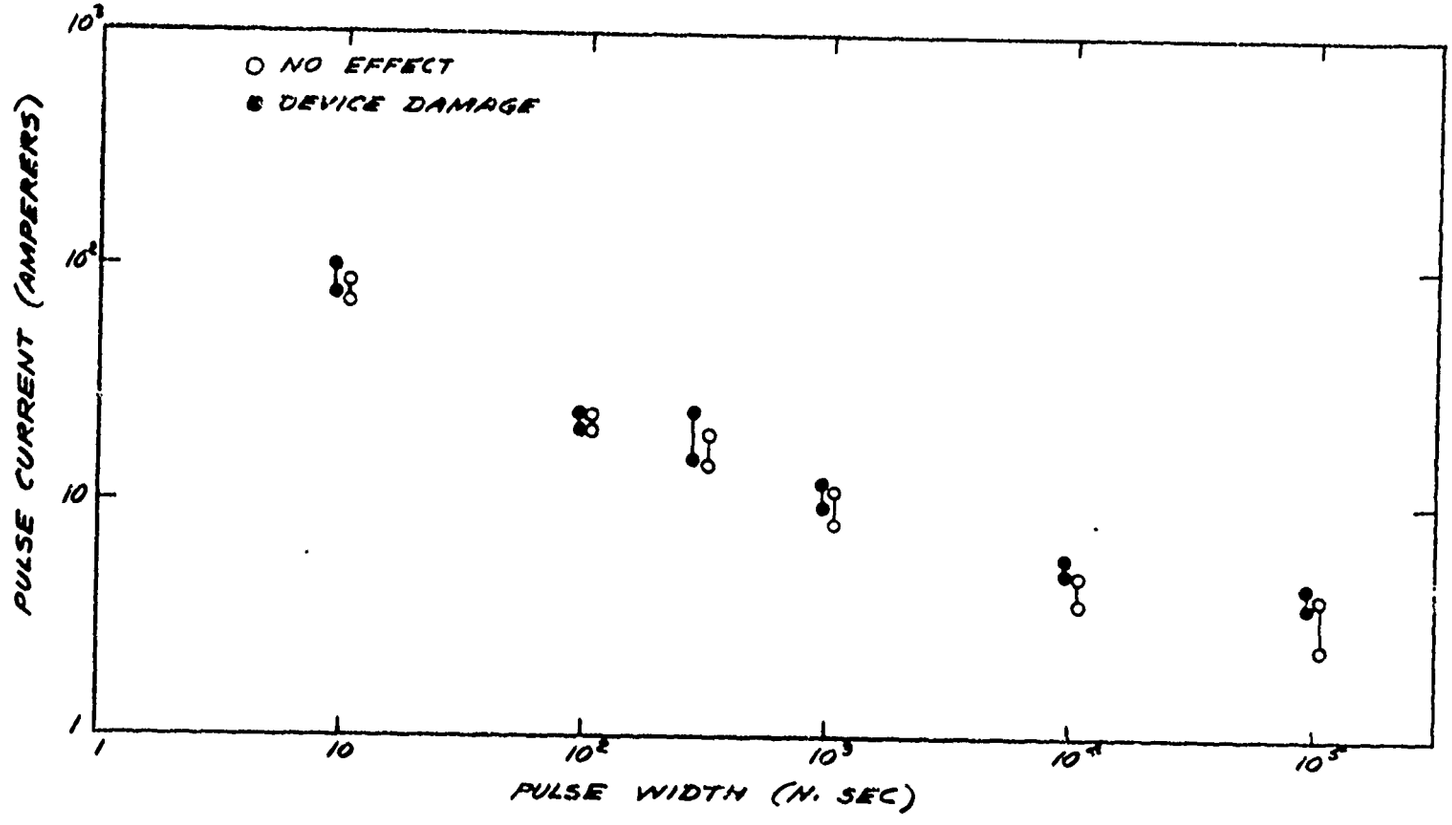

Figure 55. Pulse Response Characteristics of the Gate-to-Source, Drain Open Configuration.

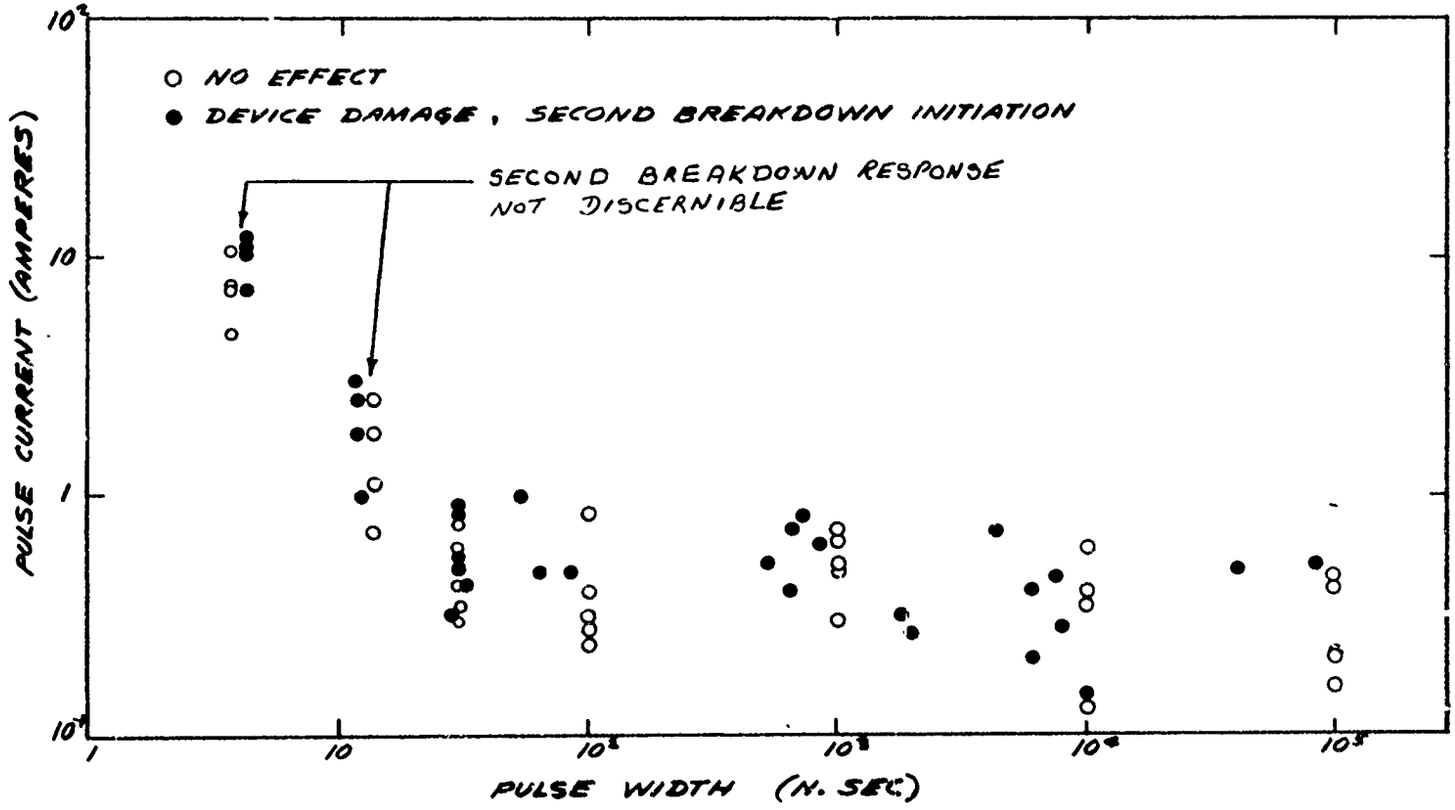

Figure 56. Pulse Response Characteristics of the Source-to-Gate, Drain Open Configuration.

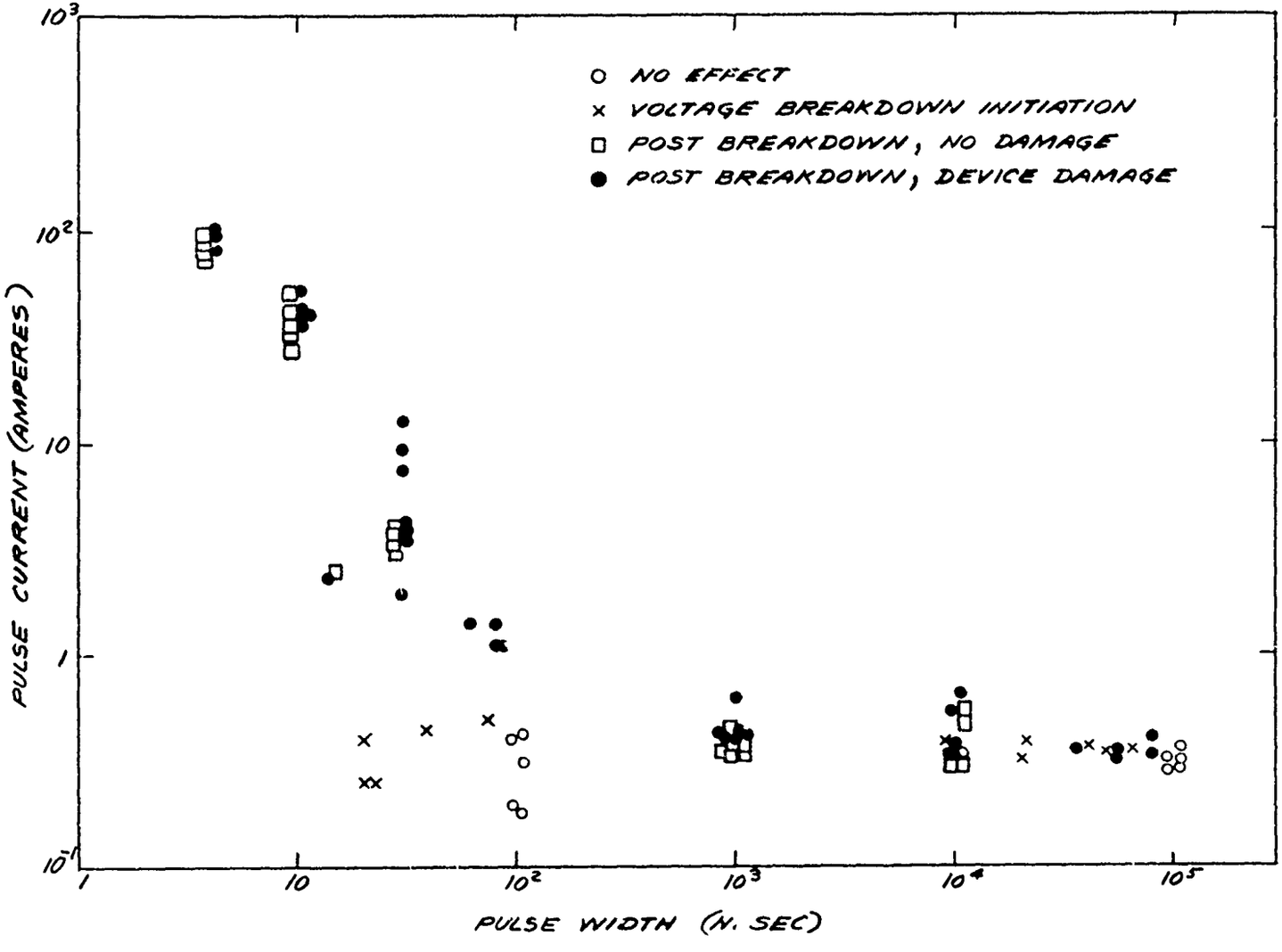

Figure 57. Pulse Response Characteristics of the Source-to-Drain, Gate Open Configuration.

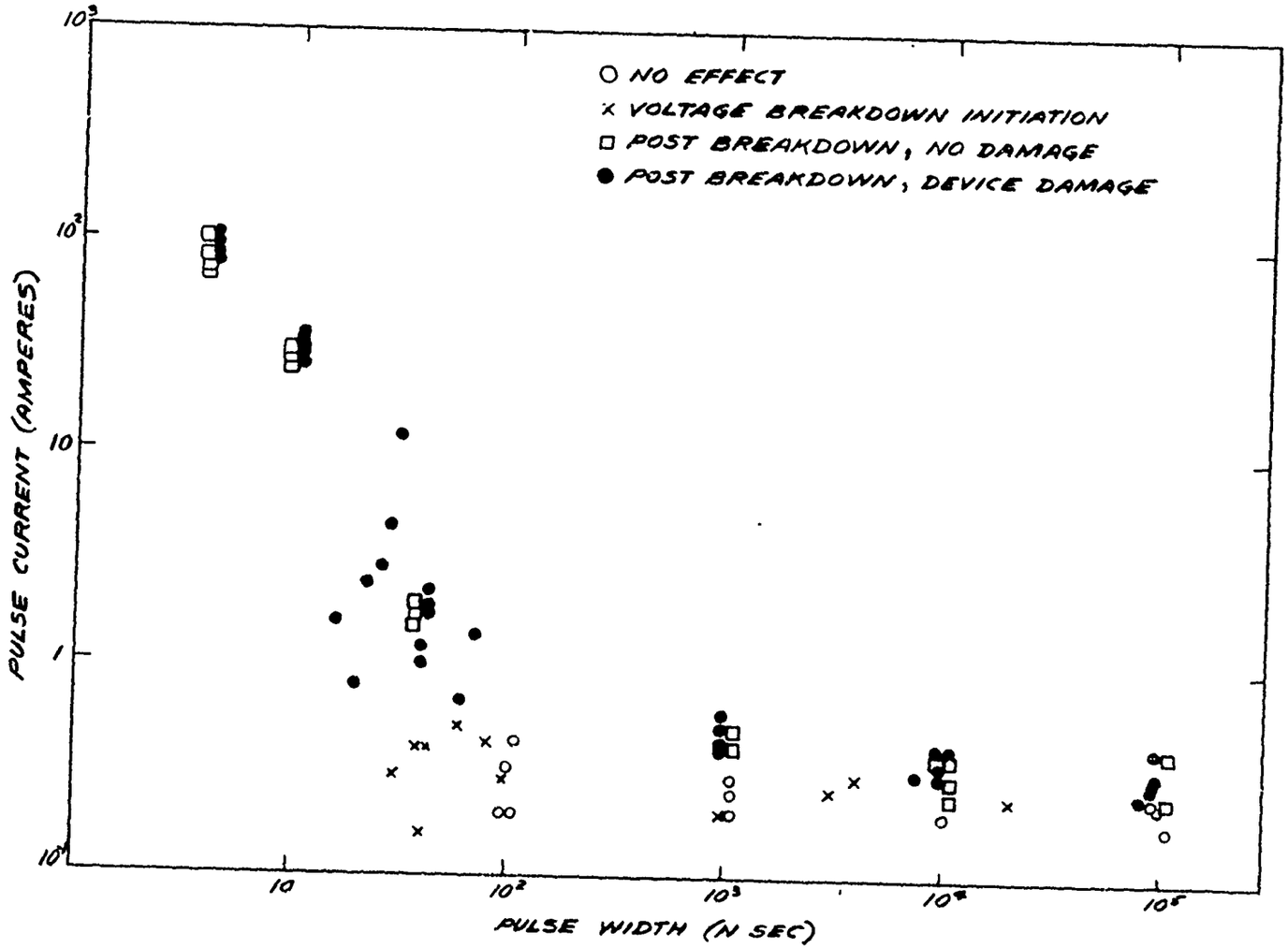

Figure 58. Pulse Response Characteristics of the Drain-to-Source, Gate Open Configuration.

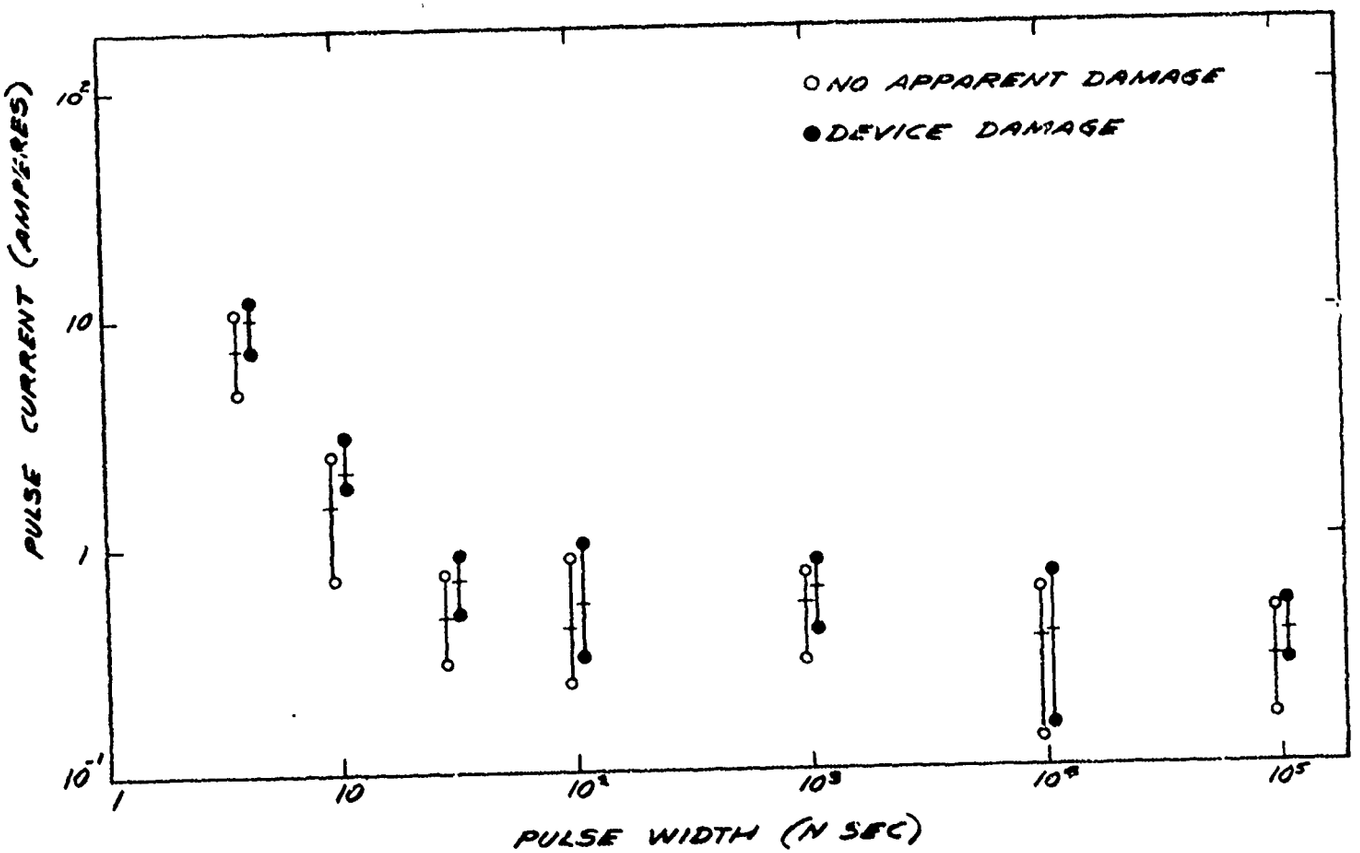

Figure 59. Pulse Damage Current Characteristics of the Source-to-Gate, Drain Open Configuration.

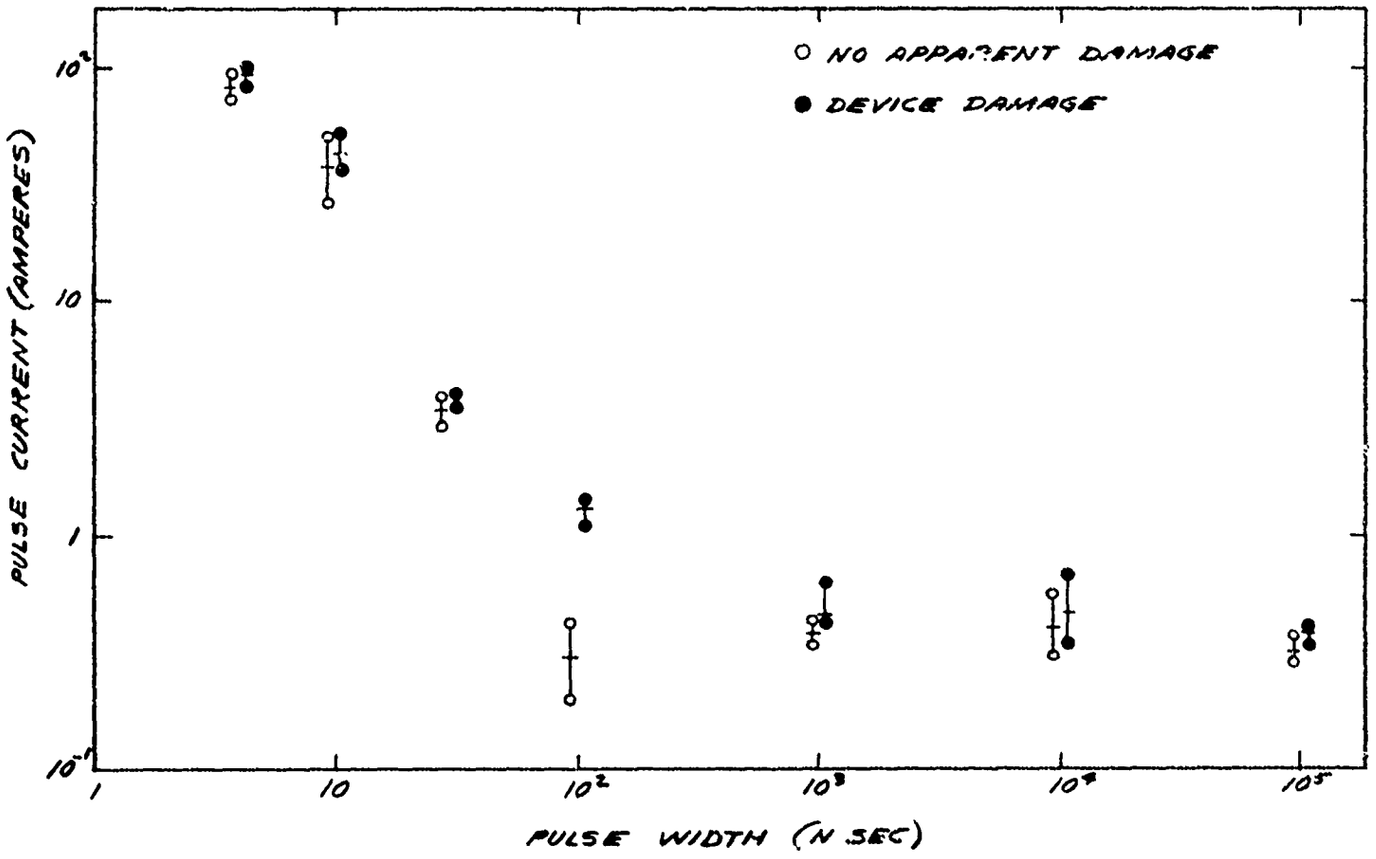

Figure 60. Pulse Damage Current Characteristics of the Source-to-Drain, Gate Open Configuration.

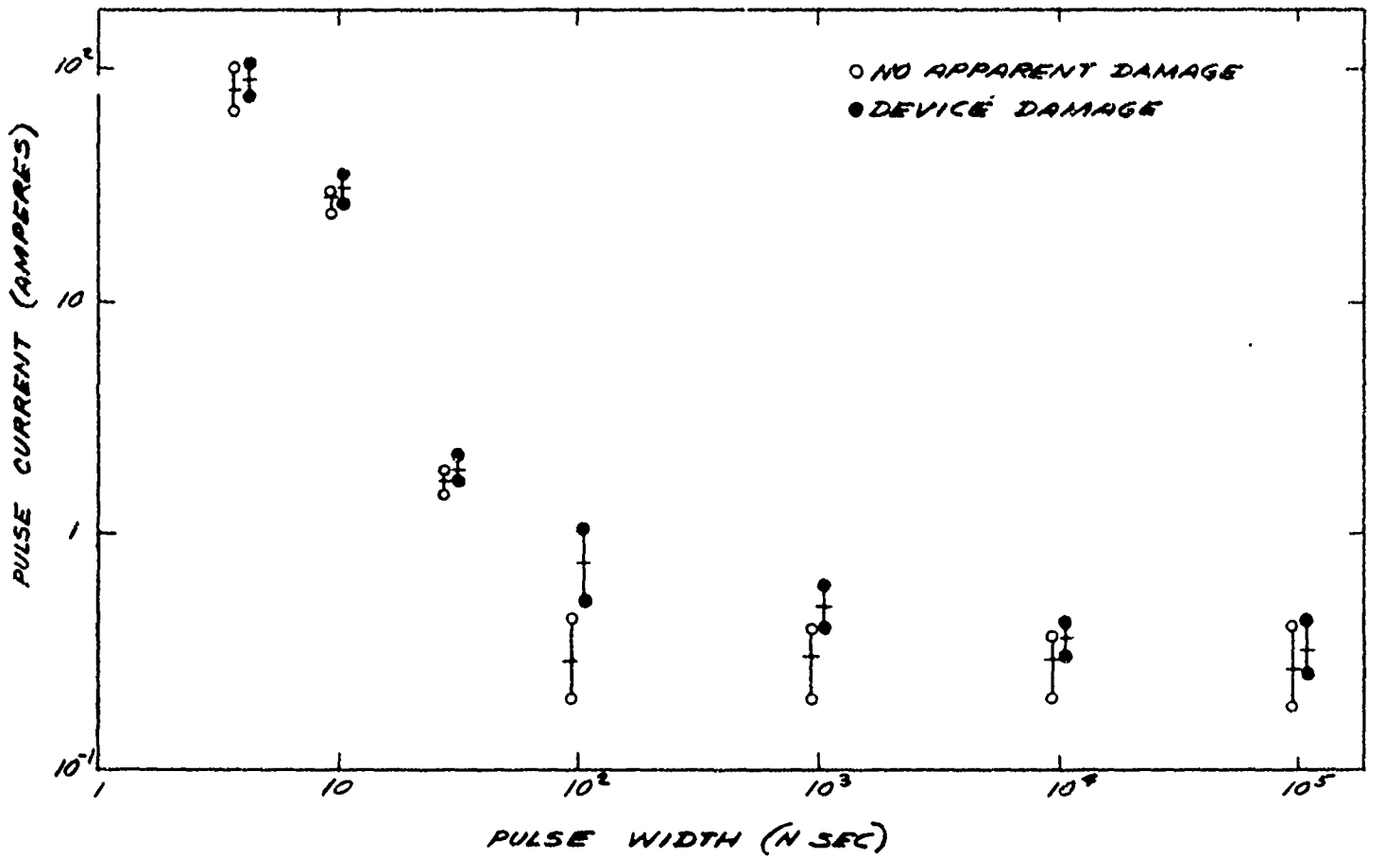

Figure 61. Pulse Damage Current Characteristics of the Drain-to-Source, Gate Open Configuration.

mentally observed and do not include the various aspects of second breakdown shown in Figures 56, 57 and 58. The similarity between the form of the time dependent damage characteristics for all three conditions can be seen. Table 7 shows a summary of the pulse damage aspects with respect to the effects on various device operating parameters. The parameters shown are forward transconductance (Y_{FS} at V_{DS} = 10 Volts, V_{GS} = -1 Volt), gate-source breakdown voltage (BV_{GS} at I_{GS} = 50 μa), gate-source forward voltage (VF_{GS} at I_{GS} = 1 ma), gate-drain breakdown voltage (BV_{GD} at I_{GD} = 50 μa), gate-drain forward voltage (VF_{GD} at I_{GD} = 1 ma), drain-source on voltage (VD_{on} at I_D = 10 ma, V_{GS} = 0 Volts), the gate-to-source and drain leakage current (I_{GSD} at V_{GSD} = 20 Volts) and the pinch-off voltage (V_p at I_{DS} = 10 μa and V_{DS} = 10 Volts). The primary damage effect in the S-G, D-S, and S-D polarities was a degradation in the G-S and G-D reverse junction characteristics. The forward junction characteristics were relatively unaffected, as was Y_{FS}, VD_{on} and V_p. Substantial gate leakage current increases were observed, though. In the G-S polarity large metallization damage accompanied by internal open circuits were observed.

Long[4] has proposed a number of damage mechanisms which could be possible in JFET structures. These are current mode second breakdown, surface breakdown and a thermal model based on heating in the channel opening in pinch-off and modeled as an infinitely long, small diameter cylinder to describe the heating conditions along a substantial portion of the entire gate length. The thermal model provides a reasonable fit to the data in the greater than 30 nanosecond range. The current mode second breakdown and surface breakdown considerations likewise provide a qualitative explanation of the greater than 30 nanosecond characteristics. The near linear rise in damage current level below 30 nanoseconds, however, may be associated with the current required to charge the junction capacitance to a critical voltage level and could indicate a surface breakdown mechanism. The exact failure mechanisms associated with the 2N4392 device, though, have not been established at this time. Further definition of the JFET current gain and other conduction phenomena under high injection levels is required to achieve a firmer understanding of the failure mechanisms.

An indication of the relative unimportance of DC bias on JFET vulnerability at both the long and short pulse widths is given in Table 8. Here, the JFET was biased well into pinch-off by a -10 Volt D.C. level on the gate and the drain-source terminal pair damage level for both pulse polarities was evaluated and compared to the unbiased condition. Device vulnerability was evaluated in both the low current level (1 microsecond pulse width) and high current level (10 nanosecond pulse width) damage regions. In neither case did the DC bias conditions alter the vulnerability levels of the device.

---

[4]Long, D.M. and Swant, D.H., "Burnout of Junction Field Effect Transistors", IEEE Transactions on Nuclear Science, Volume NS-20, #6, pp.149-157, December 1973.

Table 7. Pulse Power Damage Effects in the Motorola 2N4392 N-Channel JFET

PULSE POLARITY	PULSE WIDTH (μ SEC)	DEVICES TESTED	SEC. BKDN. RESPONSE	SEC. BKDN. DAMAGE	DEVICES EXHIBITING PARAMETER CHANGE							
					Y_{FR}	ΔV_{GS}	VF_{GS}	ΔV_{GD}	VF_{GD}	VD_{ON}	t_{OSD}	V_P
G-S, D OPEN	100	5	0		5*	5*	5*	5	5	5	5	5*
	10	5	0		5*	5*	5*	3	2	5	4	5*
	1	5	0		5*	5*	5*	0	0	5*	5	5*
	0.1	4	0		4*	4*	4*	2	0	4*	2	4*
	0.03	5	0		5*	5*	5*	1	0	5*	3	5*
	0.01	5	0		5*	5*	5*	2	0	5*	2	5*
S-G, D OPEN	100	5	5	5	5	5	5	5	5	0	5	2
	10	5	5	5	1	5	4	5	4	1	5	1
	1	5	5	5	3	5	0	5	2	1	5	0
	0.1	5	5	5	4	5	2	3	2	0	5	1
	0.03	6	6	6	0	6	0	1	0	4	6	0
	0.01	5	7	0	1	6	1	2	1	0	5	0
	0.003	5	7	0	0	6	0	0	0	4	5	0
D-S, G OPEN	100	5	5	3	2	5	0	5	0	0	3	3
	10	5	5	1	1	5	0	5	1	0	0	0
	1	5	5	3	1	5	0	5	1	1	5	2
	0.1	5	5	5	0	5	1	5	0	1	5	1
	0.03	10	10	5	0	1	0	9	0	2	8	0
	0.01	5	7	0	1	5	0	5	0	1	1	0
	0.003	5	7	0	1	5	0	5	0	3	3	2
S-D, G OPEN	100	5	5	5	0	5	0	0	0	0	4	0
	10	5	5	1	0	5	0	0	0	0	4	0
	1	5	5	0	1	5	0	5	0	0	5	0
	0.1	5	5	5	0	5	0	0	0	0	4	0
	0.03	10	10	4	0	8	0	2	0	1	10	0
	0.01	5	7	0	0	5	0	0	0	0	0	0
	0.003	5	7	0	5	4	1	2	1	4	2	1
					A	B	B	B	B	C	D	D

* = OPEN CIRCUIT
A = LESS THAN 2X INCREASE & DECREASE
B = DECREASE
C = INCREASE & DECREASE
D = INCREASE

Table 8. D.C. Bias Effects on the Drain-Source Square Wave Vulnerability of Motorola 2N4392 N-Channel JFET's

Pulse Polarity	Pulse Width	Gate Bias	Number Devices Tested	Experimental Damage Current (amperes)					
				Non Damage			Damage		
				Min.	Avg.	Max.	Min.	Avg.	Max.
D to S	1 μsec	Open	5	0.20	0.30	0.41	0.40	0.49	0.60
	1 μsec	-10 volts thru 10 K ohm	5	0.24	0.40	0.49	0.28	0.48	0.56
	10 nsec	Open	5	24	28	30	26	31	35
	10 nsec	-10 volts thru 10 K ohm	5	29	32	38	34	37	45
S to D	1 μsec	Open	5	0.34	0.37	0.43	0.41	0.46	0.62
	1 μsec	-10 volts thru 10 K ohm	5	0.44	0.59	0.64	0.50	0.63	0.72
	10 nsec	Open	5	26	37	50	36	41	51
	10 nsec	-10 volts thru 10 K ohm	5	22	27	36	28	33	40

Table 9 shows the effects of multiple square wave pulses on the damage level of the forward biased gate-source junction. Here, metallization burnout is the damage mechanism and the data shown corresponds to the current levels required to produce metallization burnout in the JFET. The thermal aspects of metallization damage are illustrated in the experimental damage data. The multiple pulse square wave damage shows, for example, the increased current level required for metallization burnout as the "off time" between subsequent pulses increases. These characteristics are indicative of increased thermal cooling during the pulse off time and the corresponding higher level required to raise the metallization temperature up to the failure point. These results are in agreement with those previously obtained[1] on other metallization testing.

Table 10 shows the effects of bipolarity square wave pulses on the gate-source junction. Under single square wave pulsing the source-to-gate polarity of the JFET is about 20 times more vulnerable than the gate-to-source polarity. The experiments were performed by first pulsing the device in the gate-to-source polarity and then reversing the pulse such that the source-to-gate polarity was then stressed. The off time between the two pulses was varied from zero to 300 nanoseconds. No significant effects on the source-to-gate damage level are observed when the gate-to-source polarity is first stressed with an equal amplitude current pulse. Similar results are observed if one also used an equal amplitude damped sine wave as shown. If, however, the gate-to-source polarity is stressed at a five times higher current pulse than the source-to-gate direction, then the damage level for source-to-gate is increased by a factor of about three. Interestingly enough, if a 300 nanosecond delay is used between bipolar pulses, then the source to gate vulnerability returns to its original lower level. A similar effect has been observed in mesa diodes which were subject to surface breakdown. Hence, the observations may indicate a surface problem in the device. This, however, is far from conclusive if based on the one experimental observation noted here.

Table 11 shows the results of the bipolarity evaluation of the drain-source terminal pair. Here, a 5 MHz damped sine wave with equal positive and negative amplitudes was used for the pulse shape. No significant difference in vulnerability level was observed for these conditions.

Table 9. Effects of Multiple Square Waves on the Damage Level of the Forward Bias Gate-Source Junction of Motorola 2N4392 JFET's

Pulse Shape	Number Devices Tested	Experimental Damage Current (amperes)					
		Non Damage			Damage		
		Min.	Avg.	Max.	Min.	Avg.	Max.
100 ns on, 0 ns off, 100 pulses	5	3.7	4.4	5.0	5.0	5.4	5.7
100 ns on, 300 ns off, 100 pulses	5	10	11	12	12	12.5	13
100 ns on, 1 μs off, 100 pulses	5	12	13	14			
100 ns on, infinity off	5	15	16	19	15	18.5	24
300 ns on, 300 ns off, 100 pulses	5	5	7.4	9	8	8.8	11
300 ns on, infinity off	5	15	16	19	15	18.5	24

Table 10. Effects of Bipolarity Square Wave Pulses on the Damage Level of the Gate-Source Junction of Motorola 2N4392 JFET's

	Number Devices Tested	Experimental Damage Current (amperes)					
		Non Damage			Damage		
		Min.	Avg.	Max.	Min.	Avg.	Max.
G-S, 100 nsec, single pulse	5	15	16	19	15	18.5	24
S-G, 100 nsec, single pulse	5	0.24	0.42	0.84	0.72	1	1.4
I_{G-S} 100nsec, 0 nsec off, I_{S-G} 100nsec; $I_{GS} \sim I_{SG}$	5	0.80	0.85	0.90	0.90	1	1.1
" , 300nsec off, " ; "	5	0.60	0.90	1.30	0.80	1.1	1.5
" , 0 nsec off, " ; $I_{GS} \sim 5I_{SG}$	5	2	2.70	3	2.50	3.2	4.5
" , 300nsec off, " "	5	1	1.20	1.50	1	1.4	2
I_{G-S} first pulse, 5MHz Damped sine, 8 cycles, $I_{GS} \sim I_{S-G}$	5	0.40	0.55	0.90	0.50	0.7	1.1

Table 11. Effects of Damped Sine Wave Pulses on the Damage Level of the Drain-Source Terminal Pair of the Motorola 2N4392 JFET

	Number Devices Tested	Experimental Damage Current (amperes)					
		Non Damage			Damage		
		Min.	Avg.	Max.	Min.	Avg.	Max.
D-S, 100 nsec, single pulse	5	.20	.24	.44	.52	.89	1.4
S-D, 100 nsec, single pulse	5	.18	.30	.42	1.1	1.3	1.4
I_{D-S} first pulse, 5MHz damped sine, 8 cycles, $I_{DS} \sim I_{S-D}$	5	.60	.94	1.2	0.7	1	1.3

4. Semiconductor Device Failure Analysis

The objective of the Semiconductor Device Failure Analysis Task was to physically examine a variety of semiconductor device types which were subjected to EMP pulse damage in order to determine the nature of the failure mechanisms in the respective device types. The device types examined were the 1N4148 diode, 2N918 transistor, RD211 gate expander, MEM806A MOSFET and SN5404 microcircuit which were previously subjected to pulse damage testing under Contract DAAG 39-72-C-0066, together with the 2N4392 JFET which was subjected to pulse damage testing under the present program. The failure analyses consisted of a surface examination, microprobing, surface etching, device cross-sectioning and electron microscopy.

The selection of the individual units for failure analysis was based on evaluating devices which exhibited the largest extent of electrical damage and obtaining an adequate representation of the various pulse excitations (including pulse width and polarity) and combinations of device terminal pairs which were pulsed. In many cases the construction and diffusion details of the devices were considered proprietary by the respective manufacturers and specific information could not be obtained. However, any pertinent information which was received is presented in the associated failure analysis discussions.

The failure analyses which were performed on the various device types are described below. The data is presented in photographic form. Photographs were obtained on each failure observation. In many cases the device failure sites were unable to be located due to the fact that the devices were subjected to failure threshold damage rather than extreme overkill damage. Hence, the failure sites were subtle in nature rather than gross. Here, photographs were only taken to illustrate device construction details observed during the various failure analysis steps.

4.1 1N4148 Diode

The 1N4148 diode examined was the General Electric planar, epitaxial, passivated device. The construction and diffusion details of the diode have been previously shown in Figure 3. Twelve units which exhibited the largest extent of electrical damage were selected for failure analysis. The analysis consisted of cross-sectioning the device perpendicular to the junction plane and microscopically searching for a device failure site. The procedure was very exacting in that only a thin layer of material was removed at a time followed by a subsequent microscopic examination. Of the twelve devices examined, three fractured and a possible failure site was observed in three others. The suspect damage site extended from the bottom of the anode into the epitaxial region as shown in Figure 62, and was observed midway through the cross-sectioning process. The anode, cathode and epitaxial regions of the device can also be seen.

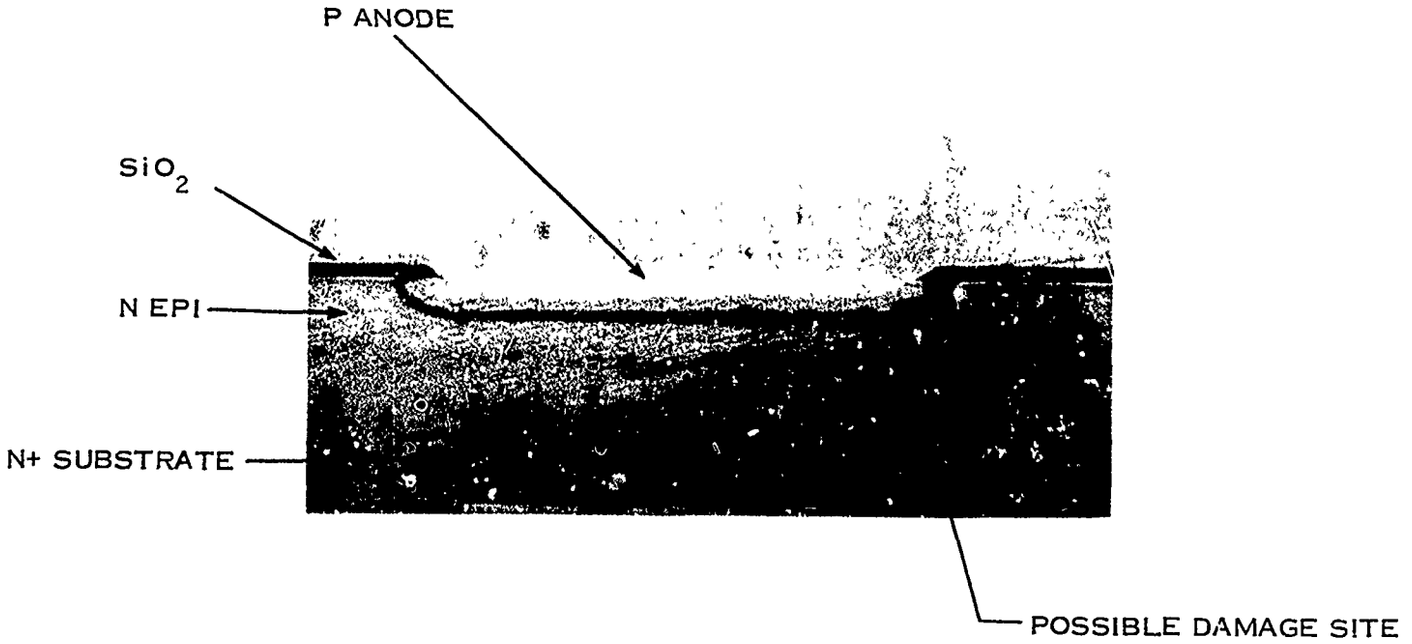

Figure 62. Cross Section Details of the General Electric 1N4148 Diode Showing a Possible Damage Site.

4.2 2N918 Transistor

The 2N918 transistor examined was the Raytheon planar, epitaxial NPN device. The chip topography and diffusion geometry of the device is shown in Figure 63. Twelve of the more extensively damaged units were selected for failure analysis. The failure analysis consisted of a surface examination, surface etching and cross-sectioning. All twelve of the units were subjected to a surface examination. Eight units were cross-sectioned perpendicular to the junction plane. In no case was a failure site observed. The typical nature of the junction regions are shown in Figure 64. Four units were subjected to a surface etching. Again, failure sites were unobservable. Figure 65 shows the surface condition of one unit after the SiO_2 and metallization were removed and just prior to deep etching.

4.3 RD211 Gate Expander

The RD211 gate expander is a dielectrically isolated micro-circuit device which was formerly manufactured by Radiation, Incorporated. The previous pulse testing which was performed on the device indicated metallization damage as the failure mechanism. The schematic diagram and equivalent diode structure of the RD211 Gate Expander is shown in Figure 66. The device consists of 8 individual diodes, 4 each of which having common anodes. Each diode is formed by using an NPN transistor structure with the base shorted to the collector. The device had been chosen as the test vehicle since it utilizes aluminum metallization and has a simple metallization pattern in that only one active semiconductor device exists between selected device terminal pairs making pulse testing of the metallization straightforward.

Eighteen units were unencapsulated and had their surface topography examined. All eighteen units showed severe signs of metallization burnout. The typical nature of the observed damage is shown in Figure 67.

4.4 2N4392 JFET

The 2N4392 JFET examined was the Motorola N-Channel, depletion mode device which was tested during the present program. Motorola considered the device geometry and diffusion details to be proprietary and no information concerning these aspects was obtained. The chip topography drawing of the device supplied by Motorola is shown in Figure 68.

Thirty units were unencapsulated and had their surface topography examined. The topography of an undamaged device, showing the various diffusion regions is shown in Figure 69. Devices which were pulsed in the Gate-to-Source polarity were observed to exhibit extensive metallization damage resulting in an open circuit of the source lead as shown in Figure 70. In many cases, junction damage

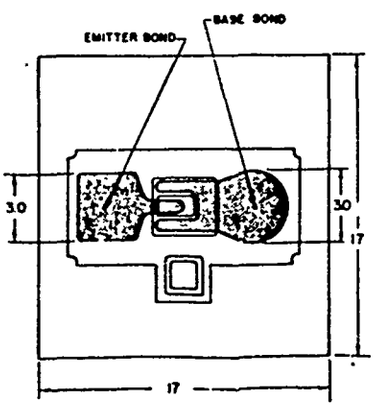

DICE THICKNESS = 8.3 ± .5
NOTE: ALL DIMENSIONS IN MILS.

EMITTER DEPTH	=	0.7 MICRONS
BASE DEPTH	=	1.5 MICRONS
EPITAXIAL DEPTH	=	6.0 MICRONS

Figure 63. Chip Topography and Diffusion Geometry of the Raytheon 2N918 Transistor.

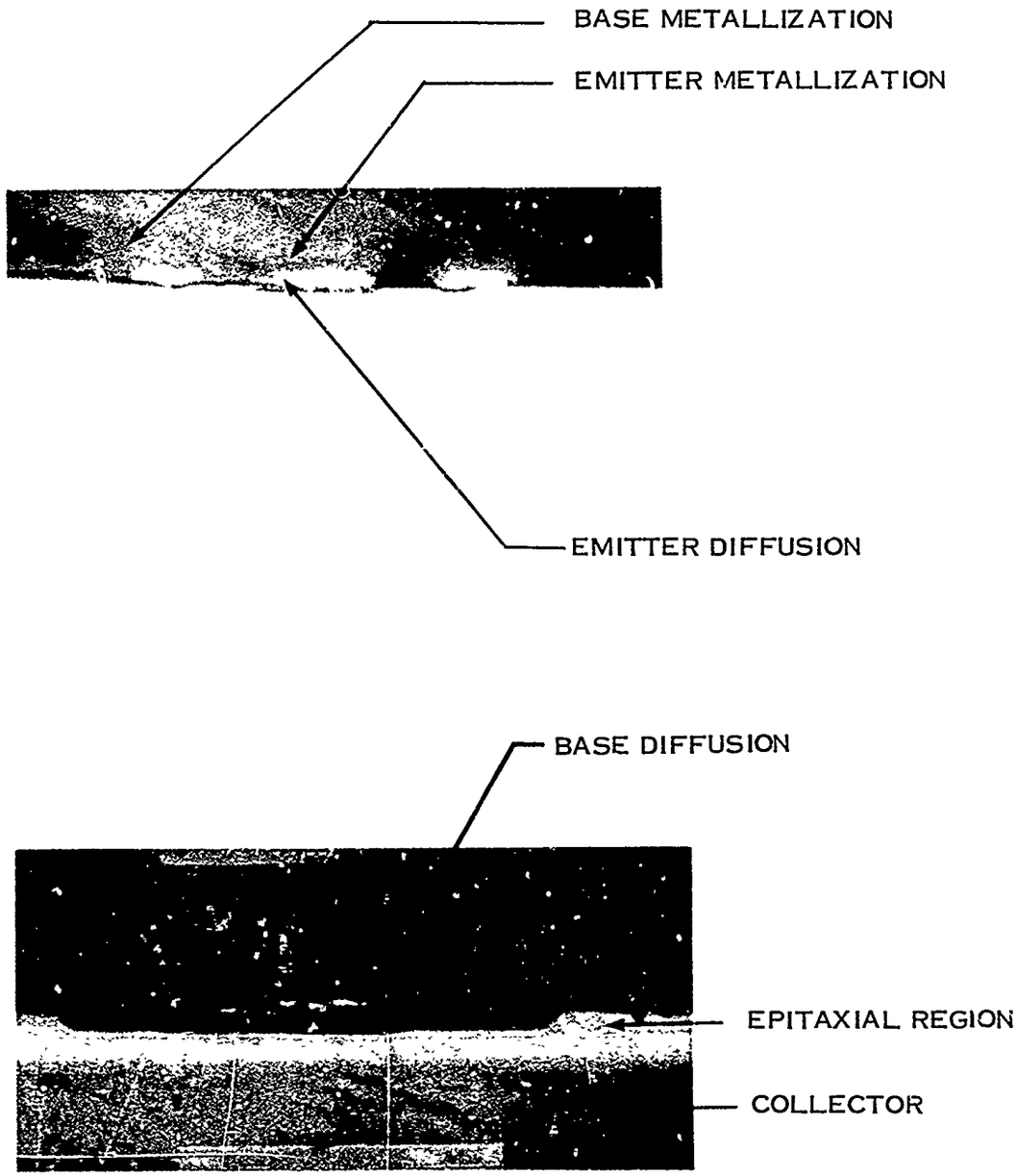

Figure 64. Cross Section Details of the Raytheon 2N918 Transistor.

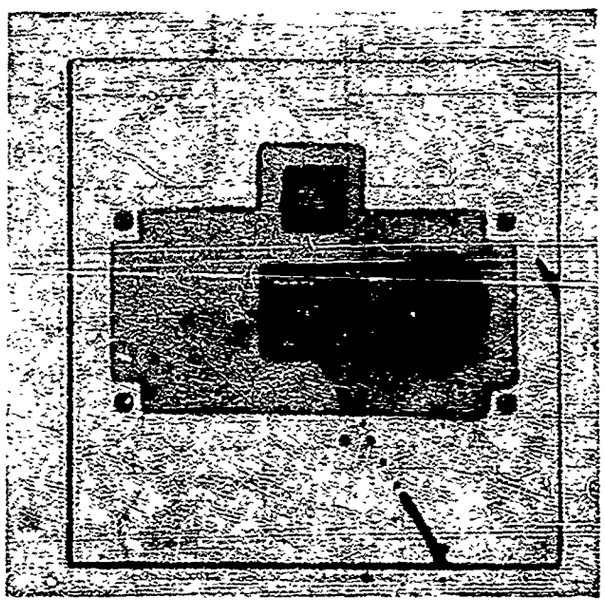

Figure 65. Surface Topography of the Raytheon 2N918 Transistor After Removal of the SiO_2 and Metallization.

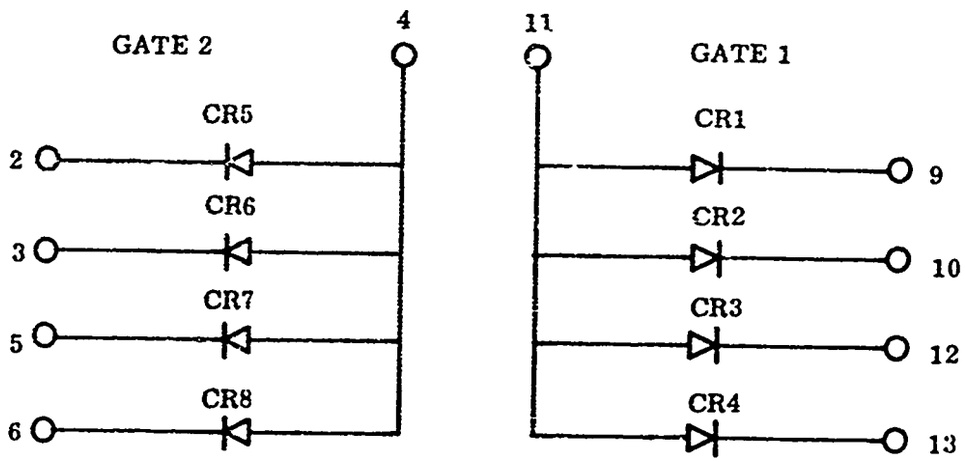

SCHEMATIC DIAGRAM

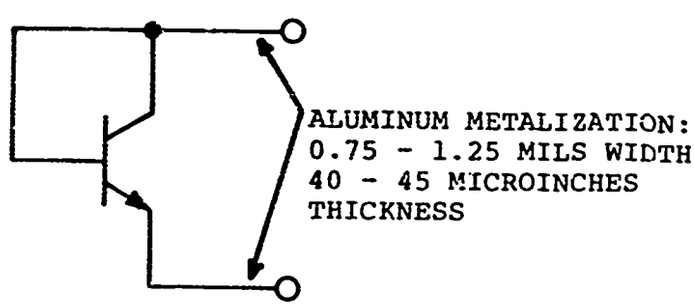

EQUIVALENT DIODE STRUCTURE

Figure 66. Schematic Diagram of the Radiation, Incorporated RD211 Gate Expander.

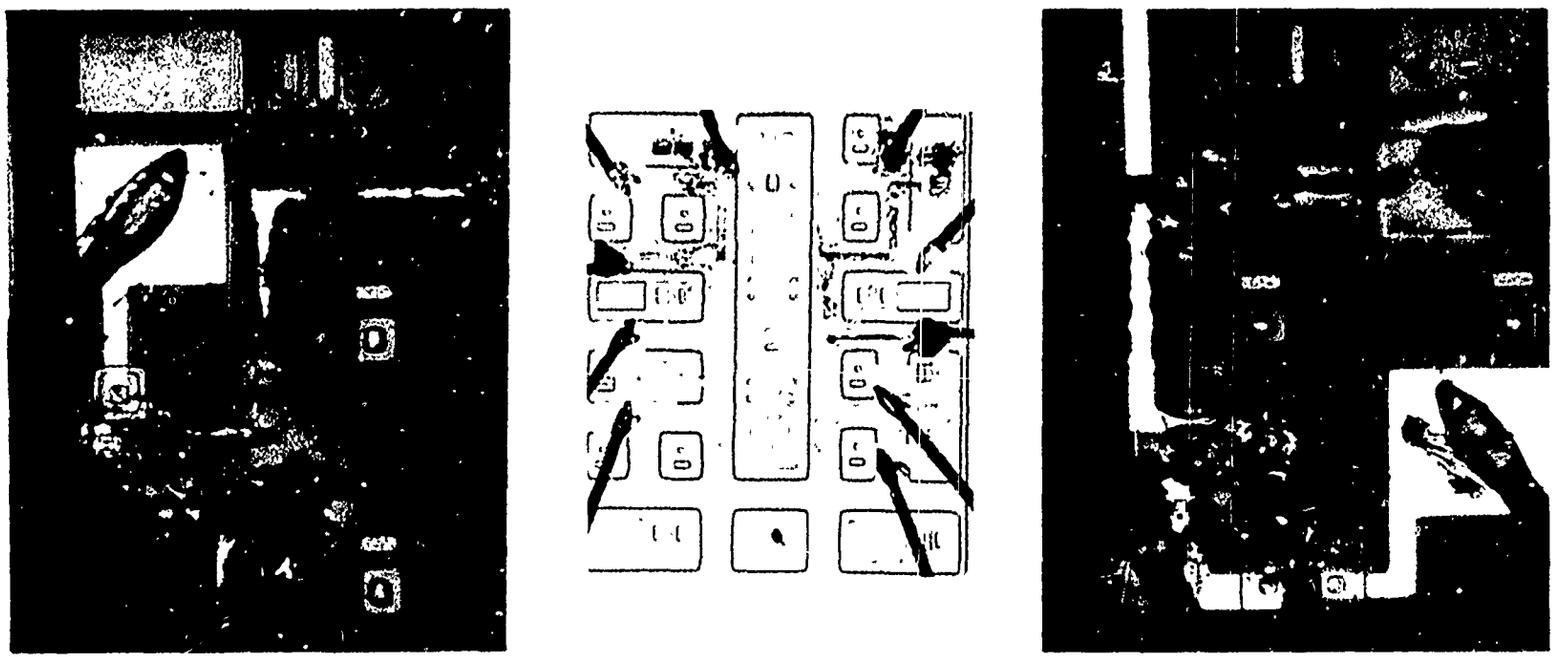

Figure 67. Metallization Damage in the Radiation, Incorporated RD211 Gate Expander.

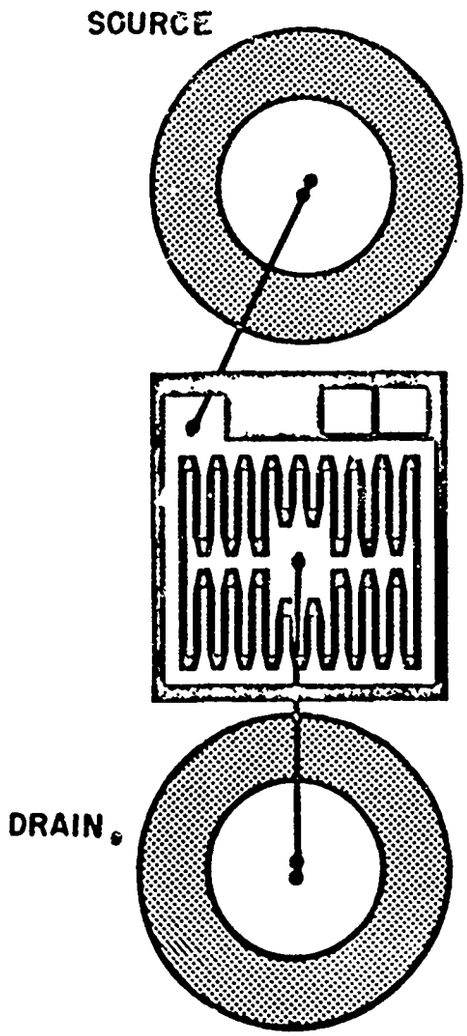

Figure 68. Chip Topography Drawing of the Motorola 2N4392 JFET (Gate Lead is in the Back of the Die).

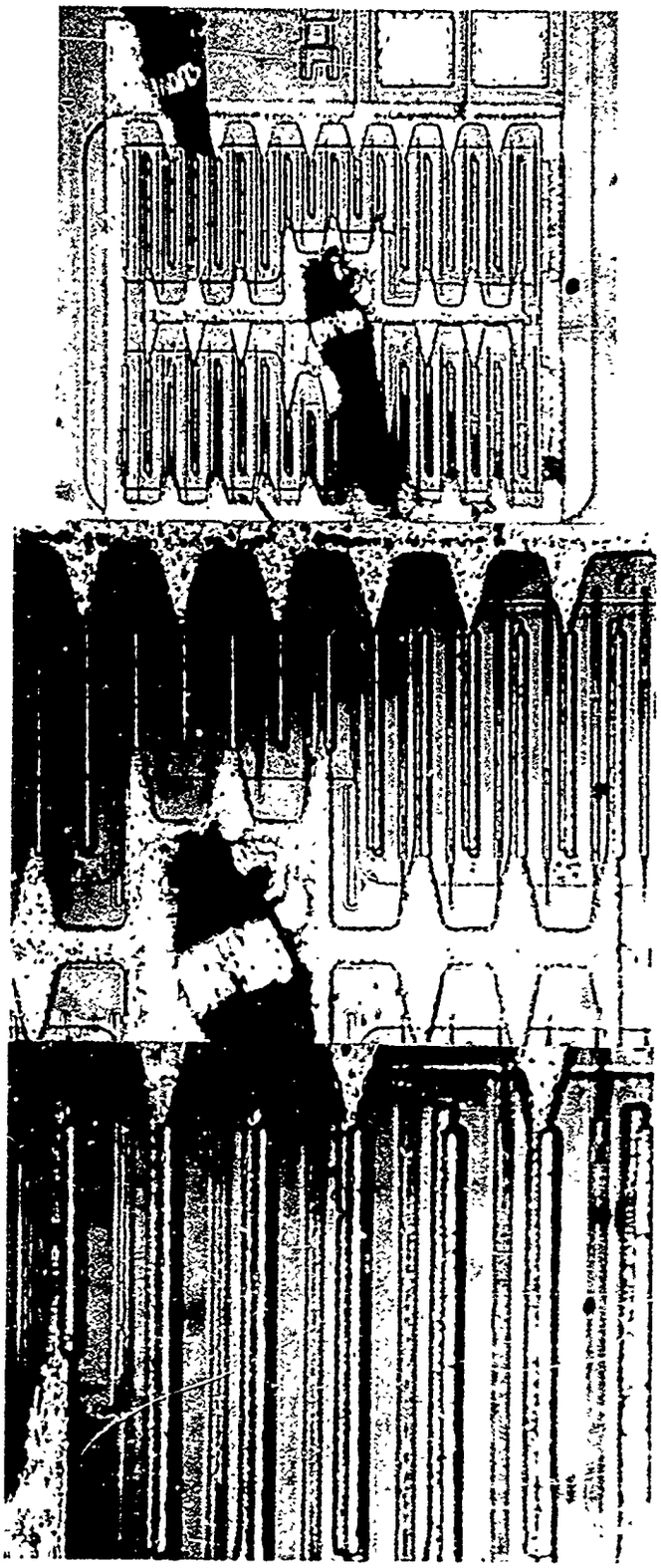

Figure 69. Chip Topography of an Undamaged Motorola 2N4392 JFET.

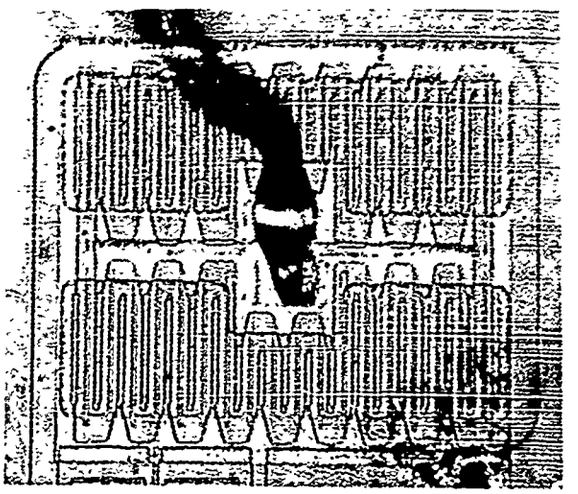

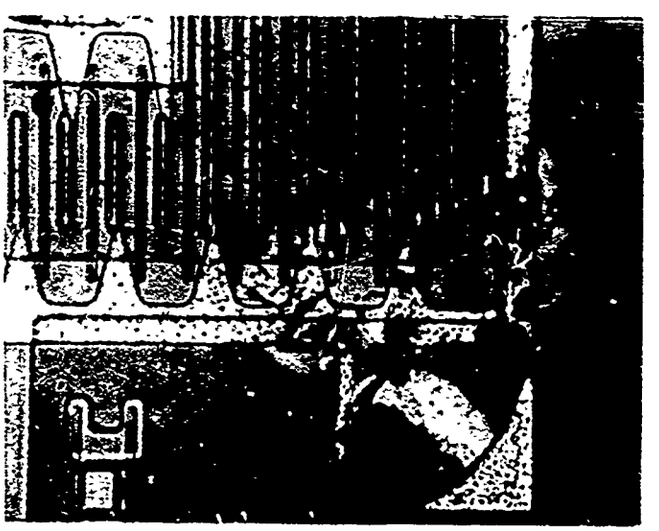

Figure 70. Metallization Damage in Motorola 2N4392 JFET's Pulsed in the Gate-to-Source Polarity.

was unobservable or very subtle for those devices which were pulsed in the drain-to-source, source-to-drain and source-to-gate polarities. Figure 71 shows a damage region which was surface observable in a unit which was pulsed in the drain-to-source polarity. The damage region is seen to extend from the drain to the gate diffusion region. Figure 72 shows a damage region which was surface observable in a unit which was pulsed in the source-to-drain polarity. The damage region is seen to be visible in the source and drain regions. A similar observation was found in a unit which was pulsed in the source-to-gate polarity, as shown in Figure 73. Here the damage region is seen to extend from the source to the gate diffusion region.

4.5 MEM806A MOSFET

The MEM806A MOSFET examined was the General Instrument Corporation P-Channel, enhancement mode device which is fabricated without a gate protection diode and utilizes an oxide-nitride gate construction. The device had been purposely chosen for test since the absence of the gate protection diode enabled the damage characteristics of the gate to be evaluated directly without being masked by damage effects in the protection diode.

The chip topography drawing supplied by General Instruments is shown in Figure 74. The device construction and diffusion geometry information supplied by General Instrument is listed below.

Resistivity of key areas

(a) Substrate resistivity - 2.6 to 4.4 ohms cm
(b) P+ Source & Drain area - 60 ohms/sq.
(c) N+ guard band resistivity - 20 ohms/sq.

Junction area dimensions and diffusion depths

(a) $A_{Drain} = 32.96$ sq. mil
$A_{Source} = 44.00$ sq. mil

(b) $X_j = 1.5\ \mu$

Oxide composition and typical thickness over key areas

t_{ox} source & drain = 10 KÅ
t_{ox} gate = 700 Å
$t_{nitride\ gate}$ = 500 Å
t_{ox} ield = 11 KÅ

} Oxide & Nitride Gate

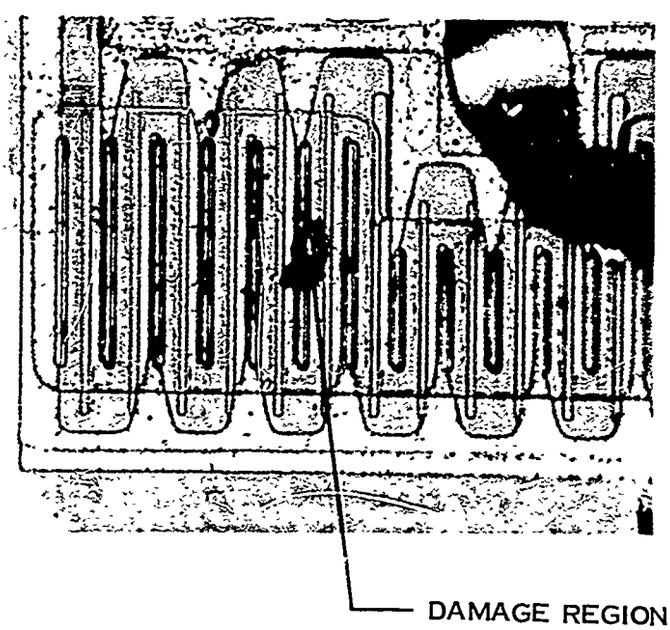

Figure 71. Surface Damage Observed in a Motorola 2N4392 JFET Pulsed in the Drain-to-Source Direction.

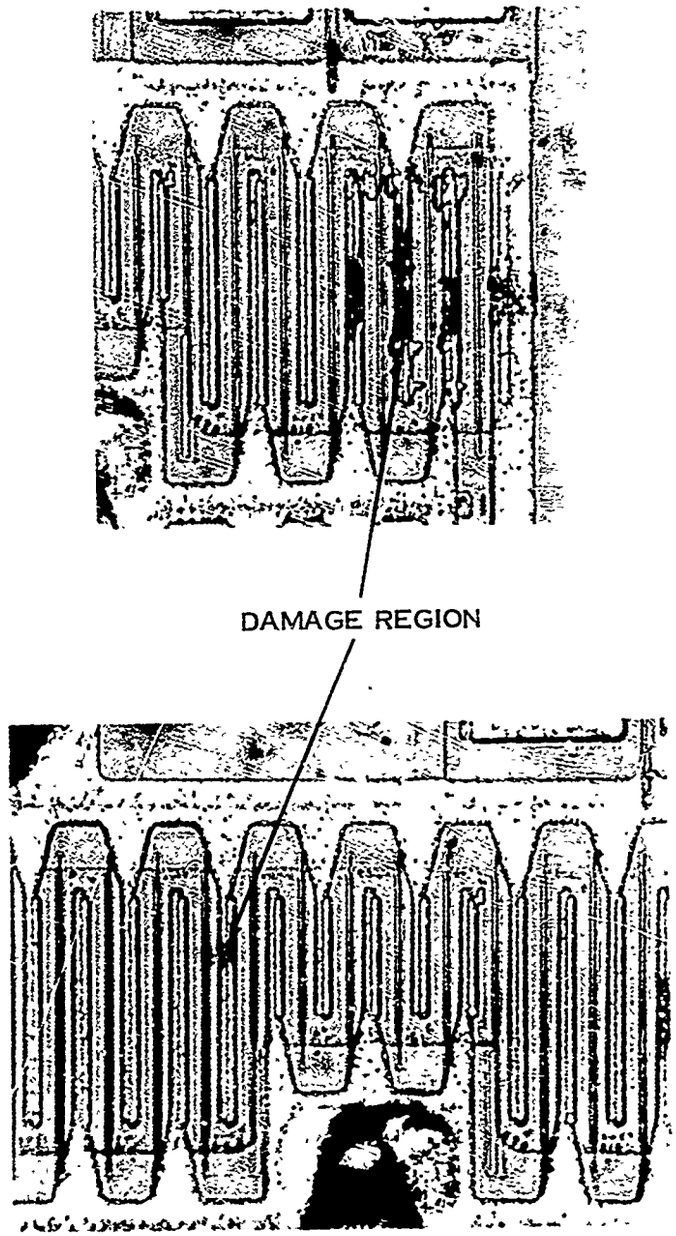

Figure 72. Surface Damage Observed in a Motorola 2N4392 JFET Pulsed in the Source-to-Drain Direction.

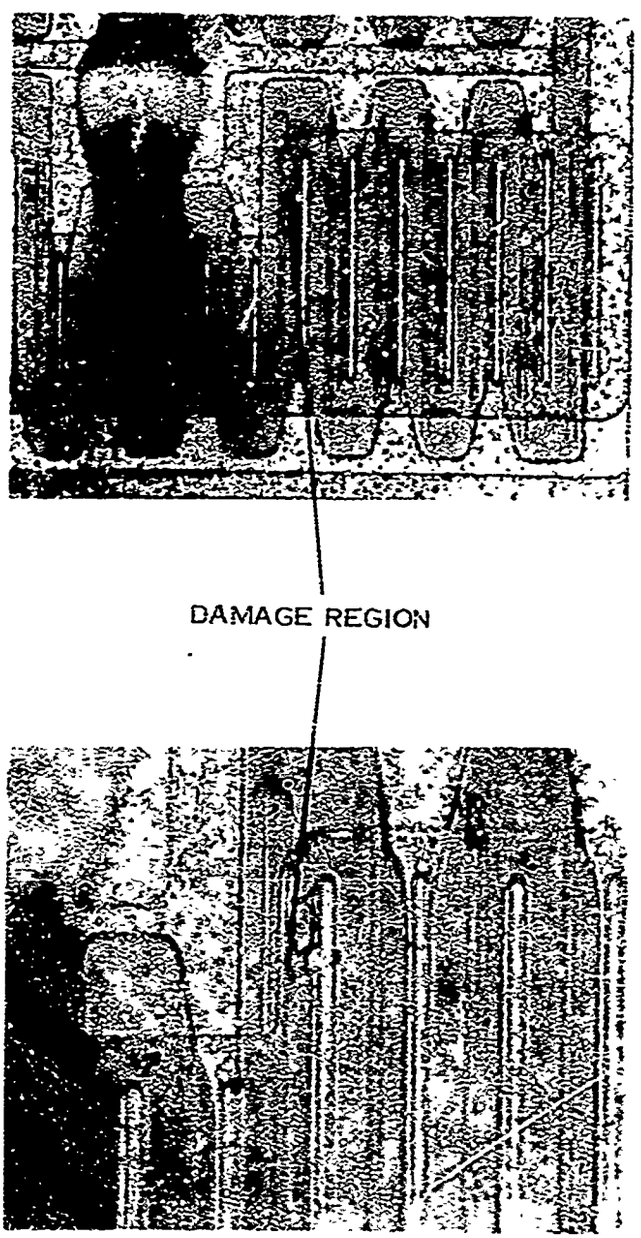

Figure 73. Surface Damage Observed in a Motorola 2N4392 JFET Pulsed in the Source-to-Gate Polarity.

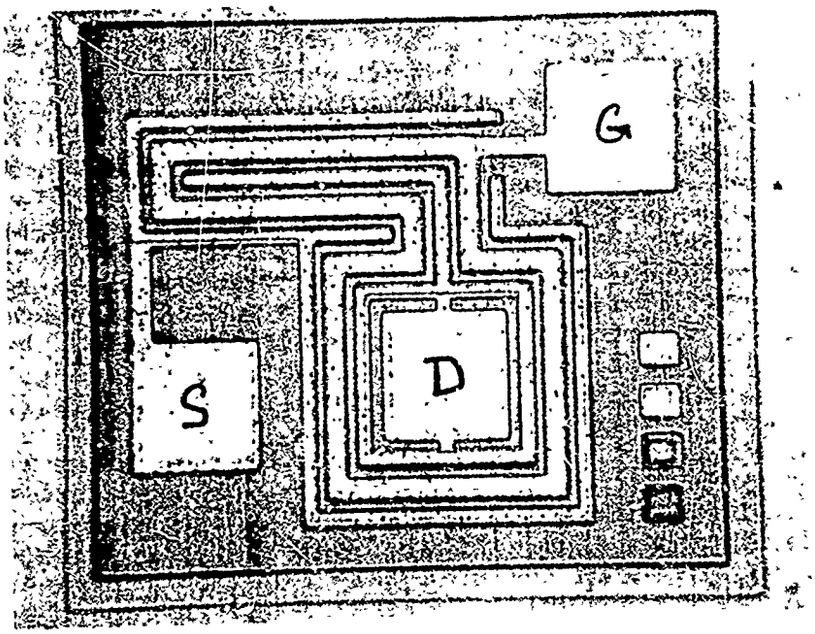

Dimensions: 21 x 24 mils

Thickness: 10 mils

Figure 74. Chip Topography Drawing of the General Instrument MEM806A MOSFET.

Surface metallization composition and thickness with approximate neck down factors over oxide steps

(a) Purity of aluminum = 99.999%

(b) $t_{aluminum}$ = 16 - 18 KÅ

(c) As oxide thickness over the step is maximum 10 KÅ there is no neck down condition observed.

Twenty-four devices were selected for failure analysis. The failure analysis consisted of a surface examination, surface etching, cross-sectioning and scanning electron microscopy examination. All units readily showed visible signs of oxide damage under the gate when unencapsulated and examined under an optical microscope. Four units were cross-sectioned perpendicular to the junction plane to observe the nature of the junction regions. The typical observations are shown in Figure 75. Twelve units were surface etched and examined under an optical microscope. Typical results are given in Figure 76 which shows the surface condition before etching and the corresponding condition after removal of the SiO_2 and metallization regions. In all cases, gate oxide damage under the gate lead and extending into the source region is clearly evident. The device shown was pulsed in the source to gate polarity. Eight units were similarly etched and then observed under a scanning electron microscope. Figure 77 shows the typical gate oxide damage effects observed on a unit which was pulsed in the gate-to-source polarity. A few devices also exhibited metallization damage. These were devices in which the post gate breakdown currents were not limited. As such, excessive current flowed through the devices after gate breakdown causing metallization burnout. The typical appearance of this is as shown in Figure 78. Here the device was pulsed in the source-drain to gate polarity and large metallization damage in the gate and source metallization can be seen.

4.6 SN5404 Microcircuit

The SN5404 device is a Hex Inverter and is from a family of Texas Instruments TTL logic element and utilizes planar construction and monolithic (junction-isolation) technology. The SN5404 device consists of six identical inverter elements interconnected to common ground and V_{CC} terminals. The schematic diagram of a single inverter is shown in Figure 79. The chip topography showing the location of the various circuit elements is given in Figure 80. The corresponding diffusion details are considered proprietary by Texas Instruments.

Sixteen units were selected for failure analysis. The analysis consisted of a surface examination and microprobing. The probe heads that were available at the time were larger than most of the

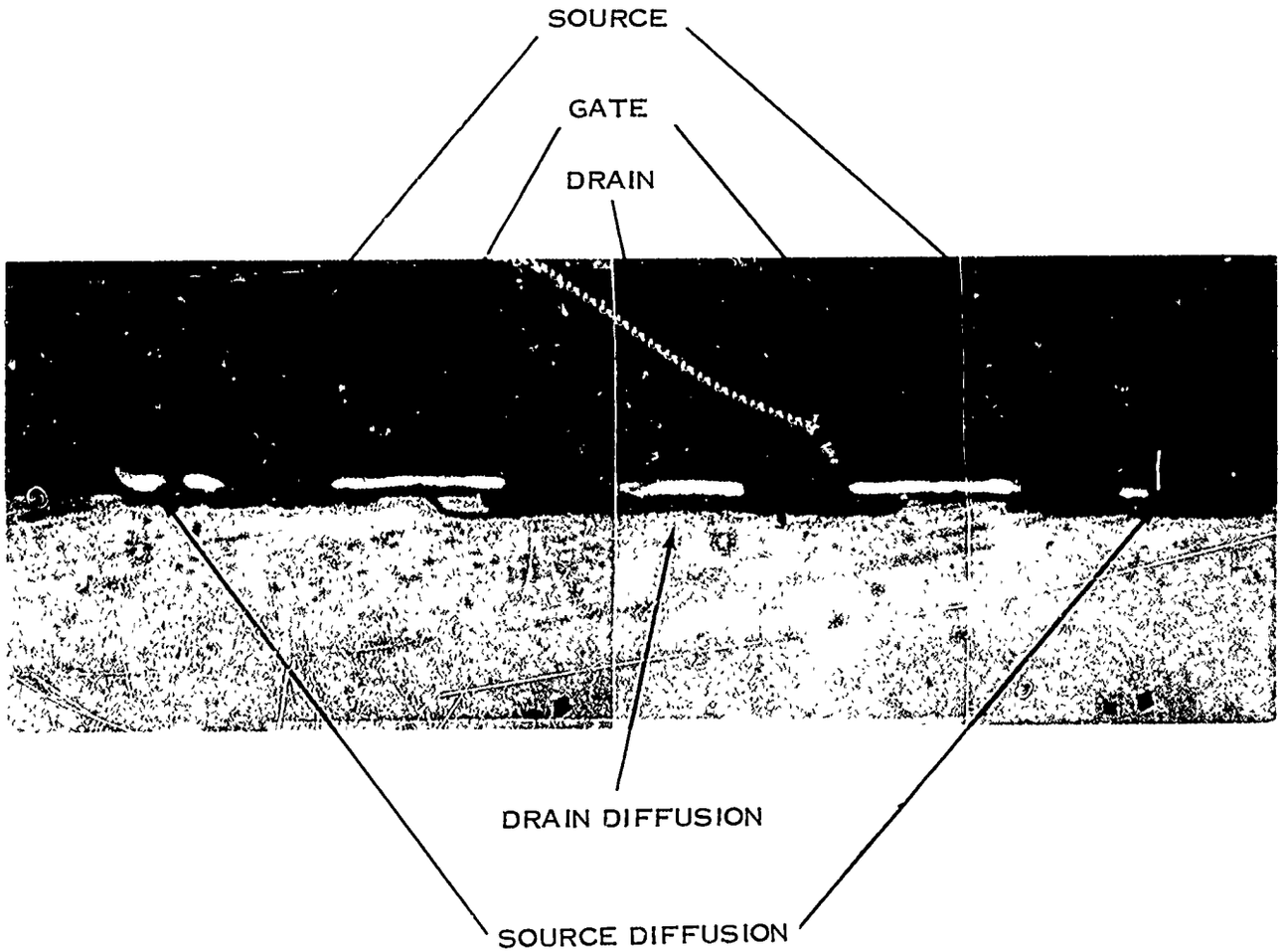

Figure 75. Cross Section Details of the General Instrument MEM806A MOSFET.

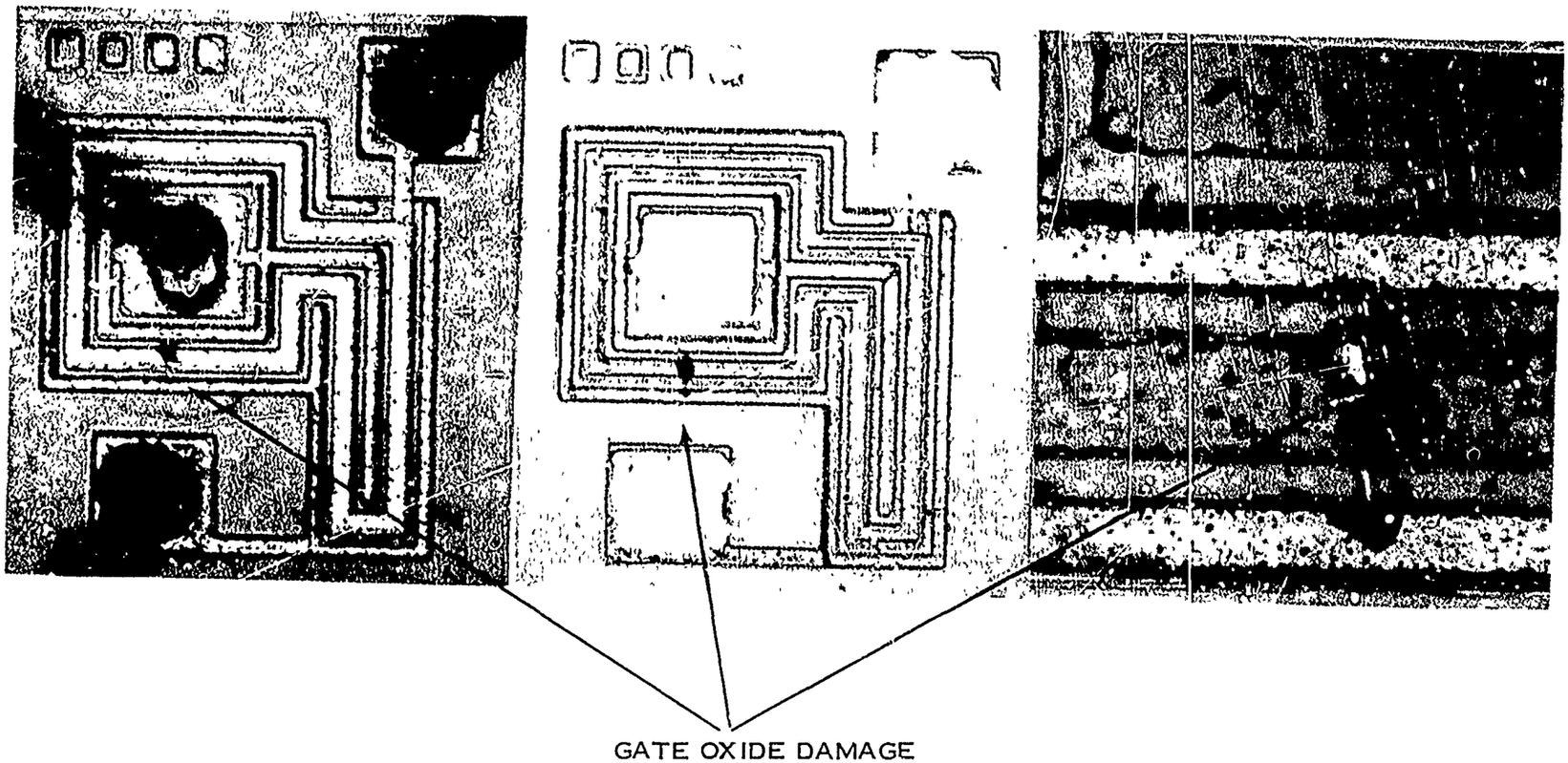

Figure 76. Surface Topography of the General Instrument MEM806A MOSFET After Removal of the SiO_2 and Metallization.

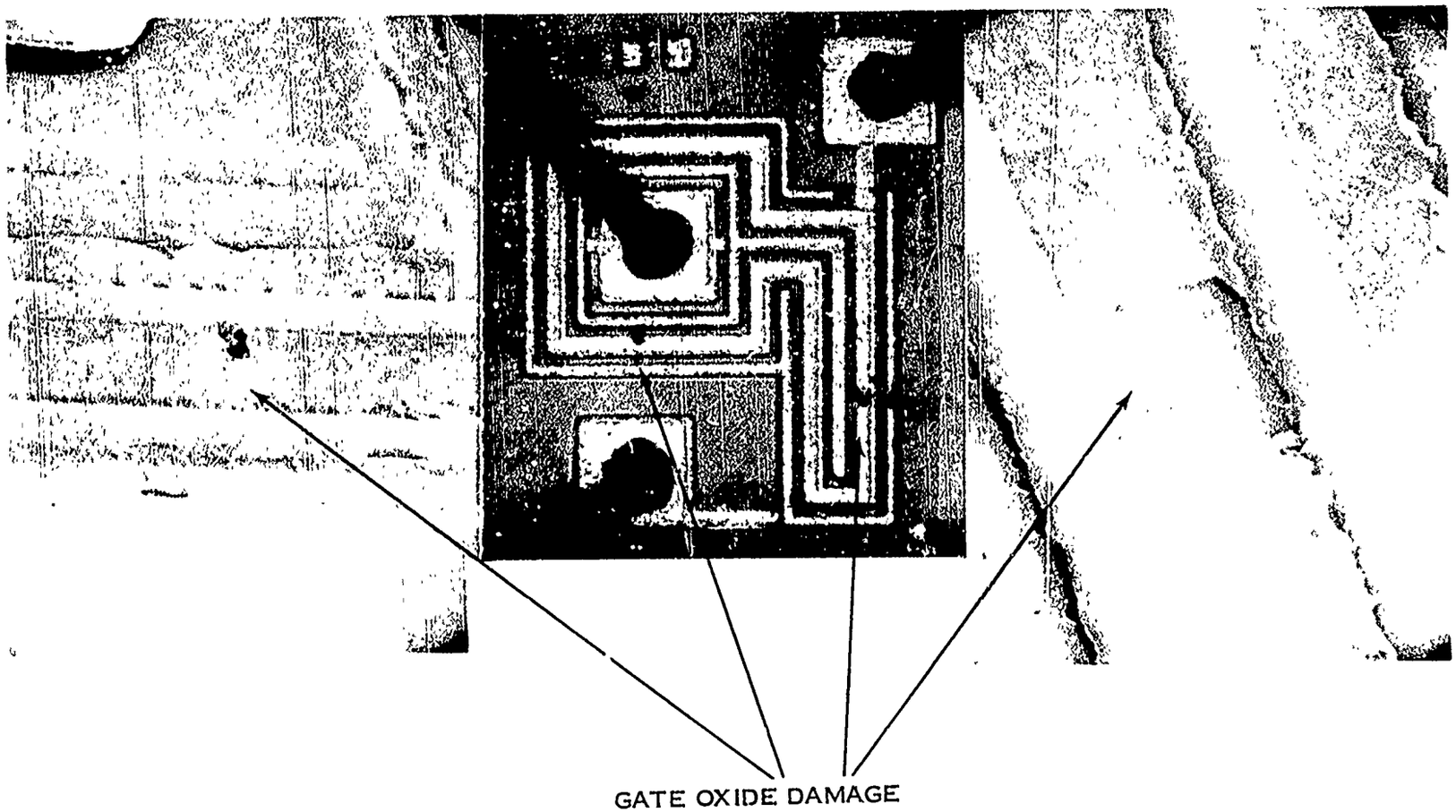

Figure 77. Gate Oxide Damage of the General Instrument MEM806A MOSFET After Removal of the SiO_2 and Metallization as Observed under a Scanning Electron Microscope.

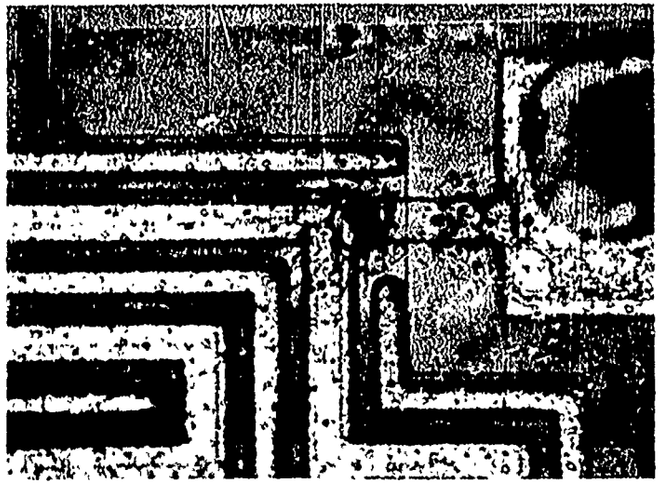

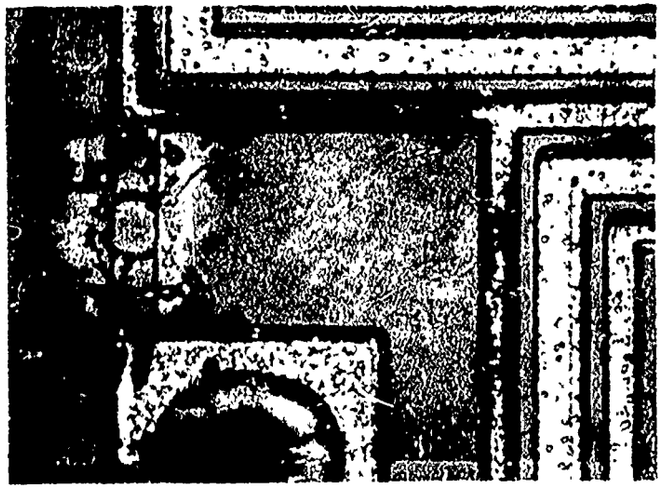

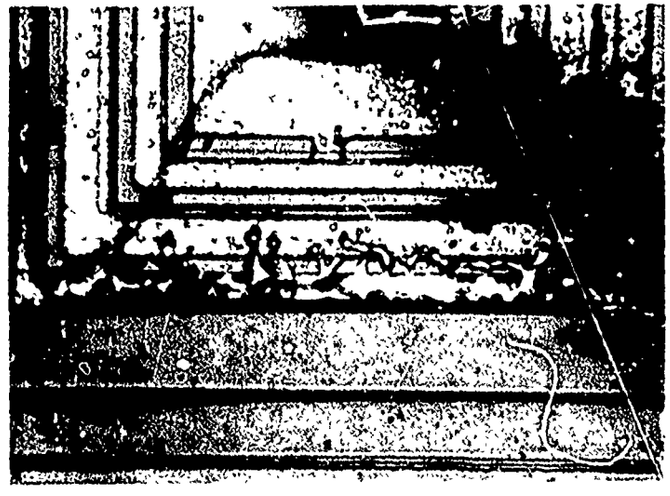

Figure 78. Metallization Damage in the General Instrument MEM806A MOSFET.

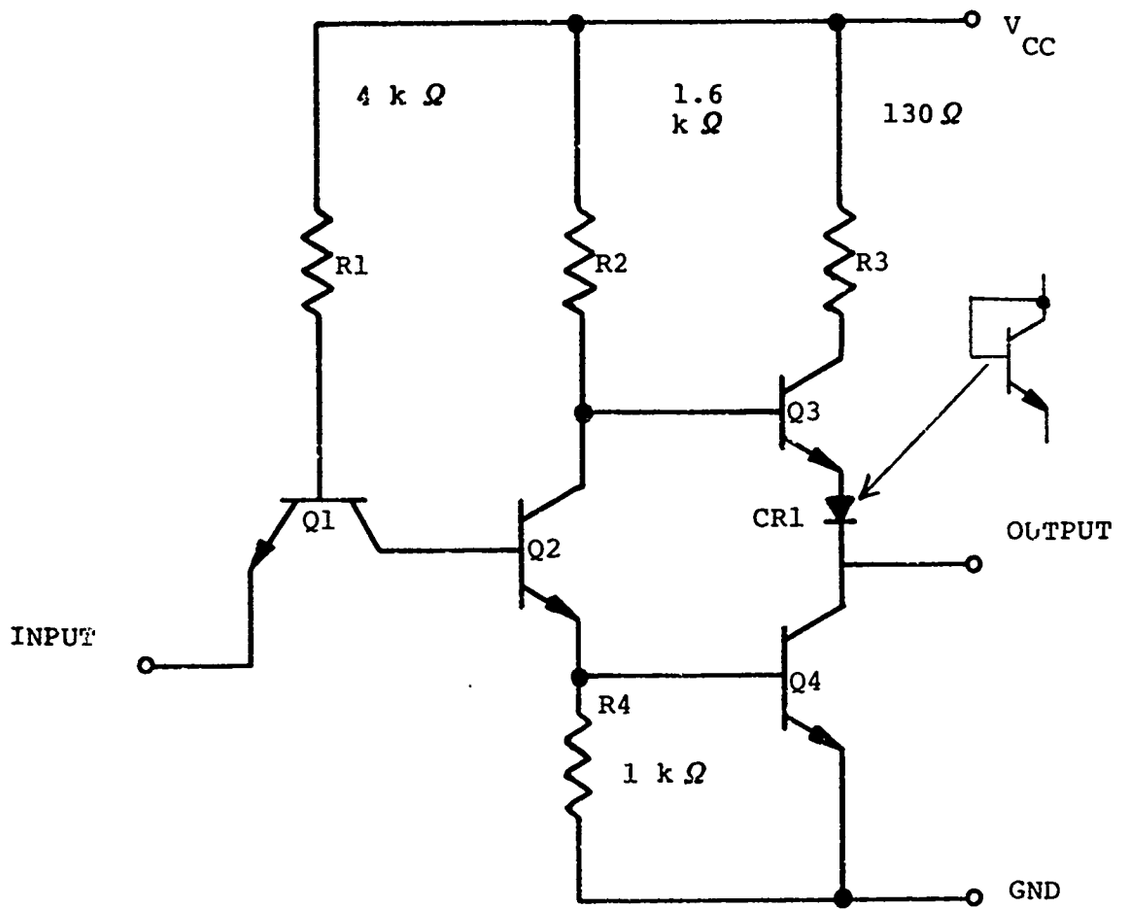

Figure 79. Schematic Diagram of Each Inverter Within the Texas Instruments SN5404 Hex Inverter.

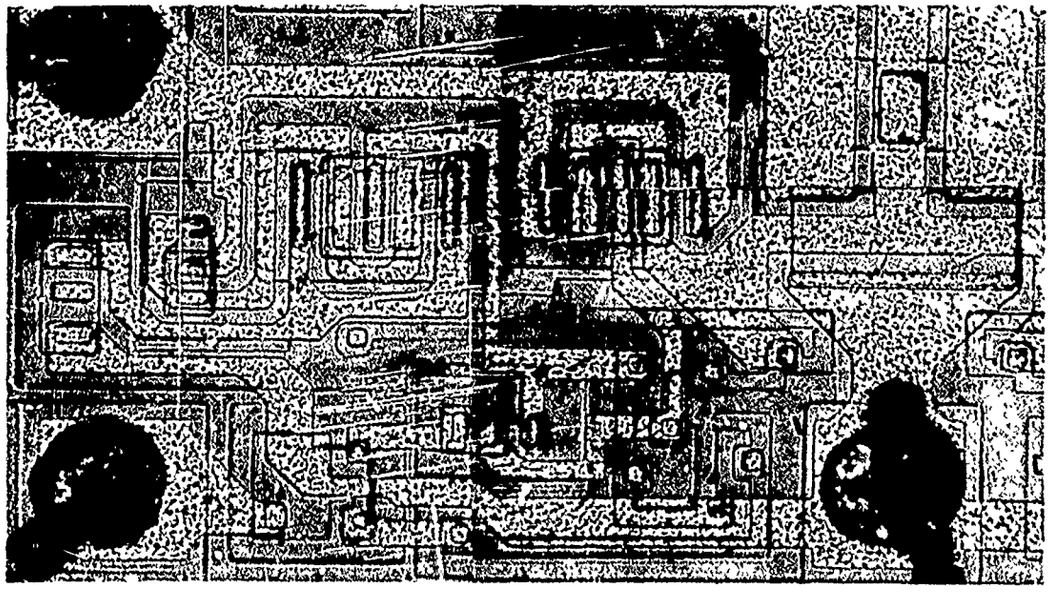

Figure 80. Chip Topography of a Single Inverter in the Texas Instruments SN5404 Hex Inverter.

diffusion regions within the device. As such, no additional information was obtained from the microprobing which was performed. The failure analysis task was terminated before adequate probe heads were received. In spite of this, however, definitive information concerning the failures in the device was obtained from just a surface examination. Here, junction damage was readily observed from just a surface examination of the devices.

Figure 81, for example, shows the typical damage observed in units which were pulsed in the input to ground and ground to input polarities. Here, failure was typically manifested as a damage region in the emitter-base junction of transistor, Q2, regardless of pulse polarity. Devices pulsed in the output to ground polarity showed damage in the emitter-collector region of transistor Q4 as shown in Figure 82. Devices pulsed in the ground to output polarity also exhibited damage in transistor Q4, but in many cases, it was manifested by open metallization in the emitter as shown in Figure 83. Device pulsing through the V_{CC} and ground terminal pair resulted in multi-circuit damage due to the commonality of the V_{CC} and ground connections. In the V_{CC} to ground polarity junction damage in diode CR1 and damage to resistor R3 typically occurred as shown in Figure 84. Pulsing in the ground to V_{CC} polarity, however, typically produced open metallization in the common ground line as shown in Figure 85.

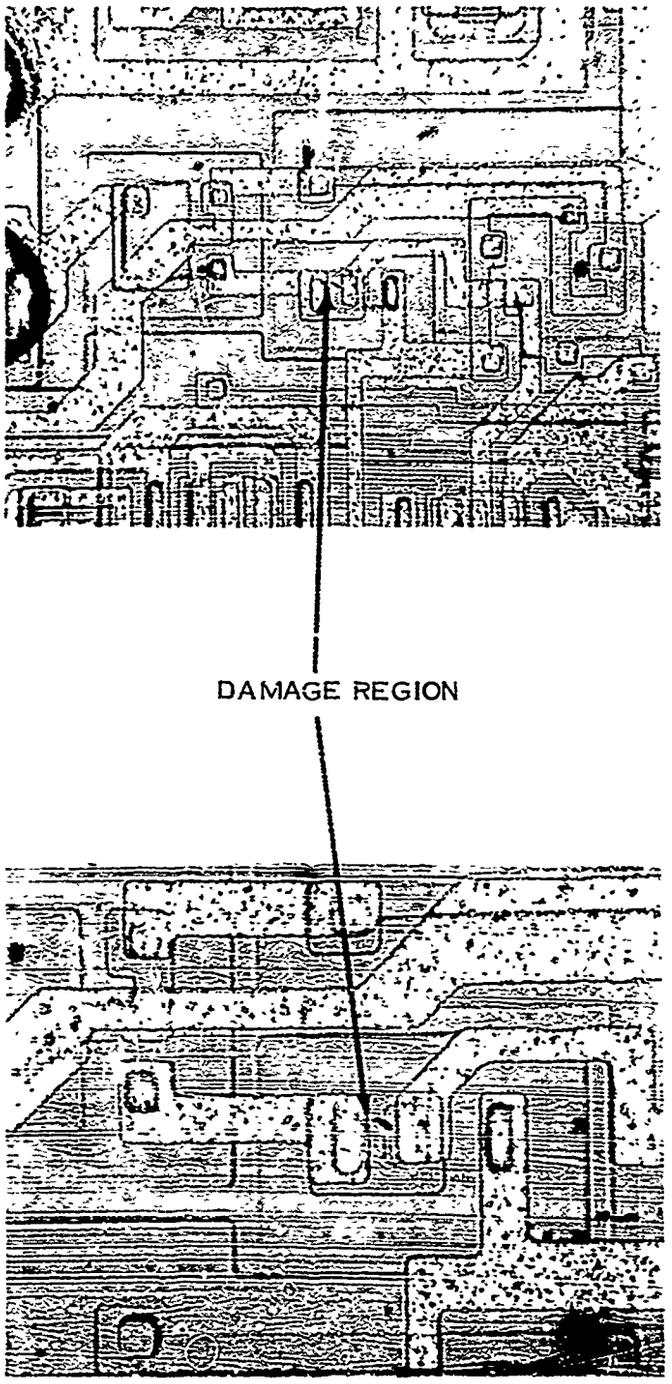

Figure 81. Junction Damage in Texas Instruments SN5404 Hex Inverters Pulsed in the Input and Ground Terminal Pair.

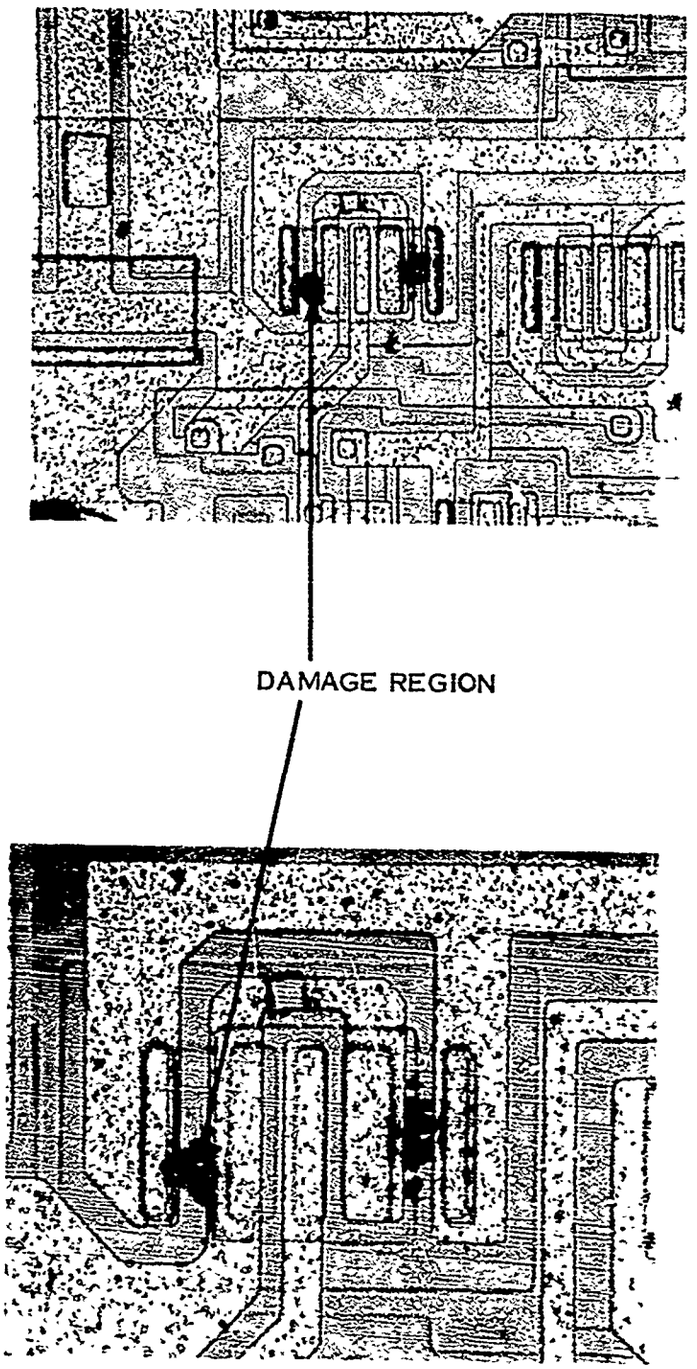

Figure 82. Junction Damage in Texas Instruments SN5404 Hex Inverters Pulsed in the Output to Ground Polarity.

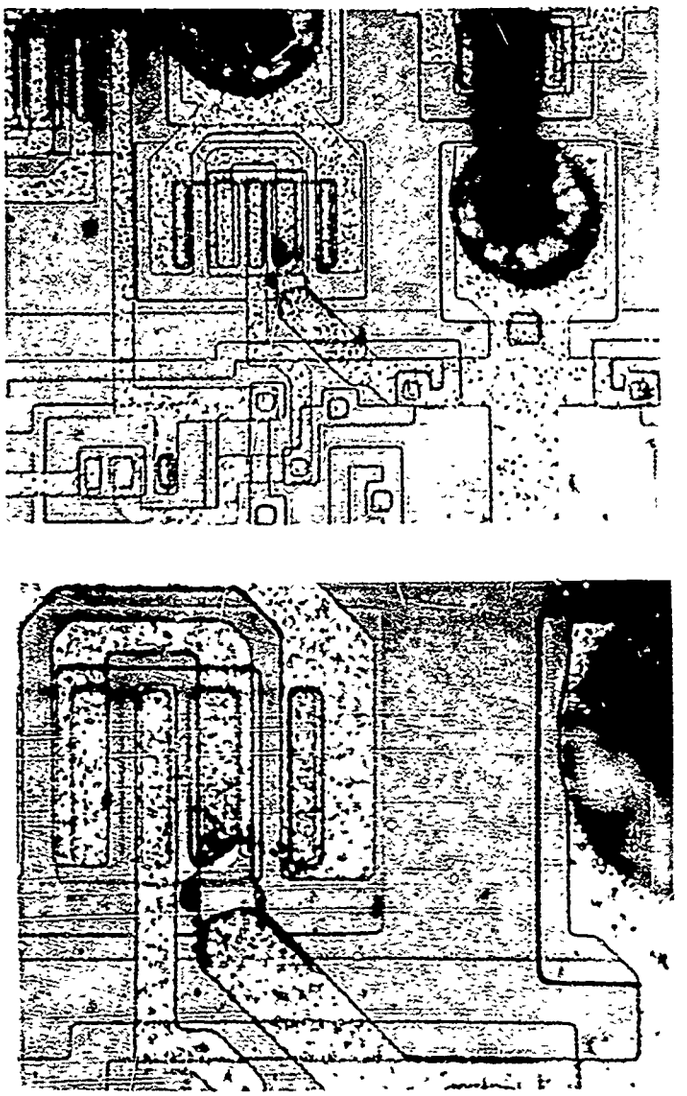

Figure 83. Metallization Damage in Texas Instruments SN5404 Hex Inverters Pulsed in the Ground to Output Polarity.

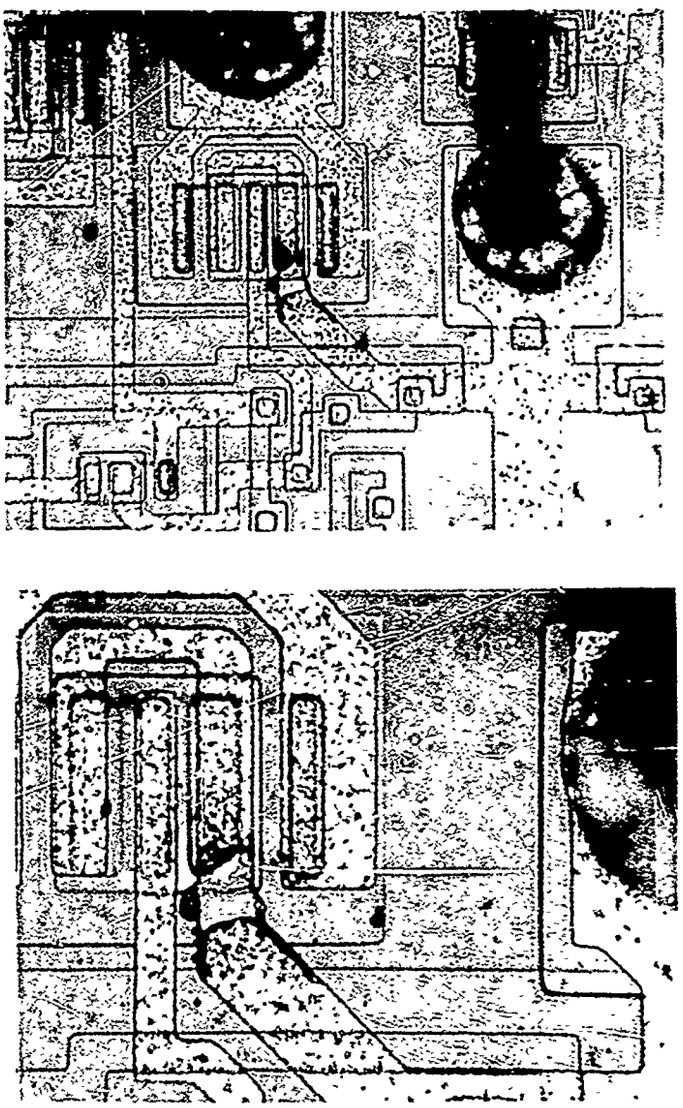

Figure 83. Metallization Damage in Texas Instruments SN5404 Hex Inverters Pulsed in the Ground to Output Polarity.

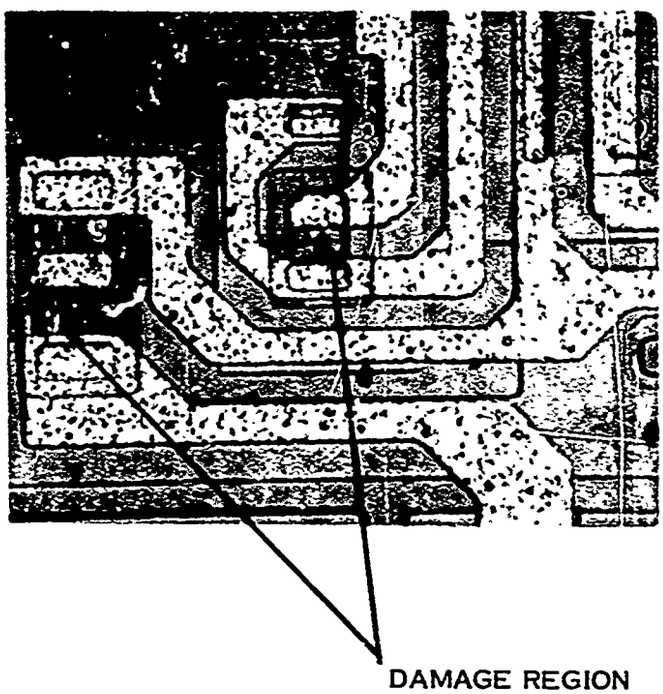

Figure 84. Junction Damage in Texas Instruments SN5404 Hex Inverters Pulsed in the V_{CC} to Ground Polarity.

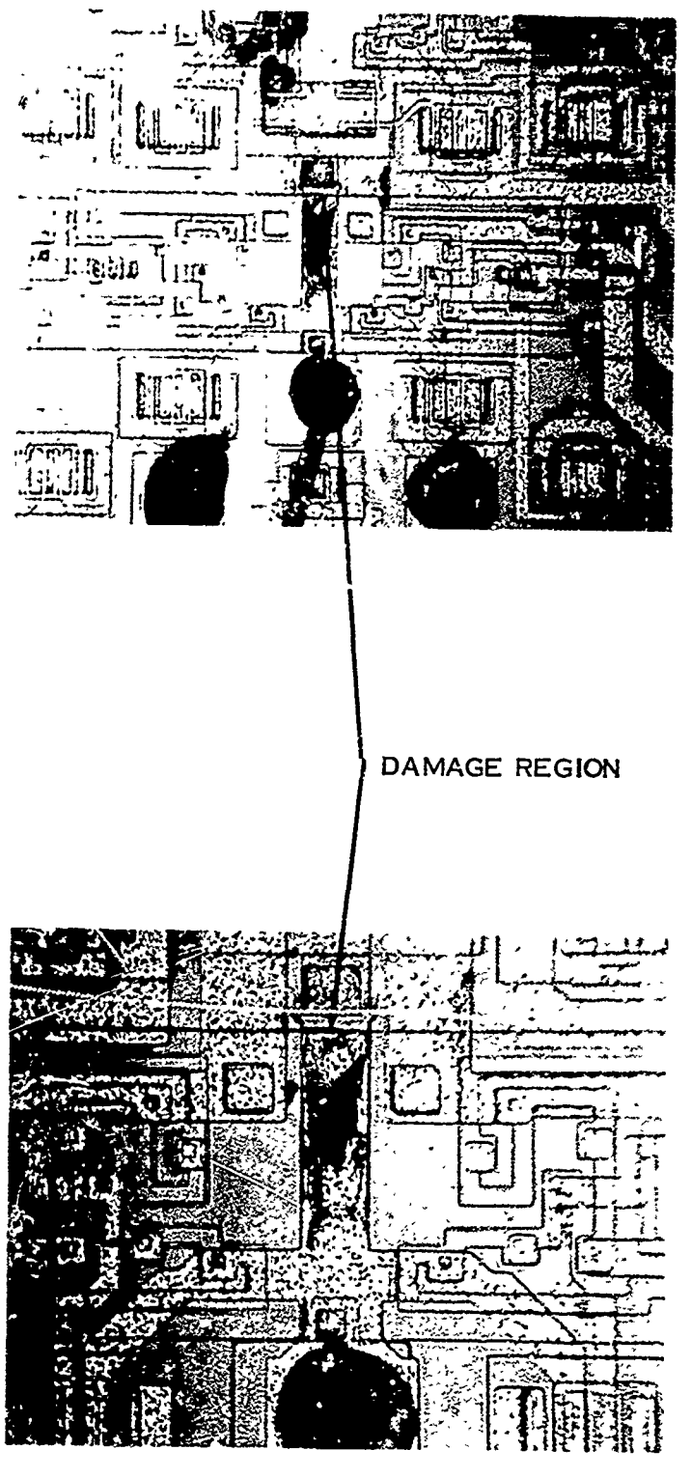

Figure 85. Metallization Damage in Texas Instruments Hex Inverters Pulsed in the Ground to V_{CC} Polarity.

5. Conclusions

Engineering type damage models to predict both surge impedance and failure levels of silicon semiconductor diodes when exposed to EMP type environments were developed from multiple regression analyses of a large experimental data base which was supplied by the U. S. Army/HDL and the U. S. Air Force/AFWL. The models were developed for both forward and reverse polarities of junction current conduction. The models are expressed in terms of published device parameters and, as such, do not require a "hands on" device evaluation. The models were developed both for conditions where the device construction was unknown and for conditions where specific device construction is known. Separate models were developed for devices functionally classified as "rectifiers, diodes and switches" and for devices functionally classified as "non-temperature compensated Zener diodes".

The analysis showed that, under high pulse current injection levels, the forward polarity surge impedance of both diode classes exhibited conductivity modulation effects whereby the impedance was inversely proportional to I^N where N was between 0.3 and 0.4. The forward polarity pulse damage in both classes of diodes was found to be due to I^2R bulk heating under non-adiabatic conditions for the pulse widths and device junction areas evaluated. The conductivity modulation effects caused the exponent of the time dependence for damage to lie in the range of 0.3 as would be expected from these effects.

Under reverse pulse polarity conditions the low and medium voltage Zener diodes also exhibited a surge impedance associated with the bulk material and also partially dependent on conductivity modulation effects. The reverse polarity surge impedance of the "rectifiers, diodes and switches" was found to be strongly dependent on both device breakdown voltage level and pulse current level. The reverse polarity pulse damage in the Zener diodes was found to be due also to I^2R bulk heating under non-adiabatic conditions. The rectifiers, diodes and switches, however, exhibited junction heating effects which were also characteristic of non-adiabatic conditions.

Extensive pulse damage testing was performed on the Motorola 2N4392 N-Channel silicon JFET. The 2N4392 is a depletion mode device designed for chopper and high speed switching applications. A total of 215 units were evaluated for various combinations of terminal pairs in biased and unbiased configurations.

In the forward polarity the gate-source junction behaves like a normal forward biased diode. Because of the relatively large junction to metallization area ratio in the device, metallization burnout occurred before junction damage. The reverse polarity gate-source junction exhibited a second breakdown response which was initiated at a relatively constant pulse current injection

level from 30 nanoseconds to 100 microseconds. Whenever second breakdown occurred, device damage resulted even though the post second breakdown currents were within a factor of 1.5 of the pre-second breakdown levels. The pulse current levels required for device damage increased sharply below 30 nanoseconds.

The pulse response and damage characteristics of the source-drain terminal are similar to the reverse bias gate-source junction. The device was observed to exhibit a second breakdown response which is initiated at a relatively constant pulse current injection level. The response was similar for either direction of pulse polarity. However, in this case, second breakdown could be initiated without producing device damage. Also, the pulse current required for damage increased sharply below 30 nanoseconds and in this region the damage levels are significantly higher than the second breakdown initiation levels.

The exact failure mechanisms associated with the 2N4392 device have not been established at this time. Further definition of the JFET current gain and other conduction phenomena under high injection levels is required to achieve a firmer understanding of the failure mechanisms. A number of competing damage mechanisms could be possible in JFET structures. These are current mode second breakdown, surface breakdown and thermal heating in the channel opening in pinch-off.

Failure analyses were performed on a variety of semiconductor device types which were subjected to EMP pulse damage. The device types examined were the 1N4148 diode, 2N918 transistor, RD211 gate expander, MEM806A MOSFET and SN5404 microcircuit which were previously subjected to pulse damage testing under Contract DAAG 39-72-C-0066, together with the 2N4392 JFET which was subjected to pulse damage testing under the present program. The failure analyses consisted of a surface examination, microprobing, surface etching, device cross-sectioning and electron microscopy. Junction and metallization damage in bipolar devices was observed. Gate oxide damage in the MOSFET device was observed while the JFET device exhibited failures which were observable on the device surface. Metallization damage was also observed in the unipolar devices.

6. Recommendations

The present program has shown that engineering type models expressed in terms of published device parameters can be developed to predict both surge impedance and failure levels of silicon semiconductor diodes when exposed to EMP type environments. The key element in the modeling effort is to segregate the various functionally classified devices into categories which exhibit common failure modes (i.e., junction effects, bulk effects, metallization, etc.) and to relate the devices in each category to some common sets of device specification parameters. In the present work, separate models were developed for devices functionally classified as "rectifiers, diodes and switches" and for devices functionally classified as "non-temperature compensated Zener diodes". These models were developed for both forward and reverse polarities of junction current conduction, and for conditions where the device construction was unknown and for conditions where specific device construction is known. Since the models are expressed in terms of published device parameters, they do not require a "hands on" device evaluation.

In view of the results shown here, it is recommended that the modelling efforts be extended to cover device types such as bipolar transistors, MOS and junction FET's and both digital and analog integrated circuits of various device construction technologies. In the almost certain event that new testing is performed in support of these activities, it is strongly recommended that particular attention be paid to selecting various device types which will give a sufficient spread in device parameters and utilizing a proper sample size in order to provide statistically meaningful correlation results. Serious consideration should be given to rejecting for test any device whose manufacturer and basic construction is unknown. Also, the quality of the test data is of utmost importance. Every effort should be made to eliminate inductive lead response and test fixture noise to the most practical extent within the realm of existing technology. Retesting should also be done to verify device identification and instrumentation validity when extreme mavericks are uncovered in the data analysis.

Additional theoretical and experimental work should definitely be performed to characterize the damage mechanisms in JFET structures, particularly in view of the interesting pulse response and damge results obtained here. A number of competing damage mechanisms such as current mode second breakdown, surface breakdown and thermal channel heating were identified as potential causes of device failure. The exact failure mechanisms, however, have not been established at this time. Further definition of the JFET current gain and other conduction phenomena under high injection levels is required to achieve a firmer understanding of the failure mechanisms.

APPENDIX A

SEMICONDUCTOR DIODE

PULSE DAMAGE DATA

The detailed pulse damage data for each diode type examined during the program is presented in this appendix. They are listed in tabular form and are sequentially ordered according to a data file number (F #). The device type and manufacturer for each corresponding data file number is given in Tables 2, 3, & 4 of Section 2. The pulse data shows the individual device serial number (S/N); the experimenter's estimate of the time to damage (TD) in microseconds; the total pulse width (TP) in microseconds; the peak pulse voltage across the device (VP) in volts; the peak pulse current through the device (IP) in amperes; the pre-test low current level breakdown voltage (VZB) in volts; the post-test breakdown voltage (VZA) in volts; the pulse polarity (POL); and, an indication as to whether damage occurred. The data on the temperature compensated zener diodes also shows the pre- and post-test forward breakdown voltage, VFB and VFA, respectively.

F#	S/N	TD	TP	VP	IP	VZB	VZA	POL	FAIL
1	2	.500	1.500	9	.30	1.2	.2	REV	YES
1	3	.500	1.500	6	.15	.6	.2	REV	YES
1	4	.300	1.500	8	.15	.5	.1	REV	YES
1	5	1.500	1.500	4	.40	.9	.9	FWD	NO
1	5	.400	1.500	5	.50	.9	.6	FWD	YES
1	6	1.500	1.500	5	.75	.6	.5	FWD	NO
1	6	.100	1.500	7	.50	.6	.5	FWD	YES
1	7	.900	1.500	5	.30	1.3	.2	REV	YES
1	8	1.500	1.500	5	.55	3.1	3.1	FWD	NO
1	8	.200	1.500	8	.95	3.1	.5	FWD	YES
2	1	3.000	3.000	1000	.20	500.0	500.0	REV	NO
2	1	4.400	7.500	1000	.15	500.0	500.0	REV	NO
2	2	3.000	3.000	8	38.00	610.0	610.0	FWD	NO
2	2	4.400	9.500	6	28.00	610.0	610.0	FWD	NO
2	2	3.200	10.000	8	38.00	610.0	580.0	FWD	NO
2	2	3.500	10.000	7	39.00	610.0	580.0	FWD	NO
3	1	.050	3.000	850	10.00	520.0	.0	REV	YES
3	3	.150	2.000	1000	3.00	500.0	.0	REV	YES
3	5	.200	4.000	850	2.00	520.0	300.0	REV	YES
3	2	3.000	3.000	12	38.00	1000.0	1000.0	FWD	NO
3	2	4.000	8.500	10	38.00	1000.0	1000.0	FWD	NO
4	1	1.000	1.000	440	8.00	370.0	370.0	REV	NO
4	1	4.000	4.000	440	7.00	370.0	370.0	REV	NO
4	2	1.000	1.000	5	15.00	350.0	350.0	FWD	NO
4	2	10.000	10.000	3	13.00	350.0	350.0	FWD	NO
4	3	10.000	10.000	440	5.00	370.0	370.0	REV	NO
6	1	.100	1.000	500	3.20	560.0	.0	REV	YES
6	1	1.000	1.000	600	.40	210.0	210.0	REV	NO
6	1	.500	1.000	920	.85	210.0	.0	REV	YES
6	2	3.000	3.000	530	.30	310.0	310.0	REV	NO
6	2	.150	3.000	850	1.00	310.0	.0	REV	YES
6	3	3.000	3.000	620	.40	350.0	350.0	REV	NO
6	3	1.900	3.000	640	.50	350.0	.0	REV	YES
6	4	8.000	8.000	650	.50	285.0	285.0	REV	NO
6	4	1.600	8.000	700	.80	285.0	.0	REV	YES
6	5	8.000	8.000	770	.45	320.0	320.0	REV	NO
6	5	7.600	8.000	800	.50	320.0	.0	REV	YES
6	6	8.000	8.000	5	12.00	290.0	290.0	FWD	NO
6	6	5.000	8.000	7	22.00	290.0	290.0	FWD	NO
6	6	4.000	8.000	9	27.00	290.0	290.0	FWD	NO

F#	S/N	TD	TP	VP	IP	VZB	VZA	PØL	FAIL
6	6	3.400	8.000	11	36.00	290.0	290.0	FWD	NØ
7	1	1.000	1.000	800	.60	220.0	220.0	REV	NØ
7	1	.900	1.000	1000	.90	220.0	.0	REV	YES
7	2	1.300	3.000	600	.40	270.0	270.0	REV	NØ
7	2	3.000	3.000	800	.80	270.0	270.0	REV	NØ
7	2	1.400	3.000	900	.90	270.0	.0	REV	YES
7	3	6.000	6.000	600	.20	240.0	240.0	REV	NØ
7	3	5.700	6.000	750	.60	240.0	.0	REV	YES
7	4	1.000	1.000	15	36.00	215.0	215.0	FWD	NØ
7	4	5.600	10.000	10	19.00	215.0	215.0	FWD	NØ
7	4	3.600	20.000	15	34.00	215.0	215.0	FWD	NØ
8	1	.200	1.000	600	1.00	240.0	240.0	REV	NØ
8	1	1.000	1.000	600	1.00	240.0	240.0	REV	NØ
8	1	.800	1.000	700	1.50	240.0	240.0	REV	NØ
8	1	.100	1.000	900	1.00	240.0	240.0	REV	NØ
8	2	4.500	4.500	600	.10	310.0	310.0	REV	NØ
8	2	.200	4.000	800	.40	310.0	310.0	REV	NØ
8	3	1.000	1.000	16	36.00	350.0	350.0	FWD	NØ
8	3	4.800	7.000	11	23.00	350.0	350.0	FWD	NØ
8	3	3.200	7.500	15	34.00	350.0	350.0	FWD	NØ
8	2	5.000	5.000	800	.70	310.0	310.0	REV	NØ
8	2	4.000	5.000	875	.80	310.0	38.0	REV	YES
8	4	8.000	8.000	600	.60	255.0	255.0	REV	NØ
8	4	4.000	8.000	650	.90	255.0	255.0	REV	NØ
8	5	8.000	8.000	675	.40	335.0	335.0	REV	NØ
8	5	.600	8.000	800	.90	335.0	4.0	REV	YES
9	1	3.700	3.700	1000	.05	725.0	725.0	REV	NØ
9	1	7.500	7.500	1000	.04	725.0	725.0	REV	NØ
9	3	3.000	3.000	11	37.00	600.0	600.0	FWD	NØ
9	3	4.000	20.000	10	37.00	600.0	600.0	FWD	NØ
10	10	.150	1.000	900	1.40	790.0	.0	REV	YES
10	8	.300	1.000	1000	1.00	820.0	840.0	REV	YES
10	4	.100	4.000	750	.80	900.0	5.0	REV	YES
10	1	1.000	1.000	5	14.00	1000.0	1000.0	FWD	NØ
10	1	.400	1.000	12	32.00	1000.0	1000.0	FWD	NØ
10	1	.200	4.000	23	40.00	1000.0	1000.0	FWD	NØ
11	1	.050	1.000	900	3.20	700.0	6.3	REV	YES
11	11	.100	2.000	1000	3.30	650.0	40.0	REV	YES
11	13	.200	4.000	1000	2.80	680.0	680.0	REV	YES
11	3	3.000	3.000	4	18.50	980.0	980.0	FWD	NØ

F#	S/N	TD	TP	VP	IP	VZB	VZA	PØL	FAIL
11	3	3.000	3.000	6	26.00	980.0	980.0	FWD	NØ
11	3	3.000	3.000	6	35.00	980.0	980.0	FWD	NØ
11	3	3.600	8.000	7	34.00	980.0	980.0	FWD	NØ
12	2	1.000	1.000	5	15.00	940.0	930.0	FWD	NØ
12	2	9.000	9.000	5	14.00	940.0	930.0	FWD	NØ
12	3	.180	.180	1000	.10	910.0	910.0	REV	NØ
12	3	1.000	1.000	1000	.10	910.0	910.0	REV	NØ
12	3	8.000	8.000	1000	.10	910.0	910.0	REV	NØ
12	4	1.000	1.000	10	34.00	830.0	830.0	FWD	NØ
12	4	9.000	9.000	5	16.00	830.0	830.0	FWD	NØ
12	4	3.200	10.000	14	32.00	830.0	830.0	FWD	NØ
13	4	1.000	1.000	5	16.00	900.0	900.0	FWD	NØ
13	4	9.000	9.000	4	14.00	900.0	900.0	FWD	NØ
13	5	1.000	1.000	10	33.00	860.0	860.0	FWD	NØ
13	5	5.200	10.000	6	18.00	860.0	860.0	FWD	NØ
13	5	3.800	10.000	9	32.00	860.0	860.0	FWD	NØ
13	5	3.200	20.000	9	32.00	860.0	860.0	FWD	NØ
14	7	4.800	6.000	8	23.00	950.0	950.0	FWD	NØ
14	7	3.300	4.000	10	30.00	950.0	950.0	FWD	NØ
14	8	5.000	5.000	1000	.10	905.0	905.0	REV	NØ
14	8	10.000	10.000	1000	.10	905.0	905.0	REV	NØ
15	1	1.000	1.000	18	32.00	3.4	3.4	REV	NØ
15	1	3.000	3.000	19	29.00	3.4	3.4	REV	NØ
15	1	5.000	8.000	14	17.00	3.4	3.4	REV	NØ
15	1	3.000	8.000	20	30.00	3.4	1.6	REV	YES
15	2	6.400	8.000	10	16.00	2.6	2.6	REV	NØ
15	2	4.000	8.000	14	25.00	2.6	2.6	REV	NØ
15	2	3.000	8.000	16	33.00	2.6	2.6	REV	NØ
15	3	4.000	8.000	16	23.00	3.6	3.6	REV	NØ
15	3	4.000	8.000	18	26.00	3.6	2.8	REV	YES
15	4	6.000	8.000	8	15.00	3.4	3.4	FWD	NØ
15	4	4.400	8.000	10	21.00	3.4	3.4	FWD	NØ
15	4	2.800	8.000	14	33.00	3.4	3.4	FWD	NØ
16	1	1.000	1.000	16	31.00	4.9	4.9	REV	NØ
16	1	3.000	3.000	16	29.00	4.9	4.9	REV	NØ
16	2	4.800	8.000	7	21.00	4.8	4.8	FWD	NØ
16	2	2.800	8.000	9	32.00	4.8	4.8	FWD	NØ
16	3	2.000	2.000	13	25.00	4.9	4.9	REV	NØ
16	3	5.000	8.000	13	24.00	4.9	4.9	REV	NØ
16	3	3.000	8.000	17	34.00	4.9	4.9	REV	NØ

F#	S/N	TD	TP	VP	IP	VZB	VZA	POL	FAIL
17	1	1.000	1.000	35	36.00	7.4	7.4	REV	NØ
17	1	4.000	4.000	25	20.00	7.4	7.4	REV	NØ
17	1	2.800	3.500	52	30.00	7.4	2.5	REV	YES
17	2	1.400	4.000	72	28.00	7.5	2.0	REV	YES
17	6	5.000	9.000	44	20.00	7.4	7.4	REV	YES
17	8	1.000	1.000	15	36.00	7.4	7.4	FWD	NØ
17	8	6.000	10.000	10	20.00	7.4	7.4	FWD	NØ
17	8	3.200	20.000	15	35.00	7.4	7.4	FWD	NØ
18	1	1.000	1.000	15	34.00	5.2	5.2	REV	NØ
18	1	3.000	3.000	16	32.00	5.2	5.2	REV	NØ
18	1	6.000	8.000	12	22.00	5.2	5.2	REV	NØ
18	1	3.000	8.000	16	32.00	5.2	5.2	REV	NØ
18	2	6.000	8.000	6	19.00	4.8	4.8	FWD	NØ
18	2	4.000	8.000	7	27.00	4.8	4.8	FWD	NØ
18	2	3.000	8.000	10	32.00	4.8	4.8	FWD	NØ
18	3	2.000	2.000	15	38.00	5.1	5.1	REV	NØ
18	3	6.000	8.000	10	16.00	5.1	5.1	REV	NØ
18	3	4.000	8.000	15	36.00	5.1	5.1	REV	NØ
19	1	6.000	6.000	10	18.50	3.8	3.8	REV	NØ
19	1	4.300	6.000	14	24.00	3.8	3.8	REV	NØ
19	1	3.000	6.000	18	36.00	3.8	3.8	REV	NØ
19	2	4.400	5.000	8	21.00	3.4	3.4	FWD	NØ
19	2	3.000	5.000	13	36.00	3.4	3.4	FWD	NØ
20	1	1.000	1.000	16	35.00	6.0	6.0	REV	NØ
20	1	3.000	3.000	22	36.00	6.0	6.0	REV	NØ
20	1	6.000	6.000	14	18.00	6.0	6.0	REV	NØ
20	1	4.000	6.000	18	28.00	6.0	6.0	REV	NØ
20	1	3.000	6.000	22	38.00	6.0	6.0	REV	NØ
20	2	1.000	1.000	9	40.00	6.2	6.2	FWD	NØ
20	2	3.000	6.000	11	38.00	6.2	6.2	FWD	NØ
20	2	4.000	8.000	11	36.00	6.2	6.2	FWD	NØ
20	3	2.000	2.000	14	19.00	6.1	6.1	REV	NØ
20	3	2.000	2.000	22	36.00	6.1	.0	REV	YES
20	4	2.000	2.000	20	32.00	6.2	6.2	REV	NØ
20	4	2.000	2.000	22	36.00	6.2	.0	REV	YES
20	5	3.000	5.000	24	34.00	6.2	6.2	REV	NØ
20	7	2.000	2.000	22	36.00	6.1	6.1	REV	NØ
20	7	3.000	8.000	23	35.00	6.1	6.1	REV	NØ
21	1	7.000	6.000	13	13.00	6.1	6.1	REV	NØ
21	1	5.000	7.000	35	23.00	6.1	6.1	REV	NØ

F#	S/N	TD	TP	VP	IP	VZB	VZA	PØL	FAIL
21	1	3.000	7.000	40	35.00	6.1	6.1	REV	NØ
21	2	6.500	6.000	7	18.00	5.8	5.8	FWD	NØ
21	2	3.000	6.000	12	36.00	5.8	5.8	FWD	NØ
22	1	2.000	2.000	19	39.00	560.0	560.0	FWD	NØ
22	1	3.200	7.000	18	37.00	560.0	560.0	FWD	NØ
22	5	4.000	4.000	315	.50	118.0	31.0	REV	YES
22	2	1.000	1.000	800	1.00	110.0	110.0	REV	NØ
22	2	.250	1.000	850	1.40	110.0	30.0	REV	YES
22	6	2.000	2.000	630	2.00	65.0	65.0	REV	NØ
22	6	1.000	2.000	710	2.00	65.0	65.0	REV	NØ
22	6	1.750	2.000	710	2.00	65.0	42.0	REV	YES
22	3	2.000	2.000	750	1.80	200.0	200.0	REV	NØ
22	3	1.500	2.000	820	2.00	200.0	17.0	REV	YES
23	1	1.000	1.000	13	8.00	5.0	5.0	REV	NØ
23	1	1.500	1.000	30	37.00	5.0	5.0	REV	NØ
23	1	5.000	5.000	25	24.00	5.0	5.0	REV	NØ
23	1	3.000	5.000	33	29.00	5.0	5.0	REV	NØ
23	2	3.000	3.000	25	23.00	4.6	4.6	REV	NØ
23	2	3.000	3.000	29	36.00	4.6	2.6	REV	YES
23	3	3.000	3.000	29	36.00	5.4	5.4	REV	NØ
23	4	4.000	3.000	20	25.00	5.5	5.5	FWD	NØ
23	4	3.000	3.000	25	34.00	5.5	5.5	FWD	NØ
23	5	3.000	5.000	26	35.00	5.0	5.0	REV	NØ
23	6	3.000	5.000	29	33.00	5.2	5.2	REV	NØ
24	2	.100	1.000	100	7.00	108.0	.0	REV	YES
24	5	.100	1.000	80	10.00	100.0	.0	REV	YES
24	6	.100	2.000	100	10.00	110.0	.0	REV	YES
26	1	1.000	1.000	30	7.50	17.0	17.0	REV	NØ
26	1	4.000	1.000	38	12.00	17.0	17.0	REV	NØ
26	1	1.600	1.000	44	10.50	17.0	10.0	REV	YES
26	2	3.000	3.000	45	11.00	17.0	17.0	REV	NØ
26	2	1.100	3.000	50	14.00	17.0	10.0	REV	YES
26	3	6.500	6.000	40	12.00	17.0	17.0	REV	NØ
26	3	1.000	6.000	55	17.00	17.0	10.0	REV	YES
26	4	1.000	1.000	7	16.00	17.0	17.0	FWD	NØ
26	4	1.000	1.000	18	23.00	17.0	17.0	FWD	NØ
26	4	1.000	1.000	12	31.00	17.0	10.0	FWD	YES
26	5	5.000	5.000	11	24.00	17.0	17.0	FWD	NØ
26	5	4.000	5.000	13	28.00	17.0	10.0	FWD	YES
27	1	1.000	1.000	380	18.00	64.0	64.0	REV	NØ

F#	S/N	TD	TP	VP	IP	VZB	VZA	PØL	FAIL
27	1	.600	1.000	400	20.00	64.0	49.0	REV	YES
27	2	1.000	3.000	319	11.00	68.0	56.0	REV	YES
27	3	.400	6.000	200	10.50	68.0	18.0	REV	YES
27	4	1.000	6.000	175	8.00	66.0	53.0	REV	YES
27	5	3.000	4.000	200	7.00	65.0	65.0	REV	NØ
27	5	4.000	4.000	250	10.00	65.0	65.0	REV	NØ
27	5	1.100	4.000	290	12.50	65.0	48.0	REV	YES
27	6	8.000	8.000	220	9.50	63.0	63.0	REV	NØ
27	6	2.000	8.000	260	12.00	63.0	42.0	REV	YES
27	7	9.000	9.000	20	10.00	67.0	67.0	FWD	NØ
27	7	5.000	8.000	20	17.00	67.0	67.0	FWD	NØ
27	7	4.000	8.000	29	30.00	67.0	67.0	FWD	NØ
28	1	.200	2.000	800	2.00	710.0	.0	REV	YES
28	3	.500	2.000	800	1.60	720.0	720.0	REV	YES
28	5	.400	5.000	800	1.50	710.0	.0	REV	YES
28	6	.200	5.000	950	1.50	850.0	.0	REV	YES
28	8	.300	8.000	950	1.70	820.0	.0	REV	YES
28	4	7.000	8.000	5	16.00	1000.0	1000.0	FWD	NØ
28	4	4.000	8.000	7	24.00	1000.0	1000.0	FWD	NØ
28	4	3.000	8.000	9	35.00	1000.0	1000.0	FWD	NØ
29	1	1.000	1.000	1000	.20	810.0	810.0	REV	NØ
29	1	3.000	3.000	1000	.10	810.0	810.0	REV	NØ
29	2	1.000	1.000	8	36.00	850.0	850.0	FWD	NØ
29	2	5.000	5.000	4	25.00	850.0	850.0	FWD	NØ
29	2	3.000	5.000	5	36.00	850.0	850.0	FWD	NØ
30	5	4.800	5.000	1000	.60	970.0	970.0	REV	NØ
30	4	1.000	1.000	5	17.00	1000.0	1000.0	FWD	NØ
30	4	5.000	5.000	5	26.00	1000.0	1000.0	FWD	NØ
30	4	3.000	5.000	6	40.00	1000.0	1000.0	FWD	NØ
31	1	1.000	1.000	12	15.00	8.6	8.6	REV	NØ
31	1	10.000	10.000	12	13.00	8.6	8.6	REV	NØ
31	2	1.000	1.000	4	14.00	8.7	8.7	FWD	NØ
31	2	10.000	10.000	3	13.00	8.7	8.7	FWD	NØ
31	3	6.000	6.000	12	14.00	8.8	8.8	REV	NØ
31	3	3.300	8.000	15	30.00	8.8	8.8	REV	NØ
31	3	6.500	6.500	4	19.00	8.8	8.8	FWD	NØ
31	3	3.200	7.500	5	30.00	8.8	8.8	FWD	NØ
31	4	6.000	7.000	11	20.00	8.9	8.9	REV	NØ
31	4	3.000	7.000	13	36.00	8.9	8.9	REV	NØ
31	5	6.500	7.000	3	17.00	8.9	8.9	FWD	NØ
31	5	3.000	7.000	6	36.00	8.9	8.9	FWD	NØ

F#	S/N	TD	TP	VP	IP	VZB	VZA	PØL	FAIL
32	1	1.000	1.000	34	15.00	31.0	31.0	REV	NØ
32	1	10.000	10.000	32	13.00	31.0	31.0	REV	NØ
32	2	1.000	1.000	3	15.00	31.5	31.5	FWD	NØ
32	2	10.000	10.000	3	13.00	31.5	31.5	FWD	NØ
32	3	6.000	6.000	38	15.00	33.0	33.0	REV	NØ
32	3	3.300	7.500	42	50.00	33.0	33.0	REV	NØ
32	3	3.300	7.500	42	50.00	33.0	33.0	REV	NØ
34	1	1.000	1.000	17	36.00	6.7	6.7	REV	NØ
34	1	5.000	6.500	13	22.00	6.7	6.7	REV	NØ
34	1	3.200	20.000	15	34.00	6.7	6.7	REV	NØ
34	2	1.000	1.000	16	40.00	6.2	6.2	FWD	NØ
34	2	2.000	3.000	15	40.00	6.2	6.2	FWD	NØ
35	1	3.000	4.000	10	36.00	1000.0	1000.0	FWD	NØ
35	2	3.000	3.000	1000	.10	580.0	580.0	REV	NØ
35	3	3.000	3.000	10	37.00	1000.0	1000.0	FWD	NØ
36	1	3.000	7.000	5	36.00	1000.0	1000.0	FWD	NØ
37	6	.700	.800	120	1.00	100.0	.0	REV	YES
37	6	.600	.600	120	1.50	100.0	.2	REV	YES
37	7	6.000	10.000	9	16.00	100.0	.0	FWD	YES
37	10	.300	2.000	120	4.00	99.0	.0	REV	YES
39	8	4.000	4.000	1000	1.40	580.0	540.0	REV	NØ
39	8	8.000	8.000	900	.90	580.0	540.0	REV	NØ
39	8	8.000	8.000	1000	1.30	580.0	740.0	REV	YES
39	6	4.000	4.000	850	.50	550.0	580.0	REV	NØ
39	6	4.000	4.000	1000	1.40	580.0	530.0	REV	YES
39	2	1.000	1.000	840	8.00	275.0	275.0	REV	NØ
39	2	4.000	4.000	840	7.00	275.0	275.0	REV	NØ
39	9	5.000	5.000	720	.25	360.0	290.0	REV	NØ
39	1	2.000	2.000	4	10.00	720.0	720.0	FWD	NØ
39	1	8.000	8.000	4	9.00	720.0	720.0	FWD	NØ
40	1	1.500	10.000	190	.60	140.0	.0	REV	YES
40	2	.150	1.000	200	2.00	135.0	17.0	REV	YES
40	3	8.500	10.000	9	5.00	125.0	34.0	FWD	YES
40	5	.500	1.000	160	.50	115.0	.0	REV	YES
40	6	2.400	6.800	170	.25	145.0	.0	REV	YES
40	7	.080	.300	180	2.00	145.0	.0	REV	YES
40	8	2.500	10.000	15	6.00	190.0	4.0	FWD	YES
40	9	6.000	9.600	12	3.50	190.0	55.0	FWD	YES

F#	S/N	TD	TP	VP	IP	VZB	VZA	PØL	FAIL
41	1	1.000	1.000	44	36.00	14.5	14.5	REV	NØ
41	1	4.000	4.000	38	23.00	14.5	14.5	REV	NØ
41	1	3.500	4.000	49	30.00	14.5	.0	REV	YES
41	2	4.200	7.000	26	35.00	14.7	14.7	REV	NØ
41	2	3.000	7.000	40	35.00	14.7	14.7	REV	NØ
41	3	3.700	7.000	52	30.00	14.8	14.8	REV	NØ
41	4	3.100	7.000	48	34.00	14.6	14.6	REV	NØ
41	5	3.700	7.000	60	30.00	14.5	.0	REV	YES
41	6	3.100	7.000	10	36.00	14.4	14.4	FWD	NØ
41	7	3.200	7.000	47	34.00	14.7	14.7	REV	NØ
43	2	2.800	3.000	25	35.00	14.0	14.0	REV	NØ
43	3	2.700	3.000	24	33.00	13.6	13.6	REV	NØ
43	4	3.000	6.000	10	36.00	13.8	13.8	FWD	NØ
44	1	1.000	1.000	36	36.00	18.0	8.0	REV	YES
44	2	3.500	7.000	32	26.00	21.0	21.0	REV	NØ
44	3	3.300	7.000	38	30.00	21.5	.0	REV	YES
44	4	3.000	4.000	40	34.00	21.0	21.0	REV	NØ
44	6	2.800	4.000	38	35.00	21.0	18.0	REV	YES
44	7	3.000	4.000	10	36.00	21.0	21.0	FWD	NØ
45	1	1.000	1.000	16	37.00	1.4	1.4	REV	NØ
45	2	4.200	5.000	8	20.00	1.6	1.6	FWD	NØ
45	2	3.000	5.000	13	36.00	1.6	1.6	FWD	NØ
46	1	1.000	1.000	15	38.00	6.4	6.4	FWD	NØ
46	1	5.000	6.000	10	20.00	6.4	6.4	FWD	NØ
46	1	3.000	6.000	15	36.00	6.4	6.4	FWD	NØ
46	2	1.000	1.000	25	39.00	6.6	6.6	REV	NØ
46	2	5.500	7.000	18	20.00	6.6	6.6	REV	NØ
46	2	3.000	7.000	26	37.00	6.6	6.6	REV	NØ
46	3	3.000	7.000	30	36.00	6.6	6.6	REV	NØ
47	3	2.000	2.000	3	19.00	650.0	650.0	FWD	NØ
47	3	3.000	2.000	5	39.00	650.0	650.0	FWD	NØ
47	5	.100	2.000	950	4.00	600.0	17.0	REV	YES
48	1	3.000	3.000	800	.40	285.0	285.0	REV	NØ
48	1	1.000	1.000	800	.35	285.0	285.0	REV	NØ
48	1	6.000	6.000	700	.15	285.0	285.0	REV	NØ
48	1	.200	6.000	900	1.80	285.0	.0	REV	YES
48	2	6.000	6.000	950	.80	80.0	80.0	REV	NØ
48	2	4.000	6.000	1000	1.00	80.0	80.0	REV	NØ

F#	S/N	TD	TP	VP	IP	VZB	VZA	PØL	FAIL
48	3	6.000	6.000	900	.40	350.0	350.0	REV	NØ
48	3	3.600	6.000	1000	.50	350.0	350.0	REV	NØ
48	4	6.000	6.000	900	.20	360.0	360.0	REV	NØ
48	4	.100	6.000	1000	2.00	360.0	2.5	REV	YES
48	5	7.000	7.000	900	.50	400.0	400.0	REV	NØ
48	5	.100	7.000	950	4.00	400.0	.0	REV	YES
48	9	.100	7.000	900	5.00	300.0	.0	REV	YES
48	10	2.000	2.000	2	15.00	350.0	350.0	FWD	NØ
48	10	4.000	5.000	5	26.00	350.0	350.0	FWD	NØ
48	10	3.000	5.000	6	36.00	350.0	350.0	FWD	NØ
49	1	3.000	3.000	25	34.00	6.5	6.5	REV	NØ
49	2	5.000	6.000	7	20.00	6.7	6.7	FWD	NØ
50	6	1.500	1.500	24	34.00	176.0	176.0	FWD	NØ
50	6	1.800	3.000	22	30.00	176.0	120.0	FWD	YES
50	7	1.300	2.000	28	33.00	180.0	16.0	FWD	YES
50	8	2.400	6.000	23	24.00	176.0	8.0	FWD	YES
50	9	4.000	6.000	16	22.00	169.0	169.0	FWD	NØ
50	9	3.300	6.000	18	24.00	169.0	144.0	FWD	YES
50	1	.150	1.000	180	6.00	168.0	8.2	REV	YES
50	2	.200	1.000	180	4.00	190.0	.0	REV	YES
50	3	.300	1.000	170	2.00	176.0	42.0	REV	YES
50	4	.800	3.000	170	.80	178.0	.0	REV	YES
50	5	3.000	3.000	175	.20	174.0	174.0	REV	NØ
50	5	1.000	3.000	170	.60	174.0	50.0	REV	YES
51	1	.100	1.000	160	5.50	124.0	13.0	REV	YES
51	2	.100	1.000	145	6.00	118.0	1.2	REV	YES
51	3	.400	2.000	150	1.00	140.0	.0	REV	YES
51	4	2.000	2.000	150	.10	142.0	142.0	REV	NØ
51	4	1.300	2.000	160	.40	142.0	.0	REV	YES
51	5	.600	7.000	135	.40	126.0	126.0	REV	NØ
51	5	.600	7.000	135	.60	126.0	.0	REV	YES
51	6	4.000	4.000	14	12.00	140.0	140.0	FWD	NØ
51	6	1.800	4.000	27	22.00	140.0	2.5	FWD	YES
51	7	.700	1.000	28	30.00	112.0	2.5	FWD	YES
51	8	1.000	1.000	32	33.00	138.0	86.0	FWD	YES
51	9	2.800	5.000	20	16.00	138.0	70.0	FWD	YES
52	1	1.000	1.000	16	38.00	11.0	11.0	REV	NØ
52	1	4.000	4.000	16	28.00	11.0	11.0	REV	NØ
52	2	5.000	7.000	15	25.00	11.0	11.0	REV	NØ
52	2	3.000	7.000	18	36.00	11.0	11.0	REV	NØ
52	3	2.000	2.000	6	37.00	11.0	11.0	FWD	NØ

F#	S/N	TD	TP	VP	IP	VZB	VZA	POL	FAIL
52	3	5.500	6.000	4	21.00	11.0	11.0	FWD	NØ
52	3	3.000	6.000	6	36.00	11.0	11.0	FWD	NØ
53	1	1.250	1.000	110	26.00	32.0	32.0	REV	NØ
53	1	1.000	1.000	150	32.00	32.0	22.0	REV	YES
53	2	2.200	4.000	100	22.00	32.5	.0	REV	YES
53	3	4.000	4.000	110	20.00	35.0	35.0	REV	NØ
53	3	3.600	4.000	115	21.00	35.0	4.0	REV	YES
53	5	3.000	7.000	85	16.50	35.0	1.0	REV	YES
53	6	6.000	7.000	9	16.00	33.5	33.5	FWD	NØ
53	6	3.000	7.000	14	36.00	33.5	33.5	FWD	NØ
53	7	7.500	7.000	90	14.50	33.0	33.0	REV	NØ
53	7	5.000	7.000	105	16.50	33.0	33.0	REV	NØ
53	7	4.400	7.000	110	19.50	33.0	.0	REV	YES
54	2	5.000	5.000	5	13.50	600.0	600.0	FWD	NØ
54	2	5.000	5.000	6	24.00	600.0	600.0	FWD	NØ
54	2	3.000	5.000	7	36.00	600.0	600.0	FWD	NØ
55	1	1.000	1.000	600	.20	415.0	415.0	REV	NØ
55	1	.250	1.000	790	4.30	415.0	410.0	REV	YES
55	2	3.000	3.000	600	.90	380.0	380.0	REV	NØ
55	2	3.000	3.000	600	5.50	380.0	380.0	REV	NØ
55	2	.800	3.000	580	8.50	380.0	380.0	REV	YES
55	3	3.000	3.000	630	9.50	410.0	400.0	REV	NØ
55	3	3.000	3.000	650	11.00	410.0	400.0	REV	NØ
55	3	2.600	3.000	580	15.00	410.0	400.0	REV	YES
55	4	3.000	3.000	620	10.00	350.0	350.0	REV	NØ
55	4	3.000	3.000	640	12.50	350.0	350.0	REV	NØ
56	3	7.000	7.000	5	20.00	1000.0	1000.0	FWD	NØ
56	3	3.400	8.000	6	30.00	1000.0	1000.0	FWD	NØ
56	7	9.000	9.000	1000	.02	860.0	860.0	REV	NØ
58	1	8.300	8.300	2000	1.00	880.0	880.0	REV	NØ
58	3	4.000	4.000	1600	1.00	800.0	800.0	REV	NØ
58	3	4.000	4.000	1750	1.00	800.0	800.0	REV	NØ
58	4	4.000	4.000	1700	.60	750.0	750.0	REV	NØ
58	6	4.000	4.000	1400	.40	725.0	725.0	REV	NØ
58	6	4.000	4.000	1700	3.00	725.0	725.0	REV	NØ
58	7	2.000	2.000	1900	2.00	870.0	870.0	REV	NØ
58	10	2.000	2.000	10	70.00	1000.0	1000.0	FWD	NØ
59	2	.150	.200	240	4.00	182.0	180.0	REV	NØ

F#	S/N	TD	TP	VP	IP	VZB	VZA	POL	FAIL
59	2	.160	.200	316	8.00	180.0	.0	REV	YES
59	4	.200	.200	272	1.00	200.0	200.0	REV	NØ
59	4	.200	.500	306	3.00	200.0	.0	REV	YES
59	5	.400	1.000	272	2.00	250.0	.0	REV	YES
59	6	.800	.800	229	.80	240.0	240.0	REV	NØ
59	7	1.000	3.000	278	1.00	235.0	.0	REV	YES
59	10	1.000	4.000	204	2.20	160.0	.0	REV	YES
59	12	3.000	4.000	180	.75	160.0	.0	REV	YES
59	13	.800	8.000	150	1.00	138.0	.0	REV	YES
59	14	.800	9.000	180	.50	160.0	.0	REV	YES
59	15	.200	6.000	170	.80	160.0	.0	REV	YES
59	16	4.000	4.000	180	.20	160.0	160.0	REV	NØ
59	16	2.000	4.000	180	.40	160.0	.0	REV	YES
59	18	3.300	4.000	210	.30	200.0	.0	REV	YES
59	19	3.000	4.500	135	.40	120.0	.0	REV	YES
59	20	.400	.400	240	.80	180.0	180.0	REV	NØ
59	20	.400	.500	230	2.00	180.0	.0	REV	YES
59	21	.400	.400	200	1.80	160.0	160.0	REV	NØ
59	21	.250	.500	220	2.00	160.0	.0	REV	YES
59	22	.300	.500	210	2.00	170.0	.0	REV	YES
59	23	.040	.048	438	13.00	200.0	110.0	REV	YES
59	24	.040	.048	368	11.00	183.0	.0	REV	YES
59	25	.048	.048	306	13.50	200.0	200.0	REV	NØ
59	25	.012	.048	350	13.60	260.0	.0	REV	YES
59	26	.030	.048	429	13.60	202.0	.0	REV	YES
59	27	.048	.048	350	11.30	185.0	19.0	REV	YES
59	29	.400	.048	293	9.00	170.0	.0	REV	YES
59	30	.024	.024	438	13.60	150.0	150.0	REV	NØ
59	30	.005	.024	875	20.60	150.0	150.0	REV	NØ
59	31	.024	.024	421	7.90	172.0	172.0	REV	NØ
59	31	.003	.024	758	6.80	172.0	.0	REV	YES
59	32	.020	.024	505	11.30	170.0	70.0	REV	YES
59	33	.024	.024	337	1.10	210.0	210.0	REV	NØ
59	33	.024	.024	505	22.70	210.0	.0	REV	YES
59	34	.024	.024	590	11.30	195.0	195.0	REV	NØ
59	35	.018	.024	758	18.10	195.0	.0	REV	YES
59	36	.004	.024	744	11.80	190.0	100.0	REV	YES
59	37	.013	.024	674	10.20	190.0	.0	REV	YES
59	40	.010	.010	675	32.60	190.0	190.0	REV	NØ
59	40	.010	.010	675	32.60	190.0	.0	REV	YES
59	41	.010	.010	420	9.00	230.0	230.0	REV	NØ
59	41	.003	.010	840	45.30	230.0	.0	REV	YES
59	43	.008	.010	690	9.00	150.0	.0	REV	YES
59	46	.010	.010	422	6.80	201.0	.0	REV	YES
59	47	.010	.010	421	9.00	180.0	180.0	REV	NØ

F#	S/N	TD	TP	VP	IP	VZB	VZA	PØL	FAIL
59	50	.005	.005	860	6.80	210.0	210.0	REV	NØ
59	50	.003	.005	880	9.00	210.0	.0	REV	YES
59	53	.005	.005	343	2.20	200.0	.0	REV	YES
60	1	1.600	1.600	4	3.80	14.0	14.0	REV	NØ
60	1	2.000	2.000	1	65.00	14.0	14.0	REV	NØ
60	2	2.300	2.300	25	50.00	14.0	5.0	REV	YES
60	3	2.300	2.300	24	70.00	14.0	14.0	REV	NØ
60	5	1.000	1.000	26	160.00	14.0	14.0	REV	NØ
60	5	1.000	1.000	30	200.00	14.0	.0	REV	YES
60	7	1.000	1.000	50	50.00	14.0	10.0	FWD	YES
60	8	1.000	1.000	130	120.00	14.0	14.0	FWD	NØ
60	9	1.900	1.900	20	125.00	14.0	14.0	FWD	NØ
60	10	1.600	1.600	17	135.00	14.0	14.0	FWD	NØ
61	1	4.500	4.700	2000	.30	1500.0	1500.0	REV	NØ
61	2	4.200	4.200	2400	2.00	1600.0	1600.0	REV	NØ
61	2	4.200	4.200	2400	4.00	1600.0	1600.0	REV	NØ
61	3	4.000	4.000	2400	1.40	1400.0	1400.0	REV	NØ
61	3	3.700	3.700	2500	4.00	1400.0	1400.0	REV	NØ
61	5	4.000	4.000	2100	.30	1300.0	1300.0	REV	NØ
61	5	4.000	3.900	2300	4.00	1300.0	1300.0	REV	NØ
61	5	4.000	4.000	2400	10.00	1300.0	1300.0	REV	NØ
61	7	7.900	7.900	1950	7.00	1500.0	1500.0	REV	NØ
61	8	7.600	7.600	1900	4.00	1400.0	1400.0	REV	NØ
62	3	4.000	4.000	1550	18.00	750.0	750.0	REV	NØ
62	3	3.200	3.200	1600	23.00	750.0	750.0	REV	NØ
62	4	.200	3.800	500	19.00	325.0	.0	REV	YES
62	8	7.800	7.800	1600	17.00	100.0	100.0	REV	NØ
62	8	3.900	3.900	1700	38.00	100.0	100.0	REV	NØ
62	9	1.800	1.800	5	90.00	225.0	225.0	FWD	NØ
62	9	1.800	1.800	5	115.00	225.0	225.0	FWD	NØ
63	1	2.200	2.200	1250	17.00	250.0	250.0	REV	NØ
63	1	.500	2.200	1350	26.00	250.0	.0	REV	YES
63	2	2.000	2.000	1450	30.00	330.0	320.0	REV	NØ
63	2	2.000	2.000	1500	32.00	330.0	.0	REV	YES
63	3	2.000	2.000	1100	25.00	320.0	320.0	REV	NØ
63	5	2.000	2.000	1240	22.00	250.0	250.0	REV	NØ
63	5	2.000	2.000	1450	32.00	250.0	250.0	REV	NØ
63	5	.400	2.000	1600	38.00	250.0	.0	REV	YES
63	6	3.200	4.000	1450	24.00	400.0	400.0	REV	NØ
63	7	3.800	3.800	1500	21.00	640.0	640.0	REV	NØ
63	7	3.800	3.800	1700	38.00	640.0	640.0	REV	NØ

F#	S/N	TD	TP	VP	IP	VZB	VZA	PØL	FAIL
63	8	3.500	3.500	20	125.00	250.0	200.0	FWD	NØ
63	9	3.400	3.400	10	120.00	320.0	320.0	FWD	NØ
63	10	3.400	3.400	5	115.00	400.0	400.0	FWD	NØ
64	2	3.800	3.800	1500	4.00	1000.0	1000.0	REV	NØ
64	2	3.800	3.800	1600	9.00	1000.0	1000.0	REV	NØ
64	3	4.000	4.000	1650	22.00	800.0	800.0	REV	NØ
64	4	4.000	4.000	1700	6.00	1000.0	1000.0	REV	NØ
64	4	.600	4.000	1750	17.00	1000.0	22.0	REV	YES
64	5	6.000	6.000	1700	26.00	660.0	660.0	REV	NØ
64	7	.100	1.200	750	35.00	525.0	8.0	REV	YES
64	9	1.300	1.300	10	60.00	1000.0	1000.0	FWD	NØ
64	9	1.000	1.000	10	125.00	1000.0	1000.0	FWD	NØ
64	10	1.800	1.800	8	130.00	190.0	190.0	FWD	NØ
65	5	.012	.048	1700	265.00	1100.0	.0	REV	YES
65	6	.012	.048	854	102.00	1600.0	.0	REV	YES
65	8	.008	.048	1290	180.00	800.0	.0	REV	YES
65	9	.010	.048	1708	193.00	950.0	.0	REV	YES
65	10	.014	.048	1540	82.00	700.0	15.0	REV	YES
65	11	.048	.048	1332	82.00	950.0	950.0	REV	NØ
65	11	.048	.048	1760	61.00	950.0	950.0	REV	NØ
65	11	.012	.048	1540	143.00	950.0	.0	REV	YES
65	12	.012	.048	1320	102.00	900.0	.0	REV	YES
65	14	.010	.024	1100	82.00	1100.0	.0	REV	YES
65	15	.020	.024	1320	82.00	1280.0	.0	REV	YES
65	16	.014	.024	1320	82.00	1000.0	.0	REV	YES
65	17	.024	.024	880	94.00	1000.0	.0	REV	YES
65	18	.024	.024	1320	54.00	1000.0	1000.0	REV	NØ
65	18	.024	.024	1760	82.00	1000.0	.0	REV	YES
65	20	.010	.024	1320	68.00	1080.0	.0	REV	YES
65	21	.024	.024	1320	102.00	955.0	950.0	REV	NØ
65	22	.010	.010	1320	13.00	950.0	.0	REV	YES
65	23	.010	.010	1760	83.00	1100.0	.0	REV	YES
65	24	.010	.010	1320	41.00	900.0	900.0	REV	NØ
65	26	.010	.010	1320	27.00	1000.0	.0	REV	YES
65	27	.010	.010	2200	13.00	1300.0	.0	REV	YES
65	28	.010	.010	2640	82.00	1000.0	.0	REV	YES
65	30	.010	.010	1760	88.00	1000.0	.0	REV	YES
65	31	.010	.010	1650	68.00	1250.0	.0	REV	YES
65	32	.005	.005	2000	67.00	950.0	950.0	REV	NØ
65	32	.005	.005	2200	110.00	950.0	950.0	REV	NØ
65	33	.003	.005	3300	110.00	800.0	800.0	REV	NØ
65	34	.005	.005	2300	50.00	1000.0	1000.0	REV	NØ
65	35	.005	.005	3000	80.00	1000.0	.0	REV	YES

F#	S/N	TD	TP	VP	IP	VZB	VZA	PØL	FAIL
66	1	4.000	4.000	160	30.00	130.0	130.0	REV	NØ
66	1	3.000	4.000	170	42.00	130.0	.0	REV	YES
66	2	.500	5.300	100	40.00	130.0	40.0	REV	YES
66	3	6.800	6.800	185	65.00	130.0	130.0	REV	NØ
66	4	2.000	2.000	160	70.00	120.0	120.0	REV	NØ
66	4	2.000	2.000	120	40.00	120.0	.0	REV	YES
66	5	2.000	2.000	170	125.00	125.0	125.0	REV	NØ
66	6	2.200	2.200	160	85.00	125.0	125.0	REV	NØ
66	6	.200	1.800	200	85.00	125.0	.0	REV	YES
66	7	1.800	1.800	800	100.00	125.0	110.0	FWD	NØ
66	9	1.800	1.700	600	160.00	125.0	125.0	FWD	NØ
66	10	2.000	2.000	600	170.00	125.0	125.0	FWD	NØ
67	3	8.000	8.000	1600	3.00	740.0	740.0	REV	NØ
67	3	8.000	8.000	1750	5.00	740.0	740.0	REV	NØ
67	4	.200	9.200	1700	6.00	550.0	.0	REV	YES
67	5	9.000	9.000	1600	4.00	680.0	680.0	REV	NØ
67	5	.800	8.200	1600	8.00	680.0	.0	REV	YES
67	6	.250	8.400	1700	6.00	740.0	.0	REV	YES
67	7	4.000	4.000	1600	8.00	560.0	560.0	REV	NØ
67	9	4.000	4.000	1900	7.00	700.0	700.0	REV	NØ
67	9	.200	4.000	1750	8.00	700.0	30.0	REV	YES
68	2	1.300	2.000	840	12.00	650.0	650.0	REV	YES
68	3	1.100	1.800	1200	5.00	650.0	650.0	REV	NØ
68	3	1.200	1.700	1400	7.50	650.0	650.0	REV	NØ
68	5	2.200	8.000	1300	4.00	670.0	.0	REV	YES
68	6	4.000	8.200	1200	3.50	450.0	.0	REV	YES
68	7	3.000	8.200	960	4.00	650.0	.0	REV	YES
68	9	4.000	4.000	1100	2.00	620.0	620.0	REV	NØ
68	9	2.200	4.000	1200	5.00	620.0	.0	REV	YES
69	2	.200	2.100	1500	8.00	1200.0	20.0	REV	YES
69	4	.100	2.000	800	20.00	550.0	.0	REV	YES
69	6	4.000	4.000	1600	1.50	1150.0	1150.0	REV	NØ
69	6	.300	4.000	1600	4.00	1150.0	100.0	REV	YES
69	8	.100	4.000	1450	3.00	1100.0	18.0	REV	YES

F#	S/N	TD	TP	VP	IP	VZB	VZA	PØL	FAIL
70	104	10.000	10.000	528	1.40	250.0	250.0	REV	NØ
70	104	4.300	10.000	696	1.60	250.0	10.0	REV	YES
70	122	10.000	10.000	465	1.30	230.0	230.0	REV	NØ
70	116	10.000	10.000	12	32.00	245.0	245.0	FWD	NØ
70	116	10.000	10.000	14	38.00	245.0	50.0	FWD	YES
70	118	10.000	10.000	16	46.00	265.0	265.0	FWD	NØ
70	118	7.600	10.000	17	59.00	265.0	250.0	FWD	YES
70	199	1.000	1.000	760	1.10	152.0	152.0	REV	NØ
70	199	.800	1.000	864	1.20	152.0	62.0	REV	YES
70	200	.630	1.000	720	1.30	160.0	20.0	REV	YES
70	203	1.000	1.000	825	.95	205.0	205.0	REV	NØ
70	203	.650	1.000	975	1.15	205.0	4.0	REV	YES
70	205	1.000	1.000	15	49.00	255.0	255.0	FWD	NØ
70	205	1.000	1.000	16	63.00	255.0	210.0	FWD	YES
70	206	1.000	1.000	9	41.00	168.0	168.0	FWD	NØ
70	206	1.000	1.000	12	47.00	168.0	80.0	FWD	YES
70	208	.100	.100	1036	2.00	240.0	240.0	REV	NØ
70	208	.063	.100	1120	3.00	240.0	230.0	REV	YES
70	209	.100	.100	770	--	150.0	150.0	REV	NØ
70	209	.037	.100	1050	6.00	150.0	5.0	REV	YES
71	67	10.000	10.000	426	.60	320.0	320.0	REV	NØ
71	67	6.200	10.000	450	.70	320.0	20.0	REV	YES
71	68	10.000	10.000	370	.30	320.0	320.0	REV	NØ
71	68	7.000	10.000	378	.50	320.0	20.0	REV	YES
71	70	10.000	10.000	392	.30	320.0	320.0	REV	NØ
71	70	2.300	10.000	400	.35	320.0	20.0	REV	YES
71	92	1.000	1.000	500	.31	340.0	340.0	REV	NØ
71	92	.250	1.000	500	.80	340.0	20.0	REV	YES
71	93	1.000	1.000	427	.52	320.0	320.0	REV	NØ
71	93	.210	1.000	470	.55	320.0	5.0	REV	YES
71	77	1.000	1.000	14	27.00	360.0	360.0	FWD	NØ
71	77	1.000	1.000	22	64.00	360.0	20.0	FWD	YES
71	80	.100	.100	502	1.60	290.0	290.0	REV	NØ
71	80	.060	.100	585	2.00	290.0	220.0	REV	YES
71	81	.100	.100	700	--	370.0	20.0	REV	YES
73	68	10.000	10.000	1760	3.70	920.0	920.0	REV	NØ
73	69	10.000	10.000	1628	3.50	890.0	890.0	REV	NØ
73	72	1.000	1.000	1392	1.30	900.0	900.0	REV	NØ
73	73	1.000	1.000	10	408.00	900.0	900.0	FWD	NØ
73	80	1.000	1.000	21	465.00	1200.0	1200.0	FWD	NØ
73	78	.100	.100	900	3.00	900.0	900.0	REV	NØ
73	78	.040	.100	1170	28.00	900.0	5.0	REV	YES

F#	S/N	TD	TP	VP	IP	VZB	VZA	PØL	FAIL
73	79	.100	.100	1575	4.00	840.0	840.0	REV	NØ
73	79	.090	.100	1580	30.00	840.0	10.0	REV	YES
74	1	10.000	10.000	1550	--	1050.0	1050.0	REV	NØ
74	1	10.000	10.000	1550	--	1050.0	10.0	REV	YES
74	2	1.000	1.000	1450	--	620.0	620.0	REV	NØ
74	2	.700	1.000	1500	--	620.0	10.0	REV	YES
74	12	1.000	1.000	60	480.00	1000.0	1000.0	FWD	NØ
74	11	1.000	1.000	56	475.00	920.0	920.0	FWD	NØ
74	3	.100	.100	1500	1.20	640.0	640.0	REV	NØ
74	3	.050	.100	1650	3.10	640.0	20.0	REV	YES
74	4	.100	.100	1550	.60	950.0	950.0	REV	NØ
74	4	.070	.100	1800	1.60	950.0	10.0	REV	YES
75	1	10.000	10.000	1440	.29	500.0	500.0	REV	NØ
75	1	10.000	10.000	1440	.36	500.0	10.0	REV	YES
75	2	1.000	1.000	1440	.07	730.0	730.0	REV	NØ
75	2	1.000	1.000	1440	.11	730.0	10.0	REV	YES
76	200	10.000	10.000	12	38.00	3.6	3.6	REV	NØ
76	200	10.000	10.000	14	56.00	3.6	.1	REV	YES
76	201	10.000	10.000	11	40.00	3.6	3.6	REV	NØ
76	201	10.000	10.000	12	52.00	3.6	1.0	REV	YES
76	202	10.000	10.000	8	21.00	3.5	3.5	REV	NØ
76	202	10.000	10.000	13	56.00	3.5	.2	REV	YES
76	204	1.000	1.000	10	62.00	3.7	3.7	REV	NØ
76	204	.810	1.000	13	80.00	3.7	.7	REV	YES
76	14	1.000	1.000	10	36.00	2.4	2.4	REV	NØ
76	14	1.000	1.000	14	64.00	2.4	2.1	REV	YES
76	205	1.000	1.000	15	66.00	3.6	.5	REV	YES
76	208	1.000	1.000	19	136.00	3.5	3.5	FWD	NØ
76	208	1.000	1.000	20	190.00	3.5	1.4	FWD	YES
76	209	1.000	1.000	18	150.00	2.2	.4	FWD	YES
76	17	1.000	1.000	16	122.00	2.5	2.5	FWD	NØ
76	17	1.000	1.000	20	140.00	2.5	1.4	FWD	YES
76	11	.100	.100	22	120.00	2.5	2.5	REV	NØ
76	11	.100	.100	30	140.00	2.5	.6	REV	YES
76	211	.100	.100	20	120.00	2.4	2.4	REV	NØ
76	211	.100	.100	24	160.00	2.4	2.0	REV	YES
77	103	10.000	10.000	11	23.00	4.6	4.6	REV	NØ
77	103	10.000	10.000	14	50.00	4.6	1.2	REV	YES
77	104	10.000	10.000	22	51.00	4.4	.8	REV	YES
77	105	10.000	10.000	11	22.00	4.5	4.5	REV	NØ
77	105	10.000	10.000	18	51.00	4.5	.6	REV	YES

F#	S/N	TD	TP	VP	IP	VZB	VZA	PØL	FAIL
77	106	1.000	1.000	22	60.00	4.6	4.6	REV	NØ
77	106	1.000	1.000	23	70.00	4.6	2.5	REV	YES
77	107	1.000	1.000	21	70.00	4.3	4.3	REV	NØ
77	107	1.000	1.000	22	78.00	4.3	2.6	REV	YES
77	10	1.000	1.000	9	180.00	4.6	4.6	FWD	NØ
77	10	1.000	1.000	16	215.00	4.6	3.0	FWD	YES
77	11	1.000	1.000	16	180.00	4.5	4.5	FWD	NØ
77	11	1.000	1.000	16	198.00	4.5	3.3	FWD	YES
77	12	.100	.100	56	252.00	4.4	4.4	REV	NØ
77	12	.100	.100	58	260.00	4.4	3.6	REV	YES
77	13	.100	.100	63	240.00	4.4	4.4	REV	NØ
77	13	.100	.100	65	328.00	4.4	3.5	REV	YES
78	106	8.600	10.000	36	83.00	5.8	.1	REV	YES
78	108	10.000	10.000	28	49.00	5.5	5.5	REV	NØ
78	108	6.400	10.000	33	62.00	5.5	2.0	REV	YES
78	111	10.000	10.000	32	66.00	5.8	5.8	REV	NØ
78	111	7.700	10.000	42	80.00	5.8	2.7	REV	YES
78	112	.810	1.000	95	208.00	5.7	4.6	REV	YES
78	113	1.000	1.000	77	196.00	5.5	5.5	REV	NØ
78	113	1.000	1.000	80	208.00	5.5	2.1	REV	YES
78	118	.400	1.000	58	229.00	5.4	.1	REV	YES
78	114	1.000	1.000	85	376.00	5.6	5.6	FWD	NØ
78	114	1.000	1.000	85	380.00	5.6	4.2	FWD	YES
78	117	1.000	1.000	84	407.00	5.6	5.6	FWD	NØ
78	117	1.000	1.000	90	481.00	5.6	4.2	FWD	YES
78	199	.100	.100	180	465.00	5.2	5.2	REV	NØ
78	198	.100	.100	200	470.00	5.3	5.3	REV	NØ
79	199	10.000	10.000	30	49.00	6.2	6.2	REV	NØ
79	199	10.000	10.000	33	65.00	6.2	3.1	REV	YES
79	200	10.000	10.000	31	56.00	6.2	2.6	REV	YES
79	201	1.000	1.000	90	192.00	6.2	6.2	REV	NØ
79	201	.620	1.000	117	233.00	6.2	5.0	REV	YES
79	202	1.000	1.000	99	168.00	6.3	6.2	REV	YES
79	203	.920	1.000	126	240.00	6.3	6.2	REV	YES
79	204	1.000	1.000	70	328.00	6.2	6.2	FWD	NØ
79	204	1.000	1.000	78	363.00	6.2	6.1	FWD	YES
79	205	1.000	1.000	70	289.00	6.2	6.2	FWD	NØ
79	205	1.000	1.000	70	330.00	6.2	6.1	FWD	YES
79	207	.100	.100	170	352.00	6.3	6.3	REV	NØ
79	207	.100	.100	195	405.00	6.3	5.6	REV	YES
79	208	.100	.100	150	365.00	6.2	6.2	REV	NØ
79	210	.100	.100	150	504.00	6.2	6.2	REV	NØ
80	100	10.000	10.000	11	21.00	6.6	6.6	REV	NØ

F#	S/N	TD	TP	VP	IP	VZB	VZA	PØL	FAIL
80	100	1.600	10.000	13	51.00	6.6	.1	REV	YES
80	101	5.900	10.000	12	23.00	6.5	.1	REV	YES
80	102	10.000	10.000	11	15.00	6.6	6.6	REV	NØ
80	102	10.000	10.000	12	20.00	6.6	5.7	REV	YES
80	103	1.000	1.000	15	59.00	6.6	3.8	REV	YES
80	106	1.000	1.000	12	28.00	6.6	6.6	REV	NØ
80	106	1.000	1.000	15	51.00	6.6	5.2	REV	YES
80	107	1.000	1.000	14	52.00	6.5	6.5	REV	NØ
80	107	1.000	1.000	15	62.00	6.5	5.0	REV	YES
80	108	1.000	1.000	18	78.00	6.5	3.6	REV	YES
80	111	1.000	1.000	10	97.00	6.4	5.4	FWD	YES
80	112	1.000	1.000	4	58.00	6.5	6.5	FWD	NØ
80	112	1.000	1.000	10	106.00	6.5	4.6	FWD	YES
80	113	1.000	1.000	3	68.00	6.3	6.3	FWD	NØ
80	113	1.000	1.000	4	77.00	6.3	6.2	FWD	YES
80	114	.100	.100	25	189.00	6.3	6.3	REV	NØ
80	114	.100	.100	25	203.00	6.3	3.8	REV	YES
80	115	.100	.100	23	196.00	6.4	6.4	REV	NØ
80	115	.100	.100	24	231.00	6.4	.6	REV	YES
81	24	10.000	10.000	27	46.00	7.3	7.3	REV	NØ
81	24	8.500	10.000	54	84.00	7.3	7.0	REV	YES
81	117	10.000	10.000	42	65.00	7.0	7.0	REV	NØ
81	117	10.000	10.000	42	84.00	7.0	6.4	REV	YES
81	25	10.000	10.000	29	33.00	7.1	7.1	REV	NØ
81	25	5.400	10.000	37	48.00	7.1	.2	REV	YES
81	26	1.000	1.000	60	168.00	7.2	7.2	REV	NØ
81	26	1.000	1.000	70	180.00	7.2	6.6	REV	YES
81	27	1.000	1.000	170	255.00	7.0	7.0	REV	NØ
81	27	.940	1.000	164	309.00	7.0	.2	REV	YES
81	28	.330	1.000	125	320.00	7.2	.2	REV	YES
81	30	1.000	1.000	96	465.00	7.3	7.3	FWD	NØ
81	30	1.000	1.000	100	465.00	7.3	7.3	FWD	YES
81	31	1.000	1.000	180	465.00	7.0	7.0	FWD	NØ
81	32	1.000	1.000	150	465.00	7.2	7.2	FWD	NØ
82	9	10.000	10.000	45	90.00	8.2	8.2	REV	NØ
82	9	7.400	10.000	53	119.00	8.2	.1	REV	YES
82	10	10.000	10.000	60	130.00	7.7	7.7	REV	NØ
82	10	9.100	10.000	60	140.00	7.7	4.8	REV	YES
82	11	10.000	10.000	50	102.00	8.2	8.2	REV	NØ
82	11	7.000	10.000	77	120.00	8.2	.1	REV	YES
82	12	1.000	1.000	75	290.00	8.1	8.1	REV	NØ
82	12	1.000	1.000	88	319.00	8.1	8.0	REV	YES
82	13	1.000	1.000	80	315.00	7.6	7.6	REV	NØ

F#	S/N	TD	TP	VP	IP	VZB	VZA	PØL	FAIL
82	13	1.000	1.000	85	416.00	7.6	7.6	REV	YES
82	16	1.000	1.000	120	480.00	8.0	7.9	FWD	YES
82	17	1.000	1.000	60	480.00	7.6	7.6	FWD	NØ
82	17	.100	.100	160	480.00	7.6	7.6	REV	NØ
82	18	.100	.100	140	480.00	7.7	7.7	REV	NØ
83	11	10.000	10.000	38	37.00	8.8	8.8	REV	NØ
83	11	8.000	10.000	40	43.00	8.8	8.6	REV	YES
83	12	10.000	10.000	39	37.00	8.8	8.8	REV	NØ
83	12	7.100	10.000	42	44.00	8.8	8.7	REV	YES
83	67	1.000	1.000	64	90.00	8.7	8.6	REV	NØ
83	67	1.000	1.000	78	105.00	8.6	8.6	REV	YES
83	68	1.000	1.000	36	41.00	8.6	8.6	REV	NØ
83	68	1.000	1.000	60	83.00	8.6	8.5	REV	YES
83	69	1.000	1.000	72	345.00	8.5	8.5	FWD	NØ
83	69	1.000	1.000	78	350.00	8.5	8.4	FWD	YES
83	70	1.000	1.000	57	260.00	8.8	8.8	FWD	NØ
83	70	1.000	1.000	64	280.00	8.8	8.7	FWD	YES
83	71	.100	.100	160	248.00	8.8	8.8	REV	NØ
83	71	.100	.100	190	298.00	8.8	8.2	REV	YES
83	72	.100	.100	120	254.00	8.4	8.4	REV	NØ
83	72	.100	.100	170	298.00	8.4	7.7	REV	YES
84	67	10.000	10.000	42	37.00	9.2	9.2	REV	NØ
84	67	10.000	10.000	44	41.00	9.2	8.8	REV	YES
84	68	10.000	10.000	41	31.00	9.5	9.5	REV	NØ
84	68	8.600	10.000	41	36.00	9.5	3.6	REV	YES
84	72	1.000	1.000	56	61.00	9.5	9.5	REV	NØ
84	72	1.000	1.000	80	83.00	9.5	9.4	REV	YES
84	73	1.000	1.000	114	83.00	9.6	9.6	REV	NØ
84	73	1.000	1.000	118	93.00	9.6	9.5	REV	YES
84	74	1.000	1.000	77	288.00	9.4	9.4	FWD	NØ
84	74	1.000	1.000	78	312.00	9.4	5.6	FWD	YES
84	76	1.000	1.000	70	305.00	9.6	9.6	FWD	NØ
84	76	1.000	1.000	70	352.00	9.6	9.2	FWD	YES
84	69	.100	.100	140	198.00	9.7	9.7	REV	NØ
84	69	.100	.100	150	217.00	9.7	9.6	REV	YES
84	70	.100	.100	140	203.00	9.6	9.6	REV	NØ
84	70	.100	.100	150	210.00	9.6	9.2	REV	YES
86	2	4.700	10.000	20	82.00	11.1	.1	REV	YES
86	3	10.000	10.000	17	57.00	11.2	11.2	REV	NØ
86	3	7.400	10.000	19	70.00	11.2	.1	REV	YES
86	4	1.000	1.000	38	255.00	11.8	11.8	REV	NØ
86	4	1.000	1.000	40	278.00	11.8	.3	REV	YES

F#	S/N	TD	TP	VP	IP	VZB	VZA	PØL	FAIL
86	6	1.000	1.000	32	206.00	11.3	.3	REV	YES
86	7	1.000	1.000	35	210.00	11.7	11.7	REV	NØ
86	7	1.000	1.000	35	243.00	11.7	.1	REV	YES
86	8	1.000	1.000	32	495.00	12.0	12.0	FWD	NØ
86	11	1.000	1.000	28	488.00	12.0	12.0	FWD	NØ
86	28	.100	.100	--	510.00	11.9	11.9	REV	NØ
86	9	.100	.100	40	480.00	12.0	12.0	REV	NØ
86	1	10.000	10.000	22	97.00	11.8	11.8	REV	NØ
86	1	10.000	10.000	22	100.00	11.8	11.7	REV	YES
87	1	10.000	10.000	23	11.00	13.6	13.6	REV	NØ
87	1	5.200	10.000	26	15.00	13.6	13.2	REV	YES
87	2	10.000	10.000	26	14.00	13.1	13.1	REV	NØ
87	2	3.450	10.000	28	17.00	13.1	11.2	REV	YES
87	3	1.000	1.000	21	63.00	13.2	13.2	REV	NØ
87	3	.570	1.000	47	88.00	13.2	8.7	REV	YES
87	4	1.000	1.000	46	31.00	13.7	13.7	REV	NØ
87	4	.620	1.000	48	36.00	13.7	10.8	REV	YES
87	5	1.000	1.000	36	32.00	13.6	13.6	REV	NØ
87	5	1.000	1.000	38	36.00	13.6	5.2	REV	YES
87	6	1.000	1.000	34	99.00	13.2	13.2	FWD	NØ
87	6	1.000	1.000	34	110.00	13.2	9.6	FWD	YES
87	7	.100	.100	40	70.00	13.3	13.3	REV	NØ
87	8	.100	.100	110	160.00	13.5	13.5	REV	NØ
87	8	.100	.100	140	200.00	13.5	13.2	REV	YES
87	9	.100	.100	85	181.00	13.6	13.6	REV	NØ
87	9	.100	.100	100	236.00	13.6	13.4	REV	YES
88	1	10.000	10.000	26	79.00	14.7	14.7	REV	NØ
88	1	9.200	10.000	37	77.00	14.7	2.0	REV	YES
88	2	10.000	10.000	29	74.00	14.2	14.2	REV	NØ
88	2	10.000	10.000	30	80.00	14.2	6.2	REV	YES
88	3	1.000	1.000	38	219.00	14.4	14.4	REV	NØ
88	3	1.000	1.000	42	255.00	14.4	6.7	REV	YES
88	4	1.000	1.000	42	273.00	14.0	14.0	REV	NØ
88	4	1.000	1.000	42	285.00	14.0	1.8	REV	YES
88	5	1.000	1.000	32	495.00	14.6	14.6	FWD	NØ
88	6	1.000	1.000	28	540.00	14.4	14.4	FWD	NØ
88	7	.100	.100	90	595.00	14.5	14.5	REV	NØ
88	8	.100	.100	70	609.00	14.6	14.6	REV	NØ
89	1	10.000	10.000	37	43.00	22.3	22.3	REV	NØ
89	1	10.000	10.000	38	44.00	22.3	22.3	REV	YES
89	2	10.000	10.000	48	39.00	23.2	23.2	REV	NØ
89	2	10.000	10.000	43	55.00	23.2	5.0	REV	YES

F#	S/N	TD	TP	VP	IP	VZB	VZA	PØL	FAIL
89	3	1.000	1.000	41	36.00	23.4	23.4	REV	NØ
89	4	1.000	1.000	63	146.00	23.2	23.2	REV	NØ
89	4	1.000	1.000	65	165.00	23.2	7.0	REV	YES
89	5	1.000	1.000	52	126.00	22.0	22.0	REV	NØ
89	5	1.000	1.000	55	150.00	22.0	5.0	REV	YES
89	6	1.000	1.000	50	490.00	22.4	22.4	FWD	NØ
89	7	1.000	1.000	40	500.00	23.5	23.5	FWD	NØ
89	8	1.000	1.000	35	485.00	22.8	22.8	FWD	NØ
89	9	.100	.100	144	480.00	23.1	23.1	REV	NØ
89	10	.100	.100	144	49 00	23.0	23.0	REV	NØ
90	67	10.000	10.000	108	55.00	28.2	28.2	REV	NØ
90	67	7.400	10.000	114	58.00	28.2	2.0	REV	YES
90	68	10.000	10.000	109	53.00	28.2	28.2	REV	NØ
90	68	5.800	10.000	109	58.00	28.2	1.0	REV	YES
90	69	1.000	1.000	135	80.00	28.2	28.2	REV	NØ
90	69	.970	1.000	170	84.00	28.2	18.0	REV	YES
90	70	1.000	1.000	156	84.00	28.5	16.0	REV	YES
90	71	1.000	1.000	213	93.00	29.1	29.1	REV	NØ
90	71	1.000	1.000	233	105.00	29.1	26.0	REV	YES
90	72	1.000	1.000	70	516.00	28.5	28.5	FWD	NØ
90	73	1.000	1.000	75	522.00	28.3	28.3	FWD	NØ
90	112	1.000	1.000	--	213.00	28.2	28.2	FWD	NØ
90	76	.100	.100	320	170.00	28.8	28.8	REV	NØ
90	76	.100	.100	350	193.00	28.8	22.5	REV	YES
90	77	.100	.100	350	193.00	28.2	28.2	REV	NØ
90	77	.100	.100	350	218.00	28.2	16.0	REV	YES
91	3	10.000	10.000	64	77.00	32.2	32.2	REV	NØ
91	3	5.400	10.000	72	93.00	32.2	20.0	REV	YES
91	12	5.600	10.000	62	39.00	31.5	31.4	REV	YES
91	11	10.000	10.000	64	91.00	31.8	31.8	REV	NØ
91	11	4.500	10.000	68	104.00	31.8	16.0	REV	YES
91	37	10.000	10.000	76	108.00	32.5	32.5	REV	NØ
91	37	3.200	10.000	83	132.00	32.5	25.0	REV	YES
91	1	1.000	1.000	180	455.00	32.0	32.0	REV	NØ
91	2	1.000	1.000	160	324.00	32.0	32.0	REV	NØ
91	2	.630	1.000	220	475.00	32.0	13.0	REV	YES
91	7	1.000	1.000	185	350.00	31.8	31.8	REV	NØ
91	7	.920	1.000	200	405.00	31.8	15.0	REV	YES
91	4	1.000	1.000	75	488.00	31.5	31.5	FWD	NØ
91	5	1.000	1.000	88	480.00	31.0	31.0	FWD	NØ
91	8	.100	.100	--	463.00	31.8	31.8	REV	NØ
92	61	10.000	10.000	52	14.00	33.0	33.0	REV	NØ

F#	S/N	TD	TP	VP	IP	VZB	VZA	PØL	FAIL
92	61	7.000	10.000	53	18.00	33.0	7.0	REV	YES
92	63	10.000	10.000	54	16.00	33.0	33.0	REV	NØ
92	63	8.000	10.000	53	20.00	33.0	1.0	REV	YES
92	51	1.000	1.000	63	67.00	33.0	33.0	REV	NØ
92	51	1.000	1.000	80	72.00	33.0	12.0	REV	YES
92	53	1.000	1.000	75	53.00	33.0	33.0	REV	NØ
92	53	1.000	1.000	96	62.00	33.0	32.0	REV	YES
92	56	1.000	1.000	30	240.00	33.0	33.0	FWD	NØ
92	65	1.000	1.000	58	460.00	33.0	33.0	FWD	NØ
92	58	.100	.100	225	350.00	33.0	33.0	REV	NØ
92	58	.100	.100	300	450.00	33.0	21.0	REV	YES
92	84	.100	.100	210	282.00	33.5	33.5	REV	NØ
92	84	.100	.100	240	296.00	33.5	33.0	REV	YES
93	50	10.000	10.000	1008	8.40	720.0	720.0	REV	NØ
93	51	10.000	10.000	1176	7.40	700.0	700.0	REV	NØ
93	54	1.000	1.000	1750	25.80	720.0	720.0	REV	NØ
93	55	1.000	1.000	1700	28.80	680.0	680.0	REV	NØ
93	56	1.000	1.000	17	468.00	700.0	700.0	FWD	NØ
93	57	1.000	1.000	12	500.00	680.0	680.0	FWD	NØ
93	52	.100	.100	1350	23.80	680.0	680.0	REV	NØ
93	52	.048	.100	1575	68.00	680.0	150.0	REV	YES
93	53	.100	.100	1800	28.80	720.0	720.0	REV	NØ
93	53	.062	.100	1870	100.00	720.0	40.0	REV	YES
94	66	10.000	10.000	1163	8.50	720.0	720.0	REV	NØ
94	67	10.000	10.000	1440	7.50	680.0	680.0	REV	NØ
94	58	.070	1.000	2000	93.00	720.0	1.0	REV	YES
94	70	1.000	1.000	1640	27.00	700.0	700.0	REV	NØ
94	70	.070	1.000	1650	96.00	700.0	1.0	REV	YES
94	71	1.000	1.000	1750	32.00	720.0	720.0	REV	NØ
94	71	.100	1.000	1900	102.00	720.0	1.0	REV	YES
94	72	1.000	1.000	17	488.00	680.0	680.0	FWD	NØ
94	73	1.000	1.000	18	492.00	680.0	680.0	FWD	NØ
94	74	.100	.100	1500	24.00	680.0	680.0	REV	NØ
94	74	.067	.100	1920	35.00	680.0	160.0	REV	YES
94	75	.100	.100	1400	18.00	740.0	740.0	REV	NØ
94	75	.090	.100	1700	24.00	740.0	180.0	REV	YES
95	51	2.300	10.000	1400	13.00	720.0	1.0	REV	YES
95	53	10.000	10.000	1300	3.00	680.0	680.0	REV	NØ
95	53	10.000	10.000	1300	6.30	680.0	210.0	REV	YES
95	54	4.500	10.000	1250	3.40	520.0	30.0	REV	YES
95	59	10.000	10.000	950	.45	630.0	630.0	REV	NØ
95	59	7.500	10.000	1100	1.90	630.0	80.0	REV	YES

F#	S/N	TD	TP	VP	IP	VZB	VZA	PØL	FAIL
95	62	1.000	1.000	1200	1.00	520.0	520.0	REV	NØ
95	65	1.000	1.000	1200	.80	760.0	760.0	REV	NØ
95	66	1.000	1.000	7	480.00	780.0	780.0	FWD	NØ
95	67	1.000	1.000	4	480.00	1040.0	1040.0	FWD	NØ
95	60	.100	.100	1400	6.00	820.0	820.0	REV	NØ
95	60	.050	.100	1400	38.00	820.0	820.0	REV	YES
95	61	.100	.100	960	--	1180.0	1180.0	REV	NØ
95	61	.037	.100	1400	18.00	1180.0	10.0	REV	YES
96	63	10.000	10.000	1148	9.00	620.0	620.0	REV	NØ
96	64	10.000	10.000	1015	9.00	700.0	700.0	REV	NØ
96	55	1.000	1.000	1700	24.00	760.0	760.0	REV	NØ
96	55	.073	1.000	1450	50.00	760.0	30.0	REV	YES
96	56	1.000	1.000	1700	24.00	680.0	680.0	REV	NØ
96	56	.061	1.000	1700	40.00	680.0	6.0	REV	YES
96	57	1.000	1.000	12	462.00	700.0	700.0	FWD	NØ
96	58	1.000	1.000	20	462.00	720.0	720.0	FWD	NØ
96	59	.100	.100	1650	25.00	620.0	620.0	REV	NØ
96	59	.075	.100	1700	40.00	620.0	180.0	REV	YES
96	60	.100	.100	1740	25.00	640.0	640.0	REV	NØ
96	60	.075	.100	1850	35.00	640.0	200.0	REV	YES
97	64	10.000	10.000	1200	7.00	460.0	460.0	REV	NØ
97	64	7.800	10.000	1250	14.50	460.0	20.0	REV	YES
97	52	10.000	10.000	1480	1.00	530.0	530.0	REV	NØ
97	52	.160	10.000	1580	12.00	530.0	5.0	REV	YES
97	53	1.000	1.000	1280	23.00	430.0	430.0	REV	NØ
97	58	1.000	1.000	1450	52.00	530.0	530.0	REV	NØ
97	50	1.000	1.000	12	370.00	460.0	460.0	FWD	NØ
97	51	1.000	1.000	7	385.00	540.0	540.0	FWD	NØ
97	59	.100	.100	1620	15.00	560.0	560.0	REV	NØ
97	59	.049	.100	1656	37.00	560.0	20.0	REV	YES
97	60	.100	.100	950	--	440.0	440.0	REV	NØ
97	60	.045	.100	1333	--	440.0	100.0	REV	YES
98	58	10.000	10.000	1150	8.50	740.0	740.0	REV	NØ
98	59	10.000	10.000	1250	7.30	760.0	760.0	REV	NØ
98	53	1.000	1.000	1600	23.00	720.0	720.0	REV	NØ
98	53	.080	1.000	1720	30.00	720.0	20.0	REV	YES
98	55	1.000	1.000	1550	24.00	720.0	720.0	REV	NØ
98	55	.090	1.000	1750	35.00	720.0	5.0	REV	YES
98	56	1.000	1.000	16	480.00	700.0	700.0	FWD	NØ
98	57	1.000	1.000	12	495.00	720.0	720.0	FWD	NØ
98	51	.100	.100	1450	13.00	720.0	720.0	REV	NØ
98	51	.055	.100	1550	27.00	720.0	20.0	REV	YES

F#	S/N	TD	TP	VP	IP	VZB	VZA	PØL	FAIL
98	52	.100	.100	1580	21.00	740.0	740.0	REV	NØ
98	52	.068	.100	1600	30.00	740.0	60.0	REV	YES
99	57	10.000	10.000	1550	8.50	820.0	820.0	REV	NØ
99	58	10.000	10.000	1300	6.20	740.0	740.0	REV	NØ
99	52	1.000	1.000	2025	31.60	720.0	720.0	REV	NØ
99	52	.100	1.000	2060	65.80	720.0	2.0	REV	YES
99	51	1.000	1.000	1840	26.30	840.0	840.0	REV	NØ
99	54	1.000	1.000	21	480.00	760.0	760.0	FWD	NØ
99	53	1.000	1.000	21	490.00	880.0	880.0	FWD	NØ
99	55	.100	.100	1250	108.00	880.0	880.0	REV	NØ
99	56	.100	.100	1900	112.00	760.0	760.0	REV	NØ
99	56	.076	.100	2250	133.00	760.0	160.0	REV	YES
100	50	10.000	10.000	13	160.00	6.5	6.5	REV	NØ
100	52	10.000	10.000	14	190.00	6.5	6.5	REV	NØ
100	81	1.000	1.000	30	488.00	6.4	6.4	REV	NØ
100	55	1.000	1.000	35	480.00	6.4	6.4	REV	NØ
100	56	1.000	1.000	21	475.00	6.4	6.4	FWD	NØ
100	57	1.000	1.000	18	483.00	6.3	6.3	FWD	NØ
100	51	.100	.100	--	495.00	6.4	6.4	REV	NØ
100	53	.100	.100	--	240.00	6.4	6.4	REV	NØ
101	56	10.000	10.000	28	185.00	6.4	6.4	REV	NØ
101	57	10.000	10.000	28	173.00	6.3	6.3	REV	NØ
101	50	1.000	1.000	40	488.00	6.5	6.5	REV	NØ
101	51	1.000	1.000	36	458.00	6.4	6.4	REV	NØ
101	52	1.000	1.000	11	468.00	6.5	6.5	FWD	NØ
101	53	1.000	1.000	11	483.00	6.4	6.4	FWD	NØ
101	54	.100	.100	--	463.00	6.4	6.4	REV	NØ
101	55	.100	.100	--	450.00	6.4	6.4	REV	NØ
102	50	10.000	10.000	30	180.00	22.0	22.0	REV	NØ
102	51	10.000	10.000	27	178.00	21.0	21.0	REV	NØ
102	52	1.000	1.000	39	483.00	22.0	22.0	REV	NØ
102	53	1.000	1.000	42	500.00	22.0	22.0	REV	NØ
102	54	1.000	1.000	11	475.00	21.0	21.0	FWD	NØ
102	55	1.000	1.000	12	500.00	22.0	22.0	FWD	NØ
102	56	.100	.100	--	525.00	22.0	22.0	REV	NØ
102	57	.100	.100	--	510.00	22.0	22.0	REV	NØ
103	91	10.000	10.000	32	150.00	21.0	21.0	REV	NØ
103	92	10.000	10.000	33	150.00	22.0	22.0	REV	NØ
103	87	1.000	1.000	56	492.00	22.0	22.0	REV	NØ
103	88	1.000	1.000	56	498.00	22.0	22.0	REV	NØ

F#	S/N	TD	TP	VP	IP	VZB	VZA	PØL	FAIL
103	85	1.000	1.000	17	504.00	22.0	22.0	FWD	NØ
103	86	1.000	1.000	50	510.00	22.0	22.0	FWD	NØ
103	89	.100	.100	60	516.00	21.0	21.0	REV	NØ
103	90	.100	.100	75	510.00	22.0	22.0	REV	NØ
104	60	10.000	10.000	40	180.00	27.0	27.0	REV	NØ
104	51	10.000	10.000	48	170.00	26.0	26.0	REV	NØ
104	52	1.000	1.000	56	480.00	26.0	26.0	REV	NØ
104	53	1.000	1.000	56	480.00	26.0	26.0	REV	NØ
104	54	1.000	1.000	20	540.00	26.0	26.0	FWD	NØ
104	55	.100	.100	--	405.00	27.0	27.0	REV	NØ
104	56	.100	.100	80	399.00	27.0	27.0	REV	NØ
105	61	10.000	10.000	80	170.00	30.0	30.0	REV	NØ
105	63	10.000	10.000	50	165.00	30.0	30.0	REV	NØ
105	55	1.000	1.000	70	570.00	29.0	29.0	REV	NØ
105	57	1.000	1.000	18	495.00	29.0	29.0	FWD	NØ
105	58	1.000	1.000	18	492.00	30.0	30.0	FWD	NØ
105	60	.100	.100	80	438.00	29.0	29.0	REV	NØ
105	61	.100	.100	80	435.00	30.0	30.0	REV	NØ
106	50	10.000	10.000	51	144.00	36.0	36.0	REV	NØ
106	51	10.000	10.000	50	140.00	35.0	35.0	REV	NØ
106	54	1.000	1.000	80	340.00	36.0	36.0	REV	NØ
106	56	1.000	1.000	88	493.00	36.0	36.0	REV	NØ
106	57	1.000	1.000	24	476.00	36.0	36.0	FWD	NØ
106	58	1.000	1.000	24	470.00	36.0	36.0	FWD	NØ
106	52	.100	.100	74	513.00	35.0	35.0	REV	NØ
106	53	.100	.100	77	438.00	36.0	36.0	REV	NØ
107	50	10.000	10.000	213	16.00	170.0	170.0	REV	NØ
107	51	10.000	10.000	231	17.00	190.0	190.0	REV	NØ
107	55	1.000	1.000	825	143.00	200.0	200.0	REV	NØ
107	55	.730	1.000	900	160.00	200.0	160.0	REV	YES
107	56	1.000	1.000	850	165.00	190.0	190.0	REV	NØ
107	56	.930	1.000	1050	175.00	190.0	10.0	REV	YES
107	57	1.000	1.000	21	510.00	180.0	180.0	FWD	NØ
107	58	1.000	1.000	21	475.00	180.0	180.0	FWD	NØ
107	52	.100	.100	1330	332.00	180.0	180.0	REV	NØ
107	52	.043	.100	1330	390.00	180.0	178.0	REV	YES
107	54	.100	.100	1344	300.00	180.0	180.0	REV	NØ
107	54	.100	.100	1344	320.0	180.0	20.0	REV	YES
108	46	10.000	10.000	12	160.00	7.5	7.5	REV	NØ
108	47	10.000	10.000	12	172.00	7.2	7.2	REV	NØ

F#	S/N	TD	TP	VP	IP	VZB	VZA	PØL	FAIL
108	40	1.000	1.000	24	508.00	7.5	7.5	REV	NØ
108	41	1.000	1.000	24	465.00	7.2	7.2	REV	NØ
108	42	1.000	1.000	16	495.00	7.3	7.3	FWD	NØ
108	43	1.000	1.000	14	474.00	7.2	7.2	FWD	NØ
108	44	.100	.100	35	450.00	7.5	7.5	REV	NØ
108	45	.100	.100	38	465.00	7.2	7.2	REV	NØ
109	59	10.000	10.000	13	140.00	8.7	8.7	REV	NØ
109	60	10.000	10.000	20	150.00	8.6	8.6	REV	NØ
109	52	1.000	1.000	56	480.00	8.7	8.7	REV	NØ
109	55	1.000	1.000	49	480.00	8.8	8.8	REV	NØ
109	56	1.000	1.000	49	475.00	8.6	8.6	REV	NØ
109	57	1.000	1.000	28	483.00	8.6	8.6	FWD	NØ
109	58	1.000	1.000	30	470.00	8.5	8.5	FWD	NØ
109	50	.100	.100	40	485.00	8.8	8.8	REV	NØ
109	51	.100	.100	48	493.00	8.6	8.6	REV	NØ
110	28	10.000	10.000	16	192.00	11.8	11.8	REV	NØ
110	29	10.000	10.000	15	203.00	12.0	12.0	REV	NØ
110	22	1.000	1.000	30	465.00	11.6	11.6	REV	NØ
110	23	1.000	1.000	28	465.00	11.8	11.8	REV	NØ
110	24	1.000	1.000	30	510.00	11.8	11.8	FWD	NØ
110	25	1.000	1.000	20	510.00	12.0	12.0	FWD	NØ
110	27	.100	.100	52	495.00	12.0	12.0	REV	NØ
110	26	.100	.100	50	410.00	11.2	11.2	REV	NØ
111	50	10.000	10.000	40	158.00	31.0	31.0	REV	NØ
111	51	10.000	10.000	40	162.00	30.0	30.0	REV	NØ
111	54	1.000	1.000	60	480.00	31.0	31.0	REV	NØ
111	55	1.000	1.000	55	495.00	30.0	30.0	REV	NØ
111	56	1.000	1.000	15	380.00	31.0	31.0	FWD	NØ
111	57	1.000	1.000	15	516.00	31.0	31.0	FWD	NØ
111	52	.100	.100	--	540.00	30.0	30.0	REV	NØ
111	53	.100	.100	--	540.00	31.0	31.0	REV	NØ
112	48	10.000	10.000	72	216.00	42.0	42.0	REV	NØ
112	59	10.000	10.000	68	148.00	42.0	42.0	REV	NØ
112	50	1.000	1.000	65	495.00	41.0	41.0	REV	NØ
112	51	.520	1.000	96	495.00	40.0	2.0	REV	YES
112	52	1.000	1.000	90	488.00	41.0	41.0	REV	NØ
112	67	1.000	1.000	108	490.00	43.0	43.0	REV	NØ
112	88	1.000	1.000	136	504.00	43.0	28.0	REV	YES
112	53	1.000	1.000	18	495.00	40.0	40.0	FWD	NØ
112	54	1.000	1.000	23	500.00	42.0	42.0	FWD	NØ
112	55	.100	.100	100	474.00	41.0	41.0	REV	NØ

F#	S/N	TD	TP	VP	IP	VZB	VZA	POL	FAIL
112	56	.100	.100	--	570.00	43.0	9.0	REV	YES
113	50	10.000	10.000	72	140.00	49.0	49.0	REV	NO
113	51	10.000	10.000	70	140.00	49.0	49.0	REV	NO
113	54	1.000	1.000	110	495.00	50.0	50.0	REV	NO
113	55	1.000	1.000	100	492.00	48.0	48.0	REV	NO
113	56	1.000	1.000	--	504.00	48.0	48.0	FWD	NO
113	57	1.000	1.000	20	510.00	52.0	52.0	FWD	NO
113	52	.100	.100	150	510.00	49.0	49.0	REV	NO
113	53	.100	.100	140	540.00	50.0	50.0	REV	NO
114	50	10.000	10.000	117	195.00	68.0	68.0	REV	NO
114	51	10.000	10.000	119	190.00	65.0	65.0	REV	NO
114	54	1.000	1.000	144	455.00	65.0	65.0	REV	NO
114	55	1.000	1.000	140	47[illegible]0	65.0	65.0	REV	NO
114	56	1.000	1.000	17	515.00	65.0	65.0	FWD	NO
114	57	1.000	1.000	16	495.00	68.0	68.0	FWD	NO
114	52	.100	.100	150	525.00	65.0	65.0	REV	NO
114	53	.100	.100	160	495.00	66.0	66.0	REV	NO
115	58	10.000	10.000	142	.48	140.0	140.0	REV	NO
115	58	4.100	10.000	142	.50	140.0	12.0	REV	YES
115	72	10.000	10.000	124	.10	100.0	100.0	REV	NO
115	72	1.200	10.000	133	.80	100.0	2.0	REV	YES
115	50	1.000	1.000	114	1.50	114.0	114.0	REV	NO
115	50	.880	1.000	114	2.40	114.0	6.0	REV	YES
115	51	1.000	1.000	112	2.00	108.0	108.0	REV	NO
115	51	.940	1.000	114	2.30	108.0	10.0	REV	YES
115	52	1.000	1.000	13	13.00	131.0	131.0	FWD	NO
115	52	1.000	1.000	13	17.00	131.0	8.0	FWD	YES
115	53	1.000	1.000	9	12.00	110.0	110.0	FWD	NO
115	53	1.000	1.000	12	16.00	110.0	64.0	FWD	YES
115	55	.100	.100	140	2.90	130.0	130.0	REV	NO
115	55	.100	.100	140	4.80	130.0	16.0	REV	YES
115	56	.100	.100	140	2.40	124.0	124.0	REV	NO
115	56	.060	.100	170	5.50	124.0	8.0	REV	YES
117	54	10.000	10.000	1450	.25	800.0	800.0	REV	NO
117	54	8.700	10.000	1500	.40	800.0	40.0	REV	YES
117	65	1.000	1.000	1600	5.22	760.0	760.0	REV	NO
117	65	.310	1.000	1800	7.60	760.0	60.0	REV	YES
117	7	1.000	1.000	34	400.00	900.0	900.0	FWD	NO
117	8	1.000	1.000	34	410.00	900.0	900.0	FWD	NO
118	50	1.000	1.000	105	.10	109.0	109.0	REV	NO

F#	S/N	TD	TP	VP	IP	VZB	VZA	PØL	FAIL
118	50	.700	1.000	113	1.80	109.0	6.0	REV	YES
118	51	.900	1.000	113	1.90	118.0	8.0	REV	YES
118	52	1.000	1.000	11	23.00	122.0	122.0	FWD	NØ
118	52	1.000	1.000	18	20.00	122.0	12.0	FWD	YES
118	53	1.000	1.000	12	26.00	122.0	122.0	FWD	NØ
118	53	1.000	1.000	12	27.00	122.0	24.0	FWD	YES
118	54	.090	.100	140	11.00	120.0	16.0	REV	YES
118	55	.100	.100	164	6.90	122.0	122.0	REV	NØ
118	55	.098	.100	190	9.50	122.0	16.0	REV	YES
119	56	10.000	10.000	10	154.00	3.1	3.1	REV	NØ
119	57	10.000	10.000	15	150.00	3.2	3.2	REV	NØ
119	50	1.000	1.000	28	473.00	3.1	3.1	REV	NØ
119	51	1.000	1.000	28	492.00	3.2	3.2	REV	NØ
119	52	1.000	1.000	--	495.00	3.2	3.2	FWD	NØ
119	53	1.000	1.000	--	519.00	3.2	3.2	FWD	NØ
119	54	.100	.100	40	492.00	3.2	3.2	REV	NØ
119	55	.100	.100	40	465.00	3.1	3.1	REV	NØ
120	50	10.000	10.000	23	140.00	6.0	6.0	REV	NØ
120	51	10.000	10.000	26	166.00	5.9	5.9	REV	NØ
120	54	1.000	1.000	36	481.00	6.0	6.0	REV	NØ
120	57	1.000	1.000	36	510.00	6.2	6.2	REV	NØ
120	55	1.000	1.000	20	494.00	6.2	6.2	FWD	NØ
120	56	1.000	1.000	20	473.00	6.2	6.2	FWD	NØ
120	52	.100	.100	--	478.00	5.8	5.8	REV	NØ
120	53	.100	.100	--	515.00	6.0	6.0	REV	NØ
121	1	10.000	10.000	2225	.14	1200.0	1200.0	REV	NØ
121	1	1.200	10.000	2225	.15	1200.0	1000.0	REV	YES
121	2	10.000	10.000	2150	.03	1400.0	1400.0	REV	NØ
121	2	6.000	10.000	2375	.14	1400.0	10.0	REV	YES
121	3	1.000	1.000	2050	.80	1700.0	1700.0	REV	NØ
121	3	.200	1.000	2060	1.00	1700.0	500.0	REV	YES
121	4	1.000	1.000	2100	.60	2000.0	2000.0	REV	NØ
121	4	.200	1.000	2125	.80	2000.0	150.0	REV	YES
121	5	1.000	1.000	40	465.00	1200.0	1200.0	FWD	NØ
121	6	1.000	1.000	35	465.00	1840.0	1840.0	FWD	NØ
121	7	.100	.100	2310	4.50	2100.0	2100.0	REV	NØ
121	7	.090	.100	2400	6.50	2100.0	100.0	REV	YES
121	8	.100	.100	--	6.70	2050.0	2050.0	REV	NØ
121	8	.080	.100	2125	12.00	2050.0	1900.0	REV	YES
122	1	10.000	10.000	119	.01	110.0	110.0	REV	NØ
122	1	10.000	10.000	133	.02	110.0	40.0	REV	YES

F#	S/N	TD	TP	VP	IP	VZB	VZA	POL	FAIL
122	2	10.000	10.000	130	.03	105.0	105.0	REV	NØ
122	2	5.500	10.000	127	.03	105.0	1.0	REV	YES
122	3	1.000	1.000	124	.45	110.0	110.0	REV	NØ
122	3	.750	1.000	131	.63	110.0	1.0	REV	YES
122	4	1.000	1.000	128	.58	110.0	110.0	REV	NØ
122	4	.750	1.000	128	.75	110.0	1.0	REV	YES
122	5	1.000	1.000	9	9.60	105.0	105.0	FWD	NØ
122	5	1.000	1.000	10	18.00	105.0	2.0	FWD	YES
122	6	1.000	1.000	9	--	115.0	115.0	FWD	NØ
122	6	1.000	1.000	10	--	115.0	10.0	FWD	YES
122	7	.100	.100	170	--	105.0	105.0	REV	NØ
122	7	.020	.100	190	4.00	105.0	2.0	REV	YES
122	8	.100	.100	--	--	115.0	115.0	REV	NØ
122	8	.010	.100	200	--	115.0	1.0	REV	YES
123	50	10.000	10.000	26	90.00	2.4	2.4	REV	NØ
123	50	9.700	10.000	27	93.00	2.4	1.1	REV	YES
123	52	10.000	10.000	40	91.00	2.4	2.4	REV	NØ
123	52	10.000	10.000	40	94.00	2.4	2.3	REV	YES
123	56	1.000	1.000	56	170.00	2.4	2.4	REV	NØ
123	56	1.000	1.000	60	196.00	2.4	2.3	REV	YES
123	58	1.000	1.000	74	246.00	2.4	2.4	REV	NØ
123	58	1.000	1.000	83	273.00	2.4	1.7	REV	YES
123	60	1.000	1.000	75	363.00	2.4	2.4	FWD	NØ
123	60	1.000	1.000	80	405.00	2.4	1.7	FWD	YES
123	61	1.000	1.000	67	346.00	2.5	2.5	FWD	NØ
123	61	1.000	1.000	67	384.00	2.5	1.6	FWD	YES
123	53	.100	.100	--	400.00	2.5	1.8	REV	YES
123	54	.100	.100	--	413.00	2.5	2.5	REV	NØ
123	55	.100	.100	--	450.00	2.5	2.5	REV	NØ
124	6	1.000	1.000	24	450.00	1200.0	1200.0	FWD	NØ
124	7	1.000	1.000	33	465.00	1500.0	1500.0	FWD	NØ
124	8	10.000	10.000	1500	.35	1400.0	1400.0	REV	NØ
124	8	.400	10.000	1600	.37	1400.0	800.0	REV	YES
124	9	10.000	10.000	1800	.10	1600.0	1600.0	REV	NØ
124	9	.400	10.000	1800	.12	1600.0	600.0	REV	YES
124	1	.100	.100	1450	--	1250.0	1250.0	REV	NØ
124	1	.070	.100	1500	--	1250.0	1.0	REV	YES
124	2	.100	.100	1350	--	1100.0	1100.0	REV	NØ
124	2	.060	.100	1350	--	1100.0	10.0	REV	YES
124	4	1.000	1.000	1450	--	800.0	800.0	REV	NØ
124	4	.200	1.000	1700	--	800.0	1.0	REV	YES
124	5	1.000	1.000	1500	--	1100.0	1100.0	REV	NØ
124	5	.040	1.000	1500	--	1100.0	1.0	REV	YES

F#	S/N	TD	TP	VP	IP	VZB	VZA	PØL	FAIL
125	199	10.000	10.000	78	138.00	45.0	45.0	REV	NØ
125	200	10.000	10.000	79	131.00	44.0	44.0	REV	NØ
125	210	10.000	10.000	13	125.00	45.0	45.0	FWD	NØ
125	200	10.000	10.000	20	150.00	44.0	44.0	FWD	NØ
125	207	1.000	1.000	96	480.00	43.0	43.0	REV	NØ
125	208	1.000	1.000	88	480.00	43.0	43.0	REV	NØ
125	205	1.000	1.000	20	480.00	43.0	43.0	FWD	NØ
125	206	1.000	1.000	20	474.00	43.0	43.0	FWD	NØ
126	1	1.000	1.000	24	135.00	4.8	4.8	REV	NØ
126	1	1.000	1.000	30	180.00	4.8	.1	REV	YES
126	2	1.000	1.000	42	270.00	5.1	5.1	REV	NØ
126	2	1.000	1.000	42	280.00	5.1	.1	REV	YES
126	3	.100	.100	60	600.00	4.5	4.5	REV	NØ
126	3	.100	.100	70	450.00	4.5	2.8	REV	YES
126	5	10.000	10.000	23	130.00	4.5	4.5	REV	NØ
126	5	10.000	10.000	23	140.00	4.5	.1	REV	YES
126	8	10.000	10.000	22	130.00	4.5	4.5	REV	NØ
126	8	10.000	10.000	22	140.00	4.5	.1	REV	YES
126	11	1.000	1.000	36	285.00	5.0	5.0	REV	NØ
126	11	1.000	1.000	36	292.00	5.0	.2	REV	YES
126	12	1.000	1.000	49	370.00	4.5	4.5	REV	NØ
126	12	1.000	1.000	52	425.00	4.5	4.4	REV	YES
126	13	1.000	1.000	42	290.00	5.0	5.0	REV	NØ
126	13	1.000	1.000	51	300.00	5.0	.1	REV	YES
126	14	1.000	1.000	52	450.00	5.0	5.0	REV	NØ
126	14	1.000	1.000	55	475.00	5.0	1.0	REV	YES
126	16	1.000	1.000	40	300.00	4.8	4.8	REV	NØ
126	16	1.000	1.000	50	400.00	4.8	.1	REV	YES
126	17	1.000	1.000	65	395.00	4.5	4.5	REV	NØ
126	17	1.000	1.000	65	410.00	4.5	1.8	REV	YES
126	15	1.000	1.000	39	300.00	4.8	4.8	REV	NØ
126	15	1.000	1.000	40	300.00	4.8	.1	REV	YES
126	4	.100	.100	60	480.00	5.0	3.2	REV	YES
126	9	1.000	1.000	43	425.00	4.5	4.5	FWD	NØ
126	10	1.000	1.000	35	425.00	5.0	5.0	FWD	NØ
127	1	1.000	1.000	41	165.00	8.8	8.8	REV	NØ
127	1	1.000	1.000	51	206.00	8.8	.1	REV	YES
127	2	1.000	1.000	99	291.00	8.5	8.5	REV	NO
127	2	1.000	1.000	108	315.00	8.5	2.0	REV	YES
127	3	1.000	1.000	51	463.00	8.4	8.4	FWD	NØ
127	4	1.000	1.000	48	480.00	8.3	8.3	FWD	NØ
127	4	1.000	1.000	54	475.00	8.3	2.1	FWD	YES

F#	S/N	TD	TP	VP	IP	VZB	VZA	PØL	FAIL
127	5	.100	.100	54	463.00	8.5	8.5	FWD	NØ
127	6	.100	.100	52	450.00	8.2	8.2	FWD	NØ
127	8	10.000	10.000	36	105.00	8.5	8.5	REV	NØ
127	8	10.000	10.000	41	117.00	8.5	8.2	REV	YES
127	9	10.000	10.000	39	114.00	8.3	8.3	REV	NØ
127	9	10.000	10.000	39	118.00	8.3	.1	REV	YES
127	10	1.000	1.000	52	178.00	8.3	8.3	REV	NØ
127	10	1.000	1.000	56	206.00	8.3	.6	REV	YES
127	11	1.000	1.000	27	140.00	8.5	8.5	REV	NØ
127	11	.900	1.000	32	168.00	8.5	.1	REV	YES
127	12	1.000	1.000	62	190.00	9.0	9.0	REV	NØ
127	12	1.000	1.000	65	180.00	9.0	.2	REV	YES
127	13	1.000	1.000	65	263.00	8.5	8.5	REV	NØ
127	13	1.000	1.000	66	285.00	8.5	.1	REV	YES
127	14	1.000	1.000	50	181.00	8.8	8.8	REV	NØ
127	14	1.000	1.000	50	206.00	8.8	2.0	REV	YES
127	15	1.000	1.000	60	225.00	8.6	8.6	REV	NØ
127	15	1.000	1.000	60	255.00	8.6	1.8	REV	YES
127	16	1.000	1.000	55	200.00	8.4	8.4	REV	NØ
127	16	1.000	1.000	60	225.00	8.4	1.0	REV	YES
127	17	1.000	1.000	50	240.00	8.8	8.8	REV	NØ
127	17	1.000	1.000	52	255.00	8.8	.1	REV	YES
128	1	10.000	10.000	39	145.00	4.8	4.8	REV	NØ
128	1	10.000	10.000	45	145.00	4.8	4.6	REV	YES
128	3	10.000	10.000	32	125.00	4.6	4.6	REV	NØ
128	3	10.000	10.000	35	142.00	4.6	4.3	REV	YES
128	4	.100	.100	126	396.00	4.8	4.8	REV	NØ
128	5	.100	.100	90	400.00	4.8	4.8	REV	NØ
128	6	1.000	1.000	70	358.00	4.4	4.4	REV	NØ
128	6	1.000	1.000	72	360.00	4.4	4.2	REV	YES
128	7	1.000	1.000	55	240.00	4.4	4.4	REV	NØ
128	7	1.000	1.000	54	284.00	4.4	1.0	REV	YES
128	8	1.000	1.000	65	463.00	4.8	4.8	FWD	NØ
128	9	1.000	1.000	70	438.00	4.8	4.8	FWD	NØ
129	1	1.000	1.000	36	200.00	9.0	9.0	FWD	NØ
129	1	1.000	1.000	42	240.00	9.0	4.0	FWD	YES
129	2	1.000	1.000	64	230.00	9.0	9.0	FWD	NØ
129	2	1.000	1.000	65	250.00	9.0	1.0	FWD	YES
129	3	1.000	1.000	56	56.00	9.0	9.0	REV	NØ
129	3	1.000	1.000	58	64.00	9.0	8.0	REV	YES
129	4	1.000	1.000	72	70.00	9.0	9.0	REV	NØ
129	4	1.000	1.000	74	86.00	9.0	8.0	REV	YES
129	7	10.000	10.000	38	22.00	9.0	9.0	REV	NØ

F#	S/N	TD	TP	VP	IP	VZB	VZA	POL	FAIL
129	7	10.000	10.000	40	28.00	9.0	8.0	REV	YES
129	8	10.000	10.000	42	25.00	9.0	9.0	REV	NØ
129	8	10.000	10.000	46	27.00	9.0	8.0	REV	YES
129	5	.100	.100	120	120.00	9.0	9.0	REV	NØ
129	5	.100	.100	140	160.00	9.0	5.0	REV	YES
129	6	.100	.100	200	170.00	9.0	9.0	REV	NØ
129	6	.100	.100	280	190.00	9.0	3.0	REV	YES
130	1	1.000	1.000	140	85.00	55.0	55.0	REV	NØ
130	1	.750	1.000	150	97.00	55.0	54.0	REV	YES
130	2	1.000	1.000	133	85.00	54.0	54.0	REV	NØ
130	2	.800	1.000	145	98.00	54.0	22.0	REV	YES
130	3	1.000	1.000	52	296.00	55.0	55.0	FWD	NØ
130	3	1.000	1.000	56	316.00	55.0	12.0	FWD	YES
130	5	1.000	1.000	64	364.00	54.0	54.0	FWD	NØ
130	5	1.000	1.000	72	400.00	54.0	1.0	FWD	YES
130	4	.100	.100	200	425.00	53.0	53.0	REV	NØ
130	4	.050	.100	200	463.00	53.0	1.0	REV	YES
130	6	.100	.100	240	425.00	55.0	55.0	REV	NØ
130	6	.040	.100	240	488.00	55.0	1.0	REV	YES
130	7	10.000	10.000	90	23.00	55.0	55.0	REV	NØ
130	7	10.000	10.000	96	28.00	55.0	52.0	REV	YES
130	8	10.000	10.000	80	19.00	54.0	54.0	REV	NØ
130	8	10.000	10.000	90	23.00	54.0	51.0	REV	YES
131	21	10.000	10.000	165	.22	130.0	130.0	REV	NØ
131	21	4.800	10.000	165	.25	130.0	40.0	REV	YES
131	20	10.000	10.000	165	.22	125.0	125.0	REV	NØ
131	20	5.000	10.000	165	.23	125.0	20.0	REV	YES
131	14	1.000	1.000	122	.75	110.0	110.0	REV	NØ
131	14	.600	1.000	122	1.05	110.0	1.0	REV	YES
131	15	1.000	1.000	129	.53	120.0	120.0	REV	NØ
131	15	.900	1.000	129	.80	120.0	1.0	REV	YES
131	16	1.000	1.000	6	6.60	125.0	125.0	FWD	NØ
131	16	1.000	1.000	5	8.00	125.0	5.0	FWD	YES
131	17	1.000	1.000	5	5.10	120.0	120.0	FWD	NØ
131	17	1.000	1.000	5	7.60	120.0	1.0	FWD	YES
131	18	.100	.100	149	3.00	120.0	120.0	REV	NØ
131	18	.100	.100	155	4.10	120.0	3.0	REV	YES
131	19	.100	.100	144	2.90	110.0	110.0	REV	NØ
131	19	.100	.100	149	4.10	110.0	5.0	REV	YES
132	1	10.000	10.000	1400	2.55	810.0	810.0	REV	NØ
132	1	10.000	10.000	1430	2.64	810.0	160.0	REV	YES

F#	S/N	TD	TP	VP	IP	VZB	VZA	POL	FAIL
132	2	10.000	10.000	1520	2.70	830.0	830.0	REV	NØ
132	2	10.000	10.000	1520	2.72	830.0	20.0	REV	YES
132	3	.100	.100	1380	3.50	820.0	820.0	REV	NØ
132	3	.050	.100	1380	5.00	820.0	5.0	REV	YES
132	4	.100	.100	1390	2.90	940.0	940.0	REV	NØ
132	4	.060	.100	1425	5.30	940.0	5.0	REV	YES
132	5	1.000	1.000	1330	1.20	940.0	940.0	REV	NØ
132	5	1.000	1.000	1440	1.70	940.0	1.0	REV	YES
132	6	1.000	1.000	1380	2.10	880.0	880.0	REV	NØ
132	6	1.000	1.000	1420	2.30	880.0	1.0	REV	YES
132	7	1.000	1.000	2	410.00	880.0	880.0	FWD	NØ
132	8	1.000	1.000	1	405.00	880.0	880.0	FWD	NØ
133	16	1.000	1.000	135	1.40	120.0	120.0	REV	NØ
133	16	.600	1.000	135	1.80	120.0	1.0	REV	YES
133	17	1.000	1.000	143	.95	130.0	130.0	REV	NØ
133	17	.980	1.000	143	1.60	130.0	5.0	REV	YES
133	18	1.000	1.000	7	23.00	110.0	110.0	FWD	NØ
133	18	1.000	1.000	8	28.00	110.0	2.0	FWD	YES
133	19	1.000	1.000	8	25.00	100.0	100.0	FWD	NØ
133	19	1.000	1.000	8	27.00	100.0	20.0	FWD	YES
133	13	10.000	10.000	143	.02	130.0	130.0	REV	NØ
133	13	10.000	10.000	143	.03	130.0	1.0	REV	YES
133	14	10.000	10.000	115	.00	100.0	100.0	REV	NØ
133	14	10.000	10.000	122	.01	100.0	1.0	REV	YES
133	12	.100	.100	200	6.60	120.0	120.0	REV	NØ
133	12	.010	.100	228	9.60	120.0	1.0	REV	YES
133	15	.100	.100	185	8.50	110.0	110.0	REV	NØ
133	15	.100	.100	195	10.20	110.0	5.0	REV	YES

F#	S/N	TD	TP	VP	IP	VZB	VZA	PØL	FAIL
141	24	.125	.125	60	100.00	136.0	136.0	FWD	NØ
141	24	.300	.300	70	100.00	136.0	24.0	FWD	YES
141	25	.300	.300	45	100.00	130.0	128.0	FWD	YES
141	26	.300	.300	45	100.00	130.0	130.0	FWD	NØ
141	27	.030	.060	180	8.00	156.0	50.0	REV	YES
141	28	.040	.040	140	5.00	156.0	156.0	REV	NØ
141	29	.050	.050	140	5.00	160.0	100.0	REV	YES
141	30	.036	.036	150	8.00	168.0	168.0	REV	NØ
141	30	.100	.100	150	2.40	168.0	168.0	REV	NØ
141	30	.040	.120	160	10.00	168.0	2.8	REV	
141	31	.040	.040	140	9.00	124.0	8.0	REV	YES
141	32	.050	.050	140	3.00	156.0	156.0	REV	NØ
141	32	.030	.050	150	8.00	156.0	10.0	REV	YES
141	33	.300	.300	150	1.30	124.0	124.0	REV	NØ
141	33	.120	.300	160	3.60	124.0	45.0	REV	YES
142	1	.300	.300	50	42.00	140.0	140.0	FWD	NØ
142	1	.300	.300	70	100.00	140.0	10.0	FWD	YES
142	2	.300	.300	65	69.00	116.0	32.0	FWD	YES
142	3	.300	.300	40	45.00	130.0	130.0	FWD	NØ
142	3	.300	.300	50	54.00	130.0	86.0	FWD	YES
142	4	.300	.300	50	45.00	150.0	130.0	FWD	YES
142	5	.300	.300	40	39.00	140.0	140.0	FWD	NØ
142	5	.300	.300	50	49.00	140.0	47.0	FWD	YES
142	13	.050	.050	130	5.00	110.0	110.0	REV	NØ
142	13	.040	.050	170	15.00	110.0	42.0	REV	YES
142	12	.050	.050	140	8.40	114.0	114.0	REV	NØ
142	12	.036	.050	170	18.00	114.0	80.0	REV	YES
142	21	.040	.050	170	18.00	114.0	80.0	REV	YES
142	14	.060	.060	140	9.20	114.0	114.0	REV	NØ
142	14	.040	.050	160	10.00	114.0	38.0	REV	YES
142	15	.050	.050	180	3.20	168.0	168.0	REV	NØ
142	15	.044	.050	200	7.60	168.0	110.0	REV	YES
142	16	.050	.050	150	8.80	118.0	118.0	REV	NØ
142	16	.040	.050	170	15.00	118.0	65.0	REV	YES
142	17	.090	.100	190	2.80	164.0	50.0	REV	YES
142	18	.100	.100	170	1.80	144.0	144.0	REV	NØ
142	18	.075	.100	170	3.00	144.0	33.0	REV	YES
142	19	.100	.100	190	2.00	152.0	152.0	REV	NØ
142	19	.075	.100	190	3.60	152.0	10.0	REV	YES
142	20	.100	.100	140	4.20	108.0	108.0	REV	NØ
142	20	.085	.100	150	6.00	108.0	45.0	REV	YES
142	22	.075	.100	200	3.00	162.0	25.0	REV	YES
142	23	.060	.100	150	4.40	108.0	80.0	REV	YES

F#	S/N	TD	TP	VP	IP	VZB	VZA	POL	FAIL
142	25	.100	.100	150	2.00	128.0	128.0	REV	NØ
142	25	.080	.100	160	3.00	128.0	12.0	REV	YES
142	26	.100	.100	170	1.80	154.0	154.0	REV	NØ
142	26	.070	.100	190	2.40	154.0	60.0	REV	YES
142	27	.300	.300	120	.50	116.0	116.0	REV	NØ
142	[illegible]	.[illegible]0	.300	130	.80	116.0	52.0	REV	YES
142	[illegible]	.[illegible]0	.300	170	.60	156.0	156.0	REV	NØ
142	28	.220	.300	180	.90	156.0	5.5	REV	YES
142	29	.300	.300	130	1.30	104.0	104.0	REV	NØ
142	29	.290	.300	140	1.70	104.0	33.0	REV	YES
142	30	.300	.300	130	1.50	120.0	120.0	REV	NØ
142	30	.290	.300	140	1.70	120.0	27.0	REV	YES
142	7	.030	.030	130	4.40	110.0	110.0	REV	NØ
142	7	.030	.030	150	10.40	110.0	32.0	REV	YES
142	8	.030	.030	160	6.80	136.0	136.0	REV	NØ
142	8	.030	.030	170	9.60	136.0	92.0	REV	YES
142	6	.030	.030	200	33.00	110.0	110.0	REV	NØ
142	9	.030	.030	190	12.40	140.0	140.0	REV	NØ
142	9	.030	.030	230	18.00	140.0	5.0	REV	YES
142	10	.030	.030	200	18.00	150.0	150.0	REV	NØ
142	10	.030	.030	200	28.00	150.0	1.0	REV	YES
142	11	.030	.030	200	11.20	160.0	160.0	REV	NØ
142	11	.030	.030	210	15.00	160.0	120.0	REV	YES
143	31	.300	.300	25	100.00	116.0	116.0	FWD	NØ
143	32	.300	.300	25	100.00	116.0	116.0	FWD	NØ
143	33	.300	.300	25	100.00	116.0	116.0	FWD	NØ
143	41	.040	.050	140	16.00	130.0	3.5	REV	YES
143	42	.050	.050	130	12.00	120.0	120.0	REV	NØ
143	42	.040	.050	140	16.00	120.0	2.0	REV	YES
143	43	.050	.050	120	6.00	116.0	116.0	REV	NØ
143	43	.040	.050	130	14.00	116.0	60.0	REV	YES
143	44	.050	.050	130	3.20	142.0	142.0	REV	NØ
143	44	.040	.050	150	10.00	142.0	2.2	REV	YES
143	45	.050	.050	130	10.00	114.0	114.0	REV	NØ
143	45	.040	.050	140	14.00	114.0	113.0	REV	YES
143	46	.050	.050	120	11.60	110.0	110.0	REV	NØ
143	46	.040	.050	140	16.00	110.0	16.0	REV	YES
143	47	.050	.050	130	8.80	116.0	92.0	REV	YES
143	48	.100	.100	130	6.80	112.0	112.0	REV	NØ
143	48	.100	.100	130	9.20	112.0	9.0	REV	YES
143	49	.100	.100	120	8.00	110.0	10.0	REV	YES
143	50	.100	.100	120	6.80	104.0	104.0	REV	NØ
143	50	.080	.100	120	10.80	104.0	2.0	REV	YES
143	51	.100	.100	130	8.00	114.0	12.0	REV	YES

F#	S/N	TD	TP	VP	IP	VZB	VZA	POL	FAIL
143	52	.100	.100	130	6.80	124.0	124.0	REV	NO
143	52	.100	.100	140	9.60	124.0	4.4	REV	YES
143	53	.100	.100	120	8.00	112.0	112.0	REV	NO
143	53	.080	.100	140	12.00	112.0	25.0	REV	YES
143	54	.100	.100	140	7.60	126.0	7.0	REV	YES
143	55	.100	.100	120	5.20	110.0	110.0	REV	NO
143	55	.100	.100	130	8.00	110.0	68.0	REV	YES
143	58	.300	.300	130	2.40	114.0	114.0	REV	NO
143	58	.280	.300	140	3.20	114.0	7.0	REV	YES
143	59	.300	.300	130	2.00	120.0	120.0	REV	NO
143	59	.280	.300	130	3.00	120.0	9.0	REV	YES
143	60	.300	.300	130	2.60	110.0	35.0	REV	YES
143	34	.030	.030	110	12.00	110.0	110.0	REV	NO
143	34	.030	.030	130	27.00	110.0	19.0	REV	YES
143	35	.030	.030	120	15.00	120.0	120.0	REV	NO
143	35	.040	.040	130	20.00	120.0	33.0	REV	YES
143	56	.030	.030	120	15.00	118.0	118.0	REV	NO
143	56	.040	.040	130	20.00	118.0	23.0	REV	YES
143	37	.030	.030	140	13.00	130.0	130.0	REV	NO
143	38	.030	.030	140	13.00	116.0	116.0	REV	NO
144	60	.300	.300	80	100.00	130.0	130.0	FWD	NO
144	60	.300	.300	85	100.00	130.0	24.0	FWD	YES
144	61	.300	.300	100	100.00	136.0	2.5	FWD	YES
144	62	.300	.300	60	45.00	130.0	130.0	FWD	NO
144	62	.300	.300	75	75.00	130.0	118.0	FWD	YES
144	63	.300	.300	90	39.00	138.0	10.0	FWD	YES
144	64	.300	.300	100	100.00	140.0	140.0	FWD	NO
144	70	.040	.050	540	13.60	130.0	1.8	REV	YES
144	71	.050	.050	700	9.00	140.0	140.0	REV	NO
144	71	.024	.050	700	15.00	140.0	46.0	REV	YES
144	72	.050	.050	480	9.60	120.0	120.0	REV	NO
144	72	.050	.050	600	12.00	120.0	90.0	REV	YES
144	73	.060	.060	400	5.00	140.0	140.0	REV	NO
144	73	.028	.050	500	10.00	140.0	36.0	REV	YES
144	74	.060	.060	400	7.20	130.0	130.0	REV	NO
144	74	.020	.050	480	12.00	130.0	27.0	REV	YES
144	75	.050	.050	400	8.00	128.0	128.0	REV	NO
144	75	.050	.050	500	10.00	128.0	40.0	REV	YES
144	77	.100	.100	500	6.00	130.0	130.0	REV	NO
144	77	.040	.100	700	14.00	130.0	4.0	REV	YES
144	78	.040	.100	420	6.40	144.0	11.0	REV	YES
144	79	.100	.100	400	3.20	140.0	140.0	REV	NO
144	79	.035	.100	560	6.00	140.0	32.0	REV	YES
144	80	.100	.100	460	7.60	136.0	136.0	REV	NO

F#	S/N	TD	TP	VP	IP	VZB	VZA	PØL	FAIL
144	80	.100	.100	500	8.00	136.0	78.0	REV	YES
144	81	.100	.100	580	6.80	130.0	130.0	REV	NØ
144	81	.075	.100	600	8.00	130.0	8.0	REV	YES
144	82	.100	.100	300	9.60	124.0	124.0	REV	NØ
144	83	.100	.100	420	6.40	120.0	120.0	REV	NØ
144	83	.070	.100	540	8.40	120.0	29.0	REV	YES
144	84	.100	.100	400	3.60	124.0	124.0	REV	NØ
144	84	.075	.100	520	4.40	124.0	27.0	REV	YES
144	86	.300	.300	360	10.80	120.0	120.0	REV	NØ
144	86	.220	.300	400	12.00	120.0	1.0	REV	YES
144	87	.100	.300	380	6.00	128.0	3.0	REV	YES
144	88	.300	.300	360	4.00	140.0	140.0	REV	NØ
144	88	.160	.300	400	4.40	140.0	70.0	REV	YES
144	89	.220	.300	380	2.40	140.0	18.0	REV	YES
144	65	.030	.030	680	8.40	130.0	130.0	REV	NØ
144	65	.030	.030	950	16.00	130.0	129.0	REV	YES
144	66	.030	.030	470	7.20	140.0	50.0	REV	YES
144	85	.030	.030	480	9.60	160.0	160.0	REV	NØ
145	90	.125	.125	280	3.60	208.0	208.0	REV	NØ
145	90	.030	.125	300	10.80	208.0	.1	REV	YES
145	91	.125	.125	280	1.60	164.0	164.0	REV	NØ
145	91	.020	.125	340	5.60	164.0	25.0	REV	YES
145	92	.125	.125	420	6.40	235.0	235.0	REV	NØ
145	92	.090	.125	440	7.60	235.0	192.0	REV	YES
145	93	.125	.125	280	4.00	200.0	200.0	REV	NØ
145	93	.090	.125	280	6.40	200.0	192.0	REV	YES
145	94	.070	.125	260	10.40	140.0	4.0	REV	YES
145	95	.125	.125	300	5.60	235.0	235.0	REV	NØ
145	95	.060	.125	320	10.40	235.0	11.0	REV	YES
145	96	.125	.125	400	4.80	180.0	180.0	REV	NØ
145	96	.125	.125	420	6.80	180.0	179.0	REV	YES
145	97	.050	.125	320	6.40	240.0	6.5	REV	YES
145	98	.300	.300	40	54.00	185.0	185.0	FWD	NØ
145	98	.300	.300	45	73.00	185.0	98.0	FWD	YES
145	99	.300	.300	50	63.00	190.0	190.0	FWD	NØ
145	99	.300	.300	70	90.00	190.0	20.0	FWD	YES
146	100	.125	.125	480	7.20	116.0	116.0	REV	NØ
146	100	.125	.125	600	9.60	116.0	11.0	REV	YES
146	101	.125	.125	520	6.40	118.0	118.0	REV	NØ
146	101	.050	.125	600	12.00	118.0	5.5	REV	YES
146	102	.125	.125	540	8.00	120.0	120.0	REV	NØ
146	102	.080	.125	580	10.00	120.0	10.0	REV	YES
146	103	.125	.125	420	8.00	120.0	120.0	REV	NØ

F#	S/N	TD	TP	VP	IP	VZB	VZA	POL	FAIL
146	103	.050	.125	500	12.00	120.0	13.0	REV	YES
146	104	.125	.125	420	8.00	120.0	120.0	REV	NØ
146	104	.080	.125	460	8.00	120.0	80.0	REV	YES
146	105	.125	.125	440	6.00	118.0	118.0	REV	NØ
146	105	.090	.125	600	8.00	118.0	117.0	REV	YES
146	106	.050	.125	480	6.00	128.0	55.0	REV	YES
146	107	.125	.125	320	6.00	110.0	110.0	REV	NØ
146	107	.080	.125	560	10.00	110.0	25.0	REV	YES
146	108	.300	.300	75	90.00	124.0	124.0	FWD	NØ
146	109	.100	.100	100	87.00	118.0	118.0	FWD	NØ
146	109	.300	.300	90	69.00	118.0	13.0	FWD	YES
147	301	.100	.100	66	.40	65.0	65.0	REV	NØ
147	301	.060	.100	80	1.20	65.0	17.0	REV	YES
147	302	.100	.100	76	.20	68.0	68.0	REV	NØ
147	302	.100	.100	80	.56	68.0	42.0	REV	YES
147	303	.100	.100	80	.60	67.0	67.0	REV	NØ
147	303	.070	.100	80	.80	67.0	5.0	REV	YES
147	304	.100	.100	80	.60	68.0	68.0	REV	NØ
147	304	.070	.100	80	.80	68.0	4.0	REV	YES
147	305	.100	.100	85	.80	76.0	76.0	REV	NØ
147	305	.080	.100	90	1.00	76.0	25.0	REV	YES
147	306	.100	.100	75	.28	65.0	65.0	REV	NØ
147	306	.085	.100	75	.60	65.0	5.0	REV	YES
147	307	.100	.100	80	.60	66.0	66.0	REV	NØ
147	307	.085	.100	80	.80	66.0	45.0	REV	YES
147	308	.100	.100	75	.40	63.0	63.0	REV	NØ
147	308	.070	.100	80	.80	63.0	32.0	REV	YES
147	309	.100	.100	80	.60	68.0	68.0	REV	NØ
147	309	.070	.100	85	.80	68.0	10.0	REV	YES
147	310	.050	.050	85	2.00	66.0	66.0	REV	NØ
147	310	.030	.050	85	2.40	66.0	63.0	REV	YES
147	311	.050	.050	90	2.00	70.0	70.0	REV	NØ
147	311	.030	.050	90	2.40	70.0	20.0	REV	YES
147	312	.050	.050	75	2.00	63.0	63.0	REV	NØ
147	312	.030	.050	75	2.60	63.0	4.0	REV	YES
147	313	.050	.050	80	1.60	70.0	70.0	REV	NØ
147	313	.030	.050	80	2.00	70.0	6.0	REV	YES
147	314	.050	.050	80	1.80	66.0	66.0	REV	NØ
147	314	.030	.050	80	2.00	66.0	3.0	REV	YES
147	315	.035	.050	80	1.60	68.0	10.0	REV	YES
147	316	.300	.300	80	.15	70.0	70.0	REV	NØ
147	316	.110	.300	80	.50	70.0	24.0	REV	YES
147	317	.300	.300	80	.20	70.0	70.0	REV	NØ
147	317	.020	.300	80	.40	70.0	64.0	REV	YES

F#	S/N	TD	TP	VP	IP	VZB	VZA	PØL	FAIL
147	318	.300	.300	75	.12	68.0	68.0	REV	NØ
147	318	.200	.300	80	.24	68.0	2.0	REV	YES
147	319	.300	.300	80	.16	72.0	72.0	REV	NØ
147	319	.190	.300	85	.34	72.0	3.0	REV	YES
147	320	.300	.300	70	.12	65.0	65.0	REV	NØ
147	320	.200	.300	80	.28	65.0	21.0	REV	YES
147	321	.300	.300	70	.12	65.0	65.0	REV	NØ
147	321	.270	.300	80	.20	65.0	13.0	REV	YES
147	323	.100	.100	40	22.00	51.0	51.0	FWD	NØ
147	323	.100	.100	65	36.00	51.0	8.0	FWD	YES
147	322	.100	.100	35	23.00	63.0	63.0	FWD	NØ
147	322	.100	.100	55	40.00	63.0	20.0	FWD	YES
147	324	.100	.100	25	20.00	40.0	2.0	FWD	YES
147	325	.100	.100	35	18.00	72.0	63.0	FWD	YES
147	326	.100	.100	35	19.00	70.0	58.0	FWD	YES
147	327	.100	.100	25	20.00	66.0	45.0	FWD	YES
148	101	.100	.100	65	3.20	56.0	56.0	REV	NØ
148	101	.120	.120	70	4.20	56.0	7.0	REV	YES
148	102	.100	.100	70	3.20	61.0	61.0	REV	NØ
148	102	.100	.100	75	4.00	61.0	27.0	REV	YES
148	103	.100	.100	70	4.80	54.0	54.0	REV	NØ
148	103	.100	.100	70	5.20	54.0	26.0	REV	YES
148	104	.100	.100	70	5.00	56.0	56.0	REV	NØ
148	104	.120	.120	70	5.20	56.0	4.0	REV	YES
148	105	.100	.100	75	3.60	61.0	61.0	REV	NØ
148	105	.120	.120	75	4.20	61.0	5.0	REV	YES
148	106	.100	.100	75	3.40	63.0	63.0	REV	NØ
148	106	.100	.100	80	3.80	63.0	46.0	REV	YES
148	107	.100	.100	75	3.40	63.0	63.0	REV	NØ
148	107	.040	.100	70	3.80	63.0	3.0	REV	YES
148	108	.100	.100	70	3.60	61.0	61.0	REV	NØ
148	108	.100	.120	70	4.00	61.0	2.0	REV	YES
148	109	.100	.100	75	3.20	64.0	64.0	REV	NØ
148	109	.100	.120	80	3.60	64.0	21.0	REV	YES
148	110	.100	.100	65	4.00	55.0	55.0	REV	NØ
148	110	.120	.120	70	4.40	55.0	5.0	REV	YES
148	111	.060	.060	70	4.80	58.0	58.0	REV	NØ
148	111	.060	.060	75	6.80	58.0	3.0	REV	YES
148	112	.060	.060	70	7.20	55.0	55.0	REV	NØ
148	112	.060	.060	75	8.00	55.0	21.0	REV	YES
148	113	.060	.060	70	8.80	54.0	54.0	REV	NØ
148	113	.060	.060	75	9.60	54.0	19.0	REV	YES
148	115	.060	.060	75	8.00	62.0	62.0	REV	NØ
148	115	.040	.060	80	8.80	62.0	2.0	REV	YES

F#	S/N	TD	TP	VP	IP	VZB	VZA	PØL	FAIL
148	116	.040	.060	65	6.40	57.0	4.0	REV	YES
148	117	.060	.060	65	6.40	55.0	55.0	REV	NØ
148	117	.060	.060	70	8.00	55.0	27.0	REV	YES
148	119	.300	.300	55	.60	54.0	54.0	REV	NØ
148	119	.240	.300	60	.80	54.0	3.0	REV	YES
148	118	.300	.300	60	.70	58.0	58.0	REV	NØ
148	118	.240	.300	65	1.00	58.0	26.0	REV	YES
148	120	.300	.300	60	.80	55.0	55.0	REV	NØ
148	120	.220	.300	60	1.00	55.0	6.0	REV	YES
148	121	.300	.300	70	.30	64.0	64.0	REV	NØ
148	121	.270	.300	70	.80	64.0	3.0	REV	YES
148	122	.300	.300	55	.40	56.0	56.0	REV	NØ
148	122	.260	.300	60	.80	56.0	4.0	REV	YES
148	123	.300	.300	60	.50	56.0	56.0	REV	NØ
148	123	.300	.300	60	.80	56.0	7.0	REV	YES
148	124	.300	.300	12	18.00	55.0	55.0	FWD	NØ
148	124	.300	.300	36	75.00	55.0	.1	FWD	YES
148	125	.300	.300	12	15.00	55.0	55.0	FWD	NØ
148	125	.300	.300	40	81.00	55.0	6.0	FWD	YES
148	126	.300	.300	12	19.00	62.0	62.0	FWD	NØ
148	126	.300	.300	40	48.00	62.0	.4	FWD	YES
148	127	.300	.300	12	20.00	60.0	60.0	FWD	NØ
148	127	.300	.300	40	84.00	60.0	1.0	FWD	YES
148	128	.300	.300	12	15.00	54.0	54.0	FWD	NØ
148	128	.300	.300	40	84.00	54.0	.2	FWD	YES
148	129	.300	.300	12	15.00	62.0	62.0	FWD	NØ
148	129	.300	.300	40	78.00	62.0	.3	FWD	YES
148	131	.300	.300	10	15.00	57.0	57.0	FWD	NØ
148	131	.300	.300	36	78.00	57.0	4.0	FWD	YES
148	159	.340	1.000	60	1.30	56.0	21.0	REV	YES
148	141	.400	1.000	60	1.00	56.0	38.0	REV	YES
148	139	.700	1.000	58	.90	53.0	6.0	REV	YES
148	151	1.000	1.000	60	.44	60.0	60.0	REV	NØ
148	151	.840	1.000	65	.56	60.0	2.0	REV	YES
148	152	1.000	1.000	60	.44	56.0	56.0	REV	NØ
148	152	.720	1.000	60	.64	56.0	5.0	REV	YES
148	150	1.000	1.000	60	.44	57.0	57.0	REV	NØ
148	150	.960	1.000	60	.52	57.0	23.0	REV	YES
148	157	1.000	1.000	65	.36	57.0	57.0	REV	NØ
148	142	1.000	1.000	60	.44	64.0	64.0	REV	NØ
148	142	.940	1.000	60	.48	64.0	23.0	REV	YES
148	154	1.000	1.000	60	.68	68.0	68.0	REV	NØ
148	154	.720	1.000	60	.94	68.0	20.0	REV	YES
148	149	.440	1.000	65	1.10	56.0	24.0	REV	YES
148	144	.200	.200	60	1.40	55.0	55.0	REV	NØ

F#	S/N	TD	TP	VP	IP	VZB	VZA	PØL	FAIL
148	144	.200	.200	60	1.80	55.0	2.0	REV	YES
148	147	.200	.200	60	1.50	58.0	58.0	REV	NØ
148	147	.200	.200	65	1.80	58.0	27.0	REV	YES
148	132	.200	.200	60	1.60	53.0	53.0	REV	NØ
148	132	.200	.200	60	1.80	53.0	25.0	REV	YES
148	138	.200	.200	60	1.60	56.0	56.0	REV	NØ
148	138	.200	.200	65	1.80	56.0	3.0	REV	YES
148	156	.200	.200	60	1.60	56.0	56.0	REV	NØ
148	156	.200	.200	65	1.80	56.0	24.0	REV	YES
148	146	.200	.200	60	2.20	56.0	56.0	REV	NØ
148	146	.200	.200	60	2.40	56.0	4.0	REV	YES
148	137	.340	.400	70	1.20	63.0	26.0	REV	YES
148	134	.400	.400	60	1.12	55.0	55.0	REV	NØ
148	134	.340	.400	60	1.36	55.0	10.0	REV	YES
148	153	.400	.400	60	1.12	54.0	54.0	REV	NØ
148	153	.330	.400	60	1.40	54.0	6.0	REV	YES
148	155	.400	.400	60	1.12	54.0	54.0	REV	NØ
148	155	.290	.400	60	1.40	54.0	11.0	REV	YES
149	1	.100	.100	460	8.00	150.0	150.0	REV	NØ
149	1	.030	.100	500	10.00	150.0	.7	REV	YES
149	2	.040	.100	300	10.00	290.0	.4	REV	YES
149	3	.100	.100	400	10.00	270.0	270.0	REV	NØ
149	3	.020	.100	420	10.00	270.0	2.0	REV	YES
149	4	.100	.100	600	4.00	320.0	320.0	REV	NØ
149	4	.040	.100	680	10.00	320.0	.0	REV	YES
149	5	.100	.100	460	8.00	280.0	280.0	REV	NØ
149	5	.040	.100	480	13.00	280.0	13.0	REV	YES
149	6	.100	.100	400	8.00	270.0	270.0	REV	NØ
149	6	.030	.100	440	12.00	270.0	1.0	REV	YES
149	7	.010	.100	340	4.40	275.0	275.0	REV	NØ
149	7	.020	.100	360	10.00	275.0	1.8	REV	YES
149	8	.100	.100	380	3.60	290.0	290.0	REV	NØ
149	8	.080	.100	520	8.00	290.0	55.0	REV	YES
149	9	.100	.100	440	10.00	270.0	270.0	REV	NØ
149	9	.020	.100	460	13.00	270.0	1.6	REV	YES
149	10	.100	.100	320	4.00	260.0	260.0	REV	NØ
149	10	.050	.100	360	10.00	260.0	.2	REV	YES
149	11	.060	.060	420	8.00	280.0	280.0	REV	NØ
149	11	.020	.060	400	14.00	280.0	10.0	REV	YES
149	12	.060	.060	420	8.00	270.0	270.0	REV	NØ
149	12	.060	.060	440	14.00	270.0	68.0	REV	YES
149	13	.060	.060	440	9.60	250.0	250.0	REV	NØ
149	13	.040	.060	440	12.00	250.0	5.0	REV	YES
149	14	.060	.060	400	8.00	290.0	290.0	REV	NØ

F#	S/N	TD	TP	VP	IP	VZB	VZA	POL	FAIL
149	14	.028	.060	400	12.80	290.0	7.0	REV	YES
149	15	.060	.060	440	7.20	270.0	270.0	REV	NØ
149	15	.040	.060	480	12.00	270.0	68.0	REV	YES
149	16	.060	.060	400	8.00	260.0	260.0	REV	NØ
149	16	.040	.060	420	12.00	260.0	90.0	REV	YES
149	17	.300	.300	360	4.00	270.0	270.0	REV	NØ
149	17	.060	.300	440	10.00	270.0	3.0	REV	YES
149	18	.300	.300	320	4.40	265.0	265.0	REV	NØ
149	18	.040	.300	400	10.00	265.0	.5	REV	YES
149	19	.300	.300	360	4.00	270.0	270.0	REV	NØ
149	19	.050	.300	420	9.00	270.0	.2	REV	YES
149	20	.300	.300	360	4.00	260.0	260.0	REV	NØ
149	20	.100	.300	440	10.00	260.0	.8	REV	YES
149	21	.300	.300	320	5.00	270.0	270.0	REV	NØ
149	21	.020	.300	340	10.00	270.0	.2	REV	YES
149	22	.300	.300	340	4.80	275.0	275.0	REV	NØ
149	22	.060	.300	400	10.00	275.0	.5	REV	YES
149	23	.300	.300	3	18.00	285.0	285.0	FWD	NØ
149	23	.300	.300	5	84.00	285.0	.4	FWD	YES
149	24	.300	.300	4	81.00	280.0	280.0	FWD	NØ
149	26	.300	.300	6	84.00	235.0	235.0	FWD	NØ
149	27	.300	.300	6	84.00	275.0	275.0	FWD	NØ
149	28	.300	.300	6	84.00	270.0	270.0	FWD	NØ
150	6	300.000	300.000	7	3.90	--	--	FWD	NØ
150	6	300.000	300.000	8	4.80	--	--	FWD	YES
150	7	300.000	300.000	10	4.20	--	--	FWD	NØ
150	7	300.000	300.000	10	4.60	--	--	FWD	YES
150	8	300.000	300.000	7	3.90	--	--	FWD	NØ
150	8	300.000	300.000	8	4.60	--	--	FWD	YES
150	9	300.000	300.000	14	5.60	85.0	85.0	FWD	NØ
150	9	300.000	300.000	15	6.00	85.0	12.0	FWD	YES
150	10	300.000	300.000	11	5.80	105.0	45.0	FWD	YES
150	1	300.000	300.000	140	.03	--	--	REV	NØ
150	1	180.000	300.000	120	.04	--	--	REV	YES
150	2	300.000	300.000	140	.05	115.0	115.0	REV	NØ
150	2	235.000	300.000	145	.05	115.0	110.0	REV	YES
150	3	195.000	300.000	145	.04	120.0	105.0	REV	YES
150	4	300.000	300.000	140	.04	125.0	125.0	REV	NØ
150	4	135.000	300.000	145	.05	125.0	110.0	REV	YES
150	5	300.000	300.000	120	.04	108.0	108.0	REV	NØ
150	16	28.000	28.000	13	8.90	101.0	101.0	FWD	NØ
150	16	28.000	28.000	14	9.80	101.0	61.0	FWD	YES
150	17	28.000	28.000	13	8.90	100.0	100.0	FWD	NØ
150	17	28.000	28.000	13	8.95	100.0	11.0	FWD	YES

F#	S/N	TD	TP	VP	IP	VZB	VZA	PØL	FAIL
150	18	28.000	28.000	13	7.80	110.0	110.0	FWD	NØ
150	18	28.000	28.000	14	8.40	110.0	42.0	FWD	YES
150	19	28.000	28.000	14	9.00	100.0	100.0	FWD	NØ
150	19	28.000	28.000	15	10.00	100.0	10.0	FWD	YES
150	20	28.000	28.000	16	8.40	110.0	110.0	FWD	NØ
150	20	28.000	28.000	18	9.50	110.0	18.0	FWD	YES
150	11	28.000	28.000	130	.07	100.0	100.0	REV	NØ
150	11	24.000	28.000	120	.08	100.0	95.0	REV	YES
150	12	28.000	28.000	135	.08	105.0	105.0	REV	NØ
150	12	20.000	28.000	136	.09	105.0	80.0	REV	YES
150	13	22.000	28.000	144	.07	112.0	102.0	REV	YES
150	14	28.000	28.000	145	.06	118.0	118.0	REV	NØ
150	14	24.500	28.000	140	.06	118.0	105.0	REV	YES
150	15	24.500	28.000	135	.07	105.0	90.0	REV	YES
150	26	2.800	2.800	29	18.50	102.0	95.0	FWD	YES
150	27	2.800	2.800	22	16.00	--	--	FWD	NØ
150	27	2.800	2.800	25	18.00	--	--	FWD	YES
150	28	2.800	2.800	22	17.80	100.0	100.0	FWD	NØ
150	28	2.800	2.800	23	18.00	100.0	90.0	FWD	YES
150	29	2.800	2.800	23	17.00	--	--	FWD	YES
150	30	2.800	2.800	26	17.00	--	--	FWD	NØ
150	30	2.800	2.800	26	17.00	--	--	FWD	YES
150	21	2.900	2.900	140	.22	108.0	108.0	REV	NØ
150	21	2.500	2.900	140	.25	108.0	90.0	REV	YES
150	22	2.900	2.900	130	.26	95.0	95.0	REV	NØ
150	22	2.600	2.900	130	.26	95.0	90.0	REV	YES
150	23	2.900	2.900	130	.23	105.0	105.0	REV	NØ
150	23	2.500	2.900	130	.25	105.0	80.0	REV	YES
150	24	2.900	2.900	130	.22	--	--	REV	YES
150	25	2.900	2.900	130	.21	--	--	REV	NØ
150	25	2.900	2.900	130	.22	--	--	REV	YES
150	46	1.000	1.000	24	18.80	105.0	105.0	FWD	NØ
150	46	1.000	1.000	31	24.00	105.0	76.0	FWD	YES
150	47	1.000	1.000	28	24.00	--	--	FWD	NØ
150	47	1.000	1.000	30	25.00	--	--	FWD	YES
150	48	1.000	1.000	30	22.00	--	--	FWD	YES
150	49	1.000	1.000	33	25.00	--	--	FWD	NØ
150	49	1.000	1.000	36	25.00	--	--	FWD	YES
150	55	.320	.320	44	34.80	100.0	100.0	FWD	NØ
150	55	.320	.320	52	43.50	100.0	46.0	FWD	YES
150	56	.320	.320	42	35.00	--	--	FWD	NØ
150	56	.320	.320	45	39.00	--	--	FWD	YES
150	57	.320	.320	45	39.50	--	--	FWD	NØ
150	57	.320	.320	47	42.00	--	--	FWD	YES
150	58	.320	.320	46	44.00	105.0	105.0	FWD	NØ

F#	S/N	TD	TP	VP	IP	VZB	VZA	POL	FAIL
150	58	.320	.320	51	47.00	105.0	87.0	FWD	YES
150	59	.320	.320	53	40.00	110.0	110.0	FWD	NO
150	59	.320	.320	55	41.30	110.0	70.0	FWD	YES
150	70	.110	.110	53	64.00	--	--	FWD	NO
150	70	.110	.110	60	72.00	--	--	FWD	YES
150	71	.110	.110	60	72.00	110.0	110.0	FWD	NO
150	71	.110	.110	62	78.00	110.0	56.0	FWD	YES
150	72	.110	.110	70	72.00	120.0	64.0	FWD	YES
150	73	.110	.110	75	73.00	--	--	FWD	NO
150	73	.110	.110	76	78.00	--	--	FWD	YES
150	74	.110	.110	60	72.00	122.0	122.0	FWD	NO
150	74	.110	.110	63	80.00	122.0	105.0	FWD	YES
150	65	.110	.110	140	2.50	115.0	115.0	REV	NO
150	65	.060	.110	125	2.20	115.0	7.2	REV	YES
150	66	.110	.110	140	2.60	120.0	20.0	REV	YES
150	67	.100	.110	140	2.50	115.0	20.0	REV	YES
150	68	.110	.110	130	1.90	105.0	105.0	REV	NO
150	68	.100	.110	135	2.70	105.0	18.0	REV	YES
150	69	.110	.110	135	2.40	120.0	120.0	REV	NO
150	69	.100	.110	137	2.50	120.0	42.0	REV	YES
150	75	.035	.035	82	87.00	110.0	100.0	FWD	YES
150	76	.035	.035	60	86.00	110.0	110.0	FWD	NO
150	76	.035	.035	80	110.00	110.0	81.0	FWD	YES
150	77	.035	.035	70	77.00	112.0	112.0	FWD	NO
150	77	.035	.035	65	86.00	112.0	87.0	FWD	YES
150	78	.035	.035	65	70.00	110.0	110.0	FWD	NO
150	78	.035	.035	80	100.00	110.0	91.0	FWD	YES
150	79	.035	.035	65	88.00	110.0	100.0	FWD	YES
150	80	.035	.035	70	90.00	120.0	120.0	FWD	NO
150	80	.035	.035	85	116.00	120.0	100.0	FWD	YES
150	81	.034	.034	156	9.10	110.0	110.0	REV	NO
150	81	.024	.034	170	13.00	110.0	1.0	REV	YES
150	82	.031	.034	148	9.10	--	--	REV	YES
150	83	.034	.034	141	8.20	110.0	110.0	REV	NO
150	83	.032	.034	143	11.00	110.0	82.0	REV	YES
150	84	.034	.034	150	8.00	112.0	112.0	REV	NO
150	84	.031	.034	152	9.40	112.0	76.0	REV	YES
150	85	.034	.034	150	9.60	--	--	REV	NO
150	85	.030	.034	150	9.80	--	--	REV	YES
150	213	.010	.010	120	170.00	100.0	84.0	FWD	YES
150	21.	.010	.010	130	135.00	104.0	104.0	FWD	NO
150	214	.010	.010	150	150.00	104.0	60.0	FWD	YES
150	215	.010	.010	130	140.00	100.0	100.0	FWD	NO
150	215	.010	.010	170	130.00	100.0	88.0	FWD	YES

F#	S/N	TD	P	VP	IP	VZ	VZA	PØL	FAIL
--	---	--	--	--	--	--	---	---	----
150	216	.010	.010	80	150.00	104.0	104.0	FWD	NØ
150	216	.010	.010	140	170.00	104.0	84.0	FWD	YES
150	217	.010	.010	150	160.00	120.0	120.0	FWD	NØ
150	217	.010	.010	110	160.00	120.0	90.0	FWD	YES
150	218	.010	.010	120	175.00	--	--	FWD	NØ
150	218	.010	.010	120	175.00	--	--	FWD	YES
150	160	.012	.012	145	28.00	99.0	99.0	REV	NØ
150	160	.008	.012	172	47.00	99.0	84.0	REV	YES
150	161	.011	.012	169	39.00	98.0	90.0	REV	YES
150	162	.012	.012	161	33.00	98.0	98.0	REV	NØ
150	162	.012	.012	163	36.00	98.0	66.0	REV	YES
150	163	.012	.012	160	32.00	100.0	100.0	REV	NØ
150	163	.004	.012	160	33.00	100.0	24.0	REV	YES
150	164	.012	.012	160	32.00	100.0	100.0	REV	NØ
150	164	.012	.012	160	34.00	100.0	59.0	REV	YES
150	375	1.000	1.000	130	.30	120.0	120.0	REV	NØ
150	375	.720	1.000	130	.40	120.0	88.0	REV	YES
150	337	1.000	1.000	130	.40	115.0	115.0	REV	NØ
150	337	.880	1.000	130	.42	115.0	100.0	REV	YES
150	328	.920	1.000	125	.28	120.0	56.0	REV	YES
150	436	1.000	1.000	140	.28	120.0	120.0	REV	NØ
150	436	.820	1.000	150	.40	120.0	76.0	REV	YES
150	335	.840	1.000	130	.38	120.0	92.0	REV	YES
150	391	1.000	1.000	140	.52	120.0	120.0	REV	NØ
150	391	.960	1.000	140	.58	120.0	80.0	REV	YES
150	339	.300	.300	140	.65	120.0	120.0	REV	NØ
150	339	.240	.300	140	.80	120.0	10.0	REV	YES
150	326	.300	.300	135	.65	110.0	110.0	REV	NØ
150	326	.240	.300	135	.80	110.0	84.0	REV	YES
150	432	.250	.300	130	.70	115.0	60.0	REV	YES
150	393	.300	.300	130	.75	115.0	115.0	REV	NØ
150	393	.290	.300	130	.80	115.0	76.0	REV	YES
150	438	.200	.300	140	.65	120.0	105.0	REV	YES
150	407	.300	.300	135	.70	120.0	120.0	REV	NØ
150	407	.280	.300	140	.80	120.0	60.0	REV	YES

NØ	PT	TD	TP	VP	IP	VZB	VZA	VFB	VFA	PØL	FAIL
5	5	5.5	7.0	17.0	18.0	5.3	5.3	4.6	4.6	REV	NØ
5	5	3.2	7.0	24.0	32.0	5.3	5.3	4.6	4.6	REV	NØ
5	6	3.1	7.0	20.0	32.0	5.5	5.5	5.6	5.6	FWD	NØ
25	1	1.0	1.0	18.0	36.0	9.2	9.2	180.0	180.0	REV	NØ
25	1	5.5	7.0	15.0	20.0	9.2	9.2	180.0	180.0	REV	NØ
25	1	3.0	7.0	18.0	36.0	9.2	9.2	180.0	180.0	REV	NØ
25	2	1.0	1.0	440.0	20.0	9.2	9.2	310.0	310.0	FWD	NØ
25	2	7.0	6.0	380.0	10.0	9.2	9.2	310.0	310.0	FWD	NØ
25	2	4.0	6.0	510.0	18.0	9.2	9.2	310.0	310.0	FWD	NØ
25	3	3.8	6.0	500.0	18.0	9.3	9.3	220.0	220.0	FWD	NØ
33	1	1.0	1.0	12.0	13.0	1.0	1.0	.3	.8	REV	YES
33	2	1.0	1.0	5.0	4.0	1.0	1.0	.3	.3	REV	NØ
33	2	1.0	1.0	10.0	8.5	1.0	1.0	.3	.3	REV	YES
33	4	2.0	2.0	4.0	4.0	1.0	1.0	.2	.2	REV	NØ
33	4	2.0	2.0	6.0	6.0	1.0	1.0	1.0	.5	REV	YES
33	5	7.0	7.0	2.5	2.0	1.0	1.0	.3	.3	REV	NØ
33	5	7.0	7.0	4.0	4.0	1.0	1.0	.3	.3	REV	NØ
33	5	7.0	7.0	5.0	6.0	1.0	1.0	1.0	1.0	REV	YES
33	6	1.0	1.0	7.0	8.0	1.0	1.0	.3	.3	FWD	NØ
33	7	6.5	6.5	3.0	2.5	1.0	1.0	.2	.2	FWD	NØ
33	7	6.5	6.5	4.5	4.5	1.0	1.0	.3	.3	FWD	YES
33	8	.4	.4	9.0	8.0	1.0	1.0	.3	.3	FWD	NØ
33	8	.5	.5	10.0	13.0	1.0	1.0	.3	.3	FWD	NØ
33	8	.5	.5	13.0	14.0	.0	.0	--	--	FWD	YES
33	1	1.0	1.0	10.0	13.0	1.0	1.0	.3	.3	REV	NØ
33	1	1.0	1.0	10.0	12.0	1.6	1.6	.8	.8	REV	YES
38	1	1.0	1.0	28.0	32.0	5.9	5.9	53.0	53.0	REV	NØ
38	1	4.5	7.0	22.0	21.0	5.9	5.9	53.0	53.0	REV	NØ
38	1	3.5	7.0	28.0	31.0	5.9	5.9	53.0	53.0	REV	NØ
38	2	7.0	7.0	280.0	9.0	5.3	5.3	45.0	50.0	FWD	NØ
38	2	6.0	7.0	370.0	10.5	5.3	5.3	45.0	.5	FWD	YES
38	3	6.5	7.0	370.0	11.0	5.5	5.5	140.0	.5	FWD	YES
38	4	.2	7.0	390.0	14.0	5.6	5.6	80.0	.5	FWD	YES
42	1	.1	1.0	360.0	5.2	140.0	.0	14.0	14.0	REV	YES
42	2	.1	1.0	520.0	4.0	230.0	.0	14.0	14.0	REV	YES
42	3	.1	4.0	560.0	5.0	200.0	.0	13.8	13.8	REV	YES
42	5	3.0	4.0	26.0	36.0	240.0	240.0	14.0	14.0	FWD	NØ
42	6	.1	7.0	550.0	4.5	210.0	.0	14.0	14.0	REV	YES

NØ	PT	TD	TP	VP	IP	VZB	VZA	VFB	VFA	PØL	FAIL
57	1	1.2	5.0	38.0	20.0	5.0	3.9	5.7	5.7	REV	YES
57	3	6.7	7.0	25.0	11.0	5.2	3.1	4.9	4.9	REV	YES
57	4	.2	1.0	60.0	20.0	5.1	3.4	5.2	5.2	REV	YES
57	5	1.3	1.0	50.0	31.0	5.3	5.3	5.5	5.5	FWD	NØ
57	5	2.0	3.0	46.0	24.0	5.3	5.3	5.5	3.3	FWD	YES
57	6	3.0	3.0	47.0	26.0	5.2	5.2	5.3	5.3	FWD	NØ
57	6	2.8	3.0	50.0	28.0	5.2	5.2	5.3	4.5	FWD	YES
85	11	10.0	10.0	38.0	85.0	6.2	6.2	--	--	REV	NØ
85	11	10.0	10.0	44.0	95.0	6.2	5.2	--	--	REV	YES
85	8	10.0	10.0	42.0	116.0	5.8	5.8	--	--	REV	NØ
85	8	10.0	10.0	45.0	135.0	5.8	5.5	--	--	REV	YES
85	2	1.0	1.0	78.0	300.0	6.2	6.2	--	--	REV	NØ
85	2	1.0	1.0	84.0	340.0	6.2	5.8	--	--	REV	YES
85	4	1.0	1.0	108.0	356.0	6.3	6.3	--	--	REV	NØ
85	4	1.0	1.0	127.0	425.0	6.3	1.1	--	--	REV	YES
85	33	1.0	1.0	109.0	488.0	6.2	6.2	--	--	FWD	NØ
85	27	1.0	1.0	112.0	500.0	5.9	5.9	--	--	FWD	NØ
85	19	.1	.1	120.0	488.0	6.0	6.0	--	--	REV	NØ
85	33	.1	.1	120.0	425.0	6.2	6.2	--	--	REV	NØ
116	56	10.0	10.0	60.0	100.0	8.6	8.6	--	--	REV	NØ
116	56	10.0	10.0	60.0	130.0	8.6	8.4	--	--	REV	YES
116	58	10.0	10.0	55.0	130.0	8.6	8.6	--	--	REV	NØ
116	58	10.0	10.0	55.0	140.0	8.6	4.2	--	--	REV	YES
116	50	1.0	1.0	90.0	340.0	8.5	8.5	--	--	REV	NØ
116	50	1.0	1.0	100.0	380.0	8.5	8.3	--	--	REV	YES
116	51	1.0	1.0	110.0	380.0	8.5	8.5	--	--	REV	NØ
116	51	1.0	1.0	110.0	396.0	8.5	8.3	--	--	REV	YES
116	53	1.0	1.0	285.0	458.0	8.6	8.6	--	--	FWD	NØ
116	52	1.0	1.0	230.0	450.0	8.5	8.5	--	--	FWD	NØ
116	54	.1	.1	280.0	450.0	8.5	8.5	--	--	REV	NØ
116	55	.1	.1	250.0	450.0	8.5	8.5	--	--	REV	NØ